DUAL ROLES FOR TRANSCRIPTION FACTOR *ZIC3* IN REGULATING EMBRYONIC STEM CELL PLURIPOTENCY AND DIFFERENTIATION

LINDA LIM SHUSHAN

B.Sc (Honours)
The University of Melbourne, 2003

A THESIS SUBMITTED

FOR THE DEGREE OF DOCTOR OF PHILOSOPHY

NUS Graduate School for Integrative Sciences and Engineering

NATIONAL UNIVERSITY OF SINGAPORE

August 2008

ACKNOWLEDGEMENTS

It is a pleasure to thank the many people who made this thesis possible. My deepest thanks goes to Dr Lawrence Stanton for his invaluable guidance and steadfast belief in me. His mentorship has encouraged creativity, flexibility and room to grow, and these past 4 years have been an amazingly inspiring and enriching experience for me. I would also like to thank my thesis advisory committee, Dr Paul Robson and Dr Chan Woon Khiong, for their critical feedback along the way.

I am especially grateful to Jonathan Loh for numerous open discussions and exchange of ideas in the development of the Zic3 project. My thanks goes to Li Pin who taught me the critical foundations of stem cell culture, and to Hoi Aina and Wong Kee Yew who have been so generous in their sharing of technical experience. Special appreciation goes to Lim Yiting and Tahira Allapitchay whose work I have referred to in this thesis, and to Rory Johnson for his feedback and comments. I also wish to thank everyone in the GIS Stem Cell group for stimulating discussions and fun companionship.

Finally and most importantly, I thank my parents, who have been encouraging, supportive and incredibly giving at every turn of the corner. I am grateful far beyond what words can express for the depth of their grace, their understanding, and the genuine interest they consistently take in my work. I am immeasurably blessed to have them as my parents. Their love has made all the difference in my life - and it is to them I dedicate this thesis.

TABLE OF CONTENTS

ABSTRACT

The transcription factors Oct4, Nanog and Sox2 are key regulatory players in embryonic stem (ES) cell biology. Dissecting their transcriptional networks will provide inroads to the molecular mechanisms that direct ES cell pluripotency and early differentiation. I describe a role for a zinc finger transcription factor, Zic3, in the maintenance of ES cell pluripotency. Zic3 is expressed in ES cells and this expression is repressed upon differentiation. The binding of transcription factors Oct4, Nanog and Sox2 have been mapped to the gene regulatory region of *Zic3* in ES cells. Here I demonstrate that *Zic3* is activated downstream of these key pluripotency genes. In addition, gene expression microarray experiments have uncovered significant overlaps between the Oct4, Nanog, Sox2 and Zic3 pathways in ES cells.

Targeted repression of *Zic3* in human and mouse ES cells was performed to investigate the functional role of Zic3 in ES cells, and the results indicate that loss of Zic3 expression induces the expression of several markers of the endodermal lineage. This suggests that Zic3 plays an important role in the maintenance of pluripotency by preventing differentiation of ES cells into endoderm. This project therefore establishes a foundation for further investigation into the mechanisms involved in the maintenance of ES cell pluripotency.

Little is known about the regulatory networks that Zic3 employs to maintain pluripotency or to determine lineage specificity during embryonic development. I

have established the global regulatory targets of Zic3 in ES cells and investigated its interactions with other ES cell-associated proteins. Here I define a Zic3 consensus DNA binding motif and present evidence for the cooperative action of Zic3 with a key ES cell transcription factor, Sox2. These results include: (1) physical interaction between Zic3 and Sox2 proteins, (2) evidence for common regulatory pathways, and (3) a significant overlap between their target genes. These results indicate that Zic3 binds both in close proximity with Sox2 in ES cells and comes in direct contact with DNA.

In addition, I report that Zic3 occupies promoters of ES cell-related genes as well as genes involved in early embryonic patterning, and mesoderm and ectoderm formation. Although Zic3-bound developmental regulators are transcriptionally silent in ES cells, functional analysis indicates that Zic3 has capacity to activate these genes outside the pluripotent state. This suggests that Zic3 may confer ectoderm and mesoderm specificity during differentiation of ES cells. In support of this, I demonstrate that transient drug-induced overexpression of Zic3 in ES cells enhances the rate of neurogenesis under conditions that promote neural differentiation.

The zinc finger transcription factor, Zic3, is critical for the maintenance of ES cell pluripotency and, additionally, is a positive regulator of embryonic morphogenesis, and cardiac, skeletal and neural differentiation during embryonic development. To date, little is known about the transcriptional network that Zic3 regulates to confer ES cell pluripotency or to define lineage specificity during development. To this end, the results of my work provide key molecular insight

into the Zic3-regulated pathways that influence ES cell pluripotency and the critical lineage decisions made during differentiation. This thesis therefore extends our knowledge of ES cell transcriptional circuitry and contributes to a greater understanding of the role of Zic3 in development.

LIST OF FIGURES

LIST OF TABLES

ABBREVIATIONS

Symbol	Definition
µg	Microgram
µL	Microlitre
A-P	Anterior-posterior
AVE	Anterior visceral endoderm
BSA	Bovine serum albumin
ChIP	Chromatin immunoprecipitation
CHO	Chinese hamster ovary
DBD	DNA-binding domain
DMSO	Dimethyl sulfoxide
DNA	Deoxyribonucleic acid
D-V	Dorso-ventral
ECL	Enhanced chemiluminescence
EDTA	Ethylene Diamine Tetra-acetic Acid
ES cells	Embryonic stem cells
EtOH	Ethanol
ExE	Extra-embryonic endoderm
FCS	Fetal calf serum
FDR	False discovery rate
gDNA	Genomic DNA
GFP	Green fluorescent protein
HH	Hedgehog
HMBA	N,N'-Hexamethylenebisacetamide
HRP	Horseradish peroxidase
ICM	Inner cell mass
IVF	In-vitro fertilization
LIF	Leukemia inhibitory factor
L-R	Left-right
MAP2	Microtubule-associated protein 2
MEF	Mouse embryonic fibroblast
Neo	Neomycin resistance
PAGE	Polyacrylamide gel electrophoresis
PBS	Phosphate buffered saline

Symbol	Definition
PCR	Polymerase chain reaction
qPCR	Quantitative PCR
RA	Retinoic acid
RE	Restriction enzyme
RNA	Ribonucleic acid
RNAi	RNA interference
SCNT	Somatic cell nuclear transfer
SDS	Sodium dodecyl sulfate
TBS-T	Tris-buffered saline/Tween-20
TF	Transcription factor
ZF	Zinc finger

CHAPTER 1:

INTRODUCTION

1.1 Derivation of embryonic stem cells

The inner cell mass (ICM) of an embryonic blastocyst is a source of pluripotent cells that ultimately give rise to the embryo proper. Following implantation into the uterine wall, pluripotent ICM cells develop into both extra-embryonic endoderm as well as the three key embryonic germ layers comprising ectoderm, endoderm and mesoderm tissue[1] (Figure 1A). The unique cells of the ICM therefore represent an opportunity for the study of fundamental processes behind embryonic development and cell fate determination.

In 1981, Evans & Kaufman at the University of Cambridge made a significant breakthrough in their establishment of pluripotent ICM cells in laboratory cultures[2]. They had successfully delayed embryonic implantation to achieve enlarged blastocysts from which ICM cells could be isolated and expanded *in vitro*. Using a separate approach, developmental biologist Gail Martin independently extracted ICM cells from non-enlarged blastocysts, and aided their expansion with teratocarinoma-conditioned media, which she hypothesized contained growth factors that stimulated cell growth and prevented differentiation[3]. These ICM cells, henceforth termed “embryonic stem cells”, were shown to be pluripotent and could self-renew indefinitely in culture[2,3] (Figure 1B).

These two developments represented a significant breakthrough in the study of pluripotent cell types, and provided the basis of isolation techniques for ES cells from other species[4-6]. In 1998, knowledge gained from prior studies culminated in the landmark derivation of five human ES cell lines by Thomson et al. from the

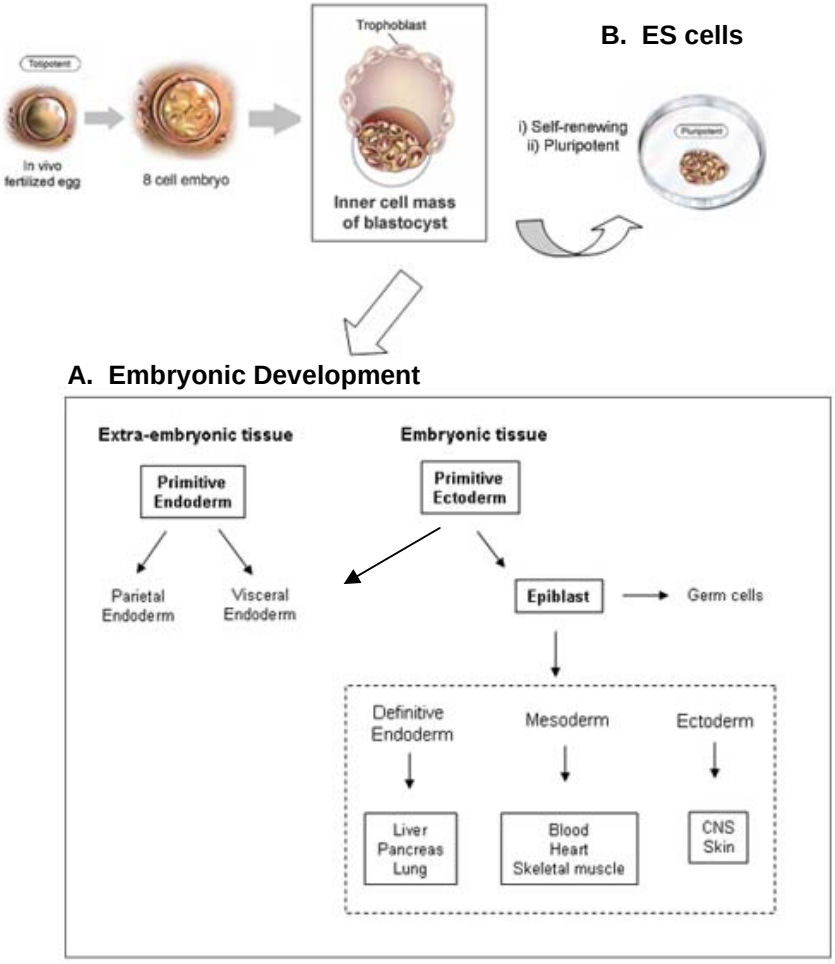

Figure 1. Contribution of the blastocyst inner cell mass to embryonic development and embryonic stem cells. (A) The ICM gives rise to extra-embryonic endoderm and the three germ layers of the embryo proper. (B) ES cells are derived from the inner cell mass of the embryonic blastocyst and can be propagated indefinitely in culture.

blastocysts of discarded *in-vitro* fertilization (IVF) embryos[7]. These cell lines demonstrated stable karyotype after several months of continuous passage, and had the ability to form extra-embryonic trophoblast and the three germ layers of the embryo proper[7]. Thomson et al. thus speculated that directed differentiation of human ES cells would one day be harnessed to treat clinical disease[7].

Today ES cells are recognized for their vast potential in a host of applications. In addition to being harnessed as a model for early embryonic development, and a vector for introduction of targeted mutations into the mouse germ-line[8,9], ES cells are viewed as an important potential tool for clinical therapy and drug discovery[10].

1.2 Regulation of embryonic stem cells

1.2.1 The key properties of ES cells

Embryonic stem cells have the capacity to self-renew indefinitely when cultured under conditions that prevent differentiation[11], and undergo rapid proliferation by symmetric division every 12 hours[12]. ES cells display an unusual cell cycle with a shortened Gap 1 (G1) phase lasting an average of 1.5 hours[13]. At the G1 phase, mammalian cells typically face a choice between entering the quiescent Gap 0 (G0) state associated with post-mitotic differentiation, or to continue through the DNA Synthesis (S) phase in preparation for mitosis (Figure 2). The G1/S transition is therefore a critical point beyond which cells are committed to dividing[14]. In ES cells, the G1 control pathways commonly found in other cell types are reduced or absent[13], resulting in prolonged maintenance of the self-renewal state.

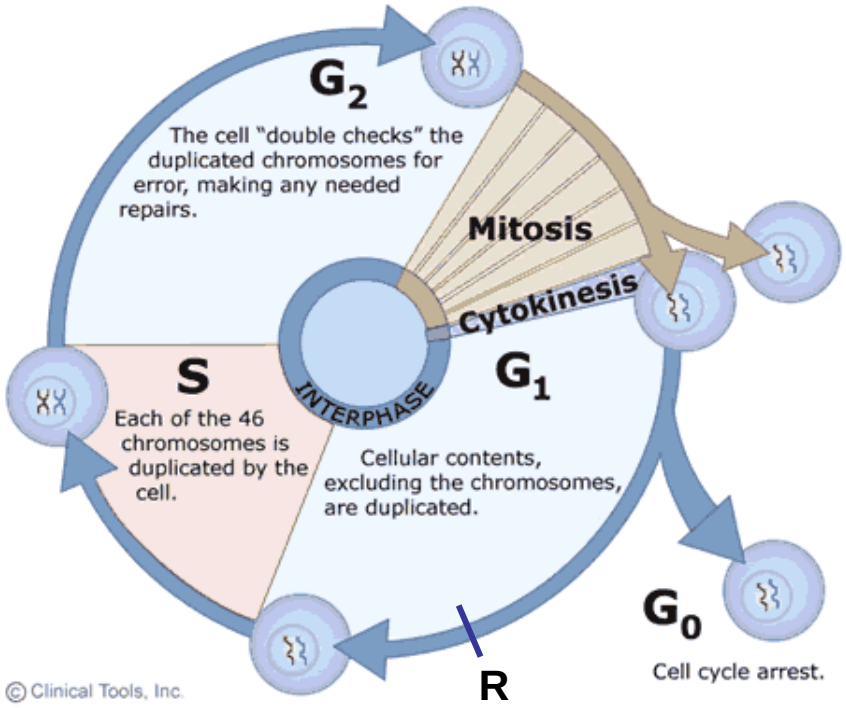

Figure 2. Components of the cell cycle. Gap 1 phase (G1) – The cell undergoes metabolic changes in preparation for division. This phase is marked by the synthesis of enzymes required for DNA replication in the S phase. Beyond the restriction point (R), the cell is committed to division and moves into the S phase. **Synthesis phase (S)** - DNA synthesis replicates the genetic material in preparation for mitosis, and each chromosome now consists of two sister chromatids. **Gap 2 phase (G2)** – A period of intense protein synthesis where cytoplasmic material mainly consisting of microtubules are produced and organized for mitosis and cytokinesis. **Mitosis (M)** – This is a relatively brief phase comprising a nuclear division (karyokinesis) followed by a cell division (cytokinesis) to produce two identical daughter cells. **Interphase (I)** - The period between mitotic divisions, G1, S and G2, are collectively known as the interphase. *Figure adapted from Clinical tools, Inc.*

Pluripotency is maintained during ES cell self-renewal through the prevention of differentiation and the promotion of proliferation[15]. Pluripotency is broadly defined as the potential to give rise to all the cells and tissues within an embryo proper, while lacking the self-organizing ability conferred by extra-embryonic tissue to generate a whole organism[15,16]. Pluripotent ES cells are characterized by the presence of ES cell surface markers (e.g. Stage-specific embryonic antigens), and specific patterns of gene expression, DNA methylation, and telomerase activity. In addition, pluripotent cells have ability to form teratomas when introduced into a host organism, generate chimeras upon injection into 8-cell embryos or blastocysts[17], and show germline transmission[18].

Studies over the past few years have revealed that transcription factor networks[19,20], epigenetic processes[21-23], and extrinsic signalling pathways[24-27] play important roles in the maintenance of ES cell pluripotency. These processes are described in greater detail in the following sections.

1.2.2 Extrinsic signalling pathways maintaining ES cell pluripotency

Embryonic stem cells are maintained by a network of extrinsic and intrinsic signals that collectively regulate the properties of pluripotency and self-renewal. A unique trademark of ES cells is their ability to propagate indefinitely without showing signs of senescence and cell death. However, the maintenance of the undifferentiated stem cell phenotype is not a cell autonomous process (Figure 3). ES cells are dependent upon exogenous factors that are supplied either by co-culture with fibroblast feeder cells, or through the use of conditioned media[28]. One key exogenous factor is leukemia inhibitory factor (LIF), a cytokine that effectively

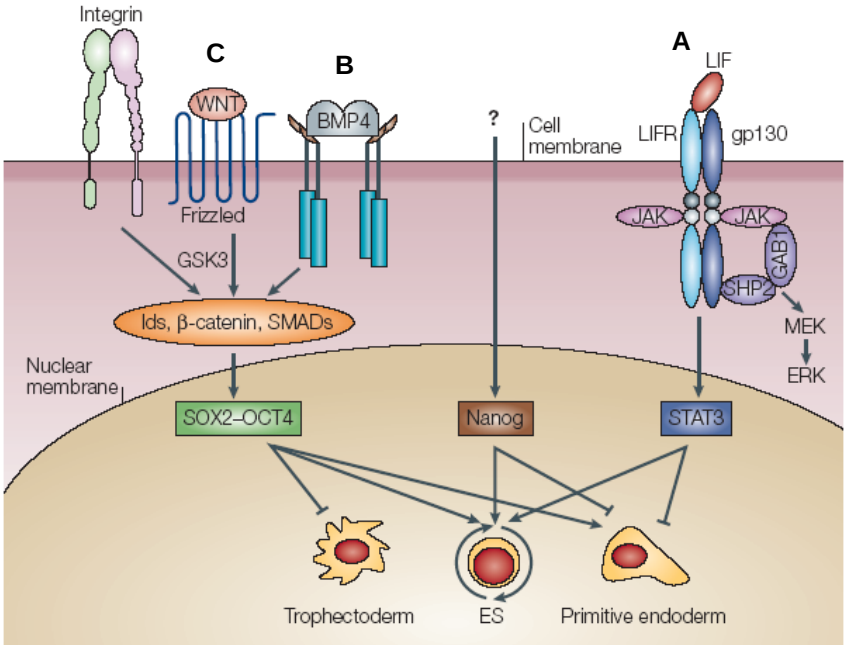

Figure 3. Signalling pathways contributing to the pluripotency of ES cells. Cell-surface receptors initiate signals that are conveyed (thin black lines) to the nucleus and affect key pluripotency transcription factors such as Oct4, Nanog, Sox2, and self-renewal transcription factors such as Stat3. These signals comprise: (A) The LIF-gp130 pathway that triggers the JAK-kinase pathway activation of Stat3, (B) the Bmp4 signalling pathway, and (C) the Wnt-Frizzled activated pathway that signals Sox2 and Oct4 activity via mediators such as β-catenin and the Smad proteins. *(Adapted from Boiani & Schöler, 2004)*

sustains mouse ES cell self-renewal in the absence of the feeders[24] (Figure 3A). The withdrawal of LIF from ES cell cultures results in a decrease in cell proliferation and induction of differentiation in mouse ES cells[25]. The expression of LIF in mouse embryonic feeder cells is stimulated by the presence of ES cells, and LIF is secreted into the media of ES cell co-cultures for the maintenance of pluripotency[29]. The importance of LIF is underscored by studies showing that feeder cells lacking a functional *Lif* gene do not effectively support ES cell propagation[30].

LIF binds to the gp130 heterodimer receptor on the cell membrane and activates downstream signaling pathways, beginning with JAK kinase-mediated recruitment of the transcription factor, Stat3 (Figure 3A). Stat3 undergoes phosphorylation and dimerization before being translocated to the nucleus, where it activates important transcriptional programs to maintain self-renewal in ES cells[25]. Significantly, studies have shown that activation of this transcription factor is sufficient to support ES cell self-renewal in medium lacking LIF[31], thus confirming that Stat3 is the downstream effector of the LIF pathway.

The LIF-Stat pathway alone is insufficient to maintain the pluripotent state in feeder-free ES cultures; additional signalling by Bmp4 is required for normal ES cell maintenance under serum-free conditions[27]. In the presence of LIF, Bmp4 contributes to the LIF pathway by the activation of Smad4, which in turn activates members of the *Id* (inhibitor of differentiation) gene family to prevent neuronal specification in mouse ES cells[27] (Figure 3B). The Bmp proteins also share their targets with the Wnt-activated ligand pathway[26] (Figure 3C). The Wnt proteins are

secreted glycoproteins that have widespread roles in tissue differentiation and organogenesis[32], and the canonical Wnt pathway is activated when a Wnt protein binds to the Frizzled receptor on the cell membrane. This leads to inhibition of Gsk3 (glycogen-synthase kinase-3) and subsequent translocation of β-catenin to the nucleus to regulate expression of downstream target genes (Figure 3C). Inhibition of the Gsk3 pathway results in the maintenance of undifferentiated mouse and human ES cells, with sustained expression of key pluripotent transcription factors *Oct4*, and *Nanog* even in the absence of LIF[33].

However Ying et al. (2008) have recently demonstrated that these extrinsic stimuli, previously thought to be critical for ES cell self-renewal, may in fact be dispensible. Small molecule-induced inhibition of the Gsk3 and phospho-ERK pathways that lie upstream of extrinsic signalling pathways resulted in replication of the pluripotent state[34], and complete bypass of cytokine signalling was demonstrated using Stat3-deficient cells. This suggests that the BMP/Smad/Id and LIF/STAT3 pathways are not instructive for self-renewal but instead shield the pluripotent state from induced phospho-ERK. These new findings indicate that ES cells may have innate self-renewal capacity and are not dependent on external signalling factors for propagation of the pluripotent state.

1.3 Transcriptional networks in ES cells

The extrinsic signalling pathways eventually reach the ES cell nucleus to activate or repress transcriptional programs responsible for the pluripotent state of the ES cells (Figure 4). Here the nuclear transcription factors Oct4, Nanog and Sox2 feature prominently in directing self-renewal and maintaining pluripotency. In early

studies of ES cells, these transcription factors were identified as potential regulators of pluripotency due to their unique expression pattern and critical roles in early development[35-39] and their function as essential regulators of cell-fate specification in many organisms[37,40]. The activity of these transcription factors also depends on the accessibility of their target genes, which are made more or less accessible by the modification of their DNA, histones, or chromatin structure[22,23,41]. In recent years, it has emerged that Oct4, Nanog and Sox2 contribute to the hallmark characteristics of ES cells by: 1) activation of target genes that encode pluripotency and self-renewal mechanisms and 2) repression of signalling pathways that promote differentiation[42] (Figure 4). These key transcription factors will be reviewed in the following section.

1.3.1 Regulation of transcription networks

Proper regulation of gene transcription is critical for activation of tissue-specific programs, and is foundational to the establishment of unique tissue properties. The biological properties of an organism are characterized by gene expression patterns that result from a dynamic interplay between transcription factors and their target genes. Delineation of transcriptional networks is therefore required to understand the molecular basis of cell fate.

Transcription factors comprise several domains that are essential for its function[43] (Figure 5). DNA-binding domains (DBD) associate with DNA in non-coding regions, and confer specificity by recognition of specific DNA sequences within the promoter of each gene. Secondly, several transcription factors also contain a signal sensing domain (SSD) which senses and transmits external signals to the

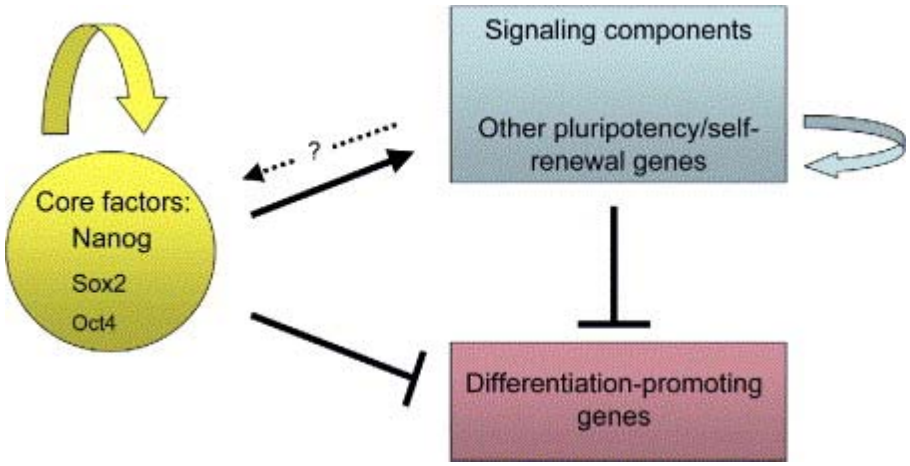

Figure 4. Role of Oct4, Nanog and Sox2 in ES cell pluripotency. Oct4, Nanog and Sox2 activate target genes in ES cells that signal the expression of pluripotency and self-renewal factors. These core ES cell transcriptional factors concurrently repress the expression of genes encoding pathways that promote ES cell differentiation. *Source: Orkin, S.H., 2005*

rest of the transcription complex to regulate gene expression (Figure 5). Finally, the trans-activating domains (TAD) of transcription factors contain binding sites for coactivator proteins (Figure 6) which signal the basal transcription proteins to initiate RNA-polymerase mediated transcription of the target gene. The transcription initiation complex in Figure 6 illustrates the core units required for activation of gene transcription, and demonstrates how signals from the transcriptional activators and repressors are transmitted via coactivator proteins to regulate the activity of RNA polymerase.

Transcription networks are built upon a series of interconnected pathways that collectively regulate the gene expression program of an organism. At the most basic level, transcription networks are organized into 6 simple motifs with specific patterns of regulation between transcription factors and their target genes[44]. These transcriptional motifs are illustrated in Figure 7. The single-input motif is a connection between a target gene and its sole transcriptional regulator, while the multiple-input motif is simultaneously regulated by a group of factors[45]. The target genes belonging to these two motifs are usually co-expressed at levels proportional to the number of transcription factors involved[46].

A feed-forward loop is established when a TF regulates the expression of a second TF, and both factors together regulate the expression of a common set of target genes[44-46]. Integrated networks characterized by these multiple feed-forward loops tend to show stable regulatory patterns[47]. Other common motifs identified in yeast include the autoregulatory and regulatory chain motifs[48]. The

Figure 5. **Functional domains of a transcription factor**. The amino acid sequence of a prototypical transcription factor is illustrated, containing a DNA-binding domain (**DBD**), a signal sensing domain (**SSD**), and a transactivation domain (**TAD**). The number and order of domains may differ in various types of transcription factors. *Adapted from Latchman, DS. (1997)*

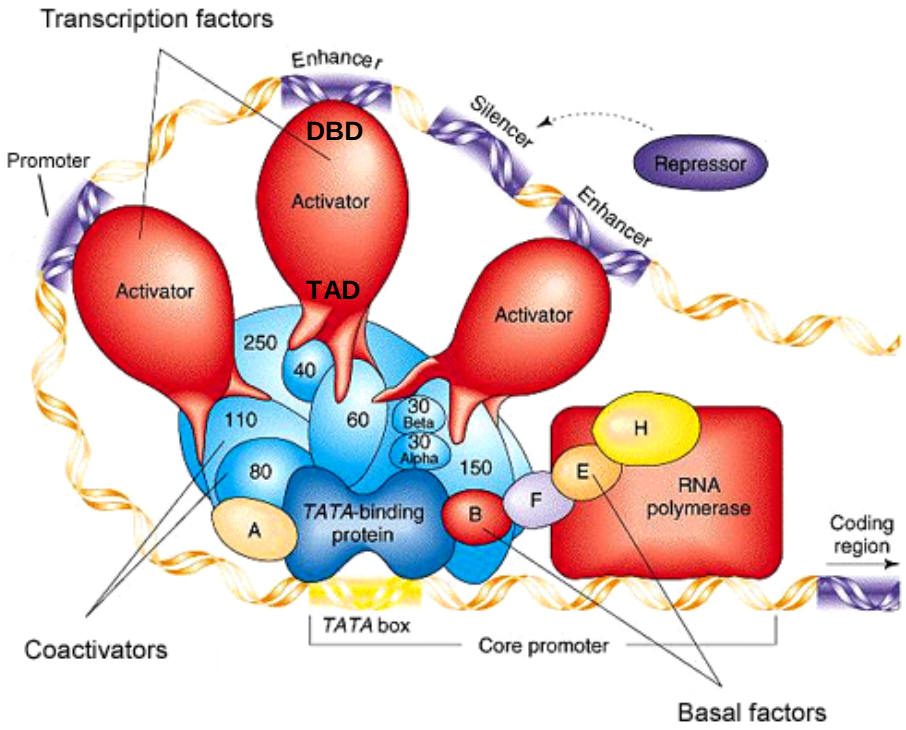

Figure 6. **Assembly of a transcription initiation complex**. Transcription factors (red) bind to promoter or enhancer regions to determine the genes that will be transcriptionally activated. The interaction of DNA binding domain (DBD) with DNA and trans-activating domain (TAD) with coactivators are represented here. Repressor proteins (grey) bind to DNA at sites known as silencers and interfere with the function of activators to decrease the rate of transcription. Co-activators (Green) are adaptor molecules that integrate activator and repressor signals and relay the results to the basal factors (blue) which position RNA polymerase at the start of the protein-coding region of a gene, and initiate the transcriptional activity of the enzyme. *Adapted from "Transcription of Eukaryotic DNA", Roanoke College, Biology 201 Chapter 11b.*

predominating motif is often determined by the type of transcriptional response required, such that an “all-or-none” response is usually characterized by single-input motifs, whereas more subtle and gradated response usually results from a combination of multiple-input motifs[47]. Together, these individual network motifs form the entire assembly of regulatory interactions known as the ‘transcriptional regulatory network’, which specifies the blueprint for gene expression patterns within an organism[44].

1.3.2 Oct4, Nanog and Sox2 are key regulators of transcription in ES cells

In ES cells Oct4, Nanog, and Sox2 co-occupy promoters of hundreds of genes that are both expressed and repressed in the pluripotent state[19,20,49] (Figure 8).

This suggests complex regulatory circuitry in which Oct4, Nanog, and Sox2 collectively and uniquely regulate downstream genes to control ES cell differentiation. Recent advances in genomic technologies have enabled the construction of transcriptional regulatory networks of Oct4, Nanog, and Sox2 in ES cells. Two groups have harnessed the chromatin-immunoprecipitation (ChIP) technique followed by genomic analysis of the target material to identify DNA bound by the three factors in human and mouse genomes[19,20,49]. Oct4, Nanog, and Sox2 were found to co-occupy a substantial portion of their target genes, suggesting that the three factors interact to regulate a large subset of common targets. Nanog shares 44.5% (345) of Oct4-bound genes in mouse ES cells[20], while 353 genes are co-bound by Oct4, Nanog, and Sox2 in human ES cells[19]. However, a comparison of the Oct4- and Nanog-bound regions revealed small

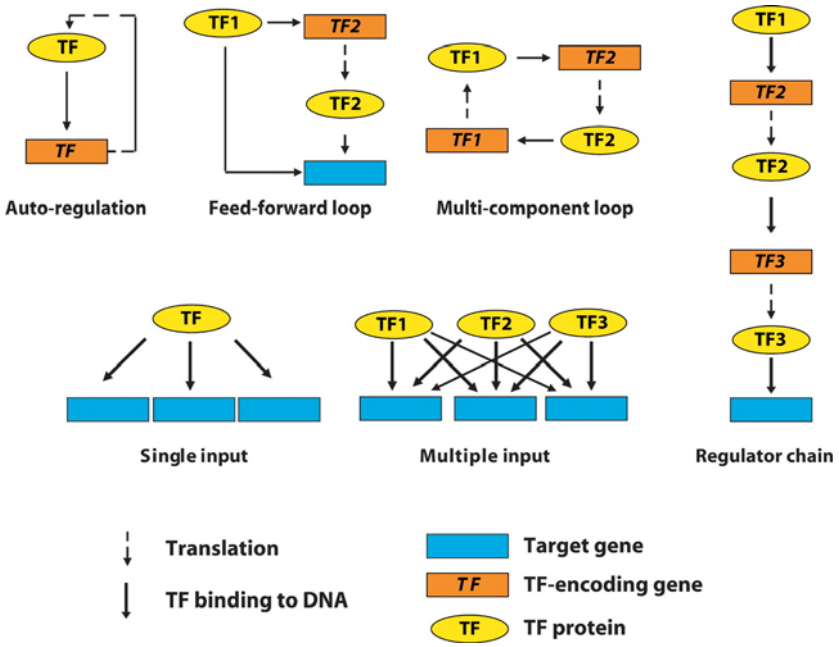

Figure 7. **The transcriptional circuit is built on basic network motifs**. The motifs in this figure represent the most common units found in transcription networks, comprising single and multiple input motifs, and autoregulatory, feed-forward, multi-component and regulator chain loops. *Source: Blais & Dynlacht, 2005*

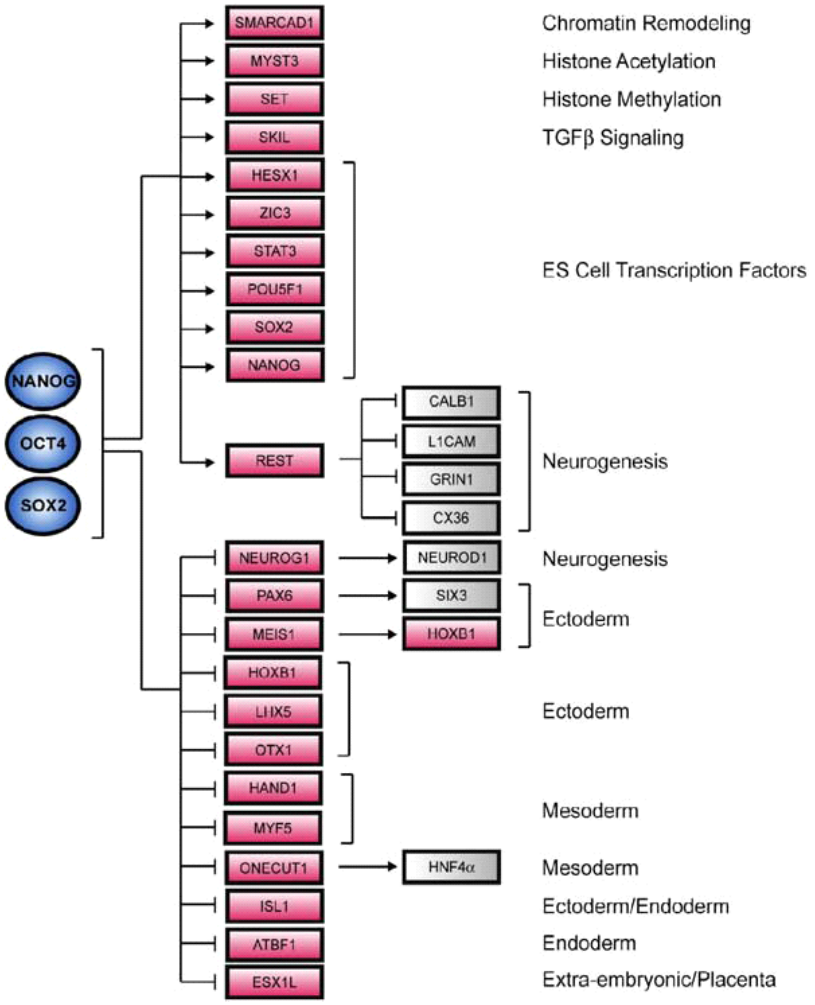

Figure 8. The core transcriptional regulatory network in ES cells. Genomics studies have enabled the elucidation of Oct4, Sox2 and Nanog networks, which reveal an integrated circuitry comprising genes that are involved in pluripotency and those that specify the development of both extra-embryonic and embryonic lineages. Boxes and circles indicate genes and proteins, respectively. Arrows represent interactions only, and not positive or negative effects. *Adapted from Boyer. et al., Cell, Vol. 122, 947–956, September 23, 2005*

overlaps between their target genes in mouse and human ES cells[20,50] (Figure 9A). The lack of similarities between their genomic targets have been attributed to the differing genomic platforms employed in the two studies, and possible genuine differences between the regulatory networks of human and mouse ES cells.

A closer examination of the Oct4, Nanog and Sox2 targets revealed that these key transcription factors occupy the promoters of both transcriptionally active and inactive genes in ES cells[19,20,49]. Among the active targets are genes encoding ES cell self-renewal genes including *Stat3* and components of the Wnt and TGF-β pathways. Amongst the inactive targets are a large number of transcriptionally silent lineage-specification genes. It was therefore concluded that Oct4, Nanog and Sox2 regulate a wide spectrum of cellular processes, and collectively function to maintain pluripotency by promoting the expression of other self-renewal genes while simultaneously preventing expression of differentiation-promoting genes involved in mesoderm, endoderm and ectoderm specification during development (Figure 8).

The assays for Oct4, Nanog and Sox2 targets revealed two regulatory motifs in the ES cell transcriptional circuitry[19]. Figure 9B represents the feed-forward loop in which Oct4 and Sox2 interact to co-activate Nanog expression, which subsequently acts in concert with these two factors to control downstream target genes. Oct4, Nanog and Sox2 also occupy the promoters of their own genes to form the interconnected auto-regulatory loops shown in Figure 9C. Collectively,

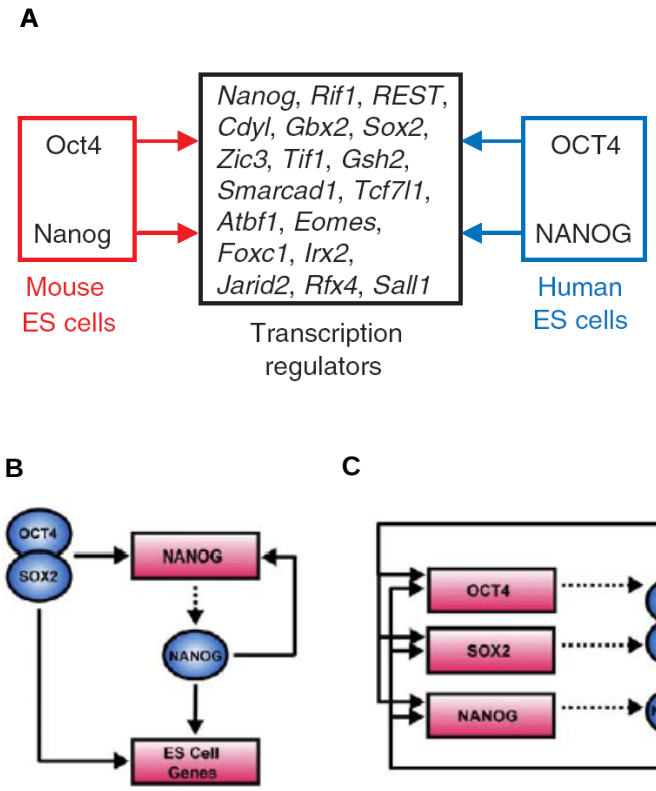

Figure 9. Transcriptional regulatory motifs between Oct4, Nanog and Sox2 and their common targets in ES Cells. (A) Oct4 and Nanog share a small subset of target genes between mouse and human ES cells. (B) Feedforward transcriptional regulatory circuitry in human ES cells. Regulators are represented by blue circles; gene promoters are represented by red rectangles. Binding of a regulator to a promoter is indicated by a solid arrow. Genes encoding regulators are linked to their respective regulators by dashed arrows. (C) The interconnected autoregulatory loop formed by Oct4, Nanog and Sox2. *Adapted from: Boyer et al., Cell. 2005 Sep 23;122(6):947-56. & Loh et al., Nat Genet. 2006 Apr;38(4):431-40*

these feedforward and auto-regulatory loops provide the advantage of reduced response time to environmental stimuli and increased stability of gene expression in ES cells.

In addition to transcription factor binding targets, a recent study was conducted to determine protein interaction patterns of key pluripotency genes[51]. The results indicate that a large subset of pluripotency-associated proteins such as Oct4, Esrrb, Rif1, and Sall4 are highly enriched within Nanog-associated complexes. Significantly, a substantial portion of the Nanog interactome members are also transcription targets of Oct4, Sox2 or Nanog in ES cells[19,20]. Moreover, a recent chromatin-immunoprecipitation assay combined with ultra-high-throughput sequencing (ChIP-sequencing) of 13 ES cell transcription factor binding sites revealed their dense occupancy patterns throughout the genome. The sites with dense TF occupancy were termed “multiple transcription-binding loci” (MTLs) of which 43.4% reflected Oct4, Nanog and Sox2 co-occupancy and were frequently associated with Smad1 and Stat3 binding[49]. This suggests that Smad1 and Stat3 share many common target sites with Nanog, Oct4, and Sox2, and reflects a point of convergence between the Smad1 and Stat3 signaling pathways with the core ES cell circuitry comprising Nanog, Oct4, and Sox2[19,20].

Interestingly, while the withdrawal of LIF and Bmp4 led to a significant reduction in binding of Stat3 and Smad1 proteins respectively, the extent of Oct4 occupancy remained unaffected. These results strongly indicate that Oct4 is central to the stability of the nucleoprotein complex[49]. The Oct4/Nanog/Sox2 MTLs also exhibit significant characteristics of enhanceosome complexes[52], such

as dense TF occupancy and an ability to enhance transcription from a distance. In addition, a second highly occurring MTL cluster comprising c-Myc, n-Myc, Zfx, and E2f1 co-occupancy was identified in ES cells. Together with the Oct4/Sox2/Nanog loci, the collective targets of these two clusters comprise 60% of genes upregulated in ES cells[49].

The recent data have therefore identified functionally-important genomic "hotspots" within the ES cell genome. These sites are extensively co-occupied by transcription factors and reflect in particular the presence of Oct4, Nanog, and Sox2 feedforward loops in ES cell transcriptional networks (Figure 9). In the following sections, I will review the properties of these three key ES cell transcriptional regulators that establish the genomic state necessary for the ES cell self-renewal and pluripotency.

1.3.2.1 Oct4

The transcription factor Oct4 is a POU-domain protein encoded by *Pou5f1*. The POU-domain family is named after three mammalian transcription factors, **P**it-l, **O**ct-l, Oct-2, and a *C. elegans* protein **U**nc-86, which share a region of homology known as the POU domain[53-57]. The POU domain is a bipartite DNA-binding domain comprising two highly conserved regions tethered by a variable linker. The 75-amino acid N-terminal region is known as the POU-specific domain, while the C-terminal 60-amino acid region, the POU homeodomain. High-affinity site-specific DNA-binding by POU domain transcription factors requires both the POU-

specific domain and the POU homeodomain. The two subdomains can cooperatively bind DNA even when they are not joined by the linker[53,57-60].

Certain transcription factors containing the POU-homeodomain are important regulators of early mammalian development[36,57,61-63]. Oct4 is expressed in the unfertilized egg and within the early embryo during the cleavage stages prior to the separation of the ICM from the trophectoderm[64]. The expression of Oct4 is then maintained in the epiblast of pre- and post-implantation embryos before becoming restricted to the migratory primordial germ cells[65,66]. In addition, Oct4 expression is downregulated in the trophectoderm, primitive endoderm and the extraembryonic and somatic lineages[66]. Interestingly, *Oct4*-deficient embryos develop to the blastocyst stage but comprise only trophectoderm cells without the ICM[38]. These *Oct4*-null embryos also specifically give rise to trophectodermal cells when dissociated and maintained *in vitro*[38]. Moreover, RNAi-mediated depletion of *Oct4* causes human ES cells to differentiate towards the trophectodermal lineage[67]. These results indicate that Oct4 plays a central role in preventing trophectodermal differentiation while maintaining the pluripotent state of the ICM during embryonic development (Figure 10).

Consistent with its role as a repressor of trophectoderm commitment, Oct4 is a negative regulator of *Cdx2*, a factor essential for the self-renewal of trophoblast stem cells and specification of the trophoblast lineage *in vivo*[68]. Moreover, overexpression of *Oct4* in mouse ES cells results in endodermal and mesodermal lineage specification[69] (Figure 10). These results collectively indicate that Oct4

has a key role in regulating ES cell pluripotency, and that precise levels of Oct4 protein are required to maintain its function in ES cells[69].

1.3.2.2 Sox2

Sox2 is a member of the Sox (SRY-related HMG box) gene family that encodes transcription factors with a high mobility group (HMG) DNA-binding domain[70]. Based on homology within and outside the HMG box, Sox2 belongs to the SoxB1 subgroup that encompasses the Sox1 and Sox3 proteins. Several lines of evidence suggest that Sox2 functions to maintain developmental potential in their target cells. Firstly, Sox2 expression is found in growing and mature oocytes[37]. Secondly, it is present in blastomeres and then later in the ICM of blastocysts and epiblasts cells[71]. *Sox2*-deficient embryos give rise to defective ICMs from which pluripotent ES cells cannot be derived (Figure 10), and subsequently, to abnormal development of the epiblast[37], and these *Sox2* null embryos also demonstrate lethality around the peri-natal stages. Third, Sox2 expression is associated with embryonic stem cells[19,20] and uncommitted precursor cells within the developing central nervous system[72] (Figure 10). Thus the expression pattern of Sox2 is similar to that of Oct4 within embryonic stem cells, and the embryonic ICM, epiblast and germ cells. However, unlike Oct4, Sox2 is also found within the multipotent cells of the extraembryonic endoderm, suggesting that Sox2 may be involved in establishment of primitive and extra-embryonic ectoderm, and that its function is not merely restricted to ES cells or pluripotency[37].

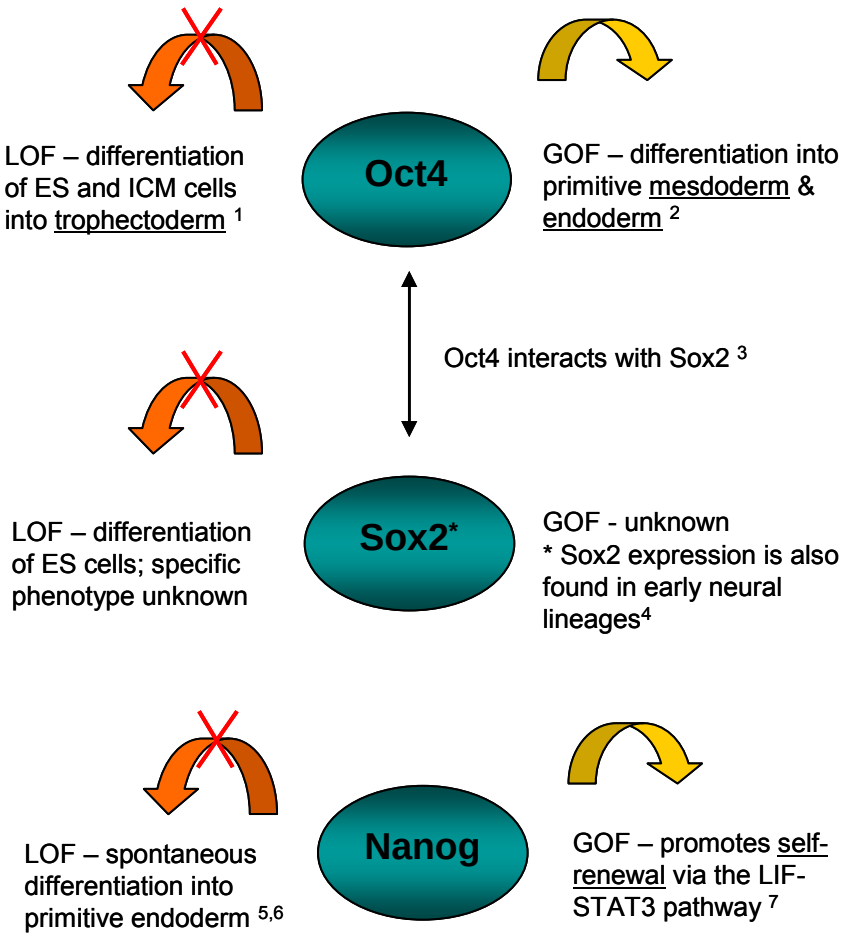

Figure 10. Gain- and Loss-of-function phenotypes of Oct4, Nanog and Sox2 in ES Cells. Loss-of-function phenotypes are described in the left column, and grain-of-function phenotypes are described in the right column.

The expression of *Sox2* in ES cells is known to be mediated by two promoter/enhancer regions on the Sox2 gene, known as SRR1 and SRR2[73]. Oct4 has recently been shown to bind and regulate an octamer recognition sequence within the SRR1 region[74], and SRR2 contains a composite sox-oct binding element 1.2 kb downstream of the *Sox2* transcription start site[73]. Binding of Oct4 or Sox2 to SRR2 is mediated by the presence of Oct4, and mutations to the SRR2 region that resulted in ablation of Oct4 binding disrupted the formation of a DNA/protein complex, and subsequent loss of SRR2 activity[73]. These results indicate that Oct4/Sox2 heterodimer occupancy of the SRR2 region is essential for the expression of Sox2. The above results are supported by structural validation of the ability of the POU and HMG domains to mediate specific protein-protein and DNA-protein interactions[75,76], and the observation that regulatory regions of a set of important Oct4/Sox2 co-regulated genes in ES cells contain an sox-oct element on which Oct4/Sox2 heterodimers bind and interact synergistically[37,77] to regulate expression of their downstream targets.

1.3.2.3 Nanog

Nanog was identified as an important ES cell transcription factor through gain-of-function studies demonstrating its ability to maintain mouse ES cells in the absence of LIF and feeder cultures[39,78] (Figure 10). The Nanog protein comprises a 96 amino acid N-terminal domain and a 150 amino acid C-terminal domain. Both the N- and C-terminal domains of mouse Nanog have the ability to trans-activate Nanog target genes, with the C-terminal domain being 7 times as active as the N-terminal one[79]. This unique arrangement of dual trans-activators may be responsible for the flexibility and specificity of Nanog to regulate downstream

targets critical for both ES cell pluripotency and differentiation. The Nanog protein also contains a homeobox domain which confers binding specificity by recognition of DNA motifs, and Nanog consensus sequences have been defined in the promoter/enhancer regions of *Rex1* and *Gata6* genes[80,81].

Nanog expression is first observed in the embryonic morula, and high levels of *Nanog* RNA persist in the early blastocyst and declines just prior to implantation[39,78]. Nanog expression is subsequently restricted to a subset of epiblast cells and is down-regulated during primitive streak formation[39,78]. The *in vivo* depletion of *Nanog* disrupts inner cell mass proliferation and prevents formation of epiblast[39,78]. *Nanog*-null embryos do not give rise to primitive ectoderm at E5.5[39], and hence subsequently do not form the three primary germ layers of the embryo. In addition, Nanog is expressed in pluripotent germ cells of the nascent gonad during embryonic development, and within in germ cell tumours and teratoma-derived cell lines[35]. These results collectively indicate that Nanog signalling is important in pluripotency and early embryonic development.

Recent studies have shown that Oct4 and Sox2 co-occupy the promoter of *Nanog* and positively regulate its expression in ES cells (Figure 9B)[19,82,83]. Nanog is known to be essential for propagation of ES cells in an undifferentiated state, and loss of Nanog results in spontaneous differentiation into primitive endoderm (Figure 10). This is similar to the cell type formed upon ectopic expression of *Gata4* and *Gata6* in ES cells[84], and it is thought that Nanog maintains pluripotency through repression of *Gata4* and *Gata6* pathways to prevent primitive endoderm differentiation in ES cells.

1.3.3 Identifying genes that contribute to stem cell pluripotency

The transcriptional networks governing the unique properties of ES cell pluripotency and self-renewal have been the focus of many genome- and proteome-wide studies to date. These approaches include high-throughput gene expression profiling to determine transcripts upregulated in the pluripotent state[85,86], chromatin-immunoprecipitation to identify targets of Oct4, Nanog and Sox2 in mouse and human ES cells[19,20,49,87], RNAi-mediated depletion of key regulators in ES cell pluripotency accompanied by global analysis of gene expression to determine affected pathways[87], and affinity purification of Nanog-associated proteins followed by mass spectrometry to establish a protein interaction network in ES cells[51].

Many transcription factors apart from Oct4, Nanog and Sox2 have recently been identified that are essential for the undifferentiated state of ES cells. An RNAi-mediated knockdown approach has demonstrated that 8 genes (*Nanog, Oct4, Sox2, Tbx3, Esrrb, Tcl1, Dppa4* and *Mm.343880*) are important for maintaining the morphology and proliferation of ES cells[87]. In addition, a genome-wide study has identified and characterized *Rif1* and *Esrrb* as important downstream effectors of Oct4 and Nanog of mouse ES cells[20]. Another study that combined a list of Oct4 binding targets with gene expression profile changes resulting from perturbations of endogenous Oct4 levels has identified *Tcl1* as a critical regulator of cell proliferation[88]. Furthermore, two separate studies have also shown that a member of the spalt-like protein family, Sall4, physically interacts with Nanog and positively regulates transcription of Oct4 in ES cells[89,90]. Two recent studies have

also demonstrated that Tcf3, a downstream effector of the Wnt pathway, is a regulator of ES cell pluripotency and self-renewal[91,92].

A series of breakthrough experiments initiated by Takahashi and Yamanaka have demonstrated the ability of four transcription factors *Oct4, Sox2, Klf4* and *c-Myc* to re-establish a pluripotent state when ectopically expressed in mouse and human embryonic fibroblasts[93,94]. Importantly, these reprogrammed cells were were able to form viable chimaeras that demonstrated germline transmission[95,96]. However, the tumorigenicity resulting from the reactivation of retroviral-transduced *c-Myc* render these induced pluripotent cells (iPS) unsuitable for transplantation[96]. To this end, another study has shown that *Nanog* and *Lin28* may be used in place of *Klf4* and *c-Myc* to successfully generate human iPS cells[97].

The above findings demonstrate that the ES cell pluripotent state is maintained by a large number of transcription factors apart from Oct4, Nanog and Sox2 in auto- and co-regulatory feedback loops. In addition, pluripotency may be re-established in differentiated cells by ectopic expression of ES cell transcription factors by various combinations of *Oct4, Nanog, Sox2, Klf4, c-Myc* and *Lin28*. These results indicate that ES cell pluripotency is a complex network encompassing a large host of transcription factors. There is therefore a critical need to dissect the ES cell transcriptional pathways to achieve a greater understanding of ES cell properties, in order to gain insight into embryonic development and important knowledge to harness these cells for effective therapy.

1.4 Properties of zinc finger transcription factor Zic3

The zinc finger transcription factor Zic3 was initially identified as a potential regulator of ES cell pluripotency due to its expression profile. Zic3 is highly expressed in mouse and human ES cells[85,86], and its expression is rapidly downregulated as the cells begin to differentiate. I have investigated the role of Zic3 in the regulation of ES cell transcriptional networks in this thesis, and the following sections therefore contain a review of the properties of Zic3 and a description of its roles in embryonic development.

1.4.1 The Zic gene family

The Zic proteins (Zinc finger protein of the cerebellum) belong to the GLI superfamily of transcription factors and are vertebrate homologues of the *Drosophila* zinc finger pair-rule protein, odd-paired (opa), essential for the parasegmental division of the *Drosophila* embryo [98]. The five known mammalian *Zic* genes (Zic1 – 5) encode five tandem C_2H_2 zinc finger domains that are highly conserved across species[98-104] (Table 1, Figure 11A). The zinc finger (ZF) domain of *Zic* family genes is characterized by an unusually long intervening sequence between the two cysteine residues of the first ZF motif. In addition, the N-terminal region contains a ZOC domain conserved between vertebrate Zic and the Drosophila Odd-paired (*Opa*) proteins[98] (Figure 11A), to which transcriptional activity has been mapped[105].

Table 1. Zic family genes in human and mouse

Species	Common name	Gene	Synonyms	Accession no.	References
Homo sapiens	human	*ZIC1*		NP_003403	Yokota et al., 1996
		ZIC2		NP_009060	Brown et al., 1998
		ZIC3		NP_003404	Gebbia et al., 1997
		ZIC4		NP_115529	
		ZIC5		NP_149123	
Mus musculus	mouse	*Zic1*		NP_033599	Aruga et al., 1994
		Zic2		BAA11115	Aruga et al., 1996a
		Zic3		NP_003404	Aruga et al., 1996a
		Zic4		NP_033602	Aruga et al., 1996b
		Zic5	*opr*	BAB18579	Furushima et al., 2000

Source: Aruga, J. Mol Cell Neurosci. 2004 Jun;26(2):205-21

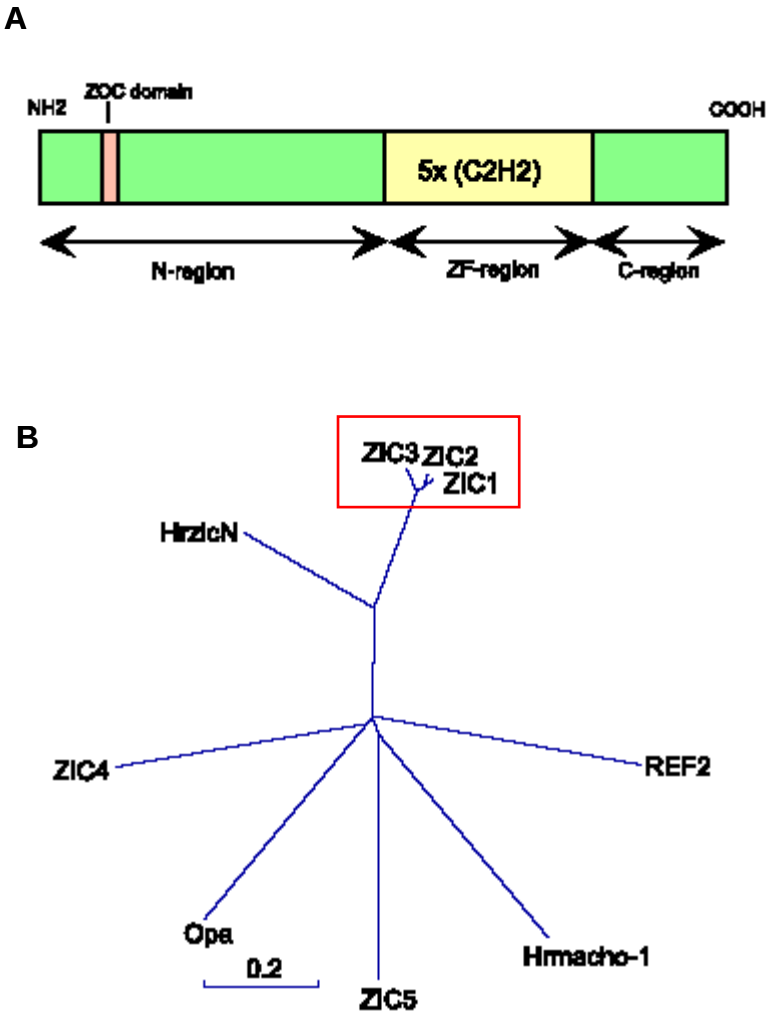

Figure 11. Structure and relationship between the Zic family proteins. (A) Structure of Zic protein family members with zinc finger (ZF) and ZOC domains indicated. (B) Phylogenic tree showing relations within the Zic family proteins, derived from a comparison of Zic family DNA sequences. The Zic1 – 3 subgroup is indicated by the red box. Adapted from: *Aruga, J. Mol Cell Neurosci. 2004 Jun;26(2):205-21*

The *Zic* genes are thought to share a common ancestral gene, and phylogenic analysis has revealed that *Zic1, Zic2* and *Zic3* are most closely related and form a subgroup among *Zic* family genes (Figure 11B). Zic3 shares overall 64% and 59% homology with Zic1 and Zic2 respectively, and this homology increases to 91% within the zinc finger domain[106] (Figure 12). Thus members of Zic family are strong candidates for redundancy in molecular signalling owing to the high degree of homology and overlapping expression observed among the members of this family. In addition, the genomic locations of gene pairs *Zic1* and *Zic4*, and *Zic*2 and *Zic5* demonstrate a head-to-head arrangement in 30-kb genomic regions, implying chromosomal duplication of an ancestral gene complex that contributes to the high complexity of *Zic* genes and the evolution of body plans during development[106].

Zic family proteins share high homology with the Gli and NKL (Gli-Kruppel zinc-finger protein) families in their zinc finger domains, where the last three C_2H_2 motifs in particular are well conserved. Gli family proteins function as transcriptional mediators of the hedgehog (Hh) signaling cascade[107,108] and are known to play critical roles in dorsoventral neural patterning[109-111]. Furthermore, characterization of the NKL/Gli protein family has shown that NKL promotes neuronal differentiation in the formation of primary neurons and other neuronal precursors[112-114]. The Zic proteins are also hypothesized to regulate genes

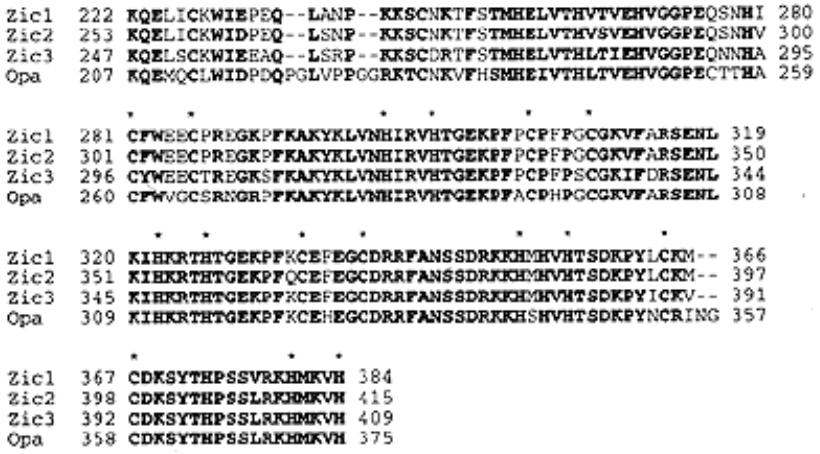

Figure 12. DNA sequence of the Zinc finger domain. The amino acid sequence alignment of zinc finger domains of the Zic, Zic2, Zic3, and Opa proteins. Bold letters indicate the conserved or similar residues among all four proteins, and the asterisks above the Zic1 line indicate the cysteine and histidine residues of a typical C2H2 motif. *Adapted from: Nakata et al., Mech Dev. 1998 Jul;75(1-2):43-51.*

involved in the hedgehog and neural development pathways, and may derive their function from these conserved zinc finger domains between the Gli and NKL families.

1.4.2 Discovery of Zic3 and its general expression domains during development

In the adult, the *Zic* genes are expressed almost exclusively in the cerebellum[98,101]. The first mammalian *Zic* family member, *Zic1,* was identified through an adult mouse cerebellum cDNA library screen[101] and *Zic3* was subsequently discovered through its shared homology of the zinc finger domain (Figure 12) by low-stringency genomic screens and cDNA cloning[98]. Although the *Zic* genes are expressed together in the adult mouse cerebellum, expression profiling revealed that they are found in partially overlapping and sometimes distinct domains during development[115,116]. The expression of *Zic3* has been identified in the mouse ectoderm and mesoderm during gastrulation, the dorsal neural tube during neurulation, and the developing brain and limb buds during organogenesis (Table 2). *Zic1* and *Zic2* expression has also been detected in these regions, and it is thought that the overlapping domains and high structural homology between Zic1, Zic2, and Zic3 may allow these proteins to function in compensatory mechanisms during development.

1.4.3 Biochemical pathways involving Zic3

The Zic and Gli family proteins physically interact through their zinc finger domains to regulate neural and skeletal patterning[117,118], and the Zic proteins are known to bind a DNA sequence highly similar to the Gli binding site, recognizing a

Table 2. Expression of Zic genes during early mouse and *xenopus* development

Zic1	*Zic2*	*Zic3*
Xenopus		
Blastula stage		
Ectoderm	Ectoderm	
Gastrula stage		
Uncommitted ectoderm	Uncommitted ectoderm	
Prospective neural plate	Prospective neural plate	Prospective neural plate
Anterior neural folds	Anterior neural folds	Anterior neural folds
Involuting mesoderm	Involuting mesoderm	Involuting mesoderm, especially organizer reg
Neurula stage		
Neural plate edges	Neural plate edges	Neural plate edges
Somites	Somites (dorsal)	
Tailbud stage		
Developing brain	Developing brain	Developing brain
Dorsal spinal cord	Dorsal spinal cord	Dorsal spinal cord
	Eye (retina)	Tail
Mouse		
Gastrulation		
	Embryonic ectoderm	Embryonic ectoderm
Embryonic mesoderm	Embryonic mesoderm	Embryonic mesoderm
Neurulation		
Dorsal neural tube	Dorsal neural tube	Dorsal neural tube
	Roof plate	
	Tailbud	Tailbud
Organogenesis		
Dorsomedial somites	Dorsomedial somites	Dorsomedial somites
Midline, developing brain	Developing brain	Developing brain
Eye (neural retina)	Eye (neural retina)	Eye (neural retina)
	Limb bud	Limb bud
Adult		
Cerebellum	Cerebellum	Cerebellum

Adapted from: Herman & El-Hodiri, Cytogenet Genome Res. 2002;99(1-4):229-35.

core motif comprising 5'-TGGGTGGTC-3'[105]. Zic/Gli interactions also facilitate the nuclear translocation of these proteins to function as transcriptional activators and repressors[103,119,120], which forms the basis of their antagonistic and synergistic features in development. As the Gli family members are well-characterized regulators of the hedgehog (HH) signaling pathway[110,121,122], it has been speculated based on interactive capacity that the Zic proteins are potential modulators of the hedgehog-mediated signaling pathway[120]. At the molecular level, Zic3 appears to function primarily as a transcriptional cofactor with the Gli proteins, with interactions occurring at the zinc-finger domain[105,120]. A Zic3 DNA-binding sequence has been identified, although its binding affinity is significantly lower than that of Gli proteins[105].

The specific pattern of *Zic3* expression during gastrulation suggests an important role in development of embryonic ectoderm and mesoderm tissue. This is supported by molecular pathways in which Zic3 has been implicated. For example the mesoderm-associated gene Brachyury induces *Zic3* expression in *Xenopus*[123], and the embryonic patterning gene Nodal is regulated by Zic3 during gastrulation through interaction with an upstream enhancer region in both mouse and *Xenopus* embryos[124]. A recent study demonstrated that Zic3 activates a 2.7kb enhancer region of Nodal at the node of the murine embryos[124]. This enhancer region, located 7.5 kb upstream of the Nodal translational start site, has been shown to be responsible for node -specific expression of Nodal in murine embryos[125]. In ectodermal development, Zic3 is a potent inducer of *Xenopus* proneural and neural crest genes[126], and is induced directly downstream of transcription factors Pbx1b and Meis1 in the *Xenopus* ectoderm[127,128].

1.5 Role of Zic3 in early embryonic development

1.5.1 The embryonic midline

The earliest reported phenotypic abnormality in *Zic3*-null mutants is a defect in establishment of the Left-Right axis[129], resulting in a congenital defect known as X-linked heterotaxy[124,130,131]. A key process in early embryonic development is the formation of positional axes. Along with the anteroposterior and dorsoventral axes, the presence of the evolutionarily conserved left-right axis is crucial for the proper morphogenesis of internal organs. Disturbances in left-right asymmetry can result in severe developmental aberrations such as (1) *situs inversus,* a complete inversion of organs relative to the L-R axis; (2) *heterotaxia* or *situs ambiguous*, the randomization of organ placement within the embryo; or (3) *isomerism*, where mirror image duplications of paired organs are observed[132].

During development, the establishment of the Left-Right (LR) axis can be described in three consecutive stages: (1) initial disruption of embryonic symmetry; (2) establishment of asymmetric gene expression; and (3) transmission of positional information to the developing organs[133]. These phases are reflected in Figure 13 and are described in greater detail in the following paragraphs.

1.5.1.1 Breaking bilateral symmetry

Left-right asymmetry is initiated in mouse embryos early in the gastrulation phase[134] (Figure 13). A series of experiments at this stage have identified an organizer, or node, as an early inducer of laterality[135,136]. The **nodal-flow model** describes a role for the monocilia at this region. Firstly, monocilia create a critical

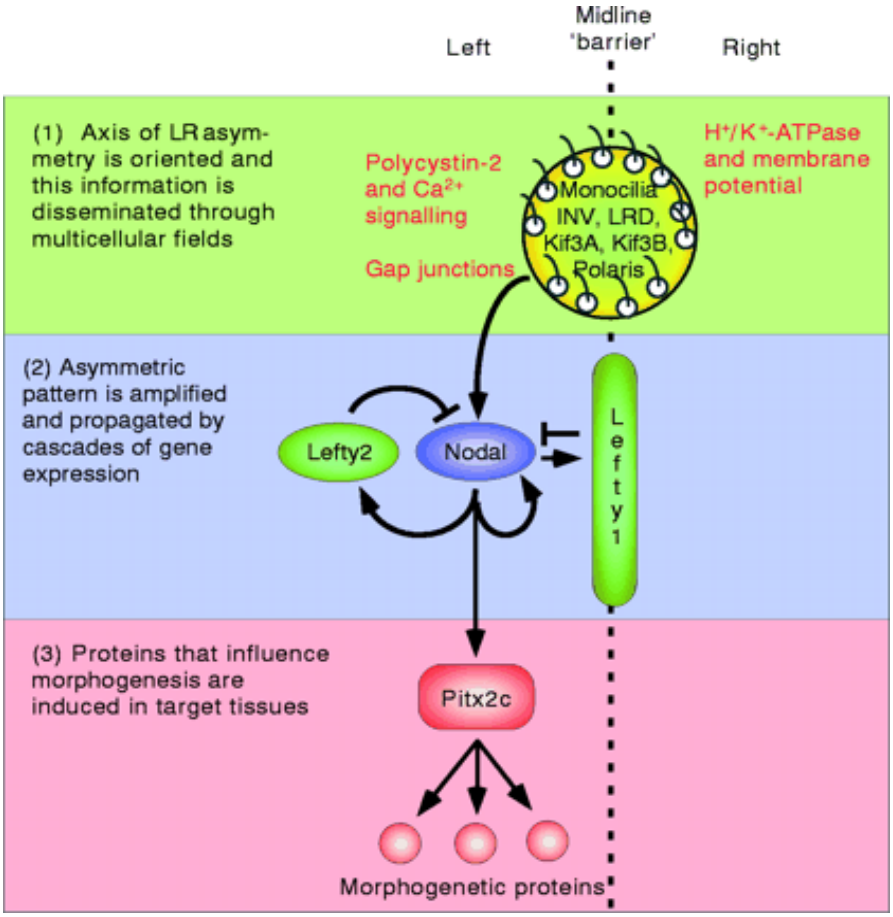

Figure 13. Determination of Left-Right asymmetry in the developing embryo. (1) Left-right asymmetry begins with an initial process that orients direction in the embryo. (2) The asymmetric pattern is propagated and amplified by cascades of gene expression that culminate in production of a Nodal protein on the left side of the embryo. (3) Nodal action is modulated by lefty proteins, in particular by constraining its action at the dorsal midline. At this stage of embryogenesis, nodal proteins regulate expression of Pitx2c and other factors that influence morphogenesis in asymmetrically developing organs (3). *Source: Mercola 2003. J Cell Sci. 2003 Aug 15;116(Pt 16):3251-7*

unidirectional flow of signalling molecules and morphogens consistently to the embryo's left[137]. The importance of this process is underscored by studies demonstrating that when cilia are rendered immotile by deletion of the left-right dynein gene (*lrd*)[138,139], or absent through mouse knockouts of the *kif3* genes[137,140], randomized laterality is observed in the resulting mutant embryos. Restoring the leftward flow in dynein (*lrd*) mutants rescued the mutant phenotype[137]. Furthermore, when an artificial rightward nodal flow was created in wildtype embryos, an inversion of laterality was observed[141]. Thus directional flow appears to be an important factor in correct handedness determination.

Based on fluid dynamics, Cartwright et al suggested that the cilia are able to direct leftward flow by capitalizing on a posterior tilt of the embryo, which impedes rightward fluid movement as the cilia stroke close to the cell surface[142]. This model has been experimentally validated, firstly through video microscopy of E8.0 mouse embryos, and secondly, through a mechanical model in which leftward velocity is shown to be proportional to the angle of tilt[143]. Further evidence from rabbit and medakafish embryos support the posterior tilt model for leftward flow that results in left-right axis development[144]. Thus recent evidence has shed some light on the role of cilia in generating unidirectional nodal flow, and demonstrates their importance in the establishment of the left-right axis during early gastrulation through facilitating the asymmetric transport of morphogens.

1.5.1.2 Asymmetric Gene Expression: Reinforcement of Left-Right Polarity

Following the break in bilateral symmetry, asymmetric gene distribution is induced in the embryo (Figure 13). At this stage, retinoic acid (RA) is a demonstrated

inducer of left side genes such as *Nodal, Lefty*, and *Pitx2*. Ectopic administration of RA resulted in misexpression of *Nodal, Lefty*, and *Pitx2* and caused abnormal situs in the developing embryo[145,146]. Conversely, the presence of RA-inhibitors caused a downregulation in the expression of *Nodal, Lefty*, and *Pitx2*[145,146]. Furthermore, studies have shown that the *cis*-regulatory region of *Nodal* contains retinoic acid response elements, and that *Lefty* expression is induced by RA in the P19 embryocarinoma cell line[125,147].

Nodal is a key morphogen that regulates specification of the left-right axis[148] (Figure 13). It has been shown to have critical functions during early murine embryogenesis and to be expressed in different tissues of the early embryo. The epiblast expression of Nodal is crucial for the establishment of the primitive streak[149,150], and the primitive endoderm expression of Nodal is important for patterning of the anterior aspects of the A-P axis[149]. Two distinct *cis*-acting regulatory elements control Nodal expression at different tissue sites: an upstream enhancer region directs node-specific expression, while an intronic enhancer controls expression in the epiblast and the visceral endoderm[125].

The importance of Nodal signalling in L-R axis formation is underscored by studies of the *lefty* genes which act as inhibitors of Nodal signalling during gastrulation[151,152], possibly through inhibition of putative Nodal receptors such as the Activin receptor, ActRIIB[152]. *Lefty* expression is found in the embryonic midline and overlaps with that of *nodal* expression (Figure 13)[151], and Lefty2 has the ability to function as a feedback inhibitor to block both *Nodal* and *Lefty2* expression on the left[153]. Significantly, *Lefty* expression has been shown to be

affected in mutant mouse backgrounds that affect organ situs[154,155]. In addition, mutations in mouse *Lefty1* lead to defects in left-right specification, including altered symmetric expression of *Lefty2* in the lateral plate mesoderm and left pulmonary isomerism[155]. The above results collectively indicate that the lefty genes are key regulators of left-right axis development.

The asymmetric expression patterns described above are dependent on an intact midline (Figure 13) consisting of two tissues - the axial mesoderm and the overlying neuroectoderm. The midline is partly derived from the node and distinguishes the left and right sides of the embryo. An intact midline is crucial for the development of L-R asymmetry, and mouse mutants with parts of the axial mesoderm disrupted, such as the notochord in *No turning* and *SIL* mice[156,157], show randomized heart looping and symmetric expression of *nodal*. These results demonstrate the importance of the midline in the maintenance of embryonic asymmetry by preventing the right lateral plate from acquiring left-sided identity.

1.5.2 Zic3 in the development of the embryonic midline

Zic3 loss-of-function mutants display both *situs ambiguous*, a partial reversal of asymmetric structures, and *situs inversus*, a complete mirror image reversal of midline organs[124,130,131]. These results imply that *Zic3* is involved in early left-right axis formation, such as the establishment of the midline node and notochord. In accordance with this, a recent study has demonstrated that *Zic3* is expressed in the node at late headfold and early somite stages of development[115]. Other groups have also shown that *Zic3* acts early in gastrulation but have

hypothesised that Zic3 affects the L-R axis following the formation of the midline by binding to and activating the Nodal promoter in the left lateral plate mesoderm[124,158].

Based on recent findings, *Zic3* expression initiates prior to gastrulation with transcript detected throughout the extra-embryonic ectoderm and within the proximal epiblast of 5.0 dpc embryos[115]. As gastrulation proceeds with the formation of the primitive streak, expression of *Zic3* is found in the primitive streak, in the wings of mesoderm of the embryonic region and in the ectoderm adjacent to the expressing mesoderm[115].

1.5.3 The *Zic3*-null mouse model

Zic3-null mice exhibit a wide spectrum of phenotypes associated with defects in left-right patterning. Fifty percent of null mice succumb to embryonic lethality over different gestational stages, and thirty percent to peri-natal lethality as a result of congenital heart defects, pulmonary isomerism and defects in the central nervous system[129]. The earliest and most profound *Zic3*-null defects have been attributed to failure in establishment of the anterior-posterior axis by the anterior visceral endoderm (AVE) prior to gastrulation[158]. In less severely affected embryos, abnormalities are observed at gastrulation in the distribution and accumulation of excess mesoderm tissue. Taken together, the defects in embryonic lethal mice demonstrate a key role for Zic3 in early embryonic patterning that encompasses anterior visceral endoderm formation, initiation of gastrulation, and primitive streak morphogenesis[158].

Laterality defects were detected in 6 out of 55 heterozygous *Zic3* female mice examined[129], indicating that both complete and partial deficiency of the X-linked *Zic3* gene result in disruption of laterality. Interestingly, a higher proportion of *Zic3* null males died *in utero* whereas *Zic3* null females died within the perinatal period, suggesting a sex-limited effect. The majority of perinatal deaths were attributable to congenital heart defects (CHD), suggesting that *Zic3* null females may be more susceptible to this defect[129]. These results indicate a role for environmental factors, potentially in combination with genetic modifying loci encompassing modifier genes and gene threshold effects, in contributing to the laterality phenotype observed in *Zic3* mutants.

The varying degrees of severity in failure to complete gastrulation displayed by *Zic3*-null mice may be attributed to compensatory mechanisms in developing embryos, as indicated by the overlapping domains of expression between Zic family, as indicated by the partially overlapping expression patterns exhibited by members of the *Zic* gene family[115,116] (Table 2). Similar to *Zic3*-null mice, previous studies in *Zic1*-deficient mice and *Zic2* knockdown mice have reported skeletal and CNS anomalies[99,159]. *Zic3* shares overall 64 and 59% homology with *Zic1* and *Zic2*, respectively, and this homology increases to 91% within the zinc finger domain. Thus members of *Zic* family are strong candidates for redundancy in molecular signaling during development.

By characterizing the early embryonic lethality of *Zic3*-null mouse embryos, a recent study has revealed a new function for Zic3 during gastrulation at a stage earlier than left-right patterning[158]. An examination of the most severely affected

Zic3-deficient embryos revealed that these mutants either fail to initiate gastrulation or undergo an initial specification of the mesodermal cell population with failure to progress[158]. It was found that *Zic3*-null embryos showed abnormalities in anterior visceral endoderm (AVE). This abnormality was reflected in the inappropriate distal localization of AVE markers such as *Cer-1* and in the absence of *Hex* expression at day 6.5 to day 7.0 when a global anterior-ward rotation of the visceral endoderm should have occurred prior to streak formation[158,160]. This rotation is critical for the conversion of the proximal-distal (P-D) polarity to the anterior-posterior (A-P) axis of the murine embryo.

It has been suggested that while the extraembryonic ectoderm seems to signal to the proximal epiblast to induce expression of proximal-posterior genes, the AVE counters this activity by repressing expression of these genes in the underlying epiblast so as to prime it for anterior patterning[160]. Thus, this failure to undergo a P-D to A-P rotation appears to be the main cause for the *Zic3*-null embryos to exhibit failure to gastrulate, establish the primitive streak, and to form mesoderm[158].

1.5.4 Zic3 mutations result in X-linked heterotaxy

A large number of congenital disorders arise from defects in embryonic midline development[129,161-164], indicating that the midline tissue of the vertebrate embryo plays a critical role in its development. In humans, Zic3 mutations are associated with X-linked heterotaxy, a disorder characterized by disruptions in embryonic laterality and midline developmental field defect[103]. In addition, clinical

abnormalities resulting from X-linked heterotaxy manifest in organs such as the spleen (asplenia or polysplenia) and lungs (bilateral trilobed or bilobed lungs), and in complex cardiovascular malformations with cardiac looping abnormalities[124,165].

Zic3-associated X-linked heterotaxy is a recessive disorder of variable clinical expression that predominantly affects males. More rarely, heterozygous females with isolated congenital heart defect are reported[119,166]. In females, functional nullisomy of the Zic3 protein can occur as a result of constitutional X-autosome translocations with one breakpoint in the *Zic3* region, leading to gene disruptions or defects arising from its ectopic position, as well as preferential inactivation of the normal X-chromosome[166].

The locus for *Zic3* in humans was initially mapped to Xq26.2 by linkage analysis in a single family and by detection of a deletion in an unrelated *situs ambiguus* male[167,168]. From this chromosomal region, *Zic3* was positionally cloned[103]. The *Zic3* mutations that gave rise to *situs ambiguus* included one frameshift, two missense and two nonsense mutations. A recent study has further established that X-linked heterotaxy in humans results from several *Zic3* mutations that render the protein unstable and absent in cells, or incapable of nuclear localization where its transcriptional effect is exerted[103,119].

1.6 Role of Zic3 in neural development

Zic3 is involved in a spectrum of processes related to neural development, from the establishment of the neuroectoderm, to the patterning of the dorsal neural tube, and finally, the development of mature dorsal neurons. These phases are summarized in Figure 14 and are described in detail in the following paragraphs.

At the beginning of gastrulation when the neuroectoderm is being established, *Zic3* expression is upregulated near the dorsal lip of the blastopore, where the dosalizing center secretes a neural inducer. As gastrulation proceeds, *Zic3* expression is extended anteriorly and is subsequently found at the border of the neural plate, where it is involved in generating dorsal neural tissue and neural crest tissue[126,169]. The expression of *Zic3* at this stage is negatively regulated by Bmp, as indicated by an increase in *Zic3* expression domain when a Bmp antagonist, noggin, or a dominant-negative Bmp receptor is overexpressed[126]. In accordance with this, it has been observed during neuroectodermal differentiation that *Zic3* is expressed by ectoderm cells only when Bmp signals are blocked by a secreted Bmp-antagonizing neural inducer[170]. Furthermore, it has been shown that the anti-neural protein, Msx1, represses *Zic3* expression through dominant negative Bmp receptors[171]. Conversely, a dominant-negative form of Msx1 was able to trigger the expression of *Zic3*[172], indicating that the inhibition of *Zic3* expression by Bmp is mediated in part by Msx1. These results collectively indicate that signalling of Bmp is essential for the proper establishment of *Zic3* expression in the ectoderm (Figure 14; early phase).

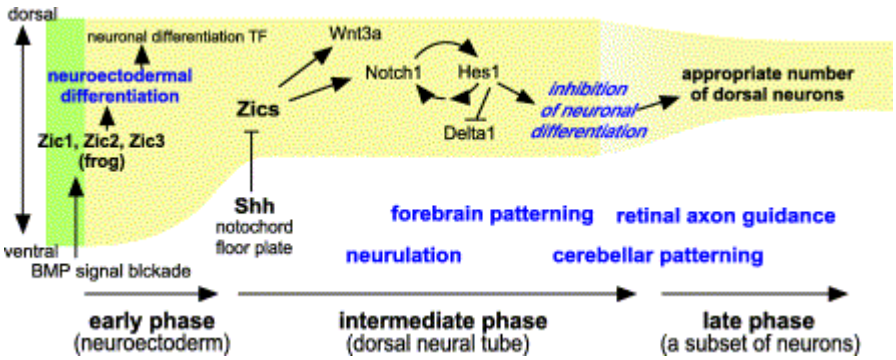

Figure 14. The role of *Zic* genes in neural development. The dorsoventral axis in neural tissue is reflected on the y-axis, and the developmental stages are shown in the x-axis. The green area indicates the region expressing *Zic*. Blue letters indicate major roles of Zic genes in neural development. *Source: Aruga, J. Mol Cell Neurosci. 2004 Jun;26(2):205-21*

The expression of *Zic3* is found in the dorsal ectoderm at the late blastula stage just prior to neuroectodermal differentiation[126]. Thus *Zic3* expression is detected earlier than most proneural genes. A study has shown that overexpression of *Zic3* at this stage resulted in an expansion of the resulting neuroectoderm[126]. In addition, ectopic expression of *Zic3* in animal cap explants induced neural crest and proneural markers. Taken together, the above data indicate that *Zic3* is a primary regulator both of neural and neural crest development, and is an inducer of pro-neural transcription factors that activate the neural differentiation program.

An alternative model for the function of Zic3 in neuroectodermal fate determination has been proposed in the context of calcium signalling. Localized calcium-expressing domains are found exclusively in the anterior dorsal part of the ectoderm, and these domains have been shown to mediate the choice between epidermal and neural tissue fates[173]. When ectodermal cell explants were treated with a voltage-sensitive calcium channel inhibitor or by a calcium-chelating reagent, *Zic3* expression was significantly reduced[174,175], indicating that *Zic3* is upregulated by the presence of calcium. Further investigation revealed an early calcium sensitive target gene, expressed in neural territories, known as arginine methyltransferase, was shown to specifically induce the expression of *Zic3*[175,176]. Arginine methyltransferase is thought to play an instructive role in the embryonic choice of determination between epidermal and neural fate[173], and its ability to regulate the expression of *Zic3* may represent another pathway by which intracellular calcium suppresses the epidermal fate and activates the neural fate[177].

Zic3 is also known to be an important regulator of neurulation (Figure 14; intermediate phase). Neural tube defects are commonly observed in the hindbrain region of *Zic3* mutant mice, in domains where *Zic3* expression is normally found in wildtype mice[106,129,178]. In addition, *Zic3*-deficient mice show hypoplastic changes in the cerebellar anterior lobe, indicating that Zic3 is involved in cerebellar patterning[106].

Zic3 is also known to regulate the process of axon targeting within the retina in the developing visual system[179] (Figure 14; late phase). During this phase, radially-positioned ganglion cell axons begin to project toward the optic disc, a small opening in the center of the retina. An expression assay determined that *Zic3* is found in a periphery-high, center-low gradient in the developing retina. During retinal cell differentiation and axonogenesis, *Zic3* expression correspondingly recedes toward the periphery of the retina[179]. Interestingly, disruption of the *Zic3* expression gradient during this process resulted in axons being misrouted to the sub-retinal space on the photoreceptor side of the retina. In contrast, misexpression of Zic3 did not affect retinal neurogenesis or lamination, and it was shown instead that the axonal mis-projection phenotype was the result of an inhibitory factor regulated by Zic3. These results suggest that Zic3 may regulate a currently unknown pathway influencing intra-retinal axon pathfinding[179]. In summary, Zic3 has been shown to regulate extensive processes in the establishment and patterning of neural tissue, and is therefore a critical factor in embryonic ectoderm development and neurogenesis.

1.7 Experimental approach and study rationale

Zic3 is preferentially expressed in the pluripotent state and has recently been identified as a target of Oct4, Nanog, and Sox2 in ES cells[19,20,179 85,86]. However, the detailed molecular networks regulated by Zic3 to confer its properties on ES cells remain unknown. Therefore I set out to address the following questions in this thesis:

1. How do Oct4, Nanog, and Sox2 regulate the expression of *Zic3*, and what results from this interaction?
2. What phenotype results from a *Zic3* loss-of-function, and what can be inferred about the role of Zic3 in the ES cells?
3. Does Zic3 interact with ES cell-related proteins to regulate pluripotency?
4. What are the targets regulated by Zic3 in ES cells, and do these genes reveal the networks that Zic3 controls to maintain pluripotency?
5. Does Zic3 repress lineage-specific genes in ES cells, and are these genes related to the established functions of Zic3 in development?

To understand the dynamics of Zic3-governed transcriptional networks in ES cells, I used a combination of gene expression analysis, *Zic3* gain- and loss-of-function experiments, co-immunoprecipitation for interacting partners of Zic3, chromatin-immunoprecipitation to identify Zic3-regulated targets, and functional annotation of these targets to gain deeper insight into Zic3-regulated processes and to establish the Zic3 regulatory network in ES cells (Figure 15). The results of these analyses are presented and discussed in Chapters 3 to 6.

A detailed knowledge of ES cell transcriptional circuitry may contribute to a more comprehensive understanding of embryonic development, and is critical for the realization of ES cell therapeutic potential. The critical need to dissect their transcriptional networks is underscored by their potential to yield critical insights into genetic mechanisms at the earliest stages of embryo development and to provide significant inroads into the properties ES cell unlimited growth and differentiation potential that will render them therapeutically useful.

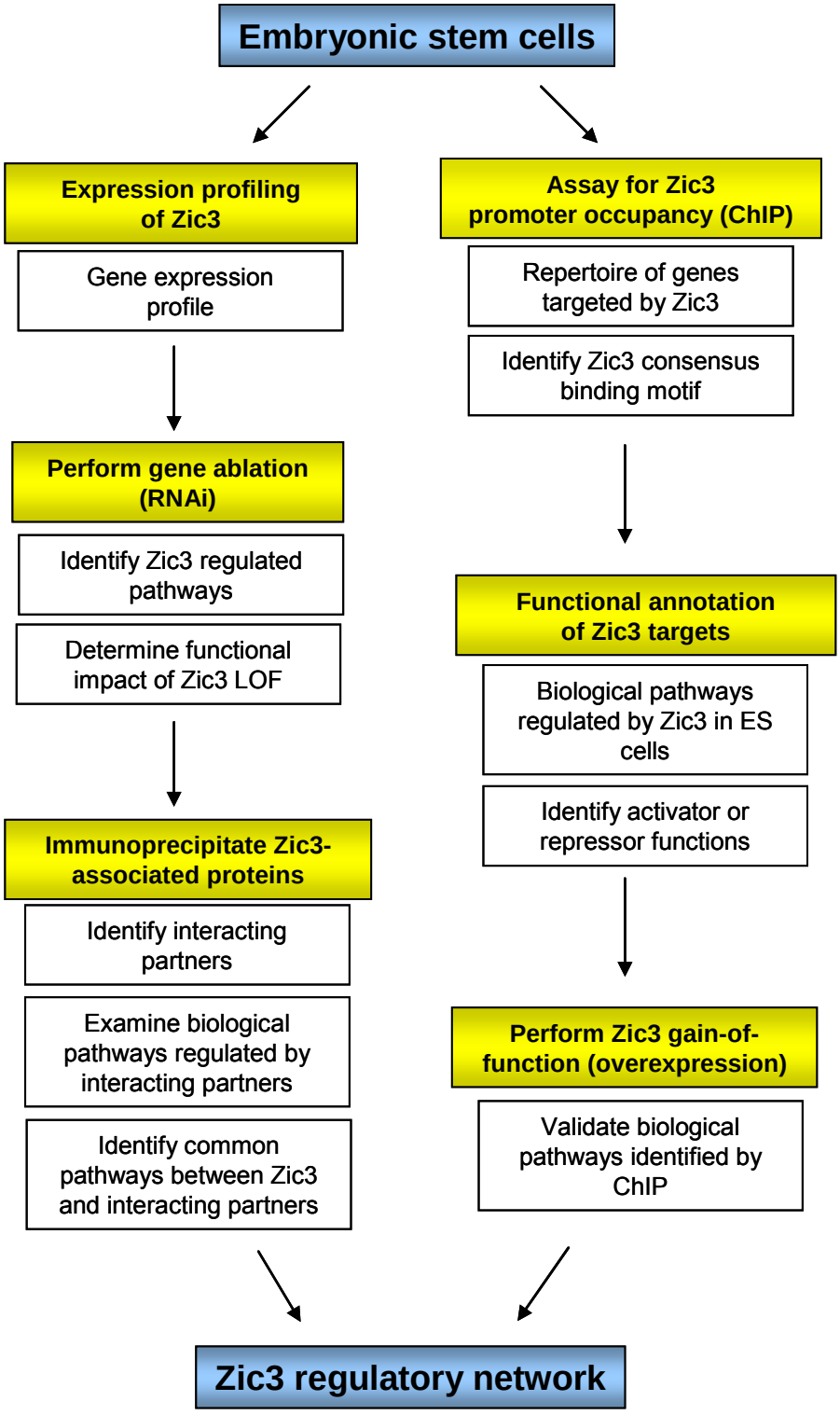

Figure 15. Experimental approach for establishing the transcriptional network of Zic3 in ES cells. Zic3 gene expression profiling, depletion of Zic3 gene expression, co-immunoprecipitation of protein complexes, chromatin-immunoprecipitation, functional annotation of Zic3 gene targets, and Zic3 gain-of-function experiments were performed to construct the Zic3 transcriptional network.

CHAPTER 2:

Methods & Materials

2.1 Molecular biology techniques

2.1.1 Cloning

The sub-cloning of DNA fragments into vectors was achieved by restriction enzyme digestion, gel purification of digested DNA, and T4 ligase treatment to yield the final construct. Restriction digests were preformed overnight at 37°C according to manufacturers' instructions (New England Biolabs). The following day, digested DNA was resolved on 1% - 1.5% agarose gels in TAE buffer, and the desired fragments were visualized under UV lighting and excised from the gel. The DNA fragments were released from agarose matrix using the Qiagen gel extraction kit according to manufacturer's instructions. The concentration of the recovered DNA was quantified by UV absorbance using the nanodrop instrument, and ligations were performed at 5:1 (insert:vector) molar ratio in 20 μl reactions containing1U of T4 DNA ligase in 1 x T4 ligase buffer (Roche) at 16°C overnight.

2.1.2 Transformation of chemically competent cells

For transformation of ligated plasmids, a 50μl aliquot of One-Shot Top10 chemically competent *E.coli* cells (Invitrogen) was thawed on ice. Approximately 10ng of ligation reaction was added to the thawed cells and gently mixed followed by incubation on ice for 30 minutes. Transformation was induced by heat-shock treatment at 42ºC for 1 minute. The cells were cooled on ice for 2 minutes, and 200μl of nutrient-rich LB-SOC was then added to the tube for incubation at 37ºC for 1 hour in a bacterial shaker. Following incubation, 50 to 300ul of the culture was plated on LB-agar plates containing the appropriate antibiotic selection, and the plates were placed in an incubator at 37ºC overnight to allow growth of bacterial colonies.

2.1.3 PCR analysis of transformants

Bacterial colonies were screened for positive ligation events as follows: 20 µl sterile PBS for inoculated with a single colony to serve as a PCR template. PCR reactions were carried out in 25 µl volumes comprising 1 x PCR buffer w/o $MgCl_2$ (ProMega), 2 mM $MgCl_2$, 0.2mM dNTPs, 0.5 µM of each forward and reverse primer, 1 U Taq Polymerase in Buffer B (ProMega), and 5 µl PBS containing template DNA. The PCR conditions were as follows: 95°C for 3 minutes, followed by 32 cycles of 95°C for 30s, 52°C for 30s, 72°C for 1 min 30s, and finally, a single cycle of 72°C for 7 minutes before holding at 4°C. PCR products were resolved on 1% agarose gels for 40 minutes at 100V to check for correct insert size.

2.1.4 Isolation of plasmid DNA from bacteria

Bacterial colonies containing positive ligation events were expanded as follows: 5 ml LB medium with appropriate antibiotic selection was inoculated for overnight culture at 37ºC. The overnight cell suspensions were centrifuged at max speed for 15 minutes to pellet bacteria. The bacterial cells were then lysed and plasmid DNA purified using the Qiagen miniprep kit according to manufacturer's instructions. The DNA was eluted in 30 – 50 µl dH2O and quantified by nanodrop to ensure a final concentration in the range of 200 – 1000 µg/ul.

2.1.5 Preparation of bacterial stocks

Bacterial stocks of successful transformation events were prepared in 33.3% sterile glycerol. The LB-glycerol suspension was vortexed to ensure thorough mixing, cooled on ice for 1 hour, and then placed at -80°C for long term storage.

2.1.6 Isolation of genomic DNA from cell lines

Confluent cell cultures were rinsed thrice with PBS and then gently scraped for release from adherent culture dishes. The cells were pelleted for 5 minutes at 500 rpm and then lysed in 3 ml DNA buffer (10 mM Tris-HCl at pH 8.0, 0.1 M EDTA, 0.5% SDS, and 100 μg/ml proteinase K) and incubated overnight at 45°C with gentle agitation. The following day, the cell lysate was treated thrice with Chloroform/ Isoamyl alcohol (24:1) as follows: An equal volume of Chloroform/ Isoamyl alcohol was added to the lysate, mixed thoroughly and centrifuged at 4°C for 10 minutes at maximum speed. The resulting supernatant was transferred to a fresh eppendorf tube and the above procedure was repeated. Following the third extraction, the supernatant was transferred into a fresh 50 ml falcon tube containing 1/10 volume 3 M sodium acetate (pH 5.2) and 3 volumes 100% isopropanol. The tube was gently inverted to allow precipitation of DNA which was then transferred into a fresh 50 ml falcon tube containing 30 ml of 70% ethanol. The DNA was rinsed in ethanol for 2 hours, then centrifuged at 4°C for 20 min at maximum speed. The DNA pellet was dried in a SpeedVac for 5 minutes and then resuspended in 1 ml sterile dH_20 for 1 hour at 37°C. The resulting genomic DNA was quantified to ensure concentrations above 1000 ng/ul, and then resolved on 1% agarose gels to check for DNA quality.

2.2 Cell culture

2.2.1 Mouse ES cell culture

Feeder-free E14 mouse ES cells were maintained on 0.1% gelatin coated dishes in E14 proliferative medium containing DMEM/15% ES FBS (Gibco), 0.1 mM

MEM non-essential amino acids (Gibco), 2 mM L-glutamine (Gibco), 0.1 mM β-mercaptoethanol (Gibco), and CHO-LIF (1,000 U/ml). The cells were passaged every 2 days with the following procedure: Each dish was rinsed twice with 1x PBS solution (Gibco) and then incubated in 3 ml 0.05% Trypsin (Gibco) for 3 minutes at 37°C to allow detachment of cells from the culture surface. The trypsin-treated cells were diluted with 7 ml E14 culture media, pelleted in a centrifuge for 5 min/500rpm, and then re-suspended in 5 ml fresh E14 culture media. The cells were then triturated to achieve a single cell suspension, and seeded in gelatin-coated plates at a density of 4.0×10^6 cells per 10 cm^2 dish.

Mouse ES cells cultured on mouse embryonic fibroblast (MEF) feeder layers were maintained in the proliferative medium described above, with the exception of CHO-LIF. The mouse ES cells were passaged every 2 days as described above and seeded at a density of 3.0×10^6 cells per 10 cm^2 dish. One day prior to passaging, 2.5×10^6 inactivated Balb/c MEFs (ref. section 2.2.3) were seeded on gelatin-coated plates and allowed to adhere to the plate surface overnight at 37°C. All cultures were maintained in an incubator at 37°C with 5% CO2.

2.2.2 Human ES cell culture

Feeder-free undifferentiated HuES9 human ES cells were maintained on matrigel-coated dishes in conditioned medium containing Knockout DMEM/10% serum replacement (Gibco), 0.1 mM MEM non-essential amino acids (Gibco), 1 mM L-glutamine (Gibco), 0.1 mM β-mercaptoethanol (Gibco), 8% plasmanate (NUH pharmacy), 12 ng/ml LIF, and 10 ng/ml human recombinant Basic Fibroblast Growth Factor (bFGF; Gibco). Conditioned media was obtained by

culturing mouse embryonic fibroblast (MEF) cells with HuES9 media. The media was collected at 24 hour intervals, filter sterilized and further supplemented with 8 ng/ml bFGF for HuES9 cell culture.

2.2.3 Isolation, expansion, and mitotic inactivation of MEF cells

Pregnant female Balb/C mice were sacrificed at day 13 post-coitum by cervical dislocation. The mouse abdomens were swabbed once with 70% Ethanol and peritoneal walls were dissected to expose the uterine horns, which were removed and placed in a 10 cm^2 dish. The uterine horns were rinsed thrice with 10 ml PBS (Gibco #14190-169) without bivalent cations. The embryos were then released from the embryonic sac and subsequently separated from the placenta and associated membranes. Dark red visceral tissue was removed and each embryo was rinsed 3 x 10 ml PBS in a fresh Petri dish.

The embryos were transferred into a new Petri dish containing a minimal amount of PBS, and were finely minced with two pairs of forceps. The fragmented tissue was placed in 2 ml Trypsin-EDTA (Gibco) per embryo, then further minced and subsequently incubated at 37°C for 15 min with gentle agitation. The Trypsin-EDTA was neutralized in a fresh 50ml conical tube containing 20 ml MEF culture medium, prepared as follows: DMEM supplemented with 10% FBS, 1% L-glutamine (v/v) and 1% Pen-step (v/v). The larger pieces of tissue were briefly allowed to settle, and the supernatant containing MEF cells was then pelleted at 500 rpm for 5 mins at room temperature. The MEF cells were then resuspended in fresh culture media warmed to 37°C, and plated at a density of 1 embryo per 10 cm^2 dish (Passage 0).

The MEF primary cultures were typically confluent within 2 days. Confluent dishes were trypsinized according to the procedure described for HEK293T cells, and re-seeded at a density of 1:5. The cells were expanded to Passage 5 and then mitotically inactivated by treatment with Mitomycin-C at 10 μg/ml for 2 hours at 37°C. The inactivated cells were then rinsed twice with PBS, trypsinzed as described above, and then resuspended in freezing media (ref. section 2.2.5) at a density of 2.5 x 10^6 cells per cryotube.

2.2.4 Maintenance of HEK293T cells

HEK 293T cells were cultured in DMEM supplemented with 10% fetal bovine serum (Gibco-Invitrogen) and 2 mM L-glutamine (Gibco-Invitrogen), and maintained in an incubator at 37°C with 5% CO2. The cells were passaged every 4 days with the following procedure: Each dish was rinsed twice with 1x PBS solution (Gibco) and incubated in 3 ml 0.25% Trypsin (Gibco) for 3 minutes at 37°C. The cells were then diluted with 7 ml 293T culture media, pelleted in a centrifuge for 5 min/500rpm, and re-suspended in 5 ml fresh 293T culture media. The cells were triturated to achieve a single cell suspension, and seeded in 10 cm^2 dishes at a density of 1.0 x 10^6 cells.

2.2.5 Cryopreservation of cell lines

Confluent cell cultures were trypsinised as described above and centrifuged for 5 minutes at 500rpm. The cells were resuspended in freezing media (70% DMEM supplemented with 20% FCS and 10% dimethyl sulphoxide) and then transferred into Nunc cryotubes at 1 ml per vial. The cryotubes were placed at -80°C

overnight in Mr Frosty containers buffered with isopropyl alcohol and then transferred to a liquid nitrogen tank the following day for long-term storage.

2.2.6 Thawing of cell lines

Frozen cryotubes were retrieved from liquid nitrogen tanks and placed immediately into a 37°C waterbath. The cells were rapidly thawed and then transferred into 10 ml of pre-warmed culture media. The cell suspension was pelleted for 5 minutes at 500 rpm, then gently resuspended in culture media and plated in 10 cm^2 tissue culture dishes to allow for overnight adhesion of cells to the vessel surface.

2.3 ES Cell-based assays

2.3.1 RNA interference (siRNA)

RNA interference (RNAi) experiments were performed with Dharmacon siGENOME SMARTpool reagents against human or mouse *Zic3*. The Dharmacon si*CONTROL* nontargeting siRNA pool was used as a negative control. Mouse ES cells were transfected according to manufacturer's instructions in 12-well plates at a density of 2 x 10^5 cells per well. Re-transfections were performed on pre-adherent cells at 48-hour intervals, and RNA expression analysis was performed on Day 5 samples. Human ES cells were transfected in 12-well plates with 2 x 10^5 cells per well in suspension. Subsequent re-transfections were performed on adherent cells at 24-hour intervals and RNA was harvested for analysis at Day 5.

2.3.2 RNA interference (shRNA)

The Oct4, Nanog, Sox2 and Zic3 shRNA sequences were designed according to criteria by Ui-tei et al. [180]. and Reynolds et al. [181], and cloned into the pSUPER.puro or pSUPER.neo-GFP shRNA vectors (Oligoengine) as per manufacturer's instructions. Details of the shRNA sequences are listed in Table 3. For shRNA experiments, E14 cells were seeded at a density of 4 x 10^5 cells per well in 6-well plates 1 day prior to transfection. The following day, the cells were transfected with 2.0 μg of shRNA construct each. Puromycin or neomycin selection was introduced 1 day post-transfection at 1.0 μg/ml, and maintained for 3 days prior to RNA isolation. The ES cells were maintained in mouse ES cell culture medium at all times.

2.3.3 Rescue of RNAi knockdown

The *Zic3* open reading frame (ORF; NM_009575) was cloned from reverse-transcribed cDNA from mouse embryonic stem cells, using the primers indicated in Table 4A. The PCR product was subsequently cloned into an overexpression construct downstream of a cytomegarovirus/chicken β-actin (CAG) promoter, which is known to drive efficient episomal expression in ES cells[69]. The RNAi-immune *Zic3* ORF R3M was generated from this construct using the QuikChange site-directed mutagenesis kit (Strategene) as per manufacturer's protocol with the primers shown in Table 4A. To perform the rescue experiments, 4 x 10^5 mouse ES cells were seeded per well in 6-well plates, and transfected according to the scheme in Table 4B. Hygromycin (1.0μg/ml) was introduced 1 day post-transfection for selection of transfected cells, and ES cell culture media containing hygromycin was refreshed daily until the cells were harvested for analysis.

Table 3. shRNA sequences for pSUPER vector

Name	Sequence
Nanog-SENSE	GATCCCCGAACTATTCTTGCTTACAATTCAAGAGATTGTAAGCAAGAATAGTTCTTTTTA
Nanog-ANTI-SENSE	AGCTTAAAAAGAACTATTCTTGCTTACAATCTCTTGAATTGTAAGCAAGAATAGTTCGGG
Sox2-SENSE	GATCCCCGAAGGAGCACCCGGATTATTTCAAGAGAATAATCCGGGTGCTCCTTCTTTTTA
Sox2-ANTI-SENSE	AGCTTAAAAAGAAGGAGCACCCGGATTATTCTCTTGAAATAATCCGGGTGCTCCTTCGGG
Zic3-SENSE	GATCCCCGAATTCGAAGGCTGTGACATTCAAGAGATGTCACAGCCTTCGAATTCTTTTTA
Zic3-ANTI-SENSE	AGCTTAAAAAGAATTCGAAGGCTGTGACATCTCTTGAATGTCACAGCCTTCGAATTCGGG
Oct4-SENSE	GATCCCCGAAGGATGTGGTTCGAGTATTCAAGAGATACTCGAACCACATCCTTCTTTTTA
Oct4-ANTI-SENSE	AGCTTAAAAAGAAGGATGTGGTTCGAGTATCTCTTGAATACTCGAACCACATCCTTCGGG
Zic3-SENSE	GATCCCCGTGCGCAGTTCCCTAACTATTCAAGAGATAGTTAGGGAACTGCGCACTTTTTA
Zic3-ANTI-SENSE	AGCTTAAAAAGTGCGCAGTTCCCTAACTATCTCTTGAATAGTTAGGGAACTGCGCACGGG

Table 4a. List of primers for the cloning Zic3 and Zic3-RNAi immune genes

Description	Primers	Set
Zic3 ORF	Forward 5'-AACACCagatctATGACGATGCTCCTGGACGGAGGCC-3' Reverse 5' -TTTTGGacgcgtTCAGACGTACCATTCGTTAAAATTG-3'.	~
Zic3 ORF R3M (RNAi immune)	Forward 5'-AACACCagatctATGACGATGCTCCTGGACGGAGGCC-3' Reverse, 5'-CTGTTGGCAAACCGTCGATCGCATCCCTCAAATTCACATT-3'	1
	Forward, 5' -AATGTGAATTTGAGGGATGCGATCGACGGTTTGCCAACAG-3' Reverse, 5'- TTTTGGacgcgtTCAGACGTACCATTCGTTAAAATTG-3'	2
	Forward, 5' - AACACCagatctATGACGATGCTCCTGGACGGAGGCC-3' Reverse, 5'- TTTTGGacgcgtTCAGACGTACCATTCGTTAAAATTG-3'	3

Table 4b. Transfection scheme for Zic3 Rescue Experiments

Experiment	Zic3 construct / 1.0 µg	RNAi construct / 1.0 µg
1	pCAGIhyg	pSUPERpuro-GFP (Non-specific control)
2	pCAGIhyg	pSUPER.puro-Zic3
3	pCAGIhyg-Zic3 R3M	pSUPER.puro-Zic3

2.3.4 Secondary ES-colony replating assay

ES cells were transfected with *Zic3*- or empty pSUPER shRNA constructs and selected 24 hours later with puromycin at 1.0 μg/ml over four days. At the end of four days few cells remained in the untransfected control wells indicating that selection was effective. The surviving cells were trypsinized as described in Section 2.2.1 and resuspended in E14 medium without LIF. Ten- or twenty-thousand cells were plated onto mouse feeder layers in six-well plates for secondary ES cell-colony formation. After seven days, emerging colonies were stained with the Wright-Giemsa stain (Sigma) according to manufacturer's instructions. Three biological replicates were performed for each experiment. The extent of differentiated colonies was defined as the percentage of unstained colonies out of the total number of colonies in the well.

2.3.5 Reprogramming assays

2.3.5.1 Viral packaging of reprogramming factors

One day prior to transfection, 8 x 10^6 Plat-E viral packing cells[182] were seeded per 10cm^2 dish, and the cells were allowed to adhere overnight at 37°C. The following day, each plate of 10cm^2 Plat-E cells was transfected with 9μg of pMXs plasmids containing *Oct4, Sox2, Klf4, c-Myc* or *Zic3*, using the Fugene 6 system (Roche) according to manufacturer's specifications. Briefly, 27μl of Fugene 6 was incubated with DMEM for 5 minutes at room temperature. pMXs DNA was then added dropwise, and gently mixed and further incubated for 15 minutes at room temperature. Following incubation, the DNA/Fugene 6 complex was added dropwise to the Plat-E cells and allowed to transfect overnight at 37°C. The transfection mix was aspirated the following day and replaced by Plat-E culture

media containing DMEM supplemented with 10% FBS, 50 units per 50 µg/ml pen/strep, 1 µg/ml puromycin (Sigma), and 100 µg/ml of blasticidin S (Funakoshi). Twenty-four hours later, the retrovirus-containing media was harvested, filter-sterilized, and supplemented with polybrene (4 mg/ml) to increase efficiency of retroviral infection.

2.3.5.2 Viral infection of fibroblast cells

Mouse embryonic fibroblast (MEF) cells were isolated from mouse embryos, expanded to Passage 6, and inactivated as described in Section 2.2.3. These inactivated MEF cells were plated as a feeder layer for the reprogramming experiment, at a density of 2.5×10^6 per gelatin-coated 10 cm^2 dish. The following day, Passage 3 balb/c fibroblasts were seeded on the inactivated feeder layer at a density of 8×10^5 per dish, and allowed to adhere overnight. Twenty-four hours later, fresh retroviral-containing media (ref section 2.3.5.2) for each reprogramming factor was mixed in equal parts to a total volume of 10 ml, and then added to the fibroblast cultures for overnight infection at 37°C. The cells were supplied daily with fresh Plat-E media (Section 2.3.5.1), and allowed to grow for 2 to 3 weeks. ES-like colonies arising from the infections were treated with the Wright-Giemsa stain (Sigma) according to manufacturer's instructions, and positive colonies were counted to assess the effectiveness of the reprogramming assay.

2.4 Establishment of clonal cell lines

2.4.1 Clonal Zic3 knockdown lines

Clonal Zic3 knockdown lines were established by transfection of shRNA constructs as described in Section 2.3.2. The Zic3 knockdown and vector control colonies were picked after 7 days of puromycin selection (1.0 µg/ml). Colonies were dissociated into single cell suspensions by treatment with 0.05% Trypsin (Gibco) and plated on puromycin-resistant mitomycin-inactivated DR4 MEFs (ATCC). In total, 15 Zic3 clonal knockdown and 7 vector control lines were established and maintained under constant puromycin selection. The lines analyzed in this thesis were maintained feeder-free in ES cell proliferative media on 0.1% gelatin-coated dishes over a period of 8 passages.

2.4.2 Clonal Zic3-inducible ES cells

The Ainv18 cell line (gift of George Daley, Harvard Medical School, Boston, MA) is an E14 mouse ES line modified for targeted gene insertion downstream of a doxycycline-responsive promoter [183]. The *Zic3* transgene was PCR-amplified from a mouse cDNA library and subcloned into the KpnI/XbaI sites of the pLox-N-tag-HA vector (George Daley, Harvard Medical School, Boston, MA) with the following primers, restriction sites indicated in uppercase: Forward 5'-tat-tat-GGT-ACC-tac-gat-gct-cct-gga-cgg-ag-3' and Reverse 5'-tcg-gca-TCT-AGA-tca-gac-gta-cca-ttc-gtt-aaa-att-g-3'. An additional nucleotide was inserted in the forward primer to allow in-frame processing of the Zic3 insert with the N-terminal HA tags.

For targeted insertion at the HPRT locus, 20 μg each of pLox-N-tag-HA-Zic3 and pSALK-Cre were transfected with Lipofectamine 2000 (Invitrogen, Carlsbad, CA) into $6x10^5$ AINV18 cells seeded in $10cm^2$ dishes. For derivation of Ainv18-*Zic3* clonal lines, mouse ESC medium was supplemented with 350 μg/ml G418 solution (Invitrogen) 24 hours after transfection and maintained for 14 days. Colonies arising from G418 selection were individually picked and expanded on neomycin-resistant MEFs. Site-specific integration was confirmed by PCR analysis with the following primers: LoxinF 5'-cta-gat-ctc-gaa-gga-tct-gga-g-3' and LoxinR 5'–ata-ctt-tct-cgg-cag-gag-ca-3'.

To induce overexpression, AINV18-*Zic3* cells were treated with 1.0 μg/mL doxycycline in mouse ESC medium. Protein was harvested to test and confirm the efficacy of regulation by doxycycline.

2.5 ES cell differentiation protocols

2.5.1 Retinoic acid differentiation

Mouse ES cells were cultured in LIF-deficient ES cell medium with all-*trans* retinoic acid (RA) at 100 nM. Retinoic acid stock powder was dissolved in DMSO to give a concentration of 0.1 M and stored at -80°C. For each differentiation experiment, an aliquot of 0.1 M RA solution was thawed and diluted 1:1000 in 100% EtOH to yield a 0.1 mM solution, which was further diluted 1:1000 in ES cell media excluding LIF for a final working concentration of 100 μM. RA-treated cells were seeded on gelatin-coated tissue culture dishes at a density of 4×10^6

cells per 10 cm^2 dish. The cells were passaged every 2 days according to the protocol in Section 2.2.1.

2.5.2 DMSO and HMBA differentiation

For differentiation, ES cells were seeded in 6-well plates at a density of 3 x 10^5 cells per well. The cells were cultured in ES cell media (detailed in Section 2.2.1) excluding LIF with 1% DMSO or 5mM HMBA. The cells were passaged and harvested for RNA extraction every 2 days according to the protocol in Section 2.2.1.

2.5.3 Neural differentiation of ES cells

To achieve neural differentiation, AINV18-*Zic3* cells were exposed to doxycycline for 48 hours in ES culture medium and then treated with N2B27 medium as previously described[184]. Briefly, ES cells were dissociated and plated onto 0.1% gelatin-coated culture dishes at a density of 0.5−1.5 x $10^4/cm^2$, in N2B27 medium comprising a 1:1 mixture of Neurobasal medium (Gibco) supplemented with B27 (Gibco), and DMEM/F12 (Gibco) supplemented with modified N2 (25 g/ml insulin, 100 g/ml apo-transferrin, 6 ng/ml progesterone, 16 g/ml putrescine, 30 nM sodium selenite and 50 g/ml bovine serum albumin fraction V (Gibco). N2B27 medium was refreshed every 2 days and the cells were observed daily under the microscope for changes in morphology.

2.6 Gene expression analysis

2.6.1 RNA extraction

RNA was extracted from mammalian cells with TriZol reagent (Invitrogen) and then further purified with the RNeasy minikit (Qiagen) according to manufacturer's instructions. RNA samples were treated with DNase for removal of genomic DNA contamination. This was performed in 100 μl reactions containing 5 μg RNA, 0.2 U/μl RNAse inhibitor, and 0.15 U/μl RNase-free DNase (ProMega). Samples were incubated at 37°C for 30 minutes, followed by heat-inactivation of enzymes at 65°C for 15 minutes. The RNA samples were then purified using two phenol extractions and one chloroform extraction, and back extractions were performed with each step using equal volumes of sterile dH_20 to minimize loss of RNA. Total RNA was precipitated, washed with 70% ethanol and finally resuspended in 30 μl of sterile nuclease-free dH_20.

2.6.2 cDNA synthesis

cDNA was synthesized with 1.0 μg total RNA using the High Capacity cDNA Archive kit (Applied Biosystems) as per manufacturer's instructions. Briefly, cDNA synthesis was performed in 100 μl reactions consisting of 1.0 μg RNA diluted in 50 μl nuclease-free dH_20, and cDNA Archive kit components: 1 x Reverse Transcriptase buffer, 5.5mM $MgCl_2$, 500 μM dNTP mix, 2.5 μM random primers, and 0.25 U/μl MultiScribe Reverse Transcriptase. Synthesis reactions were incubated in a PCR thermocycler at 25°C for 10 minutes followed by 37°C for 2 hours. The cDNA samples were stored at -20°C following synthesis.

2.6.3 Quantitative real-time PCR

Quantitative PCR assays were performed as follows: Reversed transcribed cDNA samples were diluted 10x in nuclease-free water, and added to 5.0 ul TaqMan® Universal PCR Master Mix reagent (Applied Biosystems) containing 0.5 μl of a single TaqMan probe (20x TaqMan® Gene Expression Assay reagents; Applied Biosystems). The list of TaqMan probes are provided in Table 5. Reactions were conducted in triplicate within 384-well reaction plates (ABI) at a final volume of 10 μl on the ABI Prism 7900 machine.

2.7 Protein expression analysis

2.7.1 Cell lysis and protein quantitation

Confluent cell cultures were harvested by scraping and washing with 1 x PBS solution. The cells were centrifuged for 5 minutes at 500 rpm, and then re-suspended in cell lysis buffer comprising 50 mM Tris pH 7.4, 150 mM NaCl, 2mM EDTA, 1% NP-40, 0.1% SDS, and 1 x EDTA-free Protease inhibitor (Roche). The cell lysate was incubated with rotation for 10 minutes at 4°C and was cleared by centrifugation at 12,000 rpm for 30 minutes at 4°C. The supernatant was transferred to a fresh tube and protein was quantitated using the Bradford assay (Bio-Rad Laboratories). Six bovine serum albumin (BSA) protein standards were used at 0μg, 50μg, 100μg, 200μg, 300μg and 400μg for the Bradford assay. Protein samples and standards were diluted in 0.15M NaCl prior to triplicate loadings onto a 96-well ELISA plate. Absorbance values were measured on a Sunrise Tecan Microplate Reader at A_{595} nm.

Table 5. List of marker genes used to assess lineage development in ES cells.

Gene Symbol	Description	Lineage
Sox17	SRY-box containing gene 17	Endoderm
PDGFRA	Platelet-derived growth factor receptor, alpha	Endoderm
Gata4	GATA binding protein 4	Endoderm
Gata6	GATA binding protein 6	Endoderm
Foxa2	Forkhead box A2	Endoderm
GSC	Goosecoid	Mesendoderm
Nodal	Nodal	Mesendoderm
MixL1	Mix1 homeobox-like 1	Mesendoderm
Hand1	Heart and neural crest derivatives expressed 1	Mesoderm
Nkx2.5	NK2 transcription factor related, locus 5	Mesoderm
Gata2	GATA binding protein 2	Mesoderm
Nestin	Nestin	Ectoderm
GFAP	Glial fibrillary acidic protein	Ectoderm
Pax6	Paired box gene 6	Ectoderm
TDGF1	Teratocarcinoma-derived growth factor / Cripto	Ectoderm
Sox1	SRY-box containing gene 1	Ectoderm
REST	RE1-silencing transcription factor	Ectoderm
CoREST	REST Co-repressor 1	Ectoderm
FGF5	Fibroblast growth factor 5	Ectoderm
BMP4	Bone morphogenetic protein 4	Trophectoderm
CDX2	Caudal type homeobox 2	Trophectoderm
DKK3	Dickkopf homolog 3	Wnt pathway
Gsk3beta	Glycogen synthase kinase 3 beta	Wnt pathway

2.7.2 SDS-PAGE

Denaturing polyacrylamide gel electrophoresis was conducted to resolve proteins by size. Thirty micrograms of protein was added to 6x SDS loading buffer (250 mM Tris/HCl pH6.8, 30% glycerol, 10% SDS, 5% β-mercaptoethanol, and 0.02% bromophenol blue), followed by incubation at 55°C for 5 minutes. Protein samples were loaded onto a 10% or 12% acrylamide gel for electrophoresis at 100V for 1.5 hours. The resolved protein samples were then electroblotted onto Hybond C extra nitrocellulose membrane (Amersham) for 1 hour in Western Transfer Buffer (20% Ethanol, 70% dH_20, and 1x Western Transfer Buffer stock containing 14.5g Glycine and 3.0g Tris base).

Consistency of protein loading and quality of Western blot transfer was assessed by Ponceau S staining (0.5% Ponceau S, 1% glacial acetic acid). In this protocol, the electroblotted membrane was rinsed once in Tris-buffered saline containing Tween-20 (TBS-T; 10mM Tris/HCl pH 8.0, 150mM NaCl, 0.5% Tween-20; pH 8.). Ponceau S was then applied for 30 seconds to enable visualization of proteins on the membrane, following which the membrane was rinsed twice in dH_20 and then thrice in TBS-T. The nitrocellulose membranes were immediately probed for protein (Section 2.7.3) or stored at 4°C in air-tight boxes containing TBS-T.

2.7.3 Protein detection and chemiluminescence detection

Immunodetection of proteins was carried out as follows: Nitrocellulose membranes were blocked for 1 hour at room temperature in 5% (w/v) skimmed-milk powder and 1% BSA. Protein detection was performed with goat-anti-Zic3

antibody (1:800; C-12, Santa Cruz Biotechnology) or rabbit-anti-HA (1:1000, sc-805, Santa Cruz Biotechnology), followed by HRP-conjugated donkey-anti-mouse or donkey-anti-rabbit secondary antibodies (Santa Cruz Biotechnology) at a dilution of 1:5000.

Loading consistency was determined with mouse-anti-βactin (1:3000; Invitrogen) and goat-anti-mouse HRP secondary antibodies (1:5000; Santa Cruz Biotechnology). The primary antibodies were incubated overnight at 4°C and the secondary antibodies were subsequently incubated for 1 hour at room temperature, with 3 x TBS-T rinses for 15 minutes performed in between incubations. Chemiluminescence detection was carried out using the Enhanced-Chemiluminescence (ECL) Western blotting kit (Amersham) according to manufacturer's instructions.

2.7.4 Immunocytochemistry

For imaging of Zic3 clonal knockdown lines, cells were seeded at a density of 1.0 x 10^5 cells per well on fibronectin-coated chamber slides, fixed in 4% paraformaldehyde and permeabilized with 0.3% Triton X-100. Blocking was performed with 5% FBS and 1% BSA in PBS solution for 30 minutes. Cells were stained with the following primary antibodies (1:100): goat- or mouse-anti-Oct4 (Santa Cruz Biotechnology, N-19 and C-10 respectively), rabbit-anti-Nanog (Chemicon), goat-anti-FoxA2 (M-20, Santa Cruz Biotechnology), goat-anti-Gata6 (C-20, Santa Cruz Biotechnology), or mouse-anti-CD140a (PDGFRA; eBioscience #16-1401). This was followed by the appropriate secondary

antibodies detecting mouse or goat IgG Alexa Fluor 488 (1:500; Molecular Probes) for Oct4 staining, rabbit IgG Alexa Fluor 594 (1:500; Molecular Probes) for Nanog staining, or Qdot® 655 anti-goat or anti-mouse antibodies (Molecular Probes) for FoxA2, Gata6 and PDGFRA staining (1:150) according to manufacturer's protocol. Images were captured with the Zeiss LSM 5 Duo inverted confocal microscope (Zeiss, Thornwood, NJ).

N2B27-differentiated cells were fixed at room temperature in 4% paraformaldehyde and permeabilized with 0.3% Triton X-100 in 24-well plates. Blocking was performed for 30 minutes in buffer comprising 5% FBS and 1% BSA in PBS solution. Cells were stained with the following primary antibodies: mouse-anti-Nestin (Chemicon, MAB353), rabbit-anti-TuJ1 (Covance, MRB-435P) and anti-MAP2 (Sigma-Aldrich) for 1 hour at room temperature. The cells were rinsed 3 times with blocking buffer and incubated with Alexa Fluor 488 secondary antibodies (#A11070, #A11017, #A11055; Molecular Probes) for 30 minutes. DAPI staining was performed at 1 μg/ml for 5 minutes at room temperature (D9542, Sigma) and images were captured on a Carl Zeiss Observer.D1 with AxioVision v 4.6.3 software (Carl Zeiss Inc, Thornwood, NY).

2.8 Custom production of Zic3 antibodies

A region was selected on the Zic3 protein that is not conserved among the other Zic family members (Figure 16; Clustal W protein sequence alignment). For a further test of specificity, this region was subjected to a protein BLAST search (NCBI). The peptide sequence and antibody properties are listed in Table 6.

Peptide synthesis and antibody production were performed according to the custom polyclonal antibody protocol by Biogenes GmBH (Berlin, Germany). The rabbits were immunized and boosted every 28 days for 3 months. Subsequent monthly production bleeds were affinity-purified for total IgG (tris-glycine buffer pH 7.5, 250mM NaCl, 0.02% thimerosal) and their specificity was tested by western blots. Antibodies from the 3rd production bleed were the most sensitive and produced the lowest background. These antibodies were used in our experiments.

2.9 Chromatin Immunoprecipitation (ChIP)

2.9.1 ChIP protocol

E14 cells were cultured to a density of 1 x 10^8 cells for each IP. Two biological ChIP replicates were performed per experiment. Cells were cross-linked for 10 minutes at room temperature with 1% (w/v) formaldehyde and the reaction was subsequently quenched with 125mM glycine. Nuclear fractions were isolated and the DNA was sheared to lengths of 200 to 500 bp. Antibodies against Zic3, Sox2 (sc-17320, Santa Cruz Biotechnology) and GST (sc-459 & sc-34073; Santa Cruz Biotechnology) were used for immunoprecipitation. Ten micrograms of each ChIP antibody was incubated with pre-blocked Protein G sepharose beads for 2 hours at 4°C. Following incubation, the antibody-sepharose bead complexes were rinsed, gently pelleted at 500 rpm for 1 minute at 4°C, and then resuspended in the pre-cleared (2 hour incubation at 4°C with pre-blocked protein G sepharose beads) cross-linked nuclear protein fractions for overnight incubation at 4°C. The following day, the protein-antibody-bead complexes were rinsed and pelleted by

Zic family CLUSTAL W (1.83) multiple sequence alignment (Page 1 of 2)

```
Zic1            --------------------------------------------------MLLDAGPQYPA 11
Zic2            --------------------------------------------------MLLDAGPQFPA 11
Zic3            ---------------------------------------------MTMLLDGGPQFPG 13
Zic4            ------------------------------------------------------------
Zic5            MMEPPLSKRNPPALRLADLATAQAQQLQNMTGFPVLVGPPAHSQRRAVAMHLHPRDLGTD 60


Zic1            IGVTTFGASRHHSAG-------DVAERDVGLG-------INPFADGMGAFKLNPS-SHEL 56
Zic2            IGVGSFARHHHHSAAAAAAAAAAEMQDRELSLAAA-QNGFVDSAAAHMGAFKLNPG-AHEL 69
Zic3            LGVGSFGAPRHHEMP-------NREPAGMGLNPFGDSTHAAAAAAAAAAFKLSPATAHDL 66
Zic4            ------------------------------------------------------------
Zic5            PGVASTALGPEHMAQASGQGPCPPSQGLPGLSQVPAPAARSVASGTHPGARTHPDGGGSS 120


Zic1            ASAGQTAFTSQAPG------YAAAAALGHHHHPGHVGSYS----SAAFNSTRDFLFRNRG 106
Zic2            SPGQSSAFTSQGPGAYPGSAAAAAAAAALGPHAAHVGSYS----GPPFNSTRDFLFRSRG 125
Zic3            SSGQSSAFTPQGSG--YANALGHHHHHHHHHHASQVPTYARR-ASAAFNSTRDFLFRQRG 123
Zic4            ----------------------------------MKYK----TSLVMRKRLRLYRN-- 18
Zic5            GAQASAPPPPAPPLPPSQSSSPPPPPPPPPALSGYTATNSGGGSSSGKGHSRDFVLRRDL 180
                                                   .       .    .*  : *

Zic1            --------------FG-DAAAAASAQHSLFAASAGGFGG----PHGHTDAAGHLLFSGLH 147
Zic2            --------------FG-DSAPGG-GQHGLFGPGAGGLH------HAHSDAQGHLLFPGLP 163
Zic3            --------------SGLSEAASGGGQHGLFAGSASSLHA----PAGIPEPPSYLLFPGLH 165
Zic4            ---------------TLKESSSSCGHHGPQLAAS-------------SNPS---VLPGLH 47
Zic5            SATAPAAAMHGAPLGGEQRSGSSSPQHPTPPPHPAGMFISASGTYAGRDGGGSALFPALH 240
                                 . : ..  :*      .              :     ::..*

Zic1            EQAAG-HASPN--VVNGQMRLGFSGDMYPRPEQYGQVTS---PRSE-------HYAAPQL 194
Zic2            PEQHGPHASQN--VLNGQMRLGLPGEVFGRSEQYRQVAS---PRTD-------PYSAAQL 211
Zic3            EQGAG-HPSPTGHVDNNQVHLGLRGELFGRADPYRPVAS---PRTD-------PYAASAQ 214
Zic4            EQPPQASHSRP---LNGLLRLGIPGDMYARSEPFAPGPM---ARSD-------TLATATA 94
Zic5            DSPGAPGGHP----LNGQMRLGLAAAAAAAAELYGRAEPPFAPRSGDAHYGAVAAAAAAA 296
                 .             *. ::**: .     .: :        .*:          ::.

Zic1            HG-YGPMNVNMAA-----------------HHGAG---------------------AFFR 215
Zic2            HNQYGPMNMNMGMNMAAAAAHHHH-----HHHHPG---------------------AFFR 245
Zic3            FPNYSPMNMNMGVN--------VA-----AHHGPG---------------------AFFR 240
Zic4            LHGYGGMNLTMNLT--------------APHGPG---------------------AFFR 118
Zic5            LHGYGAVNLNLNLAAAAAAAAAAGPGPHLQHHAPPPAPPPAPAPHPHHPHLPGAAGAFLR 356
                   *. :*:.:                    * .                       **:*

Zic1            YMRQP-IKQELICKWIEPEQLANPKK-------SCNKTFSTMHELVTHVTVEHVGGPEQS 267
Zic2            YMRQQCIKQELICKWIDPEQLSNPKK-------SCNKTFSTMHELVTHVSVEHVGGPEQS 298
Zic3            YMRQP-IKQELSCKWIEEAQLSRPKK-------SCDRTFSTMHELVTHVTMEHVGGPEQN 292
Zic4            YMRQP-IKQELICKWLGDDSPMSPR--------PCSKTFSTMHELVTHVTVEHVGGPEQA 169
Zic5            YMRQP-IKRELICKWLDPEELAGPPASADSGVKPCSKTFGTMHELVNHVTVEHVGGPEQS 415
                **** **:** ***:   .   *         .*.:**.******.**::******** 

Zic1            NHICFWEECPREGKPFKAKYKLVNHIRVHTGEKPFPCPFPGCGKVFARSENLKIHKRTHT 327
Zic2            NHVCFWEECPREGKPFKAKYKLVNHIRVHTGEKPFPCPFPGCGKVFARSENLKIHKRTHT 358
Zic3            NHVCYWEECPREGKSFKAKYKLVNHIRVHTGEKPFPCPFPGCGKIFARSENLKIHKRTHT 352
Zic4            NHICFWEECPRQGKPFKAKYKLVNHIRVHTGEKPFPCPFPGCGKVFARSENLKIHKRTHT 229
Zic5            SHVCFWEDCPREGKPFKAKYKLINHIRVHTGEKPFPCPFPGCGKVFARSENLKIHKRTHT 475
                .*:*:**:***:**.*******:**********************:*************** 

Zic1            GEKPFKCEFEGCDRRFANSSDRKKHMHVHTSDKPYLCKM--CDKSYTHPSSLRKHMKVHE 385
Zic2            GEKPFQCEFEGCDRRFANSSDRKKHMHVHTSDKPYLCKM--CDKSYTHPSSLRKHMKVHE 416
Zic3            GEKPFKCEFEGCDRRFANSSDRKKHMHVHTSDKPYICKV--CDKSYTHPSSLRKHMKVHE 410
Zic4            GEKPFRCEFEGCERRFANSSDRKKHSHVHTSDKPYMCKVRGCDKCYTHPSSLRKHMKVHG 289
Zic5            GEKPFKCEFDGCDRKFANSSDRKKHSHVHTSDKPYYCKIRGCDKSYTHPSSLRKHMKIHC 535
                *****:***:**:*:********** ********* **:  ***.************:* 
```

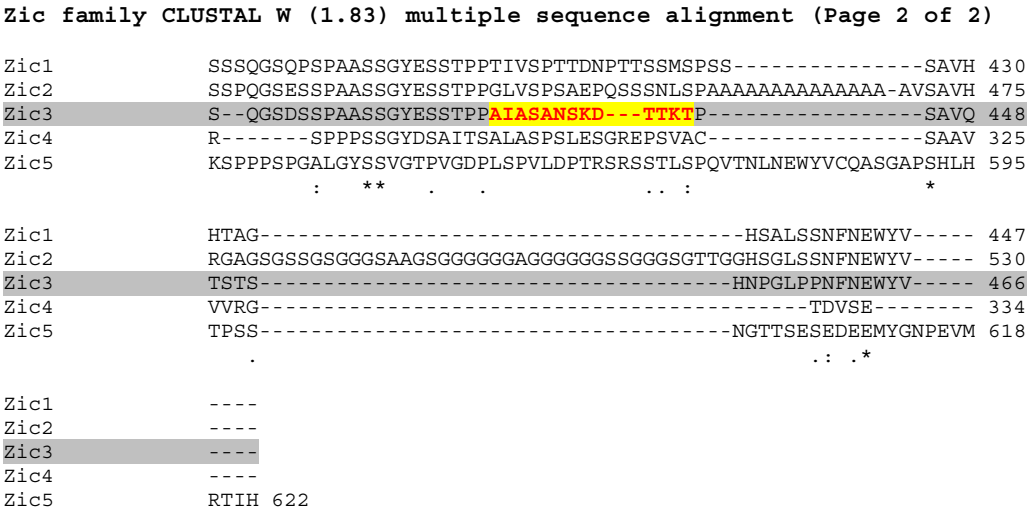

Figure 16. Zic family protien sequence alignment (Clustal W). The Zic3 protein sequence is indicated in grey, and the Zic3 antibody was raised against a unique 13 amino acid region (yellow) that is not conserved amongst the Zic family members

Table 6. Details of custom-produced Zic3 antibody

Antibody property	Details
Peptide Sequence	5'-AIASANSKDTTKT-3'
Location	Near C-terminal
Reactivity	Mus musculus (tested) Homo sapiens, Equus asinus
Applications	Western blot, co-immunoprecipitation, Chromatin-IP

Summary of peptide design
1. Binds to sequence outside high-homology zinc finger domain, and 2. Does not cross-react with other Zic family members (Figure 16) 3. Does not cross-react with other non-related proteins (BLAST seach 4. Within limits of 1 - 3 above, peptides with highest solubility were selected.

centrifugation at low speed for 1 minute at 4°C. The ChIP material was eluted from the beads at 65°C for 30 minutes, and cross-links were reversed overnight by incubation at 65°C. The following day, the samples were treated with RNaseA (0.2mg/ml) for 2 hours at 37°C, and then Proteinase K (0.2 mg/ml) at 55 °C for 1 hour. Finally, the samples were treated twice with phenol/chloroform/Isoamyl alcohol (25:24:1), then precipitated and rinsed once in 70% ethanol before re-suspension in 70µl of 10mM Tris-HCl, pH 8.0.

2.9.2 Quantitative PCR for ChIP enrichment

Quantitative PCR for ChIP enrichment was performed on the ABI PRISM 7900 machine with 1x SYBR Green PCR mastermix (Applied Biosystems), under the following conditions: 50°C for 2 minutes, 95°C for 10 minutes, and 40 cycles of 95°C for 15s and 60°C for 1 minute. Fluorescence from the amplified products was measured by laser spectral analyses on the ABI Prism 7900 machine, and the data were processed and displayed in the form of real-time amplification plots generated by the SDS software (v2.2; Applied Biosystems). ChIP fold-enrichment was determined by normalizing Threshold cycle (Ct) values of ChIP samples against sonicated whole cell DNA extract, and then subsequently to a non-enriched ChIP control region set at a value of 1. Details of primers are provided as Appendix 1.

All PCR primers gave a single product as confirmed by agarose gel electrophoresis and heat dissociation analysis[185] on the ABI Prism 7900 (Applied Biosystems), under the following conditions: 95°C for 15s, 60°C for 20s, 20

minute ramp to 95°C and 95°C for 15s. The data from this analysis were compiled by the SDS software (v2.2; Applied Biosystems) and displayed as melting curve graphs. The graphs were checked for specificity of PCR amplified product as indicated by a single, well-defined melting curve peak[185].

2.9.3 ChIP-chip assays, data processing, and statistical analysis

For analysis on mouse Agilent ChIP-on chip promoter arrays, the purified ChIP material (Section 2.9.1) was blunt-ended, ligated to linkers and PCR amplified. DNA was flurophore-labeled using Invitrogen's CGH Labeling kit (ChIP samples with Cy5; whole-cell extract with Cy3). The labeled DNA was hybridized to Agilent mouse promoter ChIP-on-chip arrays for 40 hours at 65°C (Agilent Technologies, Santa Clara, CA). Chips were washed and scanned as per manufacturer's protocol and the results were processed with Agilent's ChIP Analytics software v1.3. A *p*-value cutoff <0.001 was specified in this analysis.

To further minimize false positives, a "neighborhood voting" algorithm[19] was applied to filter for high confidence Zic3- or Sox2-enriched sites, wherein binding was considered genuine only in the presence of a second significantly enriched neighboring probe ($p < 0.005$). For analysis of ChIP-chip false discovery rate (FDR), 33 ChIP positive regions reported by the Agilent array were selected at random for PCR verification (ref. section 2.9.2). One gene out of the 33 did not give a PCR enrichment greater than our 2.5-fold threshold for positive enrichment, giving an FDR < 0.03 (Appendix 2).

2.10 Luciferase reporter assays

2.10.1 Nanog promoter assays

The 300bp *Zic3* enhancer region containing the Nanog-binding site was cloned from mouse genomic DNA (Section 2.1.6). The primers used were: forward, 5' ATATAacgcgtTTAGAGGTCAAACCAT-3', and reverse, 5'-TATATagatctTAGT AGTCAAACTGGATT-3' with restriction sites indicated in lowercase. The PCR fragment was digested with *MluI* and *BglII,* and cloned into the pGL3-Basic vector (Promega) containing a basal promoter comprising the 500bp region immediately upstream of the mouse Oct4 gene. The following constructs were transfected into cells 2.5 x 10^4 cells in 96-well plates for the luciferase assay: 100ng firefly luciferase reporter, 1.0 ng of the *Renilla* luciferase vector, pRL-SV40 plasmid normalization control, and 250ng of the respective knock-down construct. Puromycin selection (1.0μg/ml) was introduced 20 hours post-transfection and cultured for 2 days. Luciferase activity measured using the Dual Luciferase System (Promega) in a Centro LB960 96-well luminometer (Berthold Technologies).

2.10.2 Zic3 ChIP-identified promoter assays

Zic3 target regions were amplified by PCR from genomic DNA (Section 2.1.6) and sub-cloned into the NheI/BglII sites of the ProMega luciferase reporter vector pGL3. Sequences lacking a native minimal promoter were cloned upstream of the SV40 promoter for enhancer assays. DNA sequences were amplified by PCR from mouse genomic DNA with the primers listed in Appendix 3. All transfections and luciferase assays were performed as described above, and the unpaired Student's *t* test was used to determine statistical significance.

2.11 Co-immunoprecipitation experiments

The Seize-X Protein G immunoprecipitation kit (#45210, Pierce Biotechnology, Rockford, IL) was used according to the manufacturer's protocol. Briefly, antibodies were cross-linked to immobilized protein G sepharose in spin columns. Confluent 15cm^2 dishes of E14 cells (1 x 10^8 cells) were rinsed twice with PBS, and then gently scraped and pelleted at 500 rpm for 5 minutes. The cells were lysed in Co-IP lysis buffer (50 mM Tris, pH 7.6, 150 mM NaCl, 2 mM EDTA, 1% NP-40, 0.1% SDS, and 1 x EDTA-free Protease inhibitor, Roche), and centrifuged at maximum speed for 15 minutes at 4°C. The supernatant containing endogenous complexes was applied to the antibody-linked columns and incubated overnight at 4°C. Immunoprecipitated complexes were washed the following day and eluted twice from the spin columns, and the samples were resolved in 10% SDS-PAGE gels with reducing buffer.

2.12 Gene Expression arrays

2.12.1 Illumina mouse arrays

The whole-genome Illumina Mouse Ref-8 v1.1 beadchips were used for microarray analysis of RNAi-treated and Ainv18-Zic3 overexpression samples. These Illumina beadchips allow interrogation of approximately 25,600 well-annotated mouse refseq transcripts. For the microarray analyses, mRNA was harvested from 3 biological replicates per experiment. These samples were reverse-transcribed, Cy3-labeled, and hybridized to Illumina MouseRef-8 v1.1 Expression Beadchips according to the manufacturer's protocol (Illumina Inc., San Diego). Following the wash of Illumina chips, microarray signals were

scanned with an Illumina BeadStation array reader, and the data were background-normalized and assessed for quality with cluster dendrograms and DirectHyb control plots (Beadstudio v1.5, Illumina).

2.12.2 Statistical analysis of microarray data

The microarray data were processed with Genespring GX v7.3.1 (Agilent Technologies, Santa Clara). The unpaired Student's *t* test was used to determine statistical significance with Benjamini and Hochberg multiple-testing correction (FDR<0.1), and genes demonstrating ≥ 1.5-fold change were reported as statistically significant.

For statistical analysis of overlapping genes between RNAi samples, computer simulations were conducted as follows: a number of genes corresponding to the actual number of genes within each list were randomly sampled from the Illumina mouse Ref-8 v1.1 beadchip. The random gene lists were overlapped to derive a percentage, and this process was repeated 100 times to yield an average percentage overlap by chance. Finally, *p*-values were computed by comparing the 100 simulated overlaps to the actual overlap percentage using one-sample *t*-tests.

2.12.3 Functional annotations using the Panther database

The microarray gene lists were uploaded to the Panther database for functional annotations (http://www.pantherdb.org). In this analysis, the Panther Gene Expression tool set was used to classify differentially-regulated genes under

biological process groups using the “Compare Gene List” function, relative to the 25,600 Illumina mouse Ref-8 v1.1 transcripts, and the binomial test was used to identify statistically significant over- or under-represented functional categories within the Zic3 RNAi or overexpression gene lists.

CHAPTER 3:

Zic3 is involved in transcriptional regulation of ES cell pluripotency

3.1 Introduction

Embryonic stem (ES) cell pluripotency is dependent upon sustained expression of the key transcriptional regulators Oct4, Nanog and Sox2. These core factors contribute to the hallmark characteristics of ES cells by: (1) activation of target genes that encode pluripotency and self-renewal mechanisms, and (2) repression of signaling pathways that promote differentiation[42]. In ES cells Oct4, Nanog and Sox2 co-occupy promoters of hundreds of genes that are both expressed and repressed in the pluripotent state [19,20]. This suggests complex regulatory circuitry in which Oct4, Nanog and Sox2 collectively and uniquely regulate downstream genes to control ES cell differentiation. However, it remains unclear what are the downstream effectors of these transcription factors that contribute to maintaining the pluripotent status of ES cells. It also is not understood how these 'master regulators' of pluripotency are involved in controlling lineage-specific differentiation of ES cells. It is therefore useful to elucidate the transcriptional networks surrounding Oct4, Nanog and Sox2, where detailed knowledge of these pathways remain key to harnessing the potential to direct differentiation of ES cells into therapeutically useful cell types.

To expand our understanding of the transcriptional networks that control stem cell differentiation, I have focused on transcription factors whose expression is directly regulated by Oct4, Nanog and Sox2. Zic3 (Zinc finger protein of the cerebellum 3) was identified as a transcription factor of interest for two reasons. Firstly, Oct4, Nanog and Sox2 binding have been mapped to the *Zic3* promoter regions in ES cells [19,20], implying that these key factors may regulate *Zic3* expression. The overlap between mouse and human ES cells further highlights the significance of

Zic3, and suggests possible conservation of the gene's pathways between the two species. Secondly, *Zic3* demonstrates differential gene expression between the pluripotent and early differentiation phases, where its expression is higher in the pluripotent state [85,86]. The changes in gene expression between these states suggest a potential role for Zic3 in controlling differentiation of mouse and human ES cells.

Zic3 belongs to the GLI superfamily of transcription factors and is a vertebrate homologue of the *Drosophila* pair-rule gene odd-paired (opa)[98]. The five known mammalian *Zic* genes (Zic1 – 5) encode five tandem C_2H_2 zinc finger domains that are highly conserved across species[186,187], and show distinct and partially overlapping expression patterns during development[115,116]. *Zic3* shares overall 64% and 59% homology with *Zic1* and *Zic2* respectively, and this homology increases to 91% within the zinc finger domain. Thus members of Zic family are strong candidates for redundancy in molecular signaling owing to the high degree of homology and overlapping expression observed among the members of this family.

In this study, I examined the function of *Zic3* as a regulatory target of Oct4, Nanog and Sox2 in ES cells. The *Zic3* gene has been identified as a target of Oct4, Nanog and Sox2 in ES cells[19,20], and *Zic3* is preferentially expressed in pluripotent state [85,86]. Questions arising from these data are: (1) How do Oct4, Nanog and Sox2 interact with the *Zic3* regulatory region, and what results from this interaction, and, (2) What role does Zic3 play in the embryonic stem cell? In

this chapter, I have addressed these questions using the loss-of-function approach for *Zic3* and the key regulatory genes in ES cells.

3.2 Results

3.2.1 Zic3 expression is associated with ES cell pluripotency

Comprehensive expression profiling of mouse and human ES cells has resulted in the identification of numerous genes that are expressed in undifferentiated cells and quickly repressed upon differentiation[85,86]. Among these genes are transcription factors Oct4, Nanog, and Sox2, which are required to maintain pluripotency of ES cells. *Zic3* was also found to be expressed in undifferentiated ES cells and suppressed in differentiated cells, and thus, may play a role in regulating ES cell differentiation. To further characterize the expression profile of *Zic3*, I assayed its expression in mouse ES cells which were induced to differentiate over 6 days by the addition of retinoic acid (RA) (Figure 17A). Similar to the trend demonstrated by *Oct4, Nanog* and *Sox2* in differentiating ES cells, *Zic3* transcript levels decreased between 1.5- to 10-fold for each two-day interval (D2, D4, and D6) relative to the undifferentiated control (Figure 17A), and this decrease in *Zic3* mRNA levels also correlated with a downregulation of Zic3 protein expression (Figure 17B). In addition, *Zic3* expression was significantly decreased in mouse ES cells differentiated by treatment with HMBA (N,N'-Hexamethylenebisacetamide)or DMSO (Dimethyl Sulfoxide), and by aggregation into embryoid bodies (Figure 18). Collectively, these results indicate that *Zic3* is associated with mouse ES pluripotency and that its expression decreases as the ES cells differentiate.

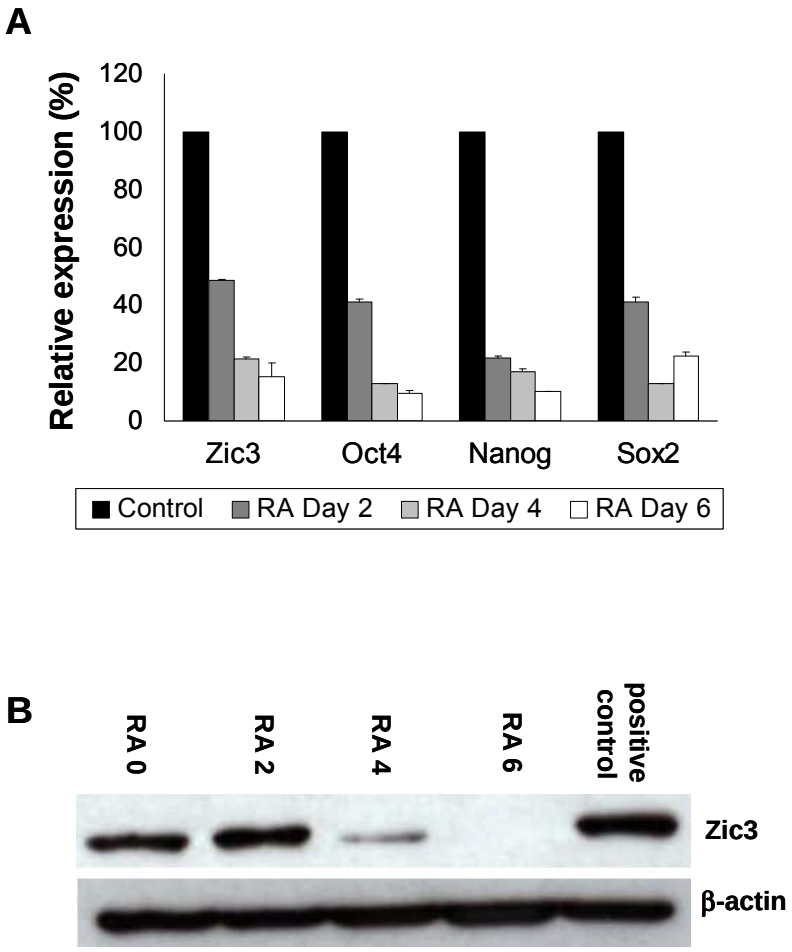

Figure 17. Profile of Zic3 expression during retinoic acid differentiation of E14 cells. (A) Real-time PCR analysis of differentiation induced by Retinoic Acid. Samples were assayed at two-day intervals (Untreated control, and treated samples Day 2, Day 4, Day 6). Mean levels ± S.E. are expressed as percentages relative to undifferentiated E14 cells (100%). The assays were conducted in duplicate and normalized to Beta-actin control. (B) Verification of Zic3 protein expression during the process of RA differentiation.

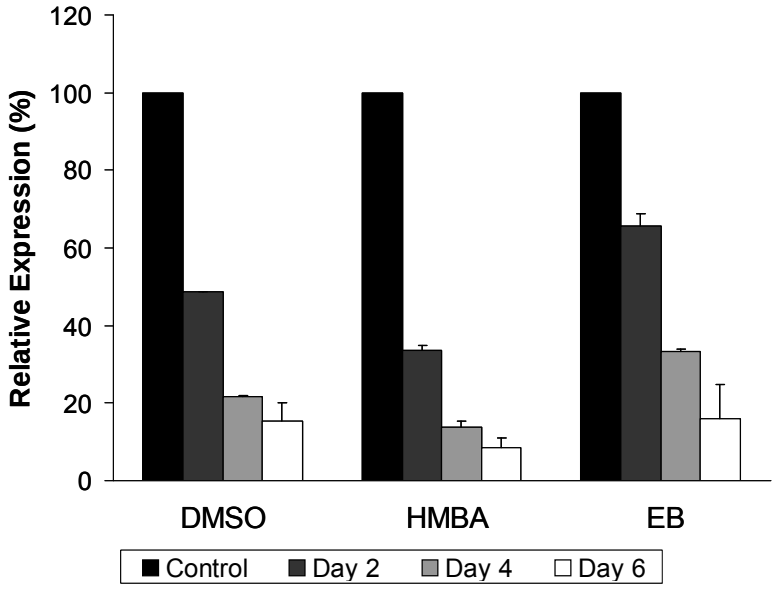

Figure 18. Zic3 expression during DMSO, HMBA and embryoid body differentiation of E14 cells. Samples were assayed at two-day intervals (Untreated control, and treated samples Day 2, Day 4, Day 6). Mean levels ± S.E. are expressed as percentages relative to undifferentiated E14 cells (100%). The assays were conducted in duplicate and normalized to Beta-actin control.

In further support of the importance of Zic3 in ES cell pluripotency, chromatin immunoprecipitation (ChIP) experiments in both mouse and human ES cells have identified binding sites for the transcription factors Oct4, Nanog and Sox2 at the *Zic3* gene locus (Figure 19)[19,20]. The binding of these transcription factors, which are demonstrated regulators of pluripotency, suggests that *Zic3* is a direct target for regulation by these TFs and may play a role in regulating ES cell differentiation.

3.2.2 Zic3 is regulated by Oct4, Nanog and Sox2

To further validate that Oct4, Sox2 and Nanog regulate *Zic3* expression, I performed gene expression knock-down experiments in mouse ES cells using RNA interference. Mouse ES cells were transfected with gene-specific siRNAs against *Oct4, Sox2,* and *Nanog* on alternate days to achieve 80-90% reduction in expression of the specific target gene as detailed in Section 2.3.1 (Figure 20A). Down-regulation of *Oct4* and *Sox2* reduced the level of endogenous *Zic3* to less than 25%, while *Nanog* RNAi reduced the level of *Zic3* to 70% (Figure 20B). These data indicate that *Zic3* expression is regulated by Oct4, Sox2, and Nanog.

It has been shown that Nanog over-expressing ES cells are resistant to differentiation induced by LIF withdrawal and RA addition[188]. As the endogenous levels of *Zic3* decreased upon RA induced differentiation (Figure 17), I was interested to determine if Nanog over-expression would sustain *Zic3* levels under RA treatment. ES cells with constitutive overexpression of Nanog were treated for two days with 0.3uM RA, alongside empty vector controls. The control cells showed a decrease in *Zic3* RNA levels typical of RA-induced differentiation. In

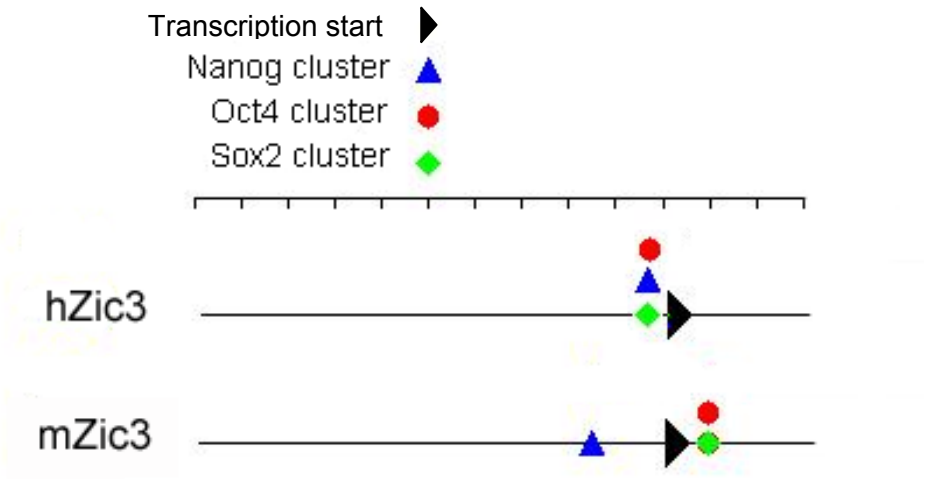

Figure 19. Oct4, Nanog and Sox2 binding sites on the Zic3 promoter. (Loh *et al.*, 2006; Sox2, H.H Ng, unpublished data) and (Boyer *et al.*, 2005). Transcription factor binding sites within 100kb up- and downstream of the Zic3 coding region are represented here. In human ES cells, Oct4, Nanog and Sox2 binding sites were located within 3.5kb upstream of the Zic3 transcription start site, while in mouse ES cells, the Nanog binding site was found within 18.5kb upstream, and the Oct4 and Sox2 binding sites were within 9.5 kb downstream of the gene respectively (Loh *et al.*, 2006). Each unit on the scale represents 10 kb.

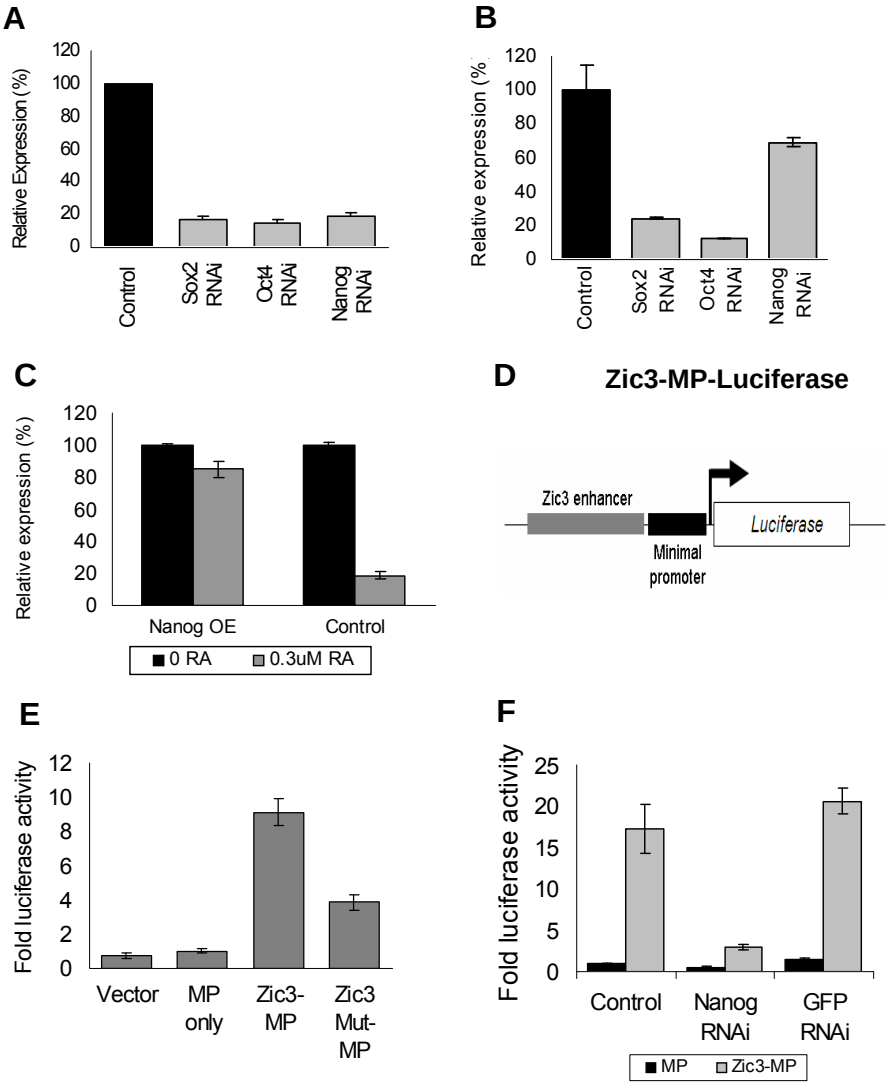

Figure 20. Oct4, Sox2 and Nanog regulate Zic3 expression. (A) Changes in endogenous gene expression levels of Oct4, Nanog and Sox2 following gene-specific RNA interference, and (B) corresponding changes in endogenous *Zic3* gene levels. cDNAs were prepared from the RNAi knockdown ES cells and analyzed using real-time PCR. The levels of the transcripts were normalized against values derived from control RNAi transfected ES cells (100%). (C) Changes in ES cell endogenous Zic3 gene level following Nanog over-expression with RA induced differentiation. Nanog over-expression cell line and control cell line were treated with no RA or 0.3μM RA for 2 days. Transcript levels of 0.3μM RA treated sample were normalized against no RA treatment sample. (D) Diagram of the construct with putative Zic3 enchancer region fused upstream of a minimal Pou5f1 promoter and firefly luciferase gene (E) The effects of luciferase activity in the absence of the putative Nanog binding site on Zic3 enhancer were tested by transfecting into ES cells. Activity were measured relative to the minimal promoter only (MP) construct without the Nanog enhancer (F) Effects of Nanog RNAi on Zic3 enhancer activity were tested by co-transfecting the Nanog RNAi with the reporter construct into ES cells and luciferase activity measured. Activity were normalized against the Control RNAi with mOct4 promoter-only construct. An RNAi targeting the GFP sequence was used as a nonspecific control.

Acknowledgments: *Data in Panels A & B were produced by the author of this thesis (Linda Lim). Panel C was produced by Jonathan Loh. The construct in Panel D was produced by Ng Huck Hui's group. Experiments in Panels E & F were independently conducted and verified by both Linda Lim and Jonathan Loh.*

contrast, mouse ES cells over-expressing Nanog sustained the level of *Zic3* at greater than 80% relative to the control ES cell line (Figure 20C). Thus, over-expression and knockdown of Nanog in ES cells results in an increase and decrease, respectively, of *Zic3*, suggesting that *Zic3* expression is regulated by Nanog, perhaps directly or indirectly.

A previous study identified a Nanog binding site in the enhancer region, 16.4 kb upstream of the transcription start site, of the *Zic3* gene[20]. Using this DNA region, I sought to determine if *Zic3* expression was directly regulated by Nanog. A 292bp portion of the *Zic3* enhancer containing the Nanog binding site was fused upstream of a minimal *Pou5f1* promoter that drives the firefly luciferase gene (Figure 20D). The minimal promoter was weakly active in ES cells, while activity of the *Zic3* enhancer region linked to the minimal promoter was 9-fold up-regulated as quantified by luciferase (Figure 20E). When the sequences of this putative Nanog binding site were deleted from the *Zic3* enhancer the corresponding reporter activity decreased (Figure 20E). *Nanog* RNAi was then transfected together with the wild-type reporter construct and the results indicated a 4-fold decrease in *Zic3* enhancer activity relative to the controls (Figure 20F). Collectively, the data show that *Zic3* expression is directly regulated by Nanog and, thus, may be a downstream effector in controlling ES cell differentiation.

3.2.3 Zic3 RNA interference in ES cells

3.2.3.1 Loss of Zic3 leads to ES cell differentiation

To investigate the role of Zic3 in ES cells I used RNA interference to achieve knockdown of gene expression. Both the siRNA and shRNA methods resulted in

a 70% reduction of *Zic3* transcript levels relative to the non-targeting controls (Figure 21A). Zic3 protein levels reflect this decrease in gene expression following *Zic3* RNAi treatment, while protein expression remained high in vector-only treated cells (Figure 21B).

Zic3 RNAi transfections resulted in a marked decrease in pluripotent colonies that stained for the stem cell surface marker alkaline phosphatase (AP)[189] relative to the mock RNAi control (Figures 22A & 22B). Following AP staining, the extent of differentiation was quantified with secondary re-plating assays that revealed a 3- to 5- fold increase in differentiated colonies in comparison with the non-targeting control (Figure 22C). In order to assess the differentiation state of *Zic3* knockdown cells, I assayed the changes in expression of key pluripotency genes (Figure 21A). Though the mouse ES cells showed clear morphological changes (Figures 22A & 22B), there were only modest decreases (15-20% siRNA experiment; 20-25% shRNA experiment) in the expression of the key pluripotency genes *Oct4* and *Sox2* (Figure 21A), while *Nano*g expression decreased 40% relative to the non-targeting control. I then performed the same experiment with human ES cells (HuES9). Although there was 70% decrease in *Zic3* transcript levels, *Oct4* and *Sox2* transcript levels remained unchanged and Nanog levels decreased by 25% (Figure 21A). These results suggest that Zic3 plays a role in maintaining ES cell pluripotency and its action is downstream of the dominant pluripotency factors Oct4, Sox2, and Nanog.

It is interesting that targeted repression of *Zic3* induced morphological differentiation of ES cells, while maintaining the expression of pluripotency marker

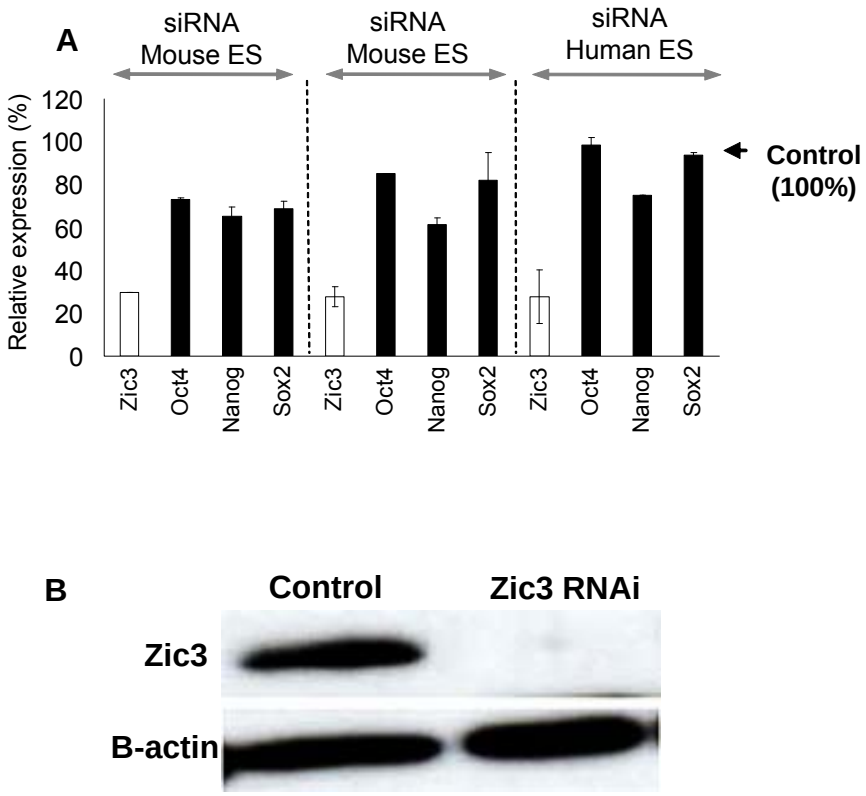

Figure 21. Effect of Zic3 RNAi on endogenous Oct4, Nanog and Sox2 levels. (A) Zic3 levels were depleted by RNA interference using siRNA and shRNA in mouse E14 cells and siRNA in human HuES9 cells. RNA was harvested between 4 to 5 days of transfection and transcript levels assayed by Real-time PCR. Shown in this figure are the levels of Zic3 transcript and the corresponding changes in Oct4, Nanog and Sox2 expression. Mean values ± S.E. are plotted as percentages relative to the non-targeting control (100%). The samples were assayed in duplicate and normalized to endogenous Beta-actin. (B) Corresponding decrease in protein levels following Zic3 RNAi treatment. Details of antibody specificity are provided in Table 6. The Zic3 protein species was depleted in the Zic3 RNAi sample, while B-actin protein levels remained high in the control. Beta-actin protein was used as a loading control.

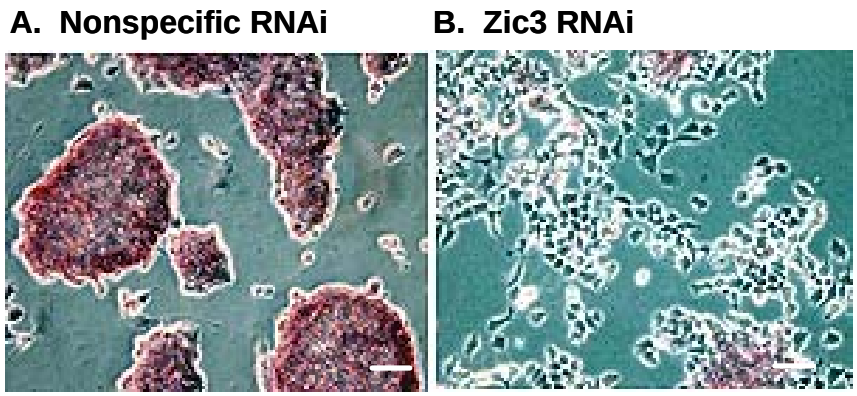

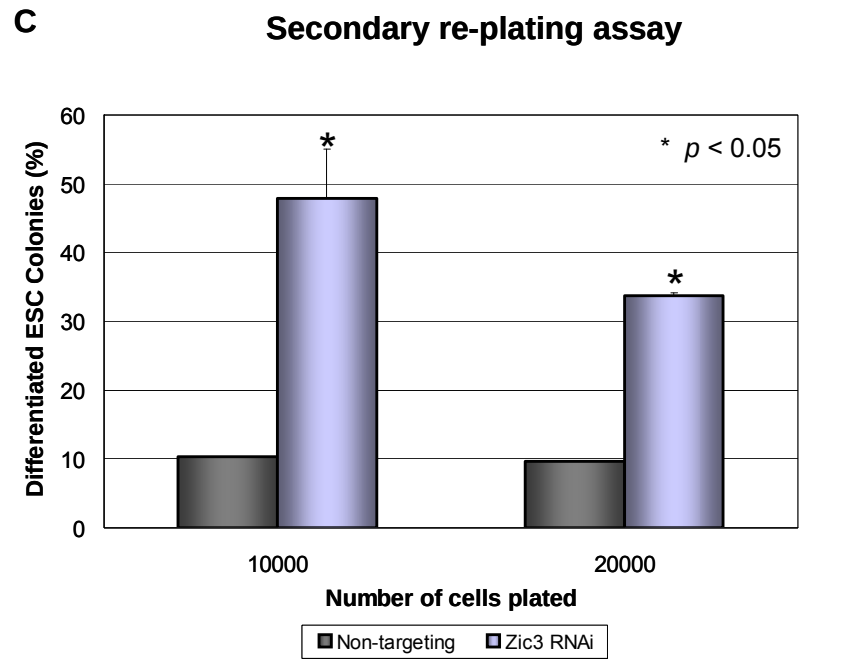

Figure 22. Effect of Zic3 RNAi on ES cell pluripotency. (A) & (B) Alkaline phosphatase staining revealed that the extent of differentiation in Zic3 RNAi-treated cells was greater than non-targeting RNAi control cells. (C) Secondary re-plating assays were used to quantitate the extent of differentiation in Zic3 RNAi cells. A 3-to-5 fold increase in differentiated colonies were observed with Zic3 RNAi relative to the non-targeting control. Scale bars, 50 μm.

genes in the transient knockdown experiments. To understand the molecular state of these cells, I examined a series of markers that represent lineage-specific ES cell differentiation. *Zic3* knockdown in mouse and human ES cells resulted in an up-regulation of a panel of endodermal markers assayed by real-time PCR (Section 2.6.3): *Sox17* (3.5-fold), *Pdgfra* (3.2- to 5.5-fold in mouse ES cells; 2.7-fold in human ES cells) and *Gata6* (2.5- to 3.5-fold) (Figure 23). In addition, two more endodermal lineage genes *Gata4* and *Foxa2* were up-regulated in the E14 RNAi cells (2.5-fold). I also assayed the expression of mesendodermal, mesodermal, ectodermal, trophectodermal and Wnt-pathway markers in *Zic3* RNAi cells. These markers remained unchanged relative to the non-targeting control in both mouse and human RNAi experiments (Figure 23) and were not statistically significant. These results indicate that Zic3 could play a specific role in maintaining ES cell pluripotency by suppressing endoderm marker expression.

3.2.3.2 Specificity of Zic3 knockdown

There was a possibility that ES cell differentiation and marker gene expression were due to off-target effects of the RNA interference. To address this concern, I designed a *Zic3* expression construct that was immune to RNA interference and tested whether this construct could rescue the knock-down phenotypes. The *Zic3* RNAi-immune expression construct was engineered with 5 silent mutations in protein coding domain sequence (Figure 24). As such, this construct (mutZic3) produces functional Zic3 protein, but due to codon degeneracy, remains resistant to RNAi targeting and degradation. This mutZic3 construct was therefore used to determine the specificity of endoderm marker upregulation produced by *Zic3* knockdown.

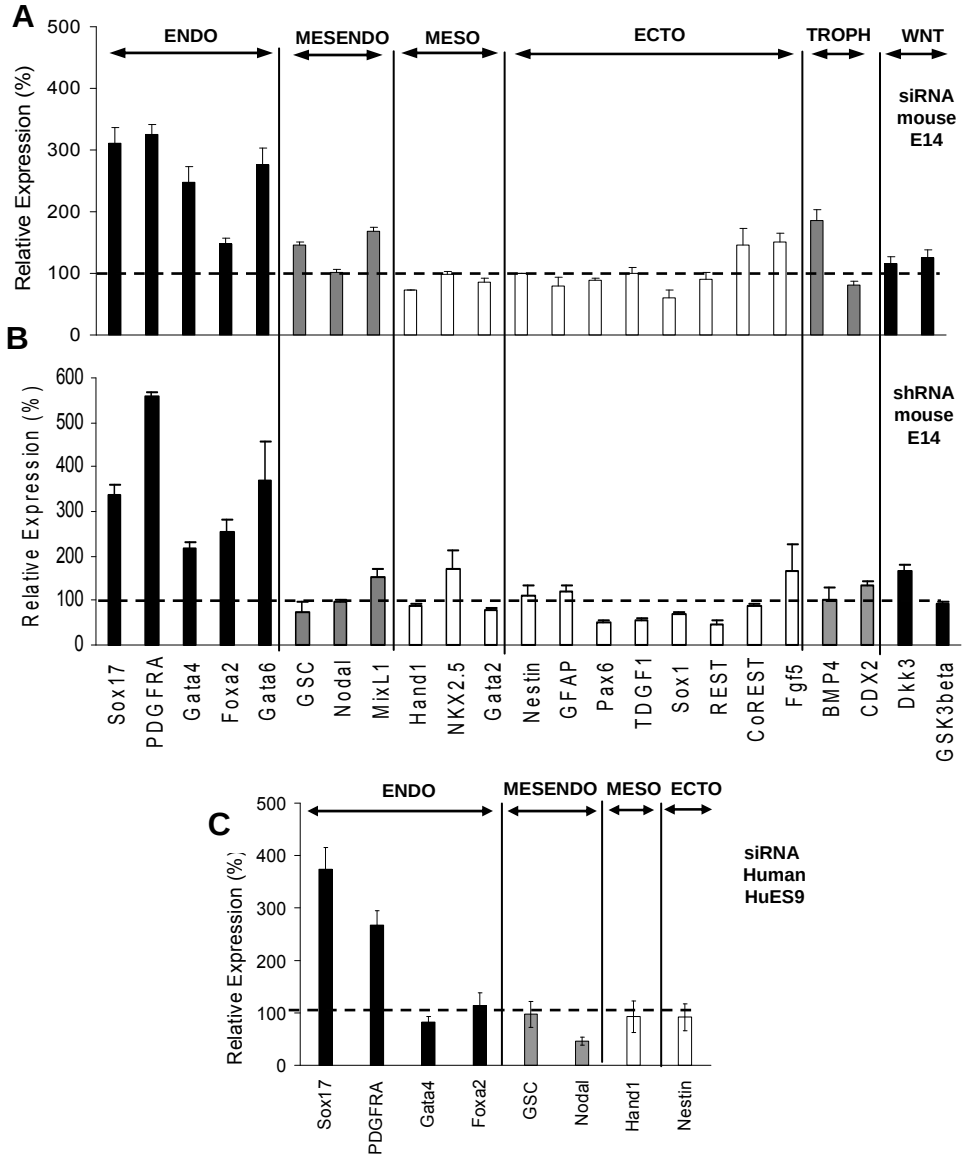

Figure 23. Effect of Zic3 RNAi on lineage marker gene expression. The panel of genes above was selected for their lineage-specificity. Transcript levels of genes from the endodermal (ENDO), mesendodermal (MESENDO), mesdodermal (MESO), ectodermal (ECTO), trophectordermal (TROPH) and Wnt pathways in mouse and human ES cells were assayed by Real-time PCR following Zic3 depletion by RNA interference. (A) siRNA in mouse E14 cells. (B) shRNA in mouse E14 cells. (C) siRNA in human HuES9 cells. Mean levels ± S.E. are expressed as percentages relative to the non-targeting control (100%). The assays were read in duplicate and results were normalized to Beta-actin.

Figure 24. Zic3 RNAi-immune construct. Diagram of the Zic3-RNAi wildtype targeted region (WT target) and the Zic3 target sequence modified to encode mutations that render immunity to RNAi targeting, while preserving functional viability due to degeneracy of the genetic code (red codons; RNAi-immune).

Acknowledgements: This construct was greated by Jonathan Loh.

The expression of endodermal markers *Foxa2, Gata4* and *Sox17* was first induced in ES cells by co-transfection of an empty overexpression vector with Zic3-RNAi, relative to cells co-transfected with empty vector and GFP-RNAi (6.5-, 10.1-, and 8.7-fold, for *Foxa2, Gata4* and *Sox17*, respectively, Figure 25, A-C). In contrast, when ES cells the RNAi-immune construct (mutZic3) was introduced into ES cells with *Zic3* RNAi, no endodermal markers were induced. (Figure 25, A-C). These experiments indicate that the RNA interference results are not due to off-target effects and further support the conclusion that Zic3 plays a role in maintaining the pluripotency of ES cells.

3.2.4 Zic3 clonal knockdown lines express endoderm lineage markers

3.2.4.1 Zic3 clonal knockdown lines

To determine if endodermal markers were upregulated in the same cells in which Zic3 was depleted, three clonal lines were generated that stably expressed *Zic3* shRNA. Figure 26 shows the morphology of these clonal lines. Panels A and B show non-targeting control lines which propagated rapidly and demonstrated the typical compact, phase-bright colonies of ES cells, suggesting that transfection of non-targeting shRNA and long-term antibiotic selection did not affect the ES-like morphology of the cells. In contrast, Panels C and D reflect the differentiated morphology of Zic3 clonal knockdown lines. These cell lines contained a mixture of phase-bright ES-like colonies and phase-dark, flattened cells with extended processes (Figure 26C and 26D). The *Zic3* knockdown lines propagated more slowly, as observed by their slower rate at attaining confluency relative to the control lines when an equal number of cells were seeded. This appeared to be a result of decreased rate of proliferation rather than increased cell death (where a

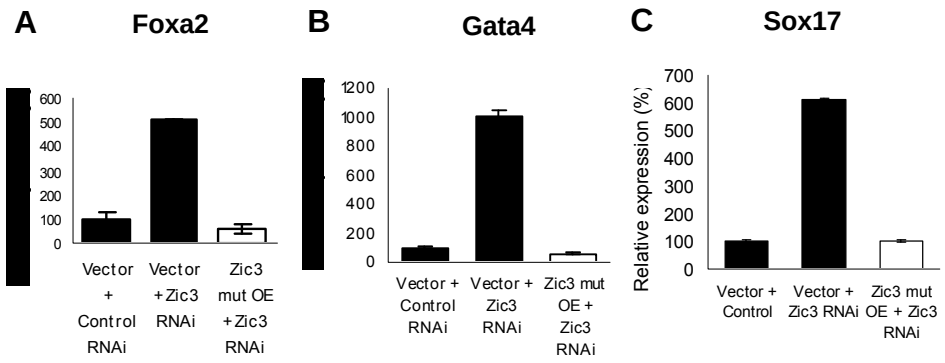

Figure 25. Zic3-immune construct specifically reverses changes in lineage marker expression levels caused by Zic3 RNAi. (A) – (C) Zic3 Rescue experiments demonstrating the specificity of Zic3 RNAi and reversibility of lineage marker expression**.** E14 cells co-transfected with the Zic3 RNAi-immune overexpression contruct and Zic3 RNAi vector demonstrated notable suppression of endodermal markers Foxa2, Gata4 and Sox17, relative to Zic3 RNAi co-transfected with the empty vector control). Zic3 immune real-time PCR analysis was conducted 3 days post-transfection. ß-actin was used as an internal control for normalization. The measurements were performed in biological triplicate with two technical replicates each and the average of the normalized ratio of target gene/ß-actin was calculated and presented with standard deviation. Relative expressions calculated with respect to the control experiment (Vector + *GFP* RNAi) at 100%. Transfection schemes are represented in Supplementary Table 1b.

The experiments were independently conducted and cross-verified by both Linda Lim and Jonathan Loh.

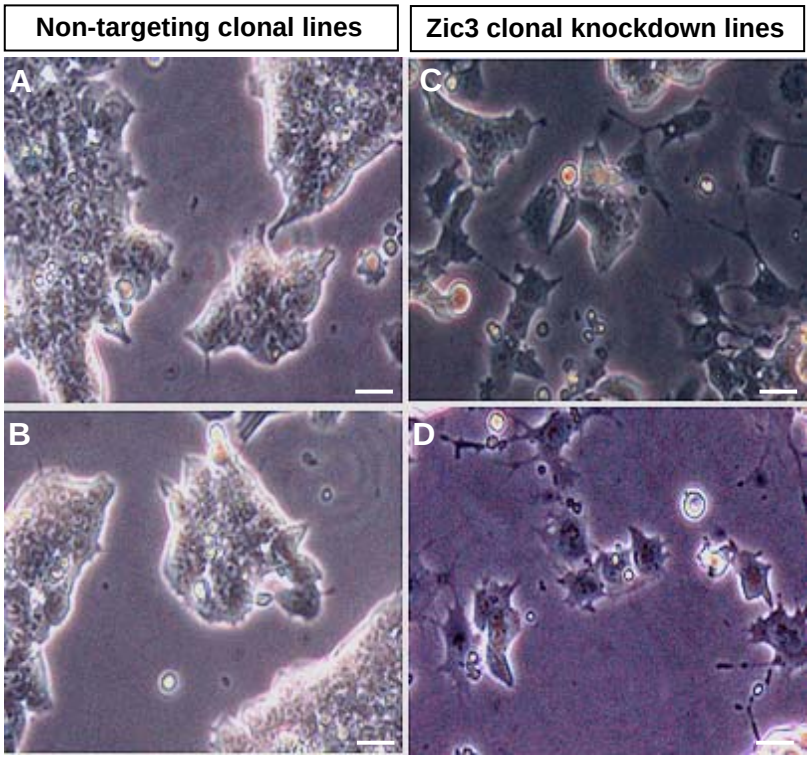

Figure 26. Morphology of Zic3 clonal knockdown lines. (A – B) Brightfield pictographs of two control lines transfected with a non-targeting control vector. These cell lines had the typical morphology of ES cells that form compact, phase-bright colonies. (C – D) Zic3 clonal knockdown lines contained a mixture of phase-bright ES-like cells and phase-dark, flattened cells with processes extended. This indicates that the Zic3 clonal knockdown lines are differentiated relative to the control lines. Scale bars, 50 μm.

significant increase in dead and floating cells was not observed in the culture media), and is a further indication of the differentiated status of the *Zic3* knockdown lines.

It was interesting that clonal cell lines with proliferative capacity could be derived from differentiated *Zic3* knockdown cells. I hypothesized that the clonal lines resulted from a subset of cells that were successfully transfected but maintained *Zic3* shRNA expression at lower levels. It was possible that this decreased amount of *Zic3* knockdown in ES cells was compatible with long-term passaging. To examine this possibility, a pSUPER shRNA construct containing EGFP (pSUPER.GFP) was used to generate *Zic3* knockdown cells (Figure 27), to enable tracking of transfected cells by GFP expression. This construct was similar to the pSUPER construct used previously, with the exception of a GFP transgene inserted upstream of the antibiotic resistance cassette. This construct has been extensively tested in our lab and produces a knockdown efficiency equivalent to that of the pSUPER vector. In addition, GFP fluorescence has been observed as a reliable indicator of vector expression.

Three days following transfection of the pSUPER.GFP constructs (Figures 28A and 29A), GFP was expressed in approximately 80% of ES cells, indicating a high rate of transfection efficiency. The non-targeting cells proliferated quickly and gave rise to small ES cell colonies at this stage (Figure 28B). In contrast, the *Zic3* knockdown cells showed differentiated morphology (Figure 29B) and were proliferating at a slower rate. This observation is consistent with the previous data

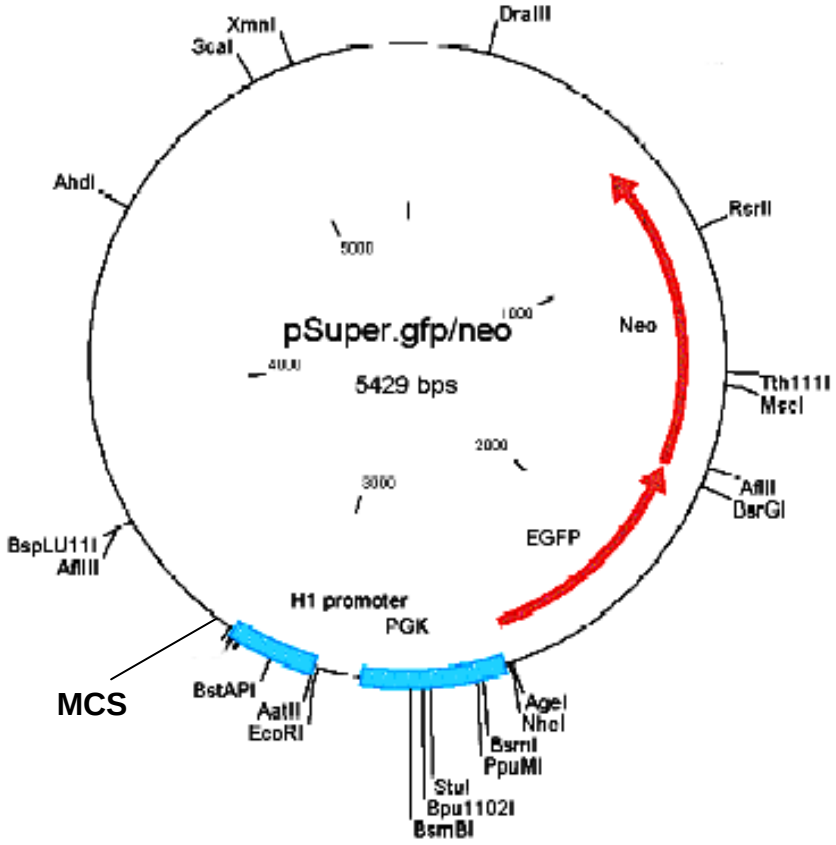

Figure 27. **pSUPER.GFP.neo construct from Oligoengine**. This construct features an shRNA cloning site (MCS) downstream of the RNA pol III H1 promoter for endogenous production of siRNA. In addition, EGFP expression and Neomycin antibiotic resistance are driven by the PGK promoter

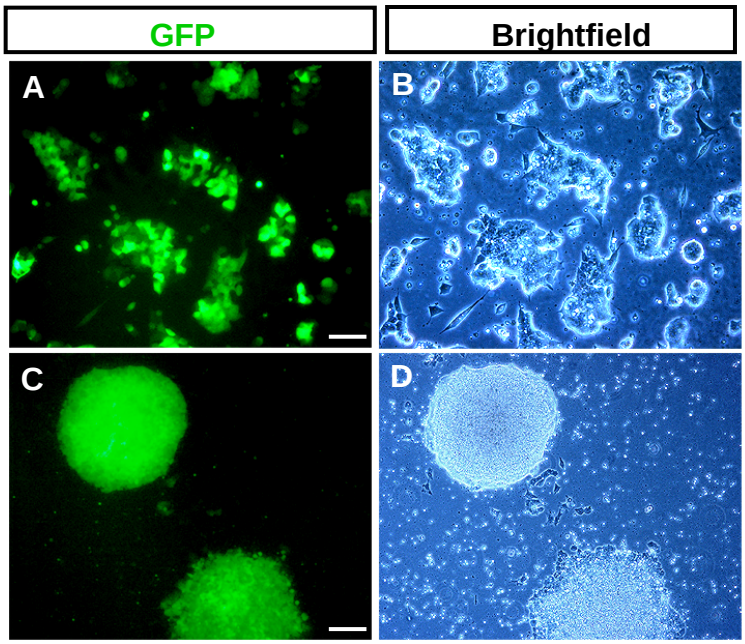

Figure 28. GFP fluorescence in mES cells transfected with non-targeting pSUPER-GFP shRNA vector. (A – B) The non-targeting control cells demonstrated robust GFP expression 3 days after transfection, with antibiotic selection introduced 24 hours post-transfection. (C – D) Three weeks post-transfection, the non-targetting pSUPER-GFP cells continued to demonstrate robust GFP expression, indicating that the shRNA construct was stably expressed in control cells undergoing long-term selection.

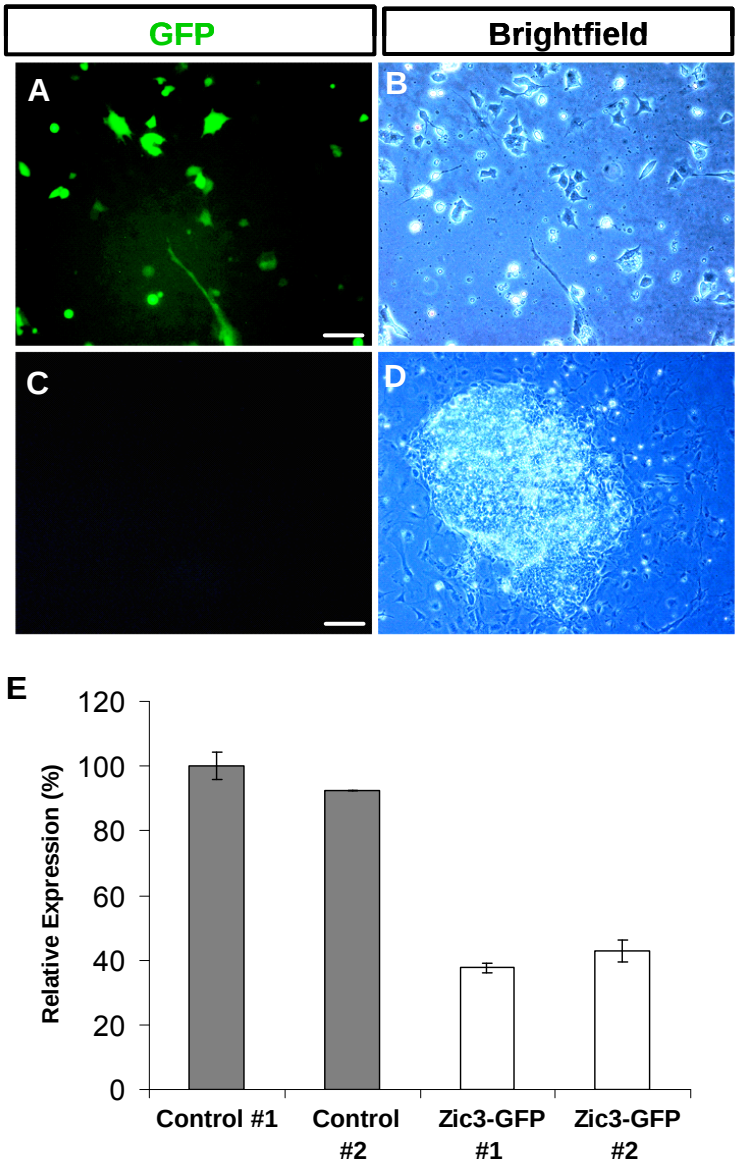

Figure 29. GFP fluorescence in mES cells transfected with the Zic3-pSUPER-GFP shRNA vector. (A – B) The Zic3 RNAi cells demonstrated robust GFP expression 3 days after transfection. The decreased proliferation rates following Zic3 knockdown resulted in smaller cell colonies compared to the controls in Figure 11. (C – D) Three weeks following transfection, the Zic3-pSUPER-GFP cells gave rise to colonies were non-fluorescent for GFP, suggesting that the cells that survived selection did not express a significant amount of shRNA. (E) Two clonal lines derived from each of the non-targetting pSUPER.GFP or Zic3-pSUPER.GFP vectors were assayed for expression of Zic3. The results indicated that, despite lack of GFP fluorescence, Zic3 expression was reduced by 60% in the Zic3 knockdown lines relative to non-targeting controls.

demonstrating that Zic3 transient knockdown resulted in ES cell differentiation (Figure 22B).

Following three weeks of antibiotic selection, robust levels of GFP expression were observed in the non-targeting knockdown cells (Figure 28C), indicating that the pSUPER.GFP vector was stably expressed in cells undergoing long-term passage. In contrast, the Zic3 knockdown cells revealed a striking lack of GFP expression (Figure 29C). This observation was surprising as colonies emerging from long-term passage of pSUPER.GFP cell lines were generally observed to have high levels of GFP fluorescence (See Appendix 4 for illustration of GFP-expressing colonies derived from knockdown an unrelated gene, *CoupTFII*). The lack of GFP expression is therefore unique to the *Zic3* knockdown cells, and it suggests that colonies present after three weeks resulted from low expression levels from the shRNA construct that conferred sufficient antibiotic resistance for cell survival, but reduced knockdown efficiency.

Clonal cell lines were derived from the non-targeting and *Zic3* knockdown cells by expansion of individual colonies at 3 weeks. Two cell lines per construct were assayed for *Zic3* expression, and the results indicate that *Zic3* was downregulated by 60% in the *Zic3* knockdown lines relative to the control lines. This knockdown is less robust than in the transient *Zic3* knockdowns where depletion of *Zic3* expression by 70% to 80% was observed (Figure 21a). The results therefore support the hypothesis that the Zic3 clonal lines resulted from a subset of transfected cells that maintained *Zic3* shRNA expression at decreased

levels, thus allowing a degree of proliferation that was compatible with long-term passage.

3.2.4.2 Endoderm genes are upregulated in Zic3 clonal knockdown lines

The *Zic3* knockdown lines derived from the non-fluorescent construct (pSUPER-Zic3) were assayed to determine the expression profile of pluripotency and lineage marker genes. As observed with the cell lines from pSUPER.GFP (Figure 29E), *Zic3* expression was downregulated approximately 60% relative to vector-only lines (Figure 30a). The pluripotency genes *Oct4* and *Sox2* were reduced between 20% to 30% relative to controls in all three clonal knockdown lines, while Nanog was reduced by 80% (Figure 30a). The endodermal genes *Pdgfra, Gata4, Gata6,* and *Sox7* were 30-fold higher than in the controls, while *Sox17* was upregulated between 60- to 80-fold, and *FoxA2* was increased by 80- to 120-fold in all three *Zic3* knockdown lines (Figure 30b). The induction of endodermal markers here was substantially greater than observed in the transient Zic3 knock-downs. Expression of mesendoderm, mesoderm, ectoderm, trophectoderm and Wnt-related genes remained essentially unchanged (<2-fold) in the Zic3 knockdown lines (Figure 30c). Thus the specific upregulation of endodermal gene expression in the clonal lines is consistent, and in fact more pronounced, with the observations in the transient knockdowns (Figure 23). It would be interesting to evaluate the *Zic3* knockdown effect in a range of clonal lines in further experiments, to correlate varying *Zic3* levels with the extent of endoderm marker upregulation.

3.2.4.2 Endoderm protein expression is upregulated in Zic3 clonal knockdown lines

To ascertain if there were corresponding increases in endodermal protein levels, immunocytochemistry was performed against FoxA2, Gata6 and PDGFRA in the clonal lines. The *Zic3* knockdown lines consistently demonstrated robust endodermal marker staining (Figure 31A) that was absent in the vector control lines (Figure 32). Oct4 staining was also observed in the cells that were positive for endodermal marker expression (Figure 31A). Interestingly, although the *Zic3* clonal knockdown lines expressed Oct4 and SSEA-1 (Figure 31B), Nanog protein expression was significantly reduced relative to the vector control lines (Figure 33). This corroborated with my earlier observation that Nanog gene expression levels were down-regulated in the Zic3 knockdown lines (Figure 30A) and raises the possibility that Nanog gene expression is directly regulated by Zic3.

3.2.5 Zic2 is able to partially compensate for the function of Zic3

Zic3 belongs to a family of transcription factors with five member proteins (Zic1 – Zic5) encoding five consecutive C_2H_2 zinc finger domains which are highly conserved across species[186,187]. In addition, the Zic family members show distinct and partially overlapping expression patterns during development[115,116]. *Zic3* shares 64% and 59% homology with the *Zic1* and *Zic2* genes respectively, and this homology increases to 91% within the zinc finger domain. It was therefore interesting that *Zic3* RNAi resulted in a 2-fold increase in *Zic2* (Figure 34a),

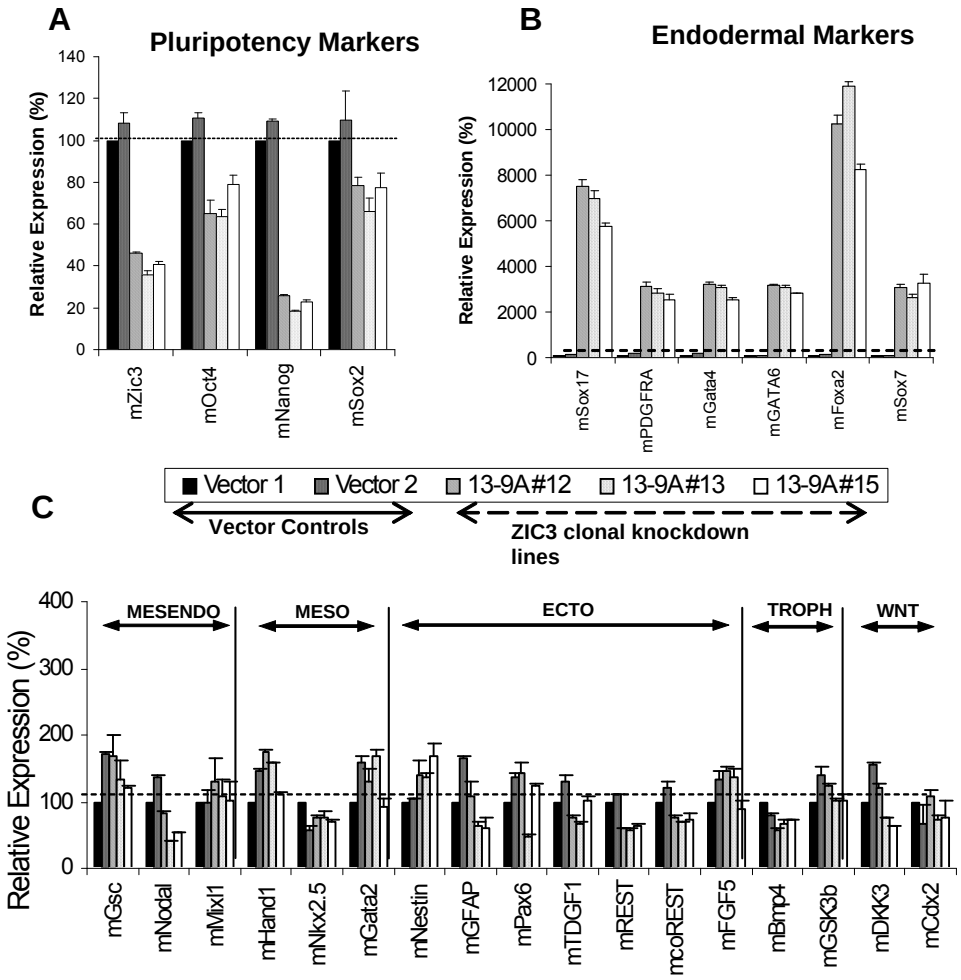

Figure 30. Zic3 knockdown clonal lines demonstrate endodermal gene marker specification. Three Zic3 knockdown clonal lines and 2 vector controls were assayed as indicated in the diagrams. (A) The pluripotency markers Oct4 and Sox2 were slightly down-regulated between 20 to 30%, while Zic3 and Nanog decreased significantly between 60 to 80% relative to the vector controls. (B) All endodermal markers assayed in the knockdown lines were significantly upregulated between 20- and 120-fold relative to the control lines. (C) Mesendodermal, mesodermal, ectodermal, trophectodermal and Wnt pathway genes did not change significantly in knockdown lines, demonstrating less than 2-fold changes relative to the vector controls. Gene expression levels were assayed by Real-time PCR. The experiments were performed in biological triplicate with two technical duplicates and normalized to endogenous Beta-actin. Mean values ± S.E. are plotted as percentages relative to the vector control.

raising the possibility that *Zic2* may be compensating for the reduction in *Zic3* levels. *Zic2* is expressed in ES cells and its expression is downregulated upon differentiation[85,86]. *Zic2* may also be regulated by Nanog as binding sites for this TF have been mapped to the Zic2 gene by chromatin immunoprecipitation (Figure 35); however the functional regulation of Zic2 by Nanog remains to be tested. Knockdown of *Zic2* expression by siRNA (75% reduction in RNA levels) did not produce any effect on lineage marker expression (Fig 34b).

In order to determine if *Zic2* compensated for the absence of *Zic3*, I performed a double RNAi experiment against *Zic2* and *Zic3* in ES cells. The double knockdown prevented *Zic2* levels from increasing in a compensatory manner as observed in the *Zic3* single knockdown (Figure 34c). Interestingly, endodermal specification was markedly enhanced following the *Zic2* and *Zic3* double knockdown as demonstrated by increased expression of *Sox17* (4.7-fold), *Pdgfra* (8.7-fold) and *Gata4* (3.1-fold), which is more robust than observed for all three markers (*Sox17*, 3.1-fold; *Pdgfra*, 3.3-fold; *Gata4*, 1.5-fold) when *Zic3* alone was reduced (Figure 34d). The results therefore indicate that, in the absence of *Zic3*, *Zic2* is able to partially compensate and downregulate endoderm gene specification in a global assay of ES cell expression.

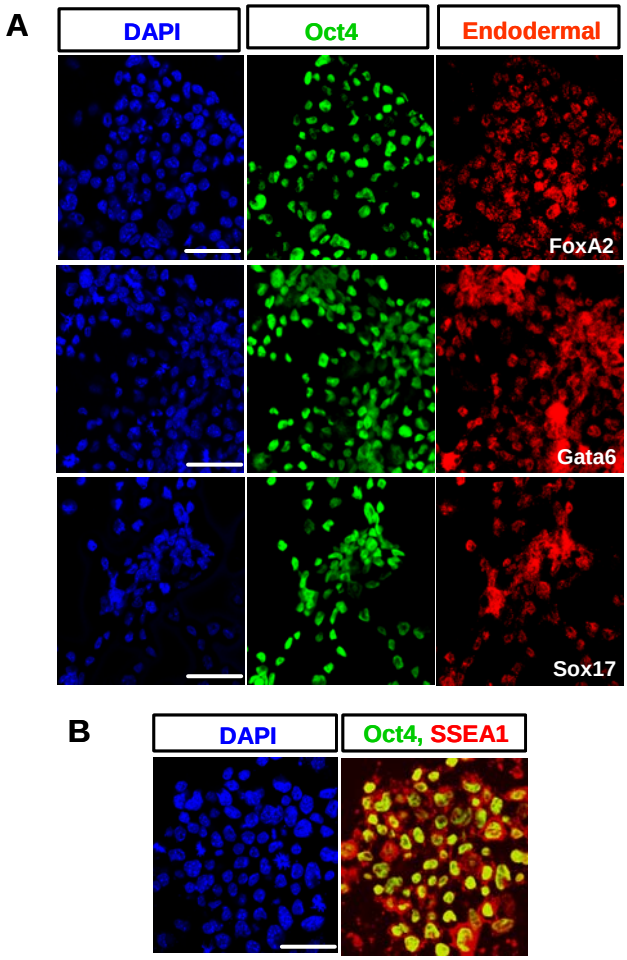

Figure 31. Protein expression in Zic3 knockdown clonal lines. (A) Oct4 protein expression was high in all three Zic3 knockdown lines, and the expression of specific endodermal marker proteins Foxa2, Gata6 and Sox17 was observed in the same cells. (B) The Zic3 knockdown lines expressed stem cell surface protein, SSEA-1, which is specific to murine ES cells. Scale bars represent 100 μm.

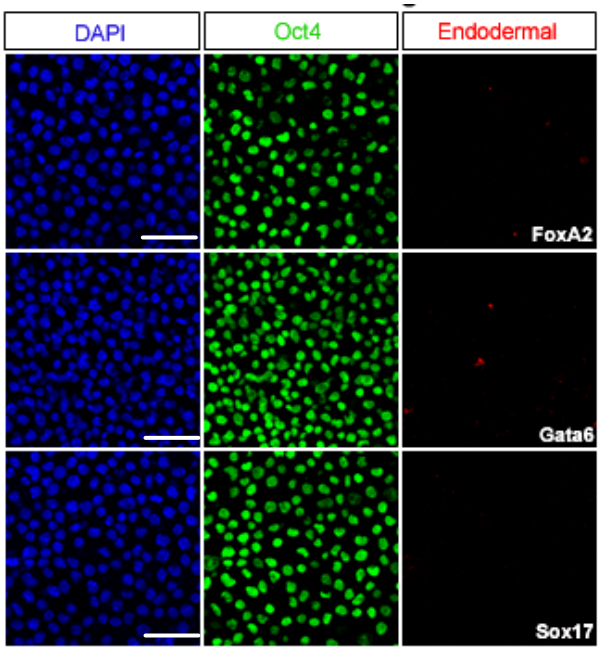

Figure 32. Endodermal marker staining for E14 cells. The negative staining here demonstrates specificity of positive staining for Zic3 knockdown clonal lines in Figure 31. Scale bars, 100 μm.

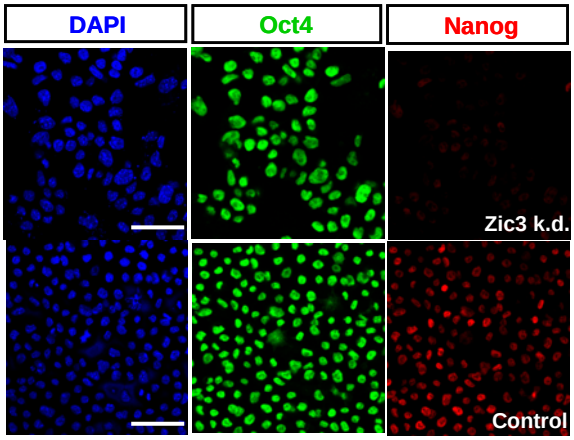

Figure 33. Nanog expression in the Zic3 knockdown lines. The Zic3 clonal knockdown lines demonstrated a significant decrease in Nanog expression.

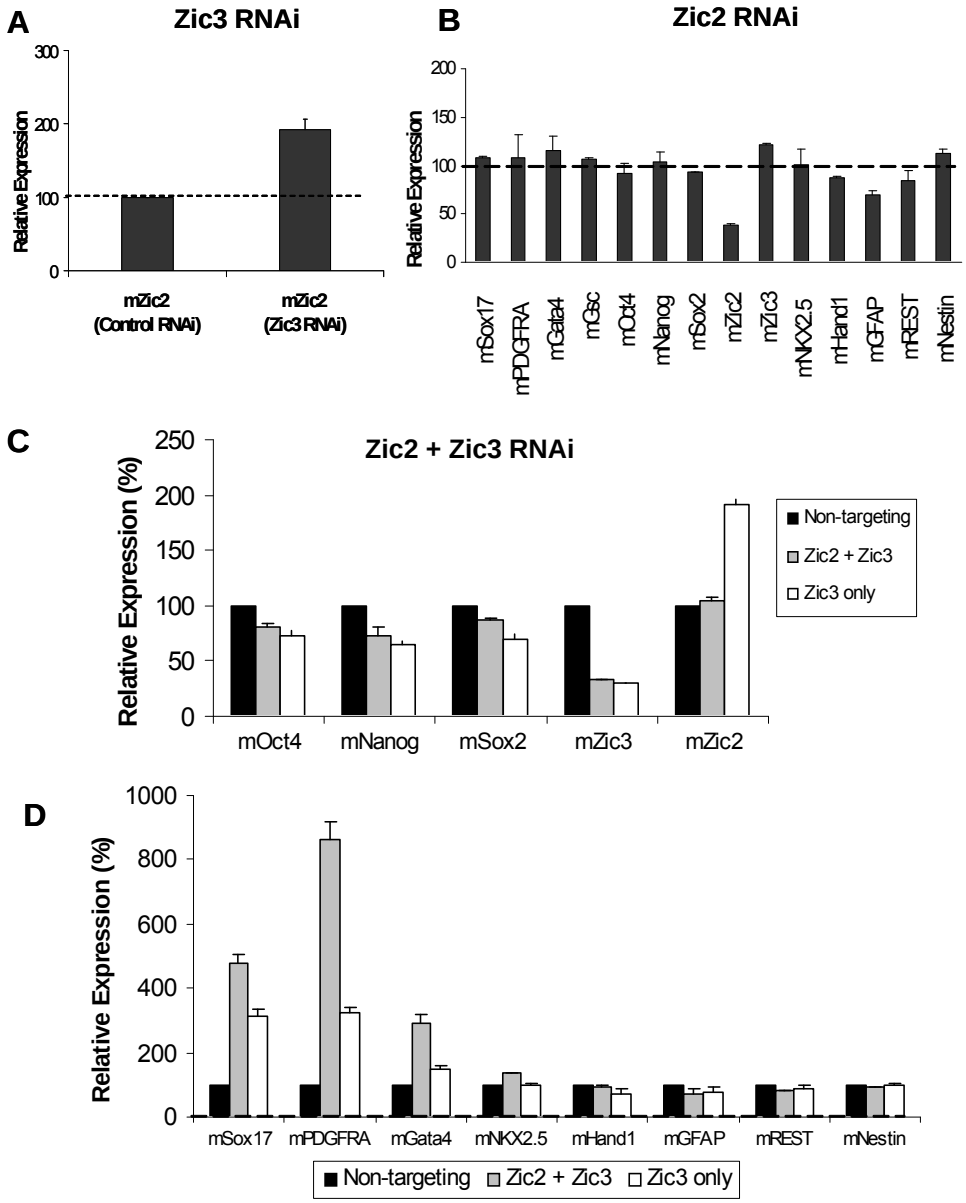

Figure 34. Effect of Zic2 and Zic3 double knockdown. The genes were assayed by Real-time PCR in triplicate and normalized to a Beta-actin control. Mean levels ± S.E. are expressed as percentages relative to the non-targeting control. (A) Zic2 gene expression increased 2-fold with Zic3 transient knockdown four days after transfection. (B) Zic2 knockdown by siRNA was specific but did not produce changes in lineage markers assayed. (C) Zic2 and Zic3 co-knockdown produced specific knockdown of Zic3 and at the same time prevented compensatory increase of Zic2 expression in ES cells. (D) The expression of endodermal lineage markers Sox17, PDGFRA and Gata4 showed a similar pattern of up-regulation as in the Zic3 single knockdown, but was substantially enhanced in this Zic2/Zic3 co-knockdown.

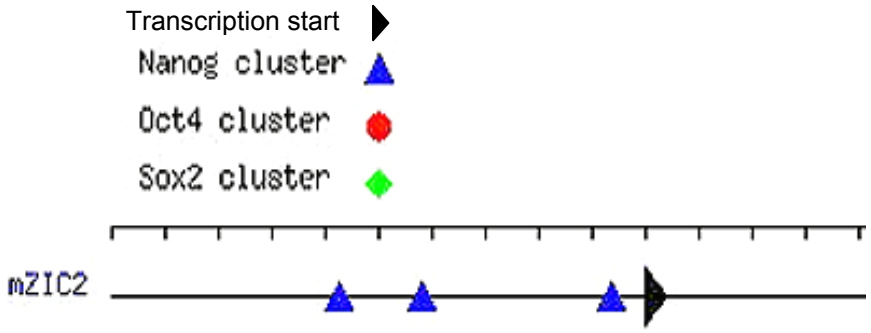

Figure 35. A summary of Oct4, Nanog and Sox2 binding sites on the Zic2 promoter. Oct4 and Sox2 binding sites were not present in this region, and three Nanog binding sites were located upstream of the Zic3 transcription start site (Loh *et al.*, 2006; Sox2). Each unit on the scale represents 10 kb.

3.3 Discussion

3.3.1 Zic3 expression is associated with the key regulators of pluripotency in ES cells.

The work presented in this chapter demonstrates that Zic3 plays a key regulatory role in controlling ES cell differentiation. Here I have demonstrated that the expression pattern of Zic3 in ES cells corresponds closely with that of known regulators of pluripotency Oct4, Nanog, Sox2, which have high levels of expression in the undifferentiated state and decrease rapidly upon differentiation (Figure 17). The findings in mouse ES cells are consistent with results from human ES cells[85]. The differences observed in Zic3 expression levels between pluripotent and early differentiation phases imply a potentially significant role for Zic3 in ES cell pluripotency. In addition, chromatin-IP mapping by us and others has revealed Oct4, Nanog and Sox2 co-occupancy on the *Zic3* regulatory region, suggesting that *Zic3* may be co-ordinately regulated by Oct4, Nanog and Sox2 in mouse and human ES cells[19,20] (Figure 19). These observations together led to my hypothesis that Zic3 functions to maintain the pluripotent state of ES cells. Here I characterized the relationship of Zic3 with that of the key stem cell regulatory factors, and uncovered a role for Zic3 in the maintenance of ES cell pluripotency.

3.3.2 Zic3 functions downstream of Oct4, Nanog and Sox2 and is positively regulated by these factors.

My first objective was to assess the nature of interactions between Oct4, Nanog and Sox2 with the *Zic3* regulatory region. This was addressed using a combinatorial approach that encompassed the results of chromatin-IP mapping

and RNAi, to demonstrate that ablation of Oct4, Nanog and Sox2 in mouse ES cells resulted in a significant decrease in *Zic3* expression (Figure 20 A-B). Since *Zic3* was previously implicated as a target of Oct4, Nanog and Sox2 in ChIP experiments[19,20], the concern of non-direct or secondary effects of RNAi was significantly reduced[45]. Thus it is likely that the binding of Oct4, Nanog and Sox2 to the *Zic3* gene regulatory region serves to enhance target gene expression, such that the key pluripotency regulators function as transcriptional activators of *Zic3* in ES cells (Figure 36). This point is underscored by the results with Nanog over-expression and binding site mutagenesis assays, which indicate a positive association between Nanog binding and Zic3 expression (Figure 20 D-F). These results therefore reveal positive functional interactions between the key pluripotency regulators and the Zic3 *gene* regulatory region.

Since transcriptional networks are also known to feature auto-regulatory loops[45,48], I also asked if the inverse relationship was true – that is, whether Zic3 regulates expression of the key regulatory genes. Here I observed that *Oct*4 and *Sox2* levels remained slightly perturbed by the ablation of *Zic3* expression (Figures 521A and 30A). In the absence of clear changes despite a robust Zic3 knockdown, the above data places *Zic3* downstream of Oct4 and Sox2 in the ES cell transcriptional networks as illustrated in Figure 36. In addition, the immunostaining experiments revealed a significant decrease in Nanog expression within the *Zic3* clonal knockdown lines (Figures 30A and 33).

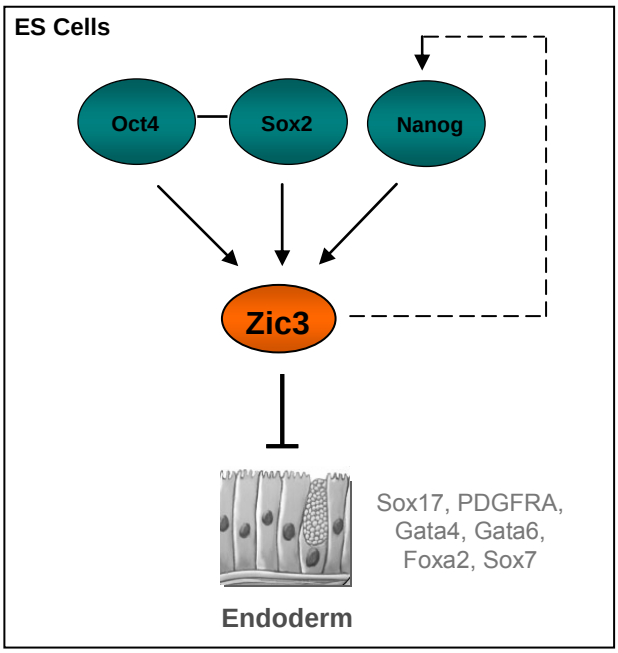

Figure 36. A model of Zic3 function in embryonic stem cells. Zic3 contributes to the maintenance of pluripotency by operating downstream of Oct4, Nanog and Sox2 to inhibit endoderm lineage specification as characterized by endodermal markers Sox17, PDGFRA, Gata4, Gata6, Foxa2 and Sox7. The presence of Zic3 also maintains the expression of the homeodomain protein Nanog, a key regulator of pluripotency in embryonic stem cells.

3.3.3 Zic3 maintains pluripotency by blocking endodermal differentiation in ES cells

Embryonic stem cells are derived from the inner cell mass of the blastocyst and, as such, are able to undergo unlimited self-renewal and differentiation into the three germ layers of the embryo – mesoderm, ectoderm and endoderm[2,3]. In the pluripotent state, ES cells remain undifferentiated and do not express specific lineage markers. I was interested in examining the effect of *Zic3* knockdown on the maintenance of ES pluripotency using specific lineage markers as an assessment of differentiation following *Zic3* knockdown. Here I demonstrate that ablation of *Zic3* expression in both mouse and human ES cells resulted in a significant increase in markers of endodermal lineage (Figures 23, 30B and 31). These results suggest that Zic3 may have an important role in preventing endodermal specification in ES cells.

Many reports support this observation: Firstly, *Zic3* knockdown in ES cells induced expression of *Gata4* and *Gata6*, and forced expression of *Gata*4 and *Gata6*in ES cells result in differentiation towards extraembryonic endoderm[84]. Further strengthening this association is the fact that all other endodermal markers assayed (*Pdgfra, Sox17* and *FoxA2*) are also expressed in extraembryonic endoderm derivatives[190]. Secondly, Zic3 regulates *Nodal* expression through direct interaction with its promoter during gastrulation and it has been shown that *Nodal* expression is essential in proper specification of the embryonic visceral endoderm[191]. This significance is underscored by studies reporting that the earliest abnormalities observed in *Zic3*-null mice are defects in proper patterning of the anterior visceral endoderm[158]. Finally, *Zic3* clonal knockdown lines exhibit a significant decrease in *Nanog* gene expression (Figure

30A and 33), and several groups have reported that RNAi-mediated depletion of *Nanog* expression resulted in an induction of extraembryonic endoderm markers *Gata4* and *Gata6*[39,192,193].

The results in this chapter indicate that Zic3 functions as a gatekeeper of pluripotency in ES cells by preventing their differentiation into cells that express endodermal markers. Corroborating with this, a significant reduction in Nanog expression was observed in the Zic3 clonal lines. This reduction is noteworthy as Nanog is a key regulator of pluripotency in ES cells[78], and it is well-established that disruption of Nanog expression results in development of extraembryonic endoderm character in ES cells[39,192,193]. Thus, I demonstrate here an important role for Zic3 in the maintenance of pluripotency in ES cells through prevention of endodermal lineage specification, and suggest that its action may in part be mediated through the key pluripotency regulator Nanog (Figure 36).

The role of Zic3 in preventing endodermal specification is further supported by evidence indicating its restricted expression within the mesoderm and ectoderm lineages during gastrulation[186]. In addition, Zic3 activity has been specifically implicated in the mesodermal and ectodermal molecular pathways in the early developing embryo[123,126-128]. These data in combination with the results in this chapter suggest that while Zic3 is instructive for mesodermal and ectodermal specification in embryonic development, it may simultaneously function as a repressor of ectopic endodermal induction in these tissues. To determine this it would be interesting to examine the differentiation capacity of *Zic3* knockdown and overexpressing cells in teratoma formation *in vivo*. In addition *Zic3*-null ES

cells may be assayed for their lineage markers under conditions that maintain ES cell pluripotency and when induced to differentiate.

3.3.4 Zic2 works in concert with Zic3 to reduce endodermal specification in ES cells

The transcription factor Zic3 shares five highly-conserved Zinc finger domains with family members Zic1, Zic2, Zic4 and Zic5[98,101,102,106]. Their partially overlapping spatial and temporal patterns of expression during early development suggests potential functional redundancy between the Zic family members[115,116]. When Zic3 expression was reduced in ES cells, an increase in *Zic2* gene levels was observed (Figure 34A). The mechanism for this upregulation remains unknown and may be addressed by an investigation of transcriptional regulators which occupy the *Zic2* promoter in ES cells. However, since *Zic2* is also differentially expressed between pluripotent and differentiation states of ES cells[85,86] and binding of the key pluripotency transcription factor Nanog has been mapped to the *Zic2* regulatory region (Figure 35), I reasoned that Zic2 may participate in the regulation of ES cell pluripotency along with Zic3.

In order to unveil the possible effects of functional redundancy between Zic2 and Zic3, a double knockdown was performed in mouse ES cells. The results indicate that repression of *Zic2* and *Zic3* expression significantly enhanced endoderm specification in ES cells (Figure 34C). The evidence that Nanog binds to the *Zic2* regulatory region suggests that it may be involved in similar pathways as Zic3 in repressing endoderm expression. Thus, Zic2 and Zic3 may participate in redundant or partially overlapping networks to silence endoderm specifying gene

expression and contribute to the maintenance of pluripotency in ES cells. It would be interesting to examine the binding targets of Zic2 to determine if it shares common targets with Zic3 to account for this redundancy.

3.4 Summary

I have demonstrated in this chapter that Zic3 is present in ES cells and that its expression is quickly repressed as the cells begin to differentiate. The expression of *Zic3* in pluripotent ES cells is also directly regulated by Oct4, Sox2, and Nanog. In addition, targeted repression of *Zic3* in both human and mouse ES cells by RNAi induced expression of several markers of the endodermal lineage. Notably, the expression of Nanog, a key pluripotency regulator and repressor of extraembryonic endoderm specification in ES cells, was significantly reduced in *Zic3* knockdown cells. This suggests that Zic3 may prevent endodermal marker expression through Nanog-regulated pathways, and that it is important in maintaining ES cell pluripotency by preventing differentiation of cells into endodermal lineages.

CHAPTER 4:

Zic3 interacts with Sox2 in ES cells

4.1 Introduction

Zic3 operates directly downstream of Oct4, Nanog and Sox2, and maintains the pluripotent state by preventing ES cells from differentiating into the endoderm lineage. These results place Zic3 within an important loop in association with the key pluripotent factors. In addition, it was recently shown that retrovirus-mediated infection of four ES cell transcription factors (Oct-3/4, Sox2, KLF4 and c-Myc) into mouse fibroblasts resulted in induced pluripotent stem (iPS) cells[93]. A recent microarray analysis of fully and partially re-programmed iPS cells revealed an upregulation of Zic3 in these cells relative to their original differentiated fibroblast states[194]. This further supports the idea that Zic3 may be at least partially involved in the process of restoring the properties of self-renewal and pluripotency during reprogramming of differentiated cells.

While the role of Zic3 in maintenance of the pluripotent state has been established, the detailed molecular pathways in which Zic3 operates in ES cells remain as yet unknown. I was therefore interested to elucidate the network of global targets regulated by Zic3, and to uncover its hitherto unknown interactions with other ES cell-associated proteins. To this end, I reported in the previous chapter that Zic3 positively regulates the expression of Nanog in ES cells in a manner similar to that of the Oct4/Sox2 heterodimer on the Nanog promoter[82,83]. Here I conducted experiments to address my hypothesis that Zic3 binds with Oct4 and/or Sox2 protein to regulate activity of the Nanog promoter, and in extension, the promoters of their common target genes in ES cells.

4.2 Results

4.2.1 Zic3 interacts with Sox2 in embryonic stem cells

In order to address my hypothesis that Zic3 is an interacting partner of the Oct4/Sox2 transcription complex, experiments were conducted to examine the capacity of Zic3 to associate with the core ES cell regulatory proteins. Here Zic3 co-immunoprecipitation (Co-IP) was performed using the Seize-X Protein G Co-IP kit (Pierce Biotechnology). This method allowed the cross-linking of Co-IP antibodies to the column to prevent their elution with the target protein complex, hence eliminating the problem of contaminating antibody heavy/light chain bands in the sample (Figure 37). To ensure adequate release of captured proteins, immunoprecipitated complexes from ES cell nuclear extracts were eluted from the column in two consecutive fractions. Following Zic3 co-IP (Figure 38), western blots were used to confirm the presence of Zic3 (55 kDa) in both eluted fractions. I subsequently checked for the presence of Sox2 and Oct4 within these fractions and found a clear Sox2 band (32 kDa) in the first eluted fraction. The Oct4 protein (47 kDa), in contrast, was not detected in the samples. These results indicate that Zic3 and Sox2 are interacting partners in ES cells.

Inverse experiments were performed to verify these observations. Corroborating with results from the Zic3 pull-down, the Oct4 co-IP yielded Oct4 protein at 47 kDa but no trace of Zic3 protein in both fractions (Figure 38). In contrast, the Sox2 co-IP yielded Sox2 and Zic3 protein in both eluted fractions (Figure 38; 32 kDa and 55 kDa respectively). To ensure that the Co-IP proteins were specifically pulled down by the antibodies used, a control pull-down was performed using

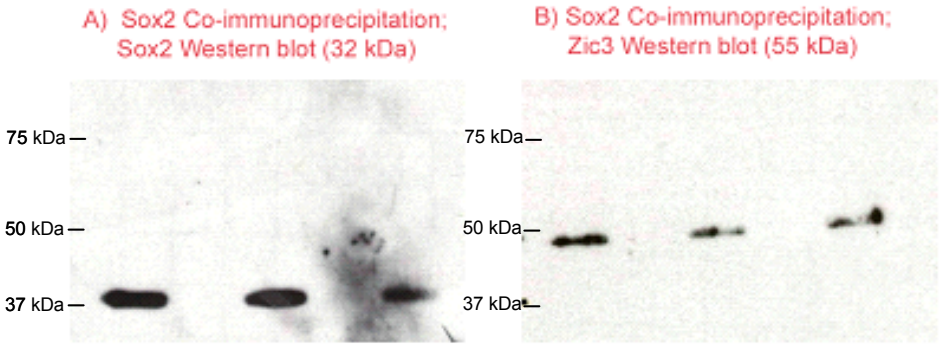

Figure 37. Sox2 Co-immunoprecipition with the Seize-X Protein G Co-IP kit (Pierce Biotechnology). Fractions 1 - 3 are displayed. (A) Presence of Sox2 protein in Sox2 Co-IP samples at 32 kDa. (B) Presence of Zic3 protein in Sox2 Co-IP samples at 55 kDa. Detection of a single protein species at the expected size confirms the specificity of the assay. Unlike traditional Co-IPs, antibodies are cross-linked to Seize-X columns and do not elute with protein complexes. The absence of additional bands in the Sox2 blot (A), for which the secondary antibody used is cross-reactive with the original co-IP antibody, indicates the lack of contamination by the Co-IP antibody's heavy and light chains (50 and 20 kDa respectively).

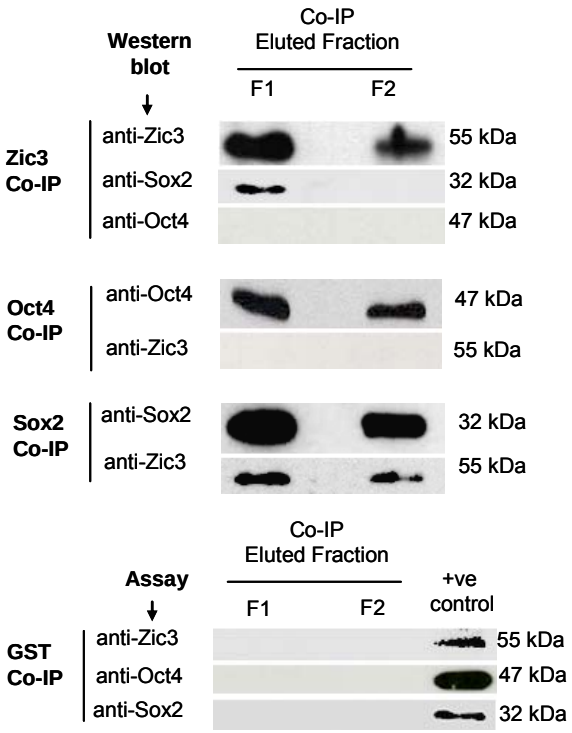

Figure 38. Zic3 and Sox2 interact in embryonic stem cells. Zic3 and Sox2 are co-immunoprecipitated in mouse ES cells (55 kDa and 32 kDa respectively), while pull-downs for Oct4 and GST did not result in Zic3 or Sox2 precipitation. Positive controls for Zic3, Oct4 and Sox3 were included to ensure sensitivity and specificity of the assay.

antibodies against GST. In these control samples, no Zic3, Oct4 or Sox2 was detected (Figure 38). Total mouse ES nuclear extract was included to confirm that western blot conditions were specific and sensitive to detect Oct4, Sox2 and Zic3. Taken together, the above results suggest that Zic3 interacts specifically with Sox2 in ES cells.

4.2.2 Zic3 shares regulatory pathways with Sox2 in ES cells

I hypothesized that as interacting partners, Zic3 and Sox2 will share regulatory pathways in mouse ES cells. To test this possibility, RNA interference of *Sox*2 and *Zic3* were performed in biological triplicate to identify commonly regulated genes. After 4 days of Zic3 knockdown, the expression of Zic3 was reduced by 80% relative to the non-targeting control (Figure 39A). In response to Zic3 knockdown, Oct4, Nanog and Sox2 expression levels were down-regulated 20%, 40% and 30%, respectively (Figure 39A).

Global gene expression changes in the RNAi samples were assayed with Illumina bead chip arrays. In response to the depletion of endogenous Zic3, a total of 1122 genes were found to be significantly regulated, of which 609 genes were up-regulated and 513 genes were down-regulated (≥1.5 fold, FDR 0.1). The complete list of genes is provided in Supplementary Tables 1A and 1B. A parallel analysis of gene expression changes was performed in ES cells after 4 days of Sox2 knockdown, where I found that the levels of *Sox2, Oct4, Nanog* and *Zic3* were down-regulated by 80% or greater relative to the non-targeting control (Figure 39B). The global gene expression assay on the *Sox2* knockdown cells

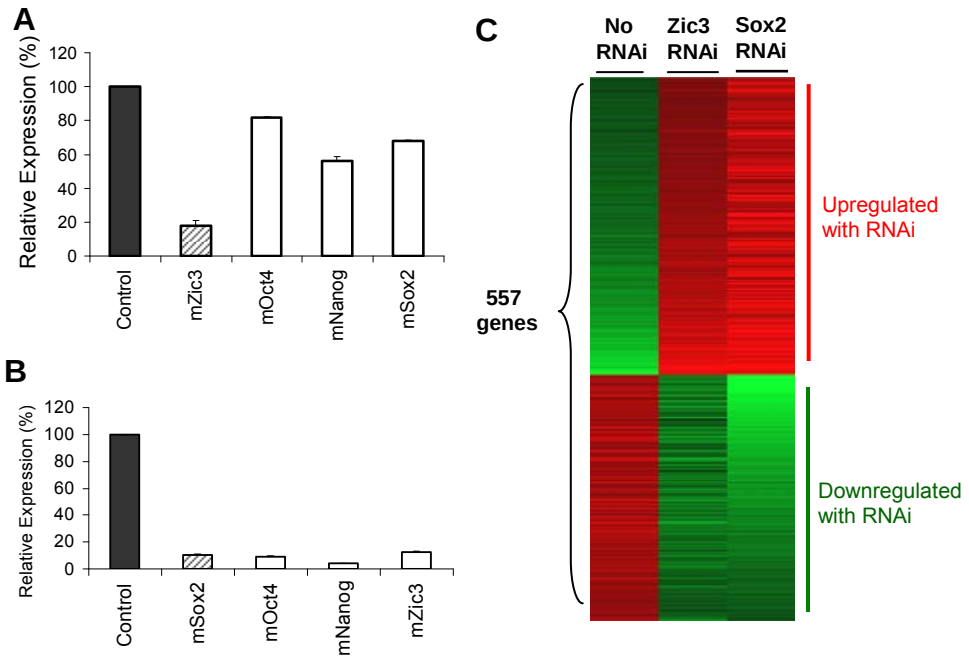

Figure 39. Gene expression profiles for Sox2 and Zic3 RNAi (A) Zic3 RNAi results in significant downregulation of endogenous Zic3 expression. The expression of Oct4, Nanog and Sox2 were also downregulated in response to Zic3 knockdown. (B) Sox2 RNAi results in significant downregulation of Sox2 expression in mouse ES cells with Oct4, Nanog and Zic3 levels correspondingly downregulated. (C) Zic3 and Sox2 RNAi samples reveal similar expression profiles for 557 genes (Fold change ≥ 1.5; FDR 0.1).

identified a total of 5445 genes that were differentially expressed (≥1.5-fold, FDR 0.1), with 2733 genes significantly up-regulated and 2712 genes down-regulated (gene lists provided in Supplementary Tables 2A and 2B). Overall, more genes were regulated by the *Sox*2 knockdown (5445 vs.1122) and the *Sox2* knockdown generally resulted in greater gene expression changes than *Zic3* knockdown. This suggests that while Zic3 and Sox2 co-regulate a subset of genes, the Zic3 transcriptional network is slightly less influential than that of Sox2.

The sets of differentially expressed genes from the Zic3 and Sox2 knockdowns were then compared, and the results indicated that 557 genes were similarly regulated in the Zic3 and Sox2 knock-down cells (Figure 39C). To assess the statistical significance of the 557 similarly regulated genes, I examined the *Zic3* and *Sox2* RNAi overlaps in greater detail (Figure 40). Amongst the genes that were up-regulated 1.5-fold or greater, 304 out of 609 genes (50%) that changed as a result of *Zic3* RNAi were similarly regulated by *Sox*2 RNAi (Figure 40A). An overlap of only 11% ± 1.3 was expected by random sampling, thus indicating that the actual 50% overlap is highly significant (p-value = 1.9725×10^{-147}). Likewise, 253 of 513 genes (49%) that were down-regulated by *Zic3* RNAi were similarly affected by *Sox2* knockdown, while an overlap of 10.7% ± 1.3 was expected by chance ($p < 6.9763 \times 10^{-146}$; Figure 40B). These results demonstrate that Zic3 and Sox2, which we have shown to physically interact, co-regulate hundreds of genes in ES cells[19,20].

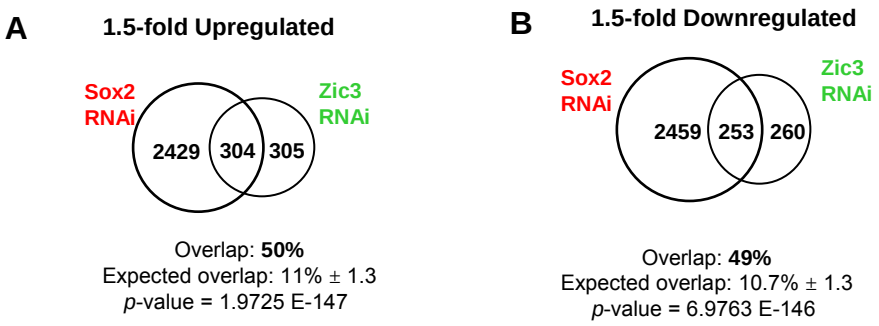

Figure 40. Significant overlap of Zic3 and Sox2 RNAi-regulated genes (A) Zic3 and Sox2 RNAi genes 1.5-fold upregulated and above show statistically significant overlap. (B) An overlap of Zic3 and Sox2 RNAi 1.5-fold downregulated and below is statistically significant.

To understand the biological implications of the gene network co-regulated by Sox2 and Zic3, the list of 557 genes was uploaded to the Panther database for biological process annotations[195]. In this analysis, the genes were clustered into functional themes and compared to a reference list to look for statistically over (+) and under-represented (-) pathways. Here I found 26 biological processes that were significantly over- or under-represented relative to all genes on the Illumina bead arrays ($p < 0.01$, Supplementary Table 3). Of these 26 pathways, the 12 highlighted in Table 7 may be broadly clustered under developmental- or stem cell-related themes. For comparison, the total number of genes from the Illumina reference list for each category is presented (#Ref list). Based on random sampling of 557 genes from the reference list (equivalent to the total number of genes in input list), the number of genes expected to cluster under each pathway is calculated (#Expected). The actual number of genes that changed as a result of RNAi (#Observed) was then compared with the #Expected to derive a *p*-value by Binomial testing. The biological processes in Table 7 are significantly over-represented in both the *Zic3* and *Sox2* RNAi gene sets. Supplementary tables 4 A - D provide the full lists of genes that cluster under each pathway. These annotations suggest that Zic3 and Sox2 are interacting partners that co-regulate pathways involved in early embryonic development, ectoderm and mesoderm specification, oncogenesis and stem-cell related functions. The genes belonging to the endoderm development pathway (Sox17, Gata6, Pdgfra) were also found in the overlapping upregulated gene set between *Zic3* and *Sox2* RNAi. However the endoderm pathway did not rank as statistically significant ($p > 0.05$) with Bionomial testing in the Panther output (Supplementary Table 3).

Table 7. Panther Biological Process annotations for significantly co-regulated genes by Zic3 and Sox2 RNAi

	PANTHER BIOLOGICAL PROCESS	# REF. LIST (Illumina)	# EXPECTED	# OBSERVED	OVER / UNDER	*p*-value
Early	Developmental processes	2057	58.5	106	+	0.0000
embryonic	Embryogenesis	146	4.15	14	+	0.0001
development	Anterior/posterior patterning	66	1.88	7	+	0.0032
Ectoderm	Ectoderm development	654	18.6	37	+	0.0001
	Neurogenesis	573	16.3	30	+	0.0012
	Segment specification	100	2.84	8	+	0.0087
Mesoderm	Mesoderm development	557	15.84	26	+	0.0100
	Muscle contraction	169	4.81	12	+	0.0039
	Muscle development	137	3.9	10	+	0.0066
Stem cell,	Cell proliferation / differentiation	850	54	24.17	+	0.0000
proliferation	Oncogenesis	376	10.69	28	+	0.0000
& oncogenesis	Oncogene	84	2.39	10	+	0.0002

Table Legend

REFERENCE - No. of genes from Reference list that clustered under specfic Panther category (Agilent mouse promoter array gene list)

OBSERVED - No. of ChIP target genes that clustered under specfic category

EXPECTED - No. of ChIP target genes that were *expected* under specfic category

OVER/UNDER - No. of observed genes vs. expected (indication of over or underrepresentation)

P-value - Probability that the number of genes observed in this category occurred by chance (Categories with $p<0.01$ are highlighted)

4.2.3 Zic3 and Sox2 co-occupy physical binding sites in mouse ES cells

Given the evidence that Zic3 and Sox2 physically interact and co-regulate developmental pathways, I hypothesized that common binding locations exist between Zic3 and Sox2 in the mouse ES genome. To address this hypothesis, chromatin immunoprecipitation (ChIP) experiments were conducted for both Zic3 and Sox2, and subsequently assayed for enriched binding sites using a mouse promoter array (Agilent Technologies, CA). These ChIP-chip arrays contain 2 x 244K probes, which interrogate promoter regions of ~17,000 transcripts. Two biological replicates were performed for each experiment.

The Zic3 ChIP-chip analysis yielded 665 significantly enriched probes at the stringent cut-off $p < 0.001$ (Supplementary Table 5). Due to the fact that maximum chromatin shear size was 500 bp, multiple 60-mer probes on the tiled array were often enriched in close proximity to each other. To account for redundant probe enrichments, each 60-bp probe was extended equally on each end to a length of 500 bp. These extended regions were then compared, and overlapping regions were merged to define unique Zic3 target regions. Using this analysis, a total of 379 Zic3 unique target promoter sites were identified (Appendix 5). A similar analysis was conducted for the Sox2 ChIP-chip samples; a total of 4400 60-mer probes were significantly enriched at $p < 0.001$ (Supplementary Table 6). These probes were extended to 500bp and then overlapped to yield a total of 1764 unique genomic locations that are occupied by Sox2 in ES cells (Appendix 6).

I was interested to determine the extent of co-binding between Zic3 and Sox2. Thus, the ChIP-chip results for Sox2 and Zic3 were compared and I found that 48.8% (185 out of 379) Zic3-enriched sites were also occupied by Sox2 (Figure 41A; details in Supplementary Table 7). This overlap was highly significant ($p < 3.69e^{-187}$) relative to an expected overlap of 5.95 ± 2.42 sites based on 100 simulations. I examined the overlaps in greater detail to determine the physical binding distance between the most highly enriched Zic3 and Sox2 probes. Figure 41B indicates that the location of the highest enriched probes for both Zic3 and Sox2 ChIPs coincided in 87 out of 185 co-bound regions (48%). This resulted in a sharp peak in the graph at 0 bp which rapidly declined further away from the Zic3 probe. These results suggest that Zic3 and Sox2 bind in very close proximity within the mouse ES genome.

Based on the degree of overlap between the most highly-enriched Zic3 and Sox2 probes, I hypothesized that Zic3 and Sox2 binding motifs would occur close to each other. The Sox2 motif has been well-characterized[20,49]; however, there were no known Zic3 motifs in the context of the ES genome. Thus, I used the binding site data described above to derive a Zic3 consensus binding motif (Figure 42A). In this analysis, 332 high-quality (normalized log2 ratio > 2) enriched 60-mer probes were selected from the list of 665 enriched probes for a *de novo* motif search. The probe sequences were equally extended on both ends to a final length of 300 bp and uploaded to the Weeder search function[196]. From the results, ubiquitously-occurring sequence motifs within promoters were filtered out[197] and the remaining motifs were assessed by frequency of their occurrence

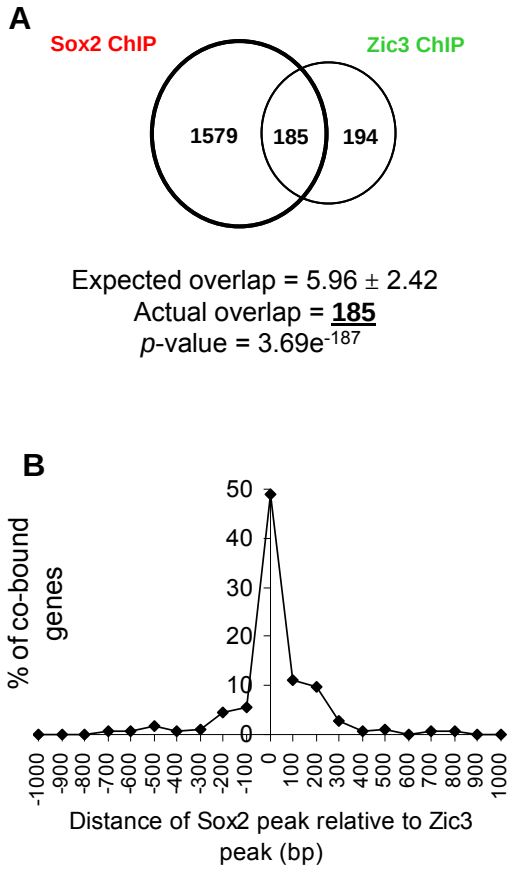

Figure 41. **Zic3 and Sox2 bind common targets in mouse ES cells.** (A) Chromatin-IP revealed 1764 promoter regions occupied by Sox2, and 379 regions occupied by Zic3. An overlap of these Sox2 and Zic3 chromatin-IP target regions is statistically significant. (B) Zic3 and Sox2 ChIP-chip peaks coincide in 48% of common target regions.

A

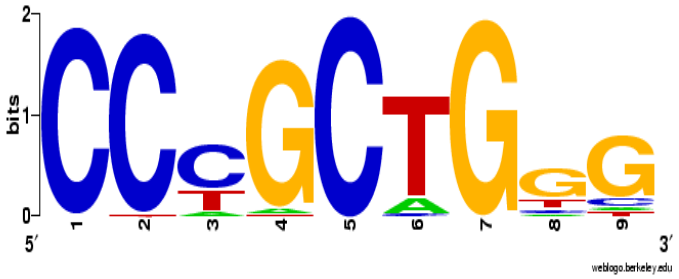

A	0	1	17	10	0	30	0	14	13
C	209	207	131	1	212	7	1	26	25
G	1	0	1	198	0	0	211	132	161
T	2	4	63	3	0	175	0	40	13

B

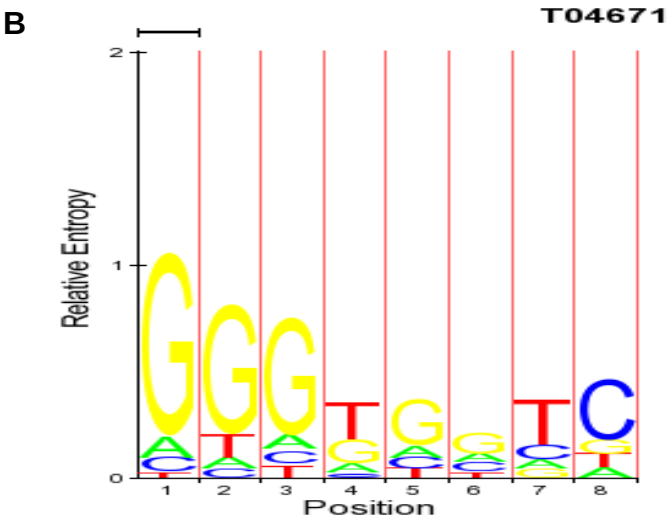

Figure 42. **The Zic3 consensus DNA binding sequence**. (A) A Zic3 consensus binding motif was derived from 212 Zic3 target regions using the Weeder motif search function. (B) A Zic3 binding motif from the T2G database established by Mizugishi et al. 2001. In this assay, 30 random oligonucleotides were incubated with GST-fused Zic3 protein. The DNA sequences bound by Zic3 protein were sequenced to determine the optimal Zic3 binding sequence.

within Zic3-bound sites using a method previously described[20]. From this analysis I identified 3 highly analogous binding motifs that correlated strongly with Zic3 enrichment. An independent search was then conducted for these 3 motifs within all Zic3 enriched regions which identified 212 positive-scoring sites. The native motif sequences were extracted from these 212 sites and aligned to generate the final Position Weight Matrix shown in Figure 42A. This motif shares some similarity with a previously reported Zic3 consensus binding site (Figure 42B; Transfac #T04671[105]). In particular, they both demonstrate heavy preference for the guanine (G) nucleotide. However, due to the fact that a greater number of Zic3 binding sequences were analyzed in these experiments, the Zic3 consensus motif presented here shows overall greater weight, and hence specificity, at each nucleotide position (Figure 42A). The binding affinity of Zic3 to this newly-defined motif may be tested by gel-shift assays and compared to that of the previously established Zic3 motif.

To determine the extent of Zic3 and Sox2 motif co-occurrence, two reciprocal analyses were performed. First, I identified the locations of Sox2 motifs within the 1764 unique Sox2 target regions described in Figure 41A (Appendix 6). I then searched for the presence of Zic3 motifs within 100 bp of the Sox2 motifs and found a total of 945 co-occurring motif regions. Figure 43A shows the relationship between the number of co-occurring motifs identified and their distance relative to the nearest Sox2 motif. Most Zic3 motifs (123 regions) were found within 10 bp of Sox2 motifs. A high number of co-occurring motifs were also found 11 to 20 bp

apart (101 regions). Beyond 20 bp, the frequency of Zic3 and Sox2 co-occurring motifs declined sharply as seen in Figure 43A.

An inverse analysis was performed with the Zic3 target regions described in Figure 41A (Appendix 5). The Zic3 motifs within these regions were identified and their sites scanned for the presence of Sox2 motifs. A total of 158 Sox2 motifs were identified within 100 bp of the Zic3 motif. Similar to the earlier observation (Figure 43A), the greatest number of Sox2 motifs were identified within 10 bps of the Zic3 motif (30 regions) and this frequency declined with separation distance (Figure 43B). Taken together, the above results indicate that Zic3 and Sox2 co-occupy physical sites in the mouse ES genome.

4.3 Discussion

4.3.1 Zic3 and Sox2 regulate a common set of pathways in ES cells

The results in this chapter demonstrate for the first time a physical interaction between Zic3 and Sox2, and evidence for their co-regulation of pathways in ES cells. Sox2 has an extended network involving a greater number of genes that change when its expression is perturbed in ES cells. Although Zic3 appears to directly or indirectly regulate fewer genes than Sox2, a significant proportion of genes that are dependent on Zic3 expression are also similarly regulated by Sox2. These genes cluster into biological pathways that reveal similar roles for Zic3 and Sox2 in the areas of stem-cell related proliferation, early embryonic

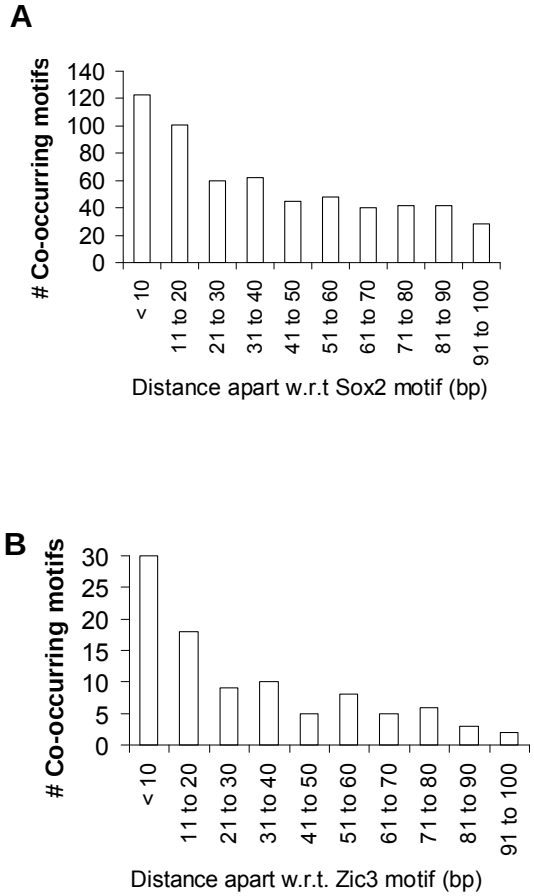

Figure 43. **Zic3 and Sox2 motifs occur in close proxmity in the mouse ES genome**. (A) Zic3-Sox2 motif distances in Sox2 target regions. (B) Zic3-Sox2 motif distances in Zic3 target regions.

development, ectoderm and mesoderm development. Evidence exists in the literature for the independent roles of Sox2 and Zic3 in several of these pathways, and in particular for neural differentiation[72,106,116,126,198,199]. These data provides further validation for the separately established functions of the two transcription factors, and present unique evidence for their co-operative action on genes related to the abovementioned contexts.

In further support of the interaction between Zic3 and Sox2, I highlight binding data demonstrating that they share a significant subset of target genes. Zic3 and Sox2 bind in close proximity on the promoters of their common targets, suggesting that they function as part of what is, at minimum, a heterodimer unit. The idea that Zic3 may associate with an ES cell protein complex is a plausible one, as reports in the literature suggest that many of the core ES cell proteins bind closely to each other [49,51], and Sox2 in particular is known to be a binding partner of Oct4 [19,83]. Hence I examined if Zic3 is associated with the Sox2-Oct4 heterodimer in ES cells. The distance between Zic3-Sox2 ChIP-chip peak enrichments was compared with that of Oct4 ChIP-sequencing peaks[49], and no significant association between the Sox2 and Oct4 binding sites (Supplementary table 8). These results suggest that Sox2 and Zic3 interact to regulate a separate subset of pathways from that of the Sox2-Oct4 heterodimer in ES cells.

4.3.2 Zic3 and Sox2 are interacting partners in ES cells

There are two possible ways in which Zic3 may bind with Sox2, either by direct contact with DNA or indirectly via Sox2 (Figure 44). A previous report suggests that Zic3 is a transcription factor with low binding affinity and is dependent on its

co-partners for specificity[105]. Thus I established three criteria to determine if Zic3 binding is dependent on that of Sox2 in ES cells: First, I assessed whether Zic3 binding sites are always located in close proximity with Sox2, and found that Zic3 sites were distinct from Sox2 in slightly over 50% of Zic3 binding targets (Figure 41A). Second, I examined if it was possible to derive an independent Zic3 motif from its ChIP-determined binding sites, and found that a consensus sequence could be detected in at least 212 Zic3 binding regions.

Third, I reasoned that if Zic3 binding was solely mediated by the binding of Sox2, then a significant association should not exist between the Zic3 and Sox2 motifs. The Sox2 binding motif has been reported as a half-site in the context of heterodimerization with Oct4[19,20,83] and more recently on its own with the use of in-depth ChIP-sequencing techiniques[49]. These Sox2 binding motifs are highly similar and many occurrences of these motifs were found within the Sox2 ChIP-chip peak binding sites, providing further validation of the accuracy of the ChIP results. Upon examination of the Zic3 and Sox2 consensus binding regions, an association between DNA binding motifs for the two transcription factors was observed (Figure 43A & B). Based on this, it is possible to conclude that the Zic3 binding motif is distinct from the Sox2 motif and yet closely associated with it, suggesting that Zic3 binds both in close proximity with Sox2 and comes in direct contact with DNA. It is still possible, however, that the binding of Zic3 is enhanced by the presence of Sox2 or that it is binding to an as yet unknown partner that is responsible for its specificity in ES cells, and these notions remain to be further elucidated with affinity purification and mass spectrometry to identify binding partners of Zic3.

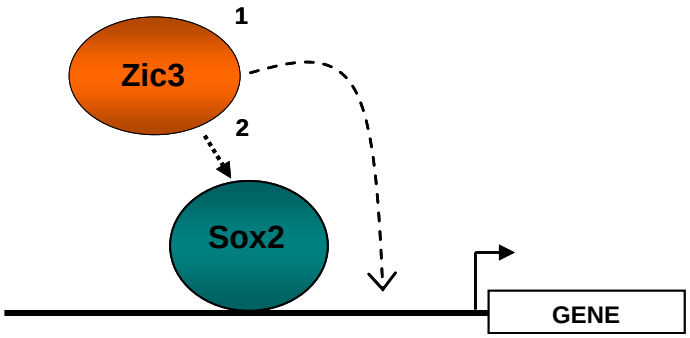

Figure 44. **Possible binding schemes for Zic3 and Sox2 in ES cells.** Zic3 and Sox2 interact in mouse ES cells. Zic3 binds to Sox2 in one of two ways: 1) By direct contact with DNA, or 2) indirectly via Sox2. Our results indicate that Zic3 has a consensus binding motif that is found in close proximity with Sox2, suggesting that Zic3 binds directly to DNA in mouse ES cells.

4.4 Summary

Little was previously known about the regulatory networks that Zic3 employs to maintain pluripotency in ES cells. Thus I have established the global regulatory targets of Zic3 in ES cells and investigated its interactions with other ES cell-associated proteins. A Zic3 consensus binding motif was defined based on DNA sequences isolated by Zic3 chromatin immunoprecipitation (ChIP), and evidence for the co-operative action of Zic3 with Sox2 was presented. These results include: (1) physical interaction between Zic3 and Sox2 proteins, (2) evidence for their common regulatory pathways, and (3) a significant overlap between their target genes. These results suggest that Zic3 binds both in close proximity with Sox2 in ES cells and comes in direct contact with DNA. This chapter therefore presents new evidence for the hitherto unknown interaction between Zic3 and Sox2 in ES cells, and provides unique molecular insight into the question of how Zic3 functions in the maintenance of ES cell pluripotency.

CHAPTER 5:

Zic3 is a regulator of lineage specification during ES cell differentiation

5.1 Introduction

In addition to its role in pluripotency, Zic3 is a positive regulator of embryonic morphogenesis and cardiac, skeletal and neural development[106,115,124,126,129,158]. During early embryogenesis, Zic3 is involved in the initiation of gastrulation and the specification of left-right asymmetry. *Zic3 null* mouse models manifest early embryonic patterning failures that encompass defects in the anterior visceral endoderm and primitive streak formation[129,158], indicating an important role for Zic3 in embryonic patterning. Complex cardiac defects also result from abnormal left-right axis formation during embryonic morphogenesis in *Zic3* knockout mice, and Zic3 has been shown to interact with Nodal in left–right patterning that gives rise to subsequent cardiac development in the mouse[124]. These studies have further indicated a Zic3-responsive enhancer that mediates *Nodal* expression at the node[124].

Zic3 expression has also been identified in developing mouse ectoderm during gastrulation[115], within the embryonic brain during organogenesis, and in the cerebellum of adult mice[186]. In addition, neural tube defects have been observed in the developing hindbrain of Zic3 knockout mouse models[129,200]. Interestingly, the overexpression of *Zic3* in the ventricular zone of the embryonic mouse telencephalon, where cortical neurons are generated during development, results in an increase of proliferating neuronal progenitors[201]. These data strongly suggest a role for Zic3 in the early specification and maintenance of neural identity. Previous reports have also demonstrated the ability of Zic3 to activate the neural differentiation program through induction of proneural gene expression in *Xenopus* tissue[126]. However, there is to date no clear understanding of the

global regulatory networks within which Zic3 operates to determine lineage specificity. Here I investigate how Zic3 confers lineage specificity during ES cell differentiation.

5.2 Results

5.2.1 Zic3 regulates the promoters of lineage-specific genes

Amongst the list of Zic3 target genes identified by chromatin-immunoprecipitation (Appendix 5) were many lineage-specific genes. In order to determine if these genes were responsive to regulation by Zic3, five arbitrarily selected target regions were tested for functional response to perturbations of Zic3 levels. Table 8 provides details on these regions including the location of Zic3 binding, the gene associated with the target region, and the response of the gene to *Zic3* RNAi or overexpression in ES cells. With the exception of *Nanog*, the other four promoter regions belonged to genes that specify lineage development. These regions were amplified from mouse ES cell genomic DNA and linked to a luciferase reporter to test for transcriptional responsiveness. The length of the target region and type of luciferase vector used, enhancer or promoter, is shown in Table 8. The *Nanog* promoter region that was cloned contained the native *Nanog* minimal promoter, while the other 4 target regions were cloned upstream of an SV40 minimal promoter to test for enhancer activity.

Zic3 enrichment was firstly verified at these 5 target regions by ChIP-PCR. Two DNA fragments approximately 200bp in length were selected for PCR amplification per target region. One PCR fragment contained the Zic3 motif while

Table 8. Luciferase assays for Zic3 target regions. DNA fragments were cloned into the pGL3 basic vector (Promoter assay) or pGL3-SV40 vector (Enhancer essay)

Zic3 Binding Location	Associated Gene	Refseq #	Regulation by Zic3 in ES cells	Luciferase Assay type / DNA Length (bp)
Promoter	Zic5-Zic2	NM_022987 NM_009574	Zic2 upregulated with Zic3 RNAi	Enhancer / 980 bp
Intron 1	Fgf5	NM_028016	Downregulated with Zic3 overexpression	Enhancer / 592 bp
Promoter	Mbtps2	NM_011803	Up with Zic3 overexpression	Enhancer / 471 bp
Intron 1	Cortistatin	NM_007745	Up with Zic3 overexpression	Enhancer / 390 bp
Promoter	Nanog	NM_028016	Down with Zic3 RNAi	Promoter / 383 bp

the other was located within 300 bps of the motif-containing fragment. The sequences of all PCR primers used are provided in Appendix 1. Figure 45 presents the fold enrichments at the 5 target regions by ChIP-PCR. The *Zic5-Zic2* divergent promoter (*Zic5/2*) and *Nanog* promoter regions were enriched between 10- to 20-fold by ChIP-PCR, while the *Cortistatin, Mbtps2* and *Fgf5* promoter regions were enriched greater than 50-fold each. These results were normalized to a region on the mouse *Chst1* promoter (NM_003654) that was not enriched by Zic3 ChIP. In contrast, a control ChIP experiment performed with a non-specific GST antibody did not enrich any of the target regions tested. Two further controls were performed with PCR primers that amplified non-Zic3 binding regions of the *Nanog* enhancer regions (Controls A and B). No Zic3 enrichment was detected at these regions, relative to the GST control. These results together confirm that the target regions selected for functional characterization are indeed occupied by Zic3 in the mouse ES genome.

Transcriptional reporter assays were performed on the five promoter regions to test for functional regulation by Zic3. Figure 46 shows the activity of the promoter regions in response Zic3 overexpression in 293T cells. The *Zic5/2* divergent promoter demonstrated the greatest increase (11-fold) in activity with Zic3 overexpression relative to the no overexpression control ($p < 0.01$). Similar to the *Zic5/2* divergent promoter, the activities of the *Fgf5* (6-fold), *Mbtps*2 (8.5-fold), *Cortistatin* (4-fold) and *Nanog* (4.5-fold) promoters were also significantly up-regulated. These activities were specific to Zic3 as overexpression of another

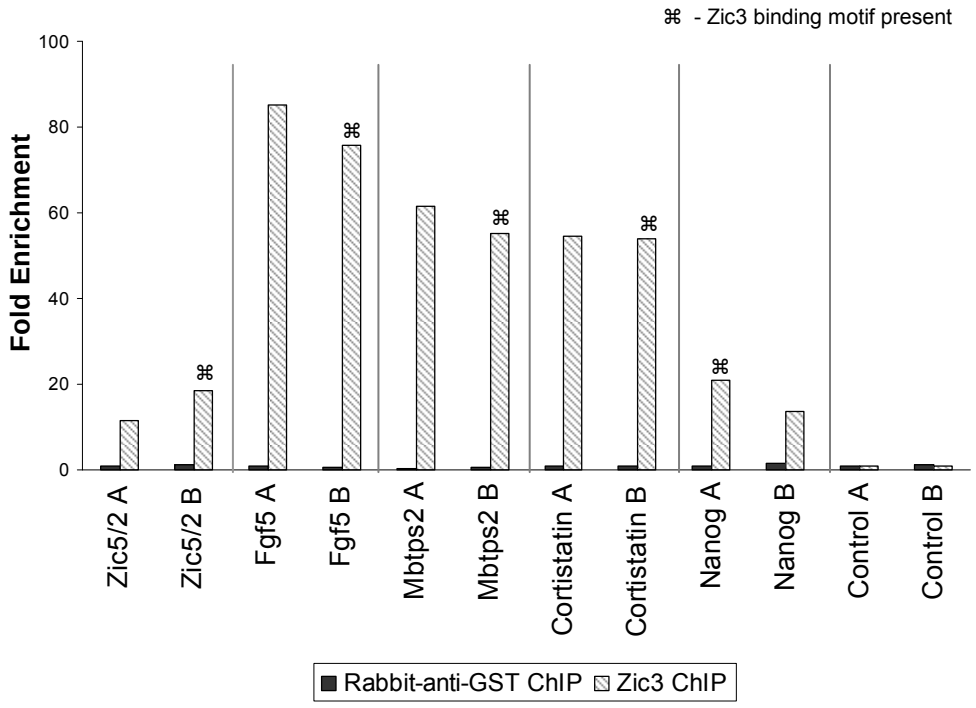

Figure 45. PCR validation of five Zic3 binding targets. Zic3 enrichment is positive by ChIP-PCR for the five target regions selected for functional validation.

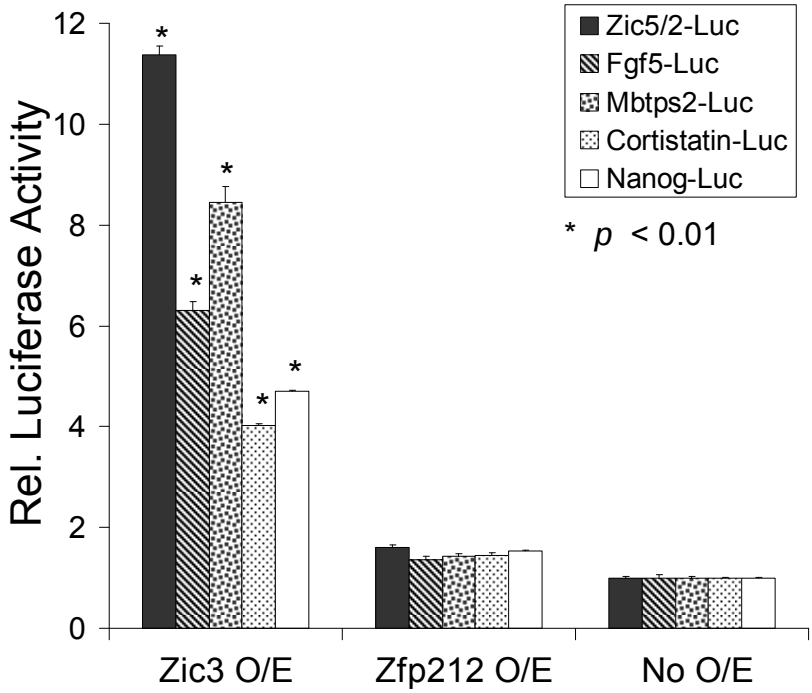

Figure 46. Transciptional responsiveness of the five Zic3 target promoter regions (HEK293T). The promoter regions were cloned into cloned into luciferase reporter vectors, and co-transfection with a Zic3 overexpression vector resulted in a significant upregulation of promoter activities in HEK 293T cells.

Zinc finger transcription factor, Zfp212, did not result in a significant increase in promoter activities (Figure 46).

The five promoter regions demonstrated robust increases in activity in 293T cells, indicating that Zic3 is an activator of these regions. However, I observed in ES cells that *Zic2* expression was up-regulated in response to *Zic3* RNAi and *Fgf5* was down-regulated with *Zic3* overexpression (Table 8), suggesting in contrast that Zic3 functions as a repressor in ES cells at these loci. To validate these observations, I performed luciferase experiments on the five promoter regions in mouse ES cells that were engineered for inducible *Zic3* expression. Two Zic3 doxycycline-inducible clonal lines were used in this analysis and three biological replicates were executed per experiment. In accordance with the earlier observations in ES cells, the activities of the *Zic5/2* divergent promoter (0.5-fold) and the *Fgf5* promoter (0.4-fold) were significantly ($p < 0.01$) down-regulated in both clonal lines in response to Zic3 overexpression (Figure 47A). As expected, the *Mbtps2* (3-fold), *Cortistati*n (2.5-fold) and *Nanog* (2.2-fold) promoter activities in both clonal lines were significantly up-regulated in response to Zic3 overexpression (Figure 47A). To confirm that the presence of doxycycline in the media did not interfere with luciferase readings, control experiments were performed with the empty vectors (pGL3 and pGL3-SV40) to demonstrate that basal luciferase activity was not affected by exposure to doxycycline (Figure 47B).

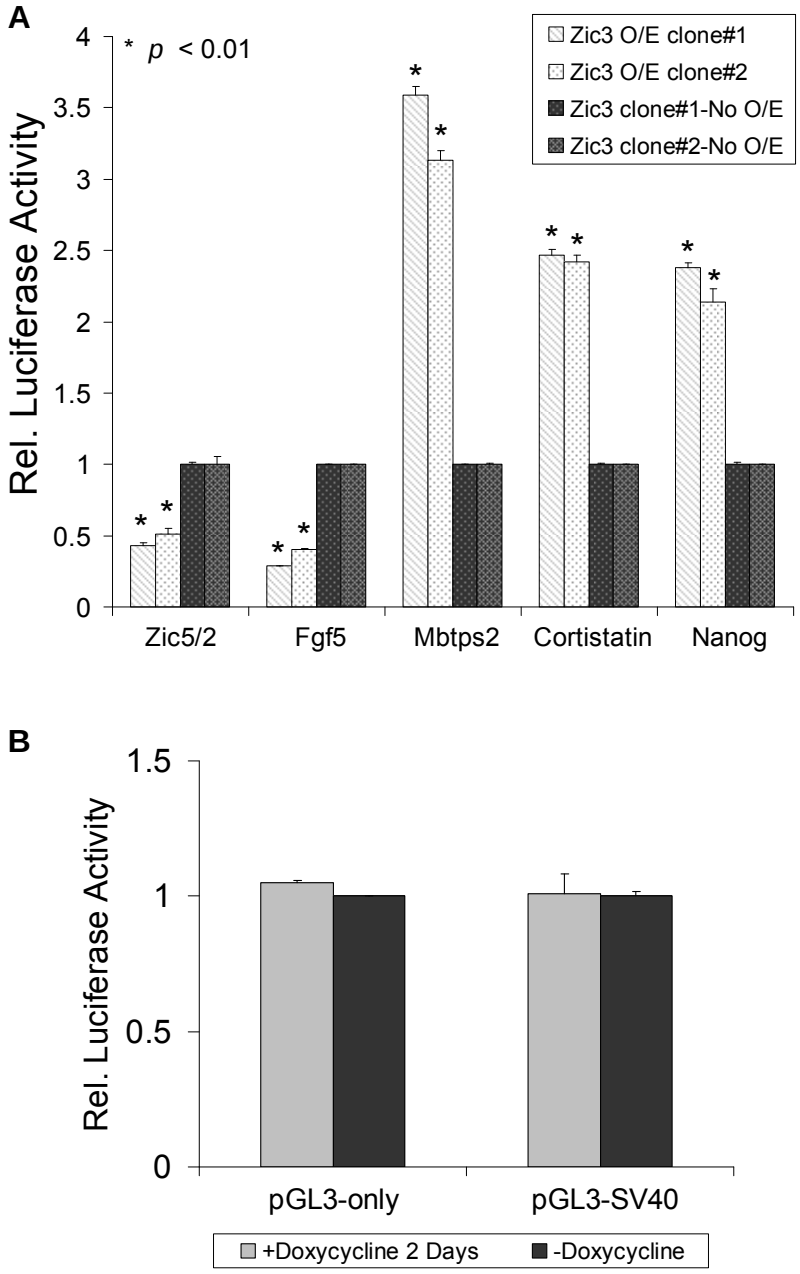

Figure 47. Transciptional responsiveness of the five Zic3 target promoter regions in mES cells. (A) The promoter regions were cloned into cloned into luciferase reporter vectors. Zic3 overexpression in mouse ES cells resulted in a downregulation of the activities of the Zic5/2 divergent promoter and the Fgf5 promoter, and an upregulation of Mbtps2, Cortistatin and Nanog promoter activities. (B) Controls for doxycycline induction in mouse ES cells, demonstrating that doxycycline does not affect the intrinsic activities of the luciferase vectors.

Finally, luciferase reporter experiments were performed in ES cells to test the activities of the five promoter regions in response to Zic3 RNAi. The promoter activities of *Zic5/2* (2.3-fold) and *Fgf5* (2-fold) were significantly up-regulated with *Zic3* RNAi, while the activities of the *Mbtps*2 (0.65-fold), *Cortistati*n (0.4-fold) and *Nanog* (0.25-fold) promoters were significantly down-regulated relative to no-RNAi controls (Figure 48). To check that the promoter activities were authentic, control experiments were performed with non-specific GFP RNAi. The five promoter activities were not significantly regulated by GFP RNAi relative to the no-RNAi experiments. The above results collectively indicate that the five promoter regions, where were identified by Zic3 ChIP experiments, are functionally responsive to Zic3 in both 293T and mouse ES cells.

5.2.2 Zic3 binds to promoters of mesoderm, ectoderm and early developmental genes

In addition to verifying the functional activity of Zic3 target regions, I was interested to define Zic3 regulated pathways in ES cells. Here I reasoned that the individual Zic3 target genes would group in specific functional pathways that reflect their function in ES cells. The list of Zic3 ChIP-chip genes was therefore analyzed by the Babelomics Fatigo+ search function (http://babelomics2.bioinfo.cipf.es/fatigoplus/ cgi-bin/fatigoplus.cgi) and classified under their relevant Gene Ontology (GO) terms for various biological processes[202]. The list of annotations at level 6 was selected for further analysis as it provided sufficient depth for functional classifications (Supplementary Table 9). Figure 49 presents a summary of the key developmental pathways identified by

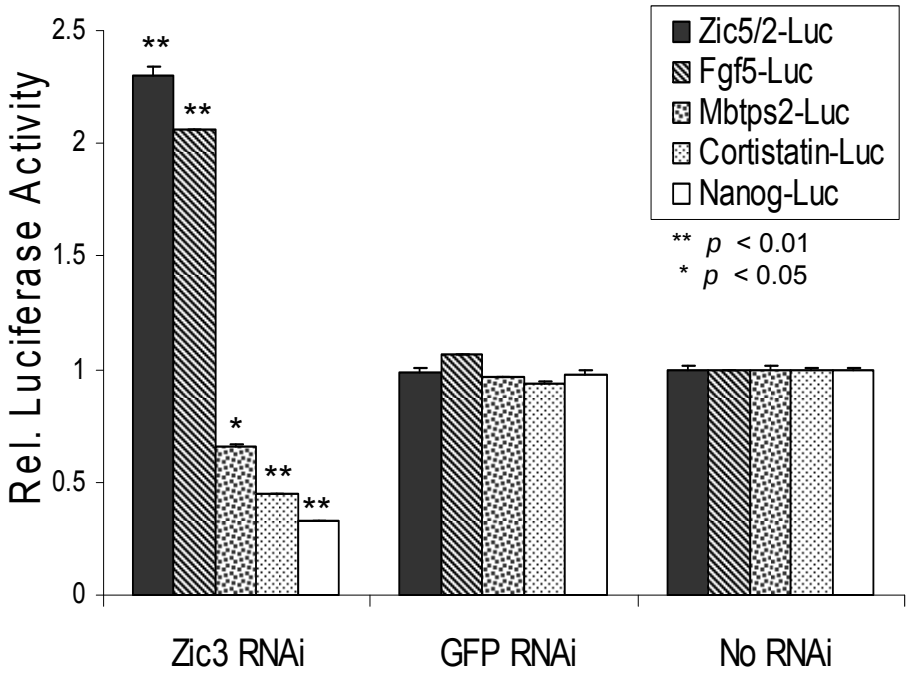

Figure 48. Transciptional responsiveness of the five Zic3 target promoter regions in mES cells. Zic3 RNAi resulted in an upregulation of Zic5/2 and Fgf5 promoter activities, and a downregulation in activities of the Mbtps2, Cortistatin and Nanog promoters in mouse ES cells.

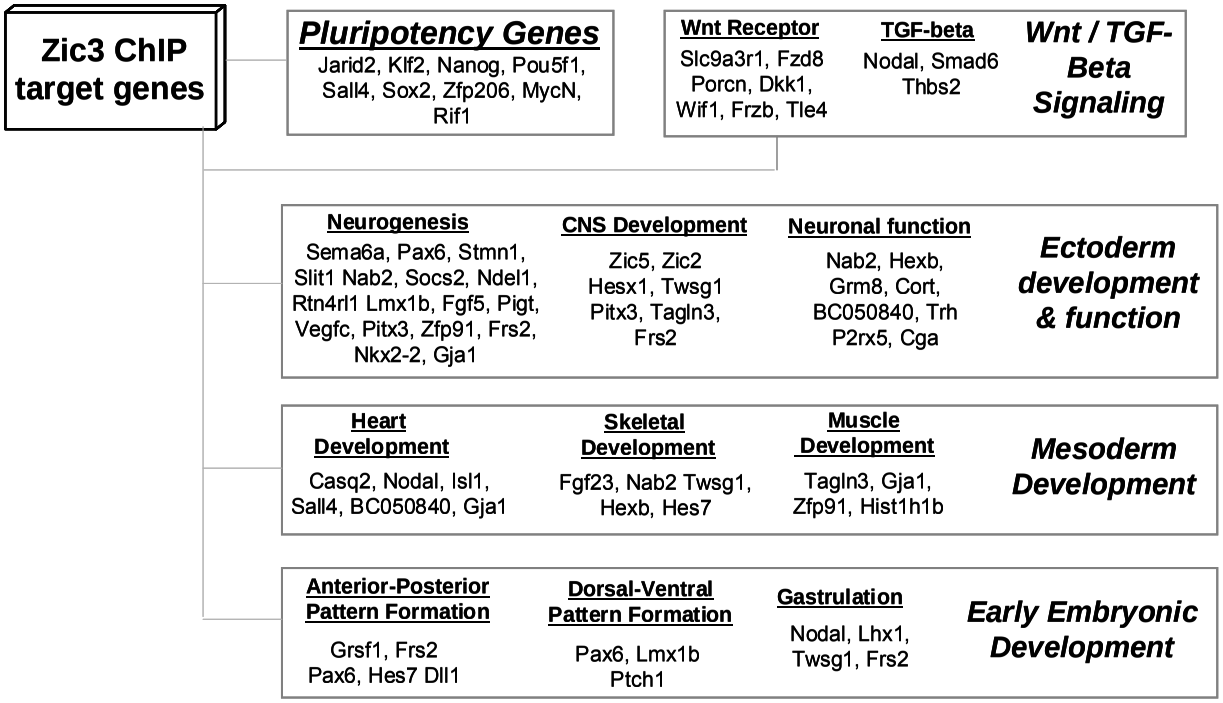

Figure 49. Zic3 target genes identified by chromatin-immunoprecipitation. Zic3 binds to the promoters of genes involved in pluripotency, Wbt/TGF-beta signalling, ectoderm development, mesoderm development, and early embryonic development

the GO search that may be broadly grouped under the following themes: Neuronal development and function, mesoderm development, Wnt signalling, and early embryonic development. As the GO database does not include annotations for pluripotency-related genes, I conducted an additional manual search for genes known to be involved in ES cell maintenance[203].

The pluripotency genes in Figure 49 provide insight into the mechanisms of Zic3 function in ES cells. To further explore the biological significance of these data, I sought to identify specific pathways in which Zic3 target genes are significantly over-represented. Hence the list of individual Zic3 target genes were compared to the Panther database of biological process annotations[195]. This list was assessed for statistically significant over (+) or under (-) representation within a pathway, relative to an expected number of genes derived from a reference list comprising the population of Agilent mouse promoter array genes. Table 9 reflects the biological pathways that are most significantly implicated by the Zic3 target genes ($p \leq 0.01$). Based on random sampling from the reference list, the processes of mRNA transcription, development, chromatin packaging and remodelling, and ectoderm development were most significantly over-represented within the Zic3 target genes.

5.2.3 Zic3 overexpression increases mesoderm and ectoderm specification

5.2.3.1 Zic3-inducible overexpression cell lines

A Zic3 inducible-expression cell line (Zic3 O/E) was established using mouse ES cells engineered for targeted gene insertion at the transcriptionally open HPRT locus[183]. Figure 50 demonstrates the specificity of regulation by doxycycline in two Zic3-overexpressing clones. Upon exposure to doxycycline for 4 days, *Zic*3 gene expression was specifically upregulated 5-fold in the Zic3-overexpressing lines relative to control lines that overexpressed GFP (Figure 50A). Corroborating with this observation, Zic3 protein expression was not detected in the clones without exposure to doxycycline (Day 0) while strong Zic3 protein expression (55kDa) was observed at days 2 and 4 in response to addition of doxycycline to the ES cell culture media (Figure 50B). These results indicate that overexpression of Zic3 in the engineered cell lines was specific and sensitive to doxycycline induction.

5.2.3.2 Zic3 overexpression leads to upregulation of ectodermal and mesodermal lineage markers

In order to assess the potential of Zic3 to induce ES cell differentiation, the GFP- and Zic3-overexpressing lines were exposed to doxycycline in the absence of LIF. This provided conditions that were conducive for general differentiation so that the lineage specification properties of Zic3 could be determined. After 4 days of doxycycline treatment in ES cell media lacking LIF, the GFP-overexpressing cells showed a mixture of phase-dark differentiated cells and phase-bright

Table 9. Panther Biological Process annotations for Zic3 ChIP-chip target genes relative to the Agilent mouse promoter array gene population

PANTHER BIOLOGICAL PROCESS	# REF. LIST (Agilent)	#OBSERVED	# EXPECTED	OVER / UNDER	*p*-value
mRNA transcription regulation	1071	56	22.87	+	0.000
mRNA transcription	1391	64	29.7	+	0.000
Nucleoside, nucleotide and nucleic acid metabolism	2522	94	53.85	+	0.000
Developmental processes	1864	66	39.8	+	0.000
Chromatin packaging and remodeling	168	11	3.59	+	0.001
Ectoderm development	595	22	12.7	+	0.010

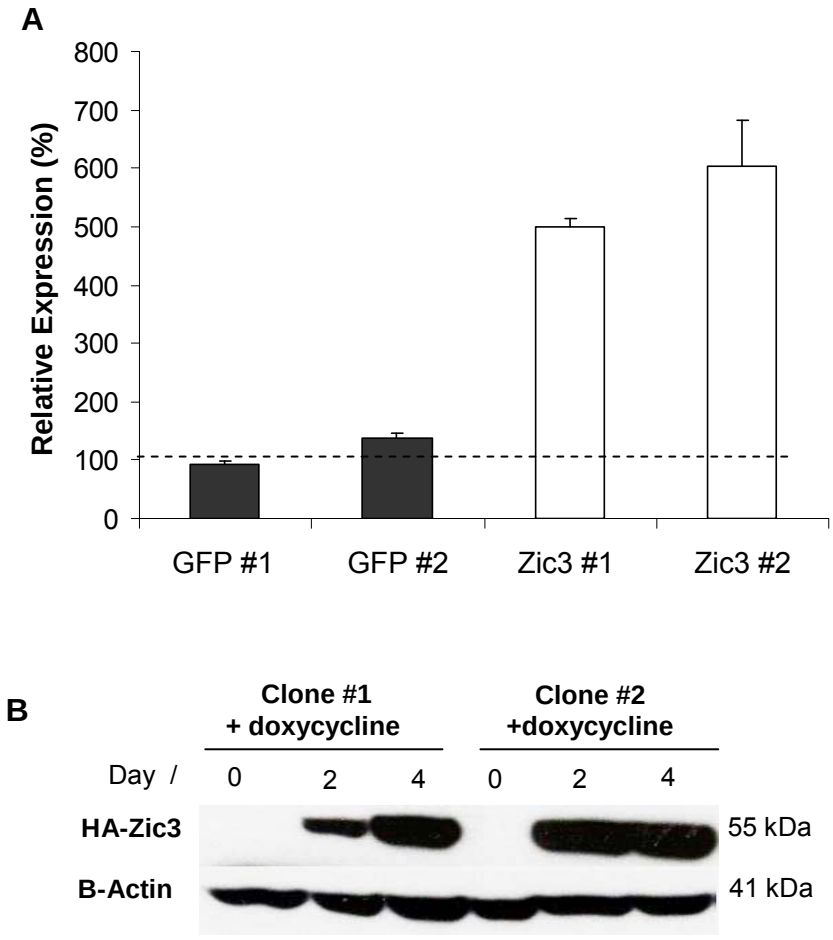

Figure 50. Expression profile of Zic3-doxcycyline inducible cell lines. (A) Zic3 overexpression cell lines are sensitive to induction by doxycycline in an overexpression cell line engineered for targeted insertion at the HPRT locus. Zic3 gene expression is upregulated in Zic3-overexpressing but not GFP control cells 4 days after exposure to doxcycline. (B) HA-tagged Zic3 protein is not detected in mouse ES without exposure to doxycyline, and is upregulated in cells exposed to doxycyline for 2 and 4 days

compact ES cell colonies (Figure 51A). In contrast, the Zic3-overexpressing cells showed very distinct signs of differentiation including phase-dark cells with extended processes, and a decreased rate of proliferation (Figure 51B). No overt increase in cell death was observed from a general survey of floating cells in the culture medium, and the rate of cell death appeared to be consistent between the GFP- and Zic3-overexpressing lines.

The GFP- and Zic3-overexpressing lines in Figure 51 were assayed for global gene expression changes. The cells at Day 4 of doxycycline induction were selected for microarray analysis as the cells earlier time-points did not demonstrate substantial change in morphology or marker expression in a preliminary real-time PCR assay. Three biological replicates were used per cell line. In this experiment, the genes that were significantly regulated in the Zic3-overexpressing lines were determined relative to the GFP-overexpressing control cells. The list of significantly regulated genes (≥ 1.5-fold; FDR 0.1, Supplementary Tables 10-11) was then uploaded to the Panther database for Biological Process annotations. In line with the functional pathways represented by Zic3 target genes (Figure 49), the results indicated a significant increase in the mesoderm and ectoderm pathways in Zic3-overexpressing cells (Table 10). These results suggest that Zic3 has the ability to confer mesoderm and ectoderm properties during ES cell differentiation.

5.2.4 Zic3 upregulates neurogenesis during ES cell neural derivation

The chromatin-IP and overexpression data suggest that Zic3 may be a significant regulator of the ectoderm specification pathway during ES cell differentiation. To determine the functional significance of these data, I examined if Zic3 overexpression was able to enhance neural induction of ES cells. Due to the fact that Zic3 is involved in the earliest stages of neural differentiation in the Xenopus embryo[126], I postulated that the presence of Zic3 during early stages of ES cell neural differentiation would enhance the rate of neurogenesis.

The N2B27 neural induction protocol was used as it involves a monolayer culture process, and is known to work with mouse ES cells[184]. Two clones each of the Zic3-overexpressing and control GFP-overexpressing cells were seeded on gelatin-coated plates and exposed to N2B27 media. The cells were induced to overexpress Zic3 or GFP by exposure to doxycycline during the first 2 days of N2B27 treatment and subsequently allowed to persist in N2B27 media without doxycycline for a further 6 days. Doxycyline induction was performed for the first two days as initial experiments indicated that maintainence of *Zic3* overexpression beyond day 2 in N2B27 prevented cells from neuronal differentiation. Corroborating with this observation, prior studies have demonstrated that Zic3 functions to maintain cells in the early undifferentiated neural progenitor state and may serve to expand the pool of neural cell numbers during embryonic ectoderm development[201].

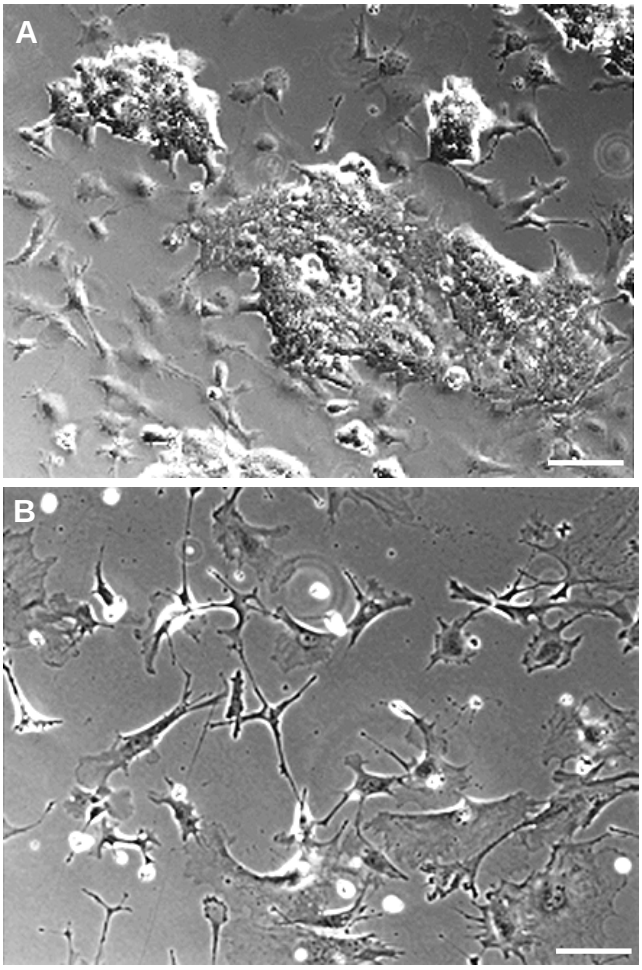

Figure 51. Zic3 overexpression cell lines differentiated more rapidly in the absence of LIF. (A) GFP-overexpressing lines show a mixture of ES-like phase-bright cells and flattened cells with extended processes after 4 days of culture in ES cell media without LIF. (B) The majority of cells in the Zic3-overexpressing cultures showed differentiated morphology with phase-dark extended processes. Scale bars, 100 μm.

Table 10. Panther Biological Process annotations for significantly regulated genes in the Zic3 overexpression samples grown in –LIF conditions, relative to the Illumina mouse Ref8-v1.1 reference gene list.

PANTHER BIOLOGICAL PROCESS	# REF. LIST (Agilent)	# EXPECTED	# OBSERVED	OVER / UNDER	*p*-value
Mesoderm development	576	355	227.42	+	0.00
Ectoderm development	729	371	287.83	+	0.00

Figure 52 shows the cells after 3 days of N2B27 treatment. As doxycycline was withdrawn just 24 hours prior to this time-point, residual GFP fluorescence was observed in the control cell lines from the earlier induction. In contrast the Zic3 overexpressing lines did not contain GFP and as such were not fluorescent. I also examined the cells at Day 3 for Nestin expression. Prior reports have indicated that the expression of this neural progenitor marker emerges between 48 to 72 hours of N2B27 treatment [184]. In accordance with previous reports[184], a small amount of Nestin in the control lines was observed at 72 hours (Day 3) while the Zic3-overexpressing lines demonstrated more intense staining for Nestin expression.

Next I examined the expression of an early neurogenesis marker, TuJ1 (β-III tubulin), and a mature neuronal marker MAP2 (microtubule associated protein 2) at days 5 and 8 of N2B27 treatment respectively. The control GFP lines expressed little TuJ1 at day 5 while the Zic3 overexpressing lines showed strong staining for this marker (Figure 53A). The expression of TuJ1 was examined at this stage in accordance with the report by Ying et al. (2003) suggesting that TuJ1 is first detected 5 days after exposure to N2B27 media. An analysis of MAP2 expression at day 8 showed a similar trend. The control GFP lines showed a small amount of MAP2 staining while the Zic3 lines demonstrated robust MAP2 expression (Figure 53B). These results show that Zic3 has the ability to enhance the process of neurogenesis and thus, is a positive regulator of neural differentiation in ES cells. Further characterization of the effect of Zic3 overexpression on neural differentiation could include a complete assay of neural

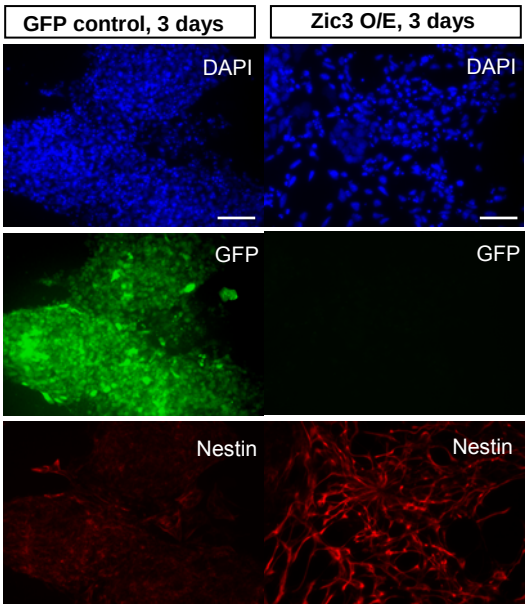

Figure 52. Zic3 overexpression enhances early neurogenesis during mouse ES differentiation. Nestin protein expression is enhanced in Zic3-overexpressing cells treated with N2B27 for 3 days. Scale bars, 100 μm.

and glial differentiation markers across different time-points, as well as fluorescence-activated cell sorting (FACs) to quantify the extent of neurogenesis.

5.3 Discussion

5.3.1 Zic3 is a regulator of lineage-specific pathways

Zic3 has clearly established roles in the context of development, and its function has been identified in embryonic morphogenesis and cardiac, skeletal, and neural differentiation[106,115,124,126,129,158]. However, the underlying Zic3 molecular networks giving rise to these processes have not been properly elucidated to date. This chapter presents novel data demonstrating the molecular pathways that Zic3 regulates in the context of development. Corroborating with observations in the literature, the chromatin-immunoprecipitation data presented here suggest that Zic3 binds to the promoters of genes involved in ectoderm development, mesoderm development, and general early embryonic development (Figure 49). In particular, the functional pathways that regulate general embryonic development and ectoderm development, encompassing genes such as *Nodal* and *Lhx1* in gastrulation, and *Fgf5* and *Zic2* in neurogenesis, are significantly over-represented amongst the target pathways identified by chromatin-IP (Table 9).

Many novel targets of Zic3 were identified, and several of these regions were tested at random for transcriptional responsiveness to Zic3. These target regions were selected to represent the diversity of pathways that Zic3 potentially regulates in both the ES cell and differentiated contexts. Amongst these target regions, the metalloprotease site-2 protease, *Mbtps2* (also known as S2P), was

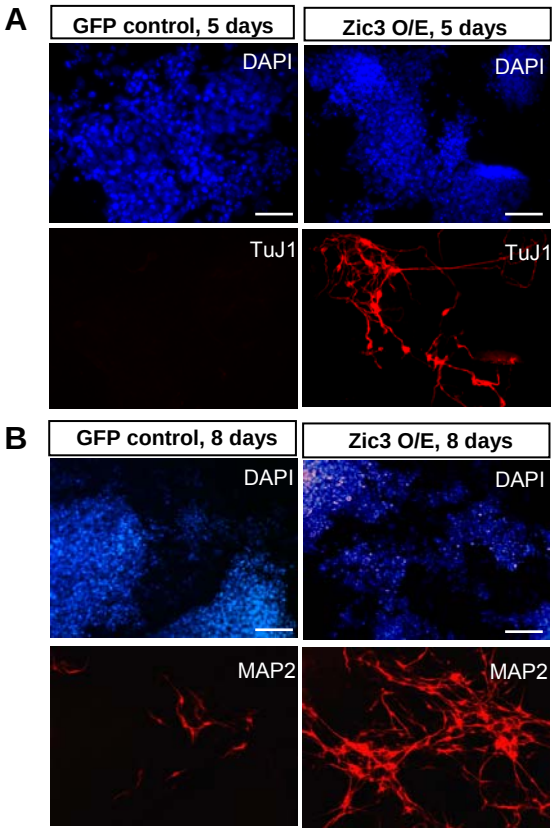

Figure 53. Zic3-overexpressing cell lines show earlier onset of neurogenesis markers. (A) An early neuronal marker, Beta-III tubulin (TuJ1), is upregulated in N2B27-treated Zic3-overexpressing cells at Day 5. (B) Mouse ES cells were treated with N2B27 for 8 days and stained for the mature neuronal marker, microtubule-associated protein 2 (MAP2). The cells overexpressing Zic3 demonstrated increased intensity of MAP2 staining. Scale bars, 100 μm.

positively regulated by Zic3 in both ES cells and HEK293T cells. Mbtps2 is an enzyme that catalyzes critical steps in cell signalling, and it is known to be involved in intra-membrane proteolysis that regulates both cholesterol homeostasis and the pathogenesis of Alzheimer's disease and Hepatitis C infections[204-206]. Mbtps2 mediates the second cleavage step in the processing of Sterol Regulatory Element-binding Proteins (SREBPs) which, when released from cell membranes, are responsible for transcriptional control of genes involved in cholesterol biosynthesis and uptake from plasma lipoproteins[207]. To date no evidence exists for *Zic3* in the regulation of intra-membrane protein cleavage or cholesterol biosynthesis. Thus the sensitivity of the *Mbtps2* promoter to Zic3 regulation could form the basis of further studies to determine the relationship between *Zic3*, *Mbtps2* and the catalysis of SREBP peptide cleavage within membranes.

The functional assays also demonstrated the capacity of Zic3 to regulate the promoters of neural genes *Zic5*/*Zic2*, *Cortistatin*, and *Fgf5*. This suggests that Zic3 has the potential to regulate the expression of these genes during ES cell differentiation and embryonic development. *Zic2* and *Zic5* belong to the Zic-family of transcription factors which share high structural homology with Zic3[106], and their expression is transcribed from a divergent promoter on chromosome 14 that is approximately 9800bp in length (Appendix 7). The functional assays in this chapter indicate that Zic3 downregulates the activity of the *Zic5*/*Zic2* promoter region in ES cells, while activating it in HEK293T cells. These results validate my earlier observation that *Zic2* expression is upregulated upon knockdown of *Zic3* in ES cells (Figure 34A), and suggest that Zic3 functions as a negative regulator of

Zic2 in ES cells. In addition, the capacity of Zic3 to activate the *Zic5*/*Zic2* divergent promoter region in HEK293T cells indicates that Zic3 may activate these genes in the context of differentiation. The significance of this is highlighted by data indicating that *Zic2, Zic3* and *Zic5* share highly overlapping expression domains in the developing dorsal brain and spinal cord[116,208]. In association with their significant structural homology, this new knowledge on the potential for Zic3 to function as a positive regulator of *Zic2* and *Zic5* in differentiated cell types may contribute to further understanding of the functional redundancy[106] between these genes. The capacity of Zic3 to function as an activator or repressor of the *Zic5*/*Zic2* promoter may be dependent on the presence of different binding partners between the pluripotent and differentiated cell contexts.

During development, *Fgf5* expression is associated the emergence of primitive ectoderm cells in the earliest stages of embryonic differentiation[29,209]. Primitive ectoderm cells arise from the inner cell mass of the embryonic blastocyst from which pluripotent ES cells are derived (Figure 1). The ability of Zic3 to downregulate Fgf5 expression in ES cells, indicated by repression of *Fgf5* in response to Zic3 overexpression and functional assays for *Fgf5* promoter activity (Table 8 & Figure 47), represents a pathway in which Zic3 may function to maintain the pluripotent state. During later stages of development, the presence of *Fgf5* is known to promote neurotrophic activity in septal cholinergic and raphe serotonergic neurons[208]. Fgf5 strongly enhances the uptake of serotonin in cholinergic and serotonergic neurons, and upregulates the choline acetyltransferase activity of rat septal cholinergic neurons[210]. Here the ability of Zic3 to upregulate *Fgf5* promoter activity in differentiated cells (Figure 46)

suggests that Zic3 promotes *Fgf5* expression and contributes to neuronal function beyond the early stages of development. Further work is required to determine the presence of Zic3 in cholinergic and serotonergic cell types, and to examine if a role exists for Zic3 in the specification of neuronal function.

Zic3 is a positive regulator of *Cortistatin* in both HEK293T and mouse ES cells. Cortistatin (CST) is a neuropeptide belonging to the somatostatin family with predominantly cortical and hippocampal expression in the central nervous system[211], and its presence is found within a subset of γ-aminobutyric acid (GABA)-releasing interneurons and hippocampal cells[212]. It has been suggested that CST-treated mice spend nearly twice the length of time in slow-wave sleep compared to saline-treated control animals[211], and it is thought that CST induces sleep by enhancing cortical neuron activity through hyperpolarization of principal cells[211,212]. In addition, it has been shown that regulated release of CST antagonizes the excitatory effects of acetylcholine neurotransmitter to promote sleep[211]. *Zic3* expression has been observed in the adult cerebellum[186]; however no functional role to date has been identified for *Zic3* in this context. The capacity of Zic3 to activate the *Cortistati*n promoter represents initial evidence for a role *Zic3* upstream of neuropeptide signalling, and further studies are required to verify the positive effect of Zic3 on *Cortistatin* expression in the developed brain.

5.3.2 Zic3 enhances neurogenesis during ES cell differentiation

In order to determine the role of Zic3 in early ES cell differentiation, a Zic3-inducible overexpression cell line was cultured in ES cell media without LIF. LIF is

able to prevent ES cell differentiation by activation of the Stat3 signalling pathway[25,31], and ES cells grown in the absence of LIF or a supporting layer of feeder cells rapidly lose their pluripotency and capacity for self-renewal. After 4 days of culture in –LIF conditions, Zic3-overexpressing cells demonstrated overt differentiated morphology with phase-dark extended processes (Figure 51). An analysis of its gene expression profile revealed that both ectoderm and mesoderm markers were significantly increased in the Zic3-overexpressing cells relative to the controls. These data suggest that Zic3 is able to confer both ectoderm and mesoderm properties on ES cells as they begin to differentiate.

In this chapter, I have provided an illustration of the principle that Zic3 is able to enhance neural specification in early ES cell differentiation. Overexpression of Zic3 resulted in an increased rate of neurogenesis when ES cells were exposed to neural differentiation conditions (Figures 52 & 53), denoted by the earlier onset of neural markers Nestin, TuJ1 (Beta-III tubulin), and MAP2 at days 3, 5 and 8 respectively. In support of the above, Zic3 is known in particular to be involved in neural development, and the overexpression of Zic3 in the ventricular zone of the embryonic mouse telencephalon, where cortical neurons are generated during development, results in an increase of proliferating neuronal progenitors[201]. A previous report has also demonstrated the ability of Zic3 to activate the neural differentiation program through induction of proneural gene expression in *Xenopus* tissue[126]. Furthermore, gene expression assays in our lab reveal that Zic3 expression is high in embryonic development and then specifically restricted to the adult brain in the mouse (Appendix 7). Taken together, these data suggest

a role for Zic3 in the early specification and maintenance of neural identity, and demonstrates conclusively that Zic3 is a potent activator of ES cell neurogenesis.

5.4 Summary

Zic3 is a positive regulator of embryonic morphogenesis, cardiac and skeletal patterning, and neural differentiation during embryonic development[106,115,124,126,129,158]. However, little is known about the networks regulated by Zic3 to determine the lineage specificity. Here I establish the target genes of Zic3 that are important during the process of development. This investigation has uncovered many novel Zic3 targets that may shed more light on its function of Zic3 in the development and function of non-pluripotent cells. In addition, the data indicate that Zic3 occupies promoters of genes involved in early embryonic patterning, and mesoderm and ectoderm formation, suggesting that Zic3 may confer ectoderm and mesoderm specificity during differentiation of ES cells. In support of this, Zic3 overexpression in differentiation-promoting conditions resulted in an over-representation of activated genes in the mesoderm and ectoderm lineage pathways. To illustrate the functional relevance of these data, I have demonstrated that transient drug-induced overexpression of Zic3 in ES cells enhances the rate of neurogenesis under conditions that promote neural differentiation. In summary, this work has elucidated a set of Zic3-regulated pathways that have the potential to influence the critical lineage decisions made during early differentiation.

CHAPTER 6:

Discussion & Future Directions

6.1 How does Zic3 maintain ES cell pluripotency?

Embryonic stem cells have the potential to generate replacement cells for damaged and diseased organs, and thus hold great promise in the field of regenerative medicine. The transcriptional networks governing the unique properties of ES cells have been the focus of many large-scale studies[19,20,51,203], and the insight gained from this work has resulted in the ability to regulate the processes of self-renewal, early differentiation, and more recently, the reprogramming of differentiated cells to the pluripotent state[93-95,213-215].

The transcriptional regulators Oct4, Nanog, and Sox2 are required for the propagation of undifferentiated ES cells in culture. These core factors contribute to the hallmark characteristics of ES cells by activating genes involved in self-renewal and pluripotency, while concurrently repressing genes involved in lineage specification[19,20]. To further elucidate the transcriptional networks that contribute to stem cell pluripotency, I have focused on transcription factors whose expression is directly regulated by Oct4, Nanog and Sox2.

Zic3 (Zinc finger protein of the cerebellum 3) is a transcription factor that encodes five tandem C_2H_2 zinc finger domains with demonstrated capacity for DNA and protein interaction[105,119,120,124]. Gene expression profiling in this thesis initially revealed that Zic3 is highly expressed in the ES cell pluripotent state and is quickly repressed upon differentiation, an observation which suggests a potential role for Zic3 in controlling differentiation of mouse and human ES cells. In addition, Oct4, Nanog and Sox2 binding have been mapped to the *Zic3* promoter regions in ES cells[19,20], implying that these key factors may regulate *Zic3*

expression. I have demonstrated in Chapter 3 that *Zic3* is directly regulated by Oct4, Nanog and Sox2 and sustains the pluripotent state through Nanog-mediated pathways. Here Zic3 functions as a gatekeeper that blocks the specification of the endoderm lineage genes, and in doing so, prevents differentiation in ES cells.

The chromatin-immunoprecipitation assays have additionally revealed that Zic3 occupies the promoters of other genes associated with the pluripotent state, including Nanog, Oct4, Sox2, *Klf2, Rif1* and *Phc1*. Zic3 may therefore function to maintain pluripotency through upregulation of key pluripotent genes Nanog, Oct4 and Sox2. Here I have demonstrated a significant overlap beween Zic3, Oct4, Nanog and Sox2 pathways (Figure 39 & Appendix 8). Furthermore, the Krüppel-like factor Klf2 shares many gene targets with Nanog, and also directly upregulates Nanog expression in ES cells[21]. Thus the association of Zic3 with the Klf2 promoter may represent another pathway by which Zic3 further modulates the expression of *Nanog* and may in part explain why *Nanog,* in particular, is substantially downregulated by Zic3 knockdown. Nanog is known to prevent differentiation of ES cells into endoderm, and downregulation of *Nanog* in ES cells leads to an upregulation of Gata4 and Gata6 expression and endoderm lineage specification[39,192,193]. It is therefore likely that Zic3 prevents differentiation of ES cells into endoderm through its maintainence of Nanog expression.

Zic3 also binds to the promoter of telomere-associated protein *Rif1*, which regulates telomere length and is hypothesized to be important for self-renewal[216], and a member of the polycomb group proteins, *Phc1*, which functions to silence

the transcription of developmental regulators in ES cells, In addition, Zic3 occupies the promoter regions of chromatin modifiers *Jarid2* and *Smarcad1*[217-219], which are known to be highly expressed in ES cells, though their roles in pluripotency and self-renewal remain as yet unknown. Zic3 may also regulate the expression of the histone methyltransferase gene, *Ehmt*2 (also known as *G9a*), which is associated with early embryonic development and transcriptional silencing in ES cells[220,221].

To date, no evidence exists for the role of Zic3 in regulating the expression of chromatin modifier genes. The above data may therefore represent additional pathways by which Zic3 could maintain the pluripotent state in ES cells, and it would be interesting to determine if Zic3 directly regulates these chromatin remodelling genes by conducting binding and mutational assays on their promoters.

6.2 Does cellular context determine activator or repressor functions of Zic3?

The question of how Zic3 operates in the opposing contexts of pluripotency and differentiation remains unresolved. Here I conceived two putative models for the role of Zic3 in pluripotency and differentiation: Firstly, Zic3 may specifically occupy the promoters of genes related to self-renewal and pluripotency in ES cells, and only bind to and regulate the promoters of lineage-specific genes as the cells exit the pluripotent phase. This model of context-dependent binding is particularly relevant given the propensity for transcription factors to associate with different partners in various spatial and temporal milieus. In support of this idea,

Zic3 is known to dimerize with the Gli proteins during development to function specifically in neural and skeletal development[105,131]. Alternatively, in a manner similar to that of Oct4, Nanog and Sox2[19,20], I postulated that Zic3 may co-occupy the epigenetically silenced promoters of developmental regulators in ES cells, thus serving to confer lineage-specific capabilities as chromatin repressive marks are relieved during differentiation.

To address this question, I examined the Zic3 targets identified by chromatin-immunoprecipitation and determined that the list comprises both ES cell-related and lineage-specific genes. It is therefore likely that Zic3 interacts with pluripotency-maintaining complexes to activate self-renewal genes and repress differentiation-specific genes in the undifferentiated state. Concurrently, Zic3 may prime the cells for differentiation into ectoderm and mesoderm lineages during differentiation by its occupancy of lineage specific promoters (Figure 49). This idea is supported by my data indicating that Zic3 represses the promoter of an early primitive ectoderm gene, *Fgf5*[29], and the divergent promoter of the neuronal differentiation genes *Zic2* and *Zic5*[106] in the ES cell state, while, in contrast, strongly activating these promoters in the differentiated HEK293T cell state (Figures 46 & 47). Thus although these Zic3-bound developmental regulators are transcriptionally silent in ES cells, the functional assays here suggest that Zic3 is able to activate these genes outside the pluripotent state. Zic3 therefore appears to function in two capacities: firstly to maintain the pluripotent state in ES cells, and secondly, to confer lineage specificity through activation of lineage development genes upon initiation of differentiation (Figure 54).

To test this hypothesis, it would be interesting to perform Zic3 chromatin-immunoprecipitation assays on embryos during axis formation and organogenesis[158]. *Zic3* null embryos at these stages demonstrate abnormalities in embryonic patterning and abnormal mesoderm and neuroectoderm allocation. This could be the result of an abnormally lateralized location of the node which normally instructs proper specification of the neuroectoderm and paraxial mesoderm[222]. The Zic3 target genes identified in ES cells that are relevant to this developmental stage include *Nodal, Lhx1, Pax6, Lmx1b, Hes7,* and *Dll1* (Figure 49). Amongst these genes, evidence exists for a genetic interaction between Zic3 and Nodal in left–right patterning and subsequent cardiac development, where significantly reduced numbers of *Zic3* $^{+/-}$ / *Nodal* $^{+/-}$ compound heterozygous mice are born[124]. In addition, Zic3 is known to mediate *Nodal* expression at the node through an upstream *Nodal* enhancer that is responsive to Zic3[124]. Apart from *Nodal*, all other Zic3 targets at this stage (Figure 49) represent newly identified pathways by which Zic3 may contribute to axis patterning and gastrulation. It therefore would be interesting to examine the genetic interaction of these genes with Zic3 using compound heterozygous mice, validate the binding of Zic3 to their promoters in embryonic tissue with chromatin-immunoprecipitation, and assay their response to Zic3 via promoter assays *in vitro* or injection into the early embryo.

The contrasting activity of Zic3 in retaining pluripotency in ES cells versus that of enhancing specific germ layers during during development may be due to its

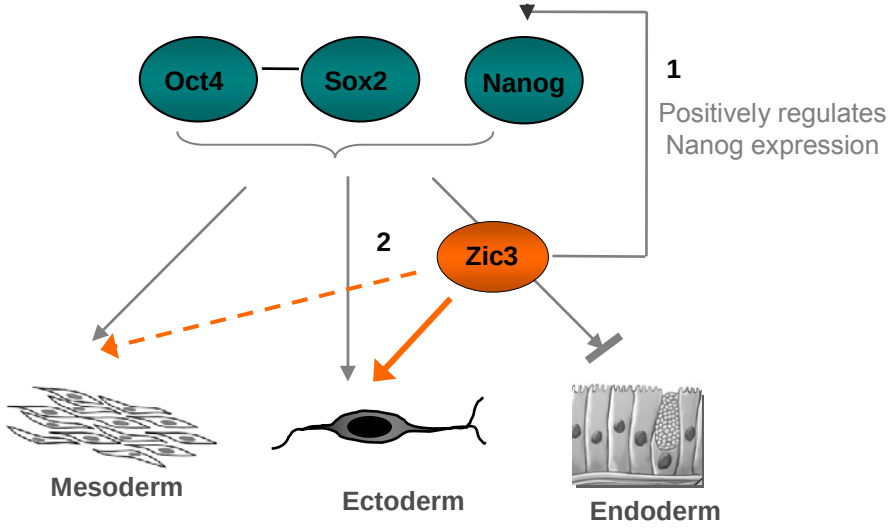

Figure 54. Illustration of the function of Zic3 in mouse ES cells. Zic3 contributes to ES cell pluripotency by: 1) Positively regulating Nanog expression and preventing mouse ES cells from expressing endodem markers, and 2) Conferring endodermal and mesodermal properties on mouse ES cells during early differentiation.

ability to associate with different factors in varying contexts. A similar molecular paradigm is observed with Sox2, which associates with Oct4 in ES cells to maintain pluripotency, while interacting with Pou2f1 to enhance lens and olfactory placode development, and with β-catenin to inhibit osteoblast differentiation[223,224].

6.3 Is Zic3 able to reprogram differentiated cells to pluripotency?

ES cells have the capacity to generate all the cells within an organism[225], and are therefore a potential donor source for cell transplantation therapies. Possible human ES cell applications include treatment of Parkinson's disease, cardiac failure and juvenile diabetes. However, the destruction of human embryos in the process of harvesting ES cells, and potential tissue rejection by the transplant recipient, pose barriers to successful ES cell therapy. One strategy to circumvent such issues is to reprogram differentiated adult cells to an ES cell-like pluripotent state and generate from them the histocompatible required tissue for therapy. It has recently been shown that differentiated cells can be reprogrammed to pluripotency through ectopic expression of ES cell transcription factors *Oct4, Sox2, c-Myc,* and *Klf4*[18,93-95,213,226]. These induced pluripotent cells (iPS) are similar to ES cells in morphology, rate of proliferation, and capacity for pluripotency indicated by teratoma formation and chimera contribution in mice[93].

A recent analysis of gene expression patterns within fully and partially reprogrammed fibroblasts revealed the presence of *Zic3* in these cells[95], suggesting that Zic3 may be at least partially involved in the process of restoring the properties of self-renewal and pluripotency as fibroblasts are reprogrammed

to an iPS state. Thus it would be interesting to assay the capacity of Zic3 to reprogram differentiated fibroblast cells.

A preliminary reprogramming assay in our lab indicated that ectopic expression of Zic3 in fibroblast cells did not yield significant numbers of ES-like colonies (Appendix 9). Overexpression of *Oct4, Sox2, c-Myc,* and *Klf*4 resulted in approximately 1000 alkaline phosphatase (AP) positive ES-like colonies, while overexpression of Zic3 in a variety of combinations with Oct4, Sox2, c-Myc, and Klf4 did not give rise to an increased number of AP-positive colonies relative to controls (Appendix 9 for details). Several factors may account for this observation. Firstly, the number of Zic3 targets in ES cells is significantly smaller than that of the key pluripotent ES cell factor Sox2 (Appendices 7 - 8), suggesting that Zic3 may regulate only a partial set of genes required for pluripotency and self-renewal. Secondly, a microarray analysis of partially reprogrammed cells expressing high levels of Zic3[95] revealed the presence of lineage-specific genes which were not detected in the fully reprogrammed state. These results suggest that Zic3 may promote the expression of lineage-specific factors in partially reprogrammed cells, and is supported by my data indicating that while Zic3 represses the promoter activity of lineage-specific factors in ES cells, it has potential to activate them in differentiated cells (Section 6.2). Therefore, Zic3 may not fully activate the program required for restoring pluripotency in differentiated fibroblast cells, due to its ability to function either as an activator or repressor of lineage-specific factors in context-dependent roles.

It is important to note that the Zic3 reprogramming assay in our lab utilized staining of a stem cell surface marker, alkaline phosphatase, to identify iPS colonies. However, it has been suggested that stem cell surface markers do not distinguish between significantly different cell states in a heterogeneous population of reprogrammed cells. For instance, both Stage-specific embryonic antigen 1 (SSEA1)-positive and -negative cells demonstrated similar gene expression profiles and DNA methylation patterns in partially reprogrammed populations[194]. Moreover, while stem cell surface antigens may serve as markers for the early reprogramming stages, activation of endogenous *Oct4*, *Nanog*, and *Sox2* is required for late reprogramming events[194,227], and the endogenous upregulation of these key pluripotent factors may thus be a better indicator of successful reprogramming. It would therefore be important to repeat the Zic3 reprogramming experiments using O*ct4*- or *Nanog*-GFP fibroblast lines[228] that enable identification of endogenous gene activation and quantification of stable ES-like induced pluripotent cell colonies.

6.4 Does Zic3 interact with Sox2 to confer neurogenic potential on ES cells?

This thesis presents evidence for a previously unknown physical interaction between Zic3 and Sox2. These transcription factors are both known to be involved in the regulation of neural progenitor cells[198,229,230], and the significance of their interaction is highlighted by reports indicating that *Sox2*[72,198,199] and *Zic3*[106,116,126] share similar patterns of expression during early development of the central nervous system. A role for Sox2 in particular has been implicated in CNS formation, primary neurons, and neural crest cells[231], and these data establish a

role for Sox2 in the initial specification of neural fate and maintenance of neural progenitor properties[198]. My results demonstrate that Zic3 and Sox2 share a subset of signalling networks in ES cells and highlight their common roles in ectoderm development, suggesting that their shared pathways may be important in neuronal specification during ES cell differentiation and embryonic development.

Due to their similar expression profiles in neural progenitors and early CNS development, it would be interesting to examine if Zic3 and Sox2 are co-localised in neural progenitor cells *in vivo,* and neural stem cells *in vitro*. To address my speculation that Zic3 and Sox2 interact and regulate common pathways during early neuronal development, chromatin-immunoprecipitation may be used to define the common targets of Zic3 and Sox2 within these cells. As the interaction between Zic3 and Sox2 is a new discovery, the dynamics of their physical association are not known. Thus it would be interesting to assay the equilibrium binding constant (K_d) of the Zic3/Sox2 dimer on a nucleotide sequence comprising both binding motifs to determine their binding affinity.

The question also remains as to whether Zic3 and Sox2 interact as a heterodimer or as part of a larger complex in the context of neural differentiation. If Zic3 and Sox2 are found to interact during neuronal development, it would be useful to explore their protein network using affinity purification and mass spectrometry. This would potentially yield insight into the protein regulatory mechanisms for maintenance of early neuronal properties of progenitor cells in embryonic development. Further work in this area could therefore contribute to validation of

the shared molecular roles of Zic3 and Sox2 potentially in the expansion of neural stem cells or promoting ectodermal specification of neural progenitors during early development, which may lead to further understanding of the process of derivation of neuronal cells from ES cells for therapeutic purposes.

6.5 Concluding remarks

This thesis highlights a role for Zic3 in the maintenance of pluripotency downstream of Oct4 and Sox2, and presents unique evidence for its function as a gatekeeper controlling differentiation of ES cells into the endoderm lineage through Nanog-mediated pathways. Having demonstrated that Zic3 plays an important role in maintenance of pluripotency, I have further mapped the target genes of Zic3 to extend our understanding of the transcriptional network that governs pluripotency and lineage specification. This has contributed to a more detailed understanding of how Zic3 may regulate pluripotency in ES cells, and identified novel pathways through which it may mediate its effects.

In addition, many lineage-specific genes were identified within the targets of Zic3. Numerous reports exist for the role of Zic3 development[116,126,158,229], and the elucidation of Zic3 binding targets in this thesis represents unique molecular insight into the function of Zic3 in these processes. These results therefore provide foundational knowledge for the dissection of transcriptional networks in Zic3-regulated developmental pathways. The data representing an interaction between Zic3 and the key stem cell pluripotent factor and neural progenitor gene, Sox2, also highlight a novel mechanism for the role of Zic3 in the maintenance of

ES cell pluripotency. In addition, it may explain how Zic3 subsequently confers neural specific properties during ES cell differentiation.

A detailed knowledge of ES cell transcriptional circuitry is fundamental to a comprehensive understanding of embryonic development and the realization of ES cell therapeutic potential. To this end, my work presents novel molecular insight into Zic3-regulated pathways that influence the state of ES cell pluripotency and the critical lineage decisions made during the process of early differentiation.

BIBLIOGRAPHY

1. Keller G. Embryonic stem cell differentiation: emergence of a new era in biology and medicine. Genes Dev 2005;19(10):1129-55.
2. Evans MJ, Kaufman MH. Establishment in culture of pluripotential cells from mouse embryos. Nature 1981;292(5819):154-6.
3. Martin GR. Isolation of a pluripotent cell line from early mouse embryos cultured in medium conditioned by teratocarcinoma stem cells. Proc Natl Acad Sci U S A 1981;78(12):7634-8.
4. Notarianni E, Galli C, Laurie S, Moor RM, Evans MJ. Derivation of pluripotent, embryonic cell lines from the pig and sheep. J Reprod Fertil Suppl 1991;43:255-60.
5. Sukoyan MA, Golubitsa AN, Zhelezova AI, Shilov AG, Vatolin SY, Maximovsky LP, Andreeva LE, McWhir J, Pack SD, Bayborodin SI and others. Isolation and cultivation of blastocyst-derived stem cell lines from American mink (Mustela vison). Mol Reprod Dev 1992;33(4):418-31.
6. Thomson JA, Kalishman J, Golos TG, Durning M, Harris CP, Becker RA, Hearn JP. Isolation of a primate embryonic stem cell line. Proc Natl Acad Sci U S A 1995;92(17):7844-8.
7. Thomson JA, Itskovitz-Eldor J, Shapiro SS, Waknitz MA, Swiergiel JJ, Marshall VS, Jones JM. Embryonic stem cell lines derived from human blastocysts. Science 1998;282(5391):1145-7.
8. Thomas KR, Deng C, Capecchi MR. High-fidelity gene targeting in embryonic stem cells by using sequence replacement vectors. Mol Cell Biol 1992;12(7):2919-23.
9. Koller BH, Hagemann LJ, Doetschman T, Hagaman JR, Huang S, Williams PJ, First NL, Maeda N, Smithies O. Germ-line transmission of a planned alteration made in a hypoxanthine phosphoribosyltransferase gene by homologous recombination in embryonic stem cells. Proc Natl Acad Sci U S A 1989;86(22):8927-31.
10. Thomson H. Bioprocessing of embryonic stem cells for drug discovery. Trends Biotechnol 2007;25(5):224-30.
11. Suda Y, Suzuki M, Ikawa Y, Aizawa S. Mouse embryonic stem cells exhibit indefinite proliferative potential. J Cell Physiol 1987;133(1):197-201.
12. Smith AG, Heath JK, Donaldson DD, Wong GG, Moreau J, Stahl M, Rogers D. Inhibition of pluripotential embryonic stem cell differentiation by purified polypeptides. Nature 1988;336(6200):688-90.
13. Burdon T, Smith A, Savatier P. Signalling, cell cycle and pluripotency in embryonic stem cells. Trends Cell Biol 2002;12(9):432-8.
14. Bartek J, Lukas J. Pathways governing G1/S transition and their response to DNA damage. FEBS Lett 2001;490(3):117-22.
15. Niwa H. How is pluripotency determined and maintained? Development 2007;134(4):635-46.
16. Boiani M, Scholer HR. Regulatory networks in embryo-derived pluripotent stem cells. Nat Rev Mol Cell Biol 2005;6(11):872-84.
17. Beddington RS, Robertson EJ. An assessment of the developmental potential of embryonic stem cells in the midgestation mouse embryo. Development 1989;105(4):733-7.
18. Yamanaka S. Pluripotency and nuclear reprogramming. Philos Trans R Soc Lond B Biol Sci 2008;363(1500):2079-87.
19. Boyer LA, Lee TI, Cole MF, Johnstone SE, Levine SS, Zucker JP, Guenther MG, Kumar RM, Murray HL, Jenner RG and others. Core transcriptional regulatory circuitry in human embryonic stem cells. Cell 2005;122(6):947-56.
20. Loh YH, Wu Q, Chew JL, Vega VB, Zhang W, Chen X, Bourque G, George J, Leong B, Liu J and others. The Oct4 and Nanog transcription network regulates pluripotency in mouse embryonic stem cells. Nat Genet 2006;38(4):431-40.
21. Jiang J, Chan YS, Loh YH, Cai J, Tong GQ, Lim CA, Robson P, Zhong S, Ng HH. A core Klf circuitry regulates self-renewal of embryonic stem cells. Nat Cell Biol 2008;10(3):353-60.

22. Lee TI, Jenner RG, Boyer LA, Guenther MG, Levine SS, Kumar RM, Chevalier B, Johnstone SE, Cole MF, Isono K and others. Control of developmental regulators by Polycomb in human embryonic stem cells. Cell 2006;125(2):301-13.
23. Fouse SD, Shen Y, Pellegrini M, Cole S, Meissner A, Van Neste L, Jaenisch R, Fan G. Promoter CpG methylation contributes to ES cell gene regulation in parallel with Oct4/Nanog, PcG complex, and histone H3 K4/K27 trimethylation. Cell Stem Cell 2008;2(2):160-9.
24. Dani C, Chambers I, Johnstone S, Robertson M, Ebrahimi B, Saito M, Taga T, Li M, Burdon T, Nichols J and others. Paracrine induction of stem cell renewal by LIF-deficient cells: a new ES cell regulatory pathway. Dev Biol 1998;203(1):149-62.
25. Niwa H, Burdon T, Chambers I, Smith A. Self-renewal of pluripotent embryonic stem cells is mediated via activation of STAT3. Genes Dev 1998;12(13):2048-60.
26. Haegele L, Ingold B, Naumann H, Tabatabai G, Ledermann B, Brandner S. Wnt signalling inhibits neural differentiation of embryonic stem cells by controlling bone morphogenetic protein expression. Mol Cell Neurosci 2003;24(3):696-708.
27. Ying QL, Nichols J, Chambers I, Smith A. BMP induction of Id proteins suppresses differentiation and sustains embryonic stem cell self-renewal in collaboration with STAT3. Cell 2003;115(3):281-92.
28. Smith AG, Hooper ML. Buffalo rat liver cells produce a diffusible activity which inhibits the differentiation of murine embryonal carcinoma and embryonic stem cells. Dev Biol 1987;121(1):1-9.
29. Rathjen J, Lake JA, Bettess MD, Washington JM, Chapman G, Rathjen PD. Formation of a primitive ectoderm like cell population, EPL cells, from ES cells in response to biologically derived factors. J Cell Sci 1999;112 (Pt 5):601-12.
30. Stewart CL, Kaspar P, Brunet LJ, Bhatt H, Gadi I, Kontgen F, Abbondanzo SJ. Blastocyst implantation depends on maternal expression of leukaemia inhibitory factor. Nature 1992;359(6390):76-9.
31. Matsuda T, Nakamura T, Nakao K, Arai T, Katsuki M, Heike T, Yokota T. STAT3 activation is sufficient to maintain an undifferentiated state of mouse embryonic stem cells. Embo J 1999;18(15):4261-9.
32. Cadigan KM, Nusse R. Wnt signaling: a common theme in animal development. Genes Dev 1997;11(24):3286-305.
33. Sato N, Meijer L, Skaltsounis L, Greengard P, Brivanlou AH. Maintenance of pluripotency in human and mouse embryonic stem cells through activation of Wnt signaling by a pharmacological GSK-3-specific inhibitor. Nat Med 2004;10(1):55-63.
34. Ying QL, Wray J, Nichols J, Batlle-Morera L, Doble B, Woodgett J, Cohen P, Smith A. The ground state of embryonic stem cell self-renewal. Nature 2008;453(7194):519-23.
35. Hart AH, Hartley L, Ibrahim M, Robb L. Identification, cloning and expression analysis of the pluripotency promoting Nanog genes in mouse and human. Dev Dyn 2004;230(1):187-98.
36. Scholer HR, Dressler GR, Balling R, Rohdewohld H, Gruss P. Oct-4: a germline-specific transcription factor mapping to the mouse t-complex. Embo J 1990;9(7):2185-95.
37. Avilion AA, Nicolis SK, Pevny LH, Perez L, Vivian N, Lovell-Badge R. Multipotent cell lineages in early mouse development depend on SOX2 function. Genes Dev 2003;17(1):126-40.
38. Nichols J, Zevnik B, Anastassiadis K, Niwa H, Klewe-Nebenius D, Chambers I, Scholer H, Smith A. Formation of pluripotent stem cells in the mammalian embryo depends on the POU transcription factor Oct4. Cell 1998;95(3):379-91.
39. Mitsui K, Tokuzawa Y, Itoh H, Segawa K, Murakami M, Takahashi K, Maruyama M, Maeda M, Yamanaka S. The homeoprotein Nanog is required for maintenance of pluripotency in mouse epiblast and ES cells. Cell 2003;113(5):631-42.
40. Hombria JC, Lovegrove B. Beyond homeosis--HOX function in morphogenesis and organogenesis. Differentiation 2003;71(8):461-76.
41. Jaenisch R, Bird A. Epigenetic regulation of gene expression: how the genome integrates intrinsic and environmental signals. Nat Genet 2003;33 Suppl:245-54.
42. Orkin SH. Chipping away at the embryonic stem cell network. Cell 2005;122(6):828-30.

43. Latchman DS. Transcription factors: an overview. Int J Biochem Cell Biol 1997;29(12):1305-12.
44. Babu MM, Luscombe NM, Aravind L, Gerstein M, Teichmann SA. Structure and evolution of transcriptional regulatory networks. Curr Opin Struct Biol 2004;14(3):283-91.
45. Blais A, Dynlacht BD. Constructing transcriptional regulatory networks. Genes Dev 2005;19(13):1499-511.
46. Yu H, Luscombe NM, Qian J, Gerstein M. Genomic analysis of gene expression relationships in transcriptional regulatory networks. Trends Genet 2003;19(8):422-7.
47. Yeger-Lotem E, Sattath S, Kashtan N, Itzkovitz S, Milo R, Pinter RY, Alon U, Margalit H. Network motifs in integrated cellular networks of transcription-regulation and protein-protein interaction. Proc Natl Acad Sci U S A 2004;101(16):5934-9.
48. Lee TI, Rinaldi NJ, Robert F, Odom DT, Bar-Joseph Z, Gerber GK, Hannett NM, Harbison CT, Thompson CM, Simon I and others. Transcriptional regulatory networks in Saccharomyces cerevisiae. Science 2002;298(5594):799-804.
49. Chen X, Xu H, Yuan P, Fang F, Huss M, Vega VB, Wong E, Orlov YL, Zhang W, Jiang J and others. Integration of external signaling pathways with the core transcriptional network in embryonic stem cells. Cell 2008;133(6):1106-17.
50. Boyer LA, Mathur D, Jaenisch R. Molecular control of pluripotency. Curr Opin Genet Dev 2006;16(5):455-62.
51. Wang J, Rao S, Chu J, Shen X, Levasseur DN, Theunissen TW, Orkin SH. A protein interaction network for pluripotency of embryonic stem cells. Nature 2006;444(7117):364-8.
52. Thanos D, Maniatis T. Virus induction of human IFN beta gene expression requires the assembly of an enhanceosome. Cell 1995;83(7):1091-100.
53. Herr W, Sturm RA, Clerc RG, Corcoran LM, Baltimore D, Sharp PA, Ingraham HA, Rosenfeld MG, Finney M, Ruvkun G and others. The POU domain: a large conserved region in the mammalian pit-1, oct-1, oct-2, and Caenorhabditis elegans unc-86 gene products. Genes Dev 1988;2(12A):1513-6.
54. Clerc RG, Corcoran LM, LeBowitz JH, Baltimore D, Sharp PA. The B-cell-specific Oct-2 protein contains POU box- and homeo box-type domains. Genes Dev 1988;2(12A):1570-81.
55. Muller MM, Ruppert S, Schaffner W, Matthias P. A cloned octamer transcription factor stimulates transcription from lymphoid-specific promoters in non-B cells. Nature 1988;336(6199):544-51.
56. Finney M, Ruvkun G, Horvitz HR. The C. elegans cell lineage and differentiation gene unc-86 encodes a protein with a homeodomain and extended similarity to transcription factors. Cell 1988;55(5):757-69.
57. Ingraham HA, Flynn SE, Voss JW, Albert VR, Kapiloff MS, Wilson L, Rosenfeld MG. The POU-specific domain of Pit-1 is essential for sequence-specific, high affinity DNA binding and DNA-dependent Pit-1-Pit-1 interactions. Cell 1990;61(6):1021-33.
58. Sturm RA, Herr W. The POU domain is a bipartite DNA-binding structure. Nature 1988;336(6199):601-4.
59. Botfield MC, Jancso A, Weiss MA. Biochemical characterization of the Oct-2 POU domain with implications for bipartite DNA recognition. Biochemistry 1992;31(25):5841-8.
60. Verrijzer CP, Alkema MJ, van Weperen WW, Van Leeuwen HC, Strating MJ, van der Vliet PC. The DNA binding specificity of the bipartite POU domain and its subdomains. Embo J 1992;11(13):4993-5003.
61. Rosner MH, Vigano MA, Ozato K, Timmons PM, Poirier F, Rigby PW, Staudt LM. A POU-domain transcription factor in early stem cells and germ cells of the mammalian embryo. Nature 1990;345(6277):686-92.
62. Ryan AK, Rosenfeld MG. POU domain family values: flexibility, partnerships, and developmental codes. Genes Dev 1997;11(10):1207-25.
63. Scholer HR, Ruppert S, Suzuki N, Chowdhury K, Gruss P. New type of POU domain in germ line-specific protein Oct-4. Nature 1990;344(6265):435-9.

64. Pesce M, Scholer HR. Oct-4: gatekeeper in the beginnings of mammalian development. Stem Cells 2001;19(4):271-8.
65. Yeom YI, Fuhrmann G, Ovitt CE, Brehm A, Ohbo K, Gross M, Hubner K, Scholer HR. Germline regulatory element of Oct-4 specific for the totipotent cycle of embryonal cells. Development 1996;122(3):881-94.
66. Palmieri SL, Peter W, Hess H, Scholer HR. Oct-4 transcription factor is differentially expressed in the mouse embryo during establishment of the first two extraembryonic cell lineages involved in implantation. Dev Biol 1994;166(1):259-67.
67. Zaehres H, Lensch MW, Daheron L, Stewart SA, Itskovitz-Eldor J, Daley GQ. High-efficiency RNA interference in human embryonic stem cells. Stem Cells 2005;23(3):299-305.
68. Niwa H, Toyooka Y, Shimosato D, Strumpf D, Takahashi K, Yagi R, Rossant J. Interaction between Oct3/4 and Cdx2 determines trophectoderm differentiation. Cell 2005;123(5):917-29.
69. Niwa H, Miyazaki J, Smith AG. Quantitative expression of Oct-3/4 defines differentiation, dedifferentiation or self-renewal of ES cells. Nat Genet 2000;24(4):372-6.
70. Kamachi Y, Uchikawa M, Kondoh H. Pairing SOX off: with partners in the regulation of embryonic development. Trends Genet 2000;16(4):182-7.
71. Pevny LH, Lovell-Badge R. Sox genes find their feet. Curr Opin Genet Dev 1997;7(3):338-44.
72. Zappone MV, Galli R, Catena R, Meani N, De Biasi S, Mattei E, Tiveron C, Vescovi AL, Lovell-Badge R, Ottolenghi S and others. Sox2 regulatory sequences direct expression of a (beta)-geo transgene to telencephalic neural stem cells and precursors of the mouse embryo, revealing regionalization of gene expression in CNS stem cells. Development 2000;127(11):2367-82.
73. Tomioka M, Nishimoto M, Miyagi S, Katayanagi T, Fukui N, Niwa H, Muramatsu M, Okuda A. Identification of Sox-2 regulatory region which is under the control of Oct-3/4-Sox-2 complex. Nucleic Acids Res 2002;30(14):3202-13.
74. Catena R, Tiveron C, Ronchi A, Porta S, Ferri A, Tatangelo L, Cavallaro M, Favaro R, Ottolenghi S, Reinbold R and others. Conserved POU binding DNA sites in the Sox2 upstream enhancer regulate gene expression in embryonic and neural stem cells. J Biol Chem 2004;279(40):41846-57.
75. Remenyi A, Lins K, Nissen LJ, Reinbold R, Scholer HR, Wilmanns M. Crystal structure of a POU/HMG/DNA ternary complex suggests differential assembly of Oct4 and Sox2 on two enhancers. Genes Dev 2003;17(16):2048-59.
76. Williams DC, Jr., Cai M, Clore GM. Molecular basis for synergistic transcriptional activation by Oct1 and Sox2 revealed from the solution structure of the 42-kDa Oct1.Sox2.Hoxb1-DNA ternary transcription factor complex. J Biol Chem 2004;279(2):1449-57.
77. Wang ZX, Teh CH, Kueh JL, Lufkin T, Robson P, Stanton LW. Oct4 and Sox2 directly regulate expression of another pluripotency transcription factor, Zfp206, in embryonic stem cells. J Biol Chem 2007;282(17):12822-30.
78. Chambers I, Colby D, Robertson M, Nichols J, Lee S, Tweedie S, Smith A. Functional expression cloning of Nanog, a pluripotency sustaining factor in embryonic stem cells. Cell 2003;113(5):643-55.
79. Pan GJ, Pei DQ. Identification of two distinct transactivation domains in the pluripotency sustaining factor nanog. Cell Res 2003;13(6):499-502.
80. Singh AM, Hamazaki T, Hankowski KE, Terada N. A heterogeneous expression pattern for Nanog in embryonic stem cells. Stem Cells 2007;25(10):2534-42.
81. Shi W, Wang H, Pan G, Geng Y, Guo Y, Pei D. Regulation of the pluripotency marker Rex-1 by Nanog and Sox2. J Biol Chem 2006;281(33):23319-25.
82. Kuroda T, Tada M, Kubota H, Kimura H, Hatano SY, Suemori H, Nakatsuji N, Tada T. Octamer and Sox elements are required for transcriptional cis regulation of Nanog gene expression. Mol Cell Biol 2005;25(6):2475-85.
83. Rodda DJ, Chew JL, Lim LH, Loh YH, Wang B, Ng HH, Robson P. Transcriptional regulation of nanog by OCT4 and SOX2. J Biol Chem 2005;280(26):24731-7.

84. Fujikura J, Yamato E, Yonemura S, Hosoda K, Masui S, Nakao K, Miyazaki Ji J, Niwa H. Differentiation of embryonic stem cells is induced by GATA factors. Genes Dev 2002;16(7):784-9.
85. Brandenberger R, Wei H, Zhang S, Lei S, Murage J, Fisk GJ, Li Y, Xu C, Fang R, Guegler K and others. Transcriptome characterization elucidates signaling networks that control human ES cell growth and differentiation. Nat Biotechnol 2004;22(6):707-16.
86. Wei CL, Miura T, Robson P, Lim SK, Xu XQ, Lee MY, Gupta S, Stanton L, Luo Y, Schmitt J and others. Transcriptome profiling of human and murine ESCs identifies divergent paths required to maintain the stem cell state. Stem Cells 2005;23(2):166-85.
87. Ivanova N, Dobrin R, Lu R, Kotenko I, Levorse J, DeCoste C, Schafer X, Lun Y, Lemischka IR. Dissecting self-renewal in stem cells with RNA interference. Nature 2006;442(7102):533-8.
88. Matoba R, Niwa H, Masui S, Ohtsuka S, Carter MG, Sharov AA, Ko MS. Dissecting Oct3/4-regulated gene networks in embryonic stem cells by expression profiling. PLoS ONE 2006;1:e26.
89. Zhang J, Tam WL, Tong GQ, Wu Q, Chan HY, Soh BS, Lou Y, Yang J, Ma Y, Chai L and others. Sall4 modulates embryonic stem cell pluripotency and early embryonic development by the transcriptional regulation of Pou5f1. Nat Cell Biol 2006;8(10):1114-23.
90. Wu Q, Chen X, Zhang J, Loh YH, Low TY, Zhang W, Sze SK, Lim B, Ng HH. Sall4 interacts with Nanog and co-occupies Nanog genomic sites in embryonic stem cells. J Biol Chem 2006;281(34):24090-4.
91. Cole MF, Johnstone SE, Newman JJ, Kagey MH, Young RA. Tcf3 is an integral component of the core regulatory circuitry of embryonic stem cells. Genes Dev 2008;22(6):746-55.
92. Tam WL, Lim CY, Han J, Zhang J, Ang YS, Ng HH, Yang H, Lim B. T-cell factor 3 regulates embryonic stem cell pluripotency and self-renewal by the transcriptional control of multiple lineage pathways. Stem Cells 2008;26(8):2019-31.
93. Takahashi K, Yamanaka S. Induction of pluripotent stem cells from mouse embryonic and adult fibroblast cultures by defined factors. Cell 2006;126(4):663-76.
94. Takahashi K, Tanabe K, Ohnuki M, Narita M, Ichisaka T, Tomoda K, Yamanaka S. Induction of pluripotent stem cells from adult human fibroblasts by defined factors. Cell 2007;131(5):861-72.
95. Wernig M, Meissner A, Foreman R, Brambrink T, Ku M, Hochedlinger K, Bernstein BE, Jaenisch R. In vitro reprogramming of fibroblasts into a pluripotent ES-cell-like state. Nature 2007;448(7151):318-24.
96. Okita K, Ichisaka T, Yamanaka S. Generation of germline-competent induced pluripotent stem cells. Nature 2007;448(7151):313-7.
97. Yu J, Vodyanik MA, Smuga-Otto K, Antosiewicz-Bourget J, Frane JL, Tian S, Nie J, Jonsdottir GA, Ruotti V, Stewart R and others. Induced pluripotent stem cell lines derived from human somatic cells. Science 2007;318(5858):1917-20.
98. Aruga J, Nagai T, Tokuyama T, Hayashizaki Y, Okazaki Y, Chapman VM, Mikoshiba K. The mouse zic gene family. Homologues of the Drosophila pair-rule gene odd-paired. J Biol Chem 1996;271(2):1043-7.
99. Brown SA, Warburton D, Brown LY, Yu CY, Roeder ER, Stengel-Rutkowski S, Hennekam RC, Muenke M. Holoprosencephaly due to mutations in ZIC2, a homologue of Drosophila odd-paired. Nat Genet 1998;20(2):180-3.
100. Yokota N, Aruga J, Takai S, Yamada K, Hamazaki M, Iwase T, Sugimura H, Mikoshiba K. Predominant expression of human zic in cerebellar granule cell lineage and medulloblastoma. Cancer Res 1996;56(2):377-83.
101. Aruga J, Yokota N, Hashimoto M, Furuichi T, Fukuda M, Mikoshiba K. A novel zinc finger protein, zic, is involved in neurogenesis, especially in the cell lineage of cerebellar granule cells. J Neurochem 1994;63(5):1880-90.
102. Aruga J, Yozu A, Hayashizaki Y, Okazaki Y, Chapman VM, Mikoshiba K. Identification and characterization of Zic4, a new member of the mouse Zic gene family. Gene 1996;172(2):291-4.

103. Gebbia M, Ferrero GB, Pilia G, Bassi MT, Aylsworth A, Penman-Splitt M, Bird LM, Bamforth JS, Burn J, Schlessinger D and others. X-linked situs abnormalities result from mutations in ZIC3. Nat Genet 1997;17(3):305-8.
104. Furushima K, Murata T, Matsuo I, Aizawa S. A new murine zinc finger gene, Opr. Mech Dev 2000;98(1-2):161-4.
105. Mizugishi K, Aruga J, Nakata K, Mikoshiba K. Molecular properties of Zic proteins as transcriptional regulators and their relationship to GLI proteins. J Biol Chem 2001;276(3):2180-8.
106. Aruga J. The role of Zic genes in neural development. Mol Cell Neurosci 2004;26(2):205-21.
107. Koebernick K, Pieler T. Gli-type zinc finger proteins as bipotential transducers of Hedgehog signaling. Differentiation 2002;70(2-3):69-76.
108. Matise MP, Joyner AL. Gli genes in development and cancer. Oncogene 1999;18(55):7852-9.
109. Ding Q, Motoyama J, Gasca S, Mo R, Sasaki H, Rossant J, Hui CC. Diminished Sonic hedgehog signaling and lack of floor plate differentiation in Gli2 mutant mice. Development 1998;125(14):2533-43.
110. Lee J, Platt KA, Censullo P, Ruiz i Altaba A. Gli1 is a target of Sonic hedgehog that induces ventral neural tube development. Development 1997;124(13):2537-52.
111. Matise MP, Epstein DJ, Park HL, Platt KA, Joyner AL. Gli2 is required for induction of floor plate and adjacent cells, but not most ventral neurons in the mouse central nervous system. Development 1998;125(15):2759-70.
112. Kim YS, Lewandoski M, Perantoni AO, Kurebayashi S, Nakanishi G, Jetten AM. Identification of Glis1, a novel Gli-related, Kruppel-like zinc finger protein containing transactivation and repressor functions. J Biol Chem 2002;277(34):30901-13.
113. Lamar E, Kintner C, Goulding M. Identification of NKL, a novel Gli-Kruppel zinc-finger protein that promotes neuronal differentiation. Development 2001;128(8):1335-46.
114. Nakashima M, Tanese N, Ito M, Auerbach W, Bai C, Furukawa T, Toyono T, Akamine A, Joyner AL. A novel gene, GliH1, with homology to the Gli zinc finger domain not required for mouse development. Mech Dev 2002;119(1):21-34.
115. Elms P, Scurry A, Davies J, Willoughby C, Hacker T, Bogani D, Arkell R. Overlapping and distinct expression domains of Zic2 and Zic3 during mouse gastrulation. Gene Expr Patterns 2004;4(5):505-11.
116. Nagai T, Aruga J, Takada S, Gunther T, Sporle R, Schughart K, Mikoshiba K. The expression of the mouse Zic1, Zic2, and Zic3 gene suggests an essential role for Zic genes in body pattern formation. Dev Biol 1997;182(2):299-313.
117. Aruga J, Mizugishi K, Koseki H, Imai K, Balling R, Noda T, Mikoshiba K. Zic1 regulates the patterning of vertebral arches in cooperation with Gli3. Mech Dev 1999;89(1-2):141-50.
118. Brewster R, Lee J, Ruiz i Altaba A. Gli/Zic factors pattern the neural plate by defining domains of cell differentiation. Nature 1998;393(6685):579-83.
119. Ware SM, Peng J, Zhu L, Fernbach S, Colicos S, Casey B, Towbin J, Belmont JW. Identification and functional analysis of ZIC3 mutations in heterotaxy and related congenital heart defects. Am J Hum Genet 2004;74(1):93-105.
120. Koyabu Y, Nakata K, Mizugishi K, Aruga J, Mikoshiba K. Physical and functional interactions between Zic and Gli proteins. J Biol Chem 2001;276(10):6889-92.
121. Alexandre C, Jacinto A, Ingham PW. Transcriptional activation of hedgehog target genes in Drosophila is mediated directly by the cubitus interruptus protein, a member of the GLI family of zinc finger DNA-binding proteins. Genes Dev 1996;10(16):2003-13.
122. Marigo V, Johnson RL, Vortkamp A, Tabin CJ. Sonic hedgehog differentially regulates expression of GLI and GLI3 during limb development. Dev Biol 1996;180(1):273-83.
123. Kitaguchi T, Mizugishi K, Hatayama M, Aruga J, Mikoshiba K. Xenopus Brachyury regulates mesodermal expression of Zic3, a gene controlling left-right asymmetry. Dev Growth Differ 2002;44(1):55-61.
124. Ware SM, Harutyunyan KG, Belmont JW. Heart defects in X-linked heterotaxy: evidence for a genetic interaction of Zic3 with the nodal signaling pathway. Dev Dyn 2006;235(6):1631-7.

125. Norris DP, Robertson EJ. Asymmetric and node-specific nodal expression patterns are controlled by two distinct cis-acting regulatory elements. Genes Dev 1999;13(12):1575-88.
126. Nakata K, Nagai T, Aruga J, Mikoshiba K. Xenopus Zic3, a primary regulator both in neural and neural crest development. Proc Natl Acad Sci U S A 1997;94(22):11980-5.
127. Kelly LE, Carrel TL, Herman GE, El-Hodiri HM. Pbx1 and Meis1 regulate activity of the Xenopus laevis Zic3 promoter through a highly conserved region. Biochem Biophys Res Commun 2006;344(3):1031-7.
128. Maeda R, Ishimura A, Mood K, Park EK, Buchberg AM, Daar IO. Xpbx1b and Xmeis1b play a collaborative role in hindbrain and neural crest gene expression in Xenopus embryos. Proc Natl Acad Sci U S A 2002;99(8):5448-53.
129. Purandare SM, Ware SM, Kwan KM, Gebbia M, Bassi MT, Deng JM, Vogel H, Behringer RR, Belmont JW, Casey B. A complex syndrome of left-right axis, central nervous system and axial skeleton defects in Zic3 mutant mice. Development 2002;129(9):2293-302.
130. Ware SM. DNA mutation analysis in heterotaxy. Methods Mol Med 2006;126:247-56.
131. Zhu L, Zhou G, Poole S, Belmont JW. Characterization of the interactions of human ZIC3 mutants with GLI3. Hum Mutat 2008;29(1):99-105.
132. Le P, Benazouzz AP, Billey C. [Situs invertus, a mirror image]. Presse Med 2003;32(37 Pt 1):1742-3.
133. Burdine RD, Schier AF. Conserved and divergent mechanisms in left-right axis formation. Genes Dev 2000;14(7):763-76.
134. Wood WB. The left-right polarity puzzle: determining embryonic handedness. PLoS Biol 2005;3(8):e292.
135. Danos MC, Yost HJ. Linkage of cardiac left-right asymmetry and dorsal-anterior development in Xenopus. Development 1995;121(5):1467-74.
136. Davidson BP, Kinder SJ, Steiner K, Schoenwolf GC, Tam PP. Impact of node ablation on the morphogenesis of the body axis and the lateral asymmetry of the mouse embryo during early organogenesis. Dev Biol 1999;211(1):11-26.
137. Nonaka S, Tanaka Y, Okada Y, Takeda S, Harada A, Kanai Y, Kido M, Hirokawa N. Randomization of left-right asymmetry due to loss of nodal cilia generating leftward flow of extraembryonic fluid in mice lacking KIF3B motor protein. Cell 1998;95(6):829-37.
138. Supp DM, Witte DP, Potter SS, Brueckner M. Mutation of an axonemal dynein affects left-right asymmetry in inversus viscerum mice. Nature 1997;389(6654):963-6.
139. Supp DM, Brueckner M, Kuehn MR, Witte DP, Lowe LA, McGrath J, Corrales J, Potter SS. Targeted deletion of the ATP binding domain of left-right dynein confirms its role in specifying development of left-right asymmetries. Development 1999;126(23):5495-504.
140. Marszalek JR, Ruiz-Lozano P, Roberts E, Chien KR, Goldstein LS. Situs inversus and embryonic ciliary morphogenesis defects in mouse mutants lacking the KIF3A subunit of kinesin-II. Proc Natl Acad Sci U S A 1999;96(9):5043-8.
141. Nonaka S, Shiratori H, Saijoh Y, Hamada H. Determination of left-right patterning of the mouse embryo by artificial nodal flow. Nature 2002;418(6893):96-9.
142. Cartwright JH, Piro O, Tuval I. Fluid-dynamical basis of the embryonic development of left-right asymmetry in vertebrates. Proc Natl Acad Sci U S A 2004;101(19):7234-9.
143. Nonaka S, Yoshiba S, Watanabe D, Ikeuchi S, Goto T, Marshall WF, Hamada H. De novo formation of left-right asymmetry by posterior tilt of nodal cilia. PLoS Biol 2005;3(8):e268.
144. Okada Y, Takeda S, Tanaka Y, Belmonte JC, Hirokawa N. Mechanism of nodal flow: a conserved symmetry breaking event in left-right axis determination. Cell 2005;121(4):633-44.
145. Chazaud C, Chambon P, Dolle P. Retinoic acid is required in the mouse embryo for left-right asymmetry determination and heart morphogenesis. Development 1999;126(12):2589-96.
146. Tsukui T, Capdevila J, Tamura K, Ruiz-Lozano P, Rodriguez-Esteban C, Yonei-Tamura S, Magallon J, Chandraratna RA, Chien K, Blumberg B and others. Multiple left-right asymmetry defects in Shh(-/-) mutant mice unveil a convergence of the shh

and retinoic acid pathways in the control of Lefty-1. Proc Natl Acad Sci U S A 1999;96(20):11376-81.
147. Oulad-Abdelghani M, Chazaud C, Bouillet P, Mattei MG, Dolle P, Chambon P. Stra3/lefty, a retinoic acid-inducible novel member of the transforming growth factor-beta superfamily. Int J Dev Biol 1998;42(1):23-32.
148. Brennan J, Norris DP, Robertson EJ. Nodal activity in the node governs left-right asymmetry. Genes Dev 2002;16(18):2339-44.
149. Varlet I, Collignon J, Robertson EJ. nodal expression in the primitive endoderm is required for specification of the anterior axis during mouse gastrulation. Development 1997;124(5):1033-44.
150. Conlon FL, Lyons KM, Takaesu N, Barth KS, Kispert A, Herrmann B, Robertson EJ. A primary requirement for nodal in the formation and maintenance of the primitive streak in the mouse. Development 1994;120(7):1919-28.
151. Bisgrove BW, Essner JJ, Yost HJ. Regulation of midline development by antagonism of lefty and nodal signaling. Development 1999;126(14):3253-62.
152. Meno C, Gritsman K, Ohishi S, Ohfuji Y, Heckscher E, Mochida K, Shimono A, Kondoh H, Talbot WS, Robertson EJ and others. Mouse Lefty2 and zebrafish antivin are feedback inhibitors of nodal signaling during vertebrate gastrulation. Mol Cell 1999;4(3):287-98.
153. Saijoh Y, Adachi H, Sakuma R, Yeo CY, Yashiro K, Watanabe M, Hashiguchi H, Mochida K, Ohishi S, Kawabata M and others. Left-right asymmetric expression of lefty2 and nodal is induced by a signaling pathway that includes the transcription factor FAST2. Mol Cell 2000;5(1):35-47.
154. Meno C, Saijoh Y, Fujii H, Ikeda M, Yokoyama T, Yokoyama M, Toyoda Y, Hamada H. Left-right asymmetric expression of the TGF beta-family member lefty in mouse embryos. Nature 1996;381(6578):151-5.
155. Meno C, Shimono A, Saijoh Y, Yashiro K, Mochida K, Ohishi S, Noji S, Kondoh H, Hamada H. lefty-1 is required for left-right determination as a regulator of lefty-2 and nodal. Cell 1998;94(3):287-97.
156. Melloy PG, Ewart JL, Cohen MF, Desmond ME, Kuehn MR, Lo CW. No turning, a mouse mutation causing left-right and axial patterning defects. Dev Biol 1998;193(1):77-89.
157. Izraeli S, Lowe LA, Bertness VL, Good DJ, Dorward DW, Kirsch IR, Kuehn MR. The SIL gene is required for mouse embryonic axial development and left-right specification. Nature 1999;399(6737):691-4.
158. Ware SM, Harutyunyan KG, Belmont JW. Zic3 is critical for early embryonic patterning during gastrulation. Dev Dyn 2006;235(3):776-85.
159. Aruga J, Minowa O, Yaginuma H, Kuno J, Nagai T, Noda T, Mikoshiba K. Mouse Zic1 is involved in cerebellar development. J Neurosci 1998;18(1):284-93.
160. Lu CC, Brennan J, Robertson EJ. From fertilization to gastrulation: axis formation in the mouse embryo. Curr Opin Genet Dev 2001;11(4):384-92.
161. Henderson DJ, Conway SJ, Greene ND, Gerrelli D, Murdoch JN, Anderson RH, Copp AJ. Cardiovascular defects associated with abnormalities in midline development in the Loop-tail mouse mutant. Circ Res 2001;89(1):6-12.
162. Triulzi F, Scotti G, di Natale B, Pellini C, Lukezic M, Scognamiglio M, Chiumello G. Evidence of a congenital midline brain anomaly in pituitary dwarfs: a magnetic resonance imaging study in 101 patients. Pediatrics 1994;93(3):409-16.
163. Clark KL, Yutzey KE, Benson DW. Transcription factors and congenital heart defects. Annu Rev Physiol 2006;68:97-121.
164. Nagai T, Aruga J, Minowa O, Sugimoto T, Ohno Y, Noda T, Mikoshiba K. Zic2 regulates the kinetics of neurulation. Proc Natl Acad Sci U S A 2000;97(4):1618-23.
165. Zhu L, Belmont JW, Ware SM. Genetics of human heterotaxias. Eur J Hum Genet 2006;14(1):17-25.
166. Fritz B, Kunz J, Knudsen GP, Louwen F, Kennerknecht I, Eiben B, Orstavik KH, Friedrich U, Rehder H. Situs ambiguus in a female fetus with balanced (X;21) translocation--evidence for functional nullisomy of the ZIC3 gene? Eur J Hum Genet 2005;13(1):34-40.

167. Kosaki K, Casey B. Genetics of human left-right axis malformations. Semin Cell Dev Biol 1998;9(1):89-99.
168. Casey B, Devoto M, Jones KL, Ballabio A. Mapping a gene for familial situs abnormalities to human chromosome Xq24-q27.1. Nat Genet 1993;5(4):403-7.
169. Nakata K, Nagai T, Aruga J, Mikoshiba K. Xenopus Zic family and its role in neural and neural crest development. Mech Dev 1998;75(1-2):43-51.
170. Grinblat Y, Sive H. zic Gene expression marks anteroposterior pattern in the presumptive neurectoderm of the zebrafish gastrula. Dev Dyn 2001;222(4):688-93.
171. Feledy JA, Beanan MJ, Sandoval JJ, Goodrich JS, Lim JH, Matsuo-Takasaki M, Sato SM, Sargent TD. Inhibitory patterning of the anterior neural plate in Xenopus by homeodomain factors Dlx3 and Msx1. Dev Biol 1999;212(2):455-64.
172. Yamamoto TS, Takagi C, Ueno N. Requirement of Xmsx-1 in the BMP-triggered ventralization of Xenopus embryos. Mech Dev 2000;91(1-2):131-41.
173. Batut J, Vandel L, Leclerc C, Daguzan C, Moreau M, Neant I. The Ca2+-induced methyltransferase xPRMT1b controls neural fate in amphibian embryo. Proc Natl Acad Sci U S A 2005;102(42):15128-33.
174. Leclerc C, Webb SE, Daguzan C, Moreau M, Miller AL. Imaging patterns of calcium transients during neural induction in Xenopus laevis embryos. J Cell Sci 2000;113 Pt 19:3519-29.
175. Leclerc C, Lee M, Webb SE, Moreau M, Miller AL. Calcium transients triggered by planar signals induce the expression of ZIC3 gene during neural induction in Xenopus. Dev Biol 2003;261(2):381-90.
176. Moreau M, Neant I, Webb SE, Miller AL, Leclerc C. Calcium signalling during neural induction in Xenopus laevis embryos. Philos Trans R Soc Lond B Biol Sci 2008;363(1495):1371-5.
177. Leclerc C, Rizzo C, Daguzan C, Neant I, Batut J, Auge B, Moreau M. [Neural determination in Xenopus laevis embryos: control of early neural gene expression by calcium]. J Soc Biol 2001;195(3):327-37.
178. Inoue T, Hatayama M, Tohmonda T, Itohara S, Aruga J, Mikoshiba K. Mouse Zic5 deficiency results in neural tube defects and hypoplasia of cephalic neural crest derivatives. Dev Biol 2004;270(1):146-62.
179. Zhang J, Jin Z, Bao ZZ. Disruption of gradient expression of Zic3 resulted in abnormal intra-retinal axon projection. Development 2004;131(7):1553-62.
180. Ui-Tei K, Naito Y, Takahashi F, Haraguchi T, Ohki-Hamazaki H, Juni A, Ueda R, Saigo K. Guidelines for the selection of highly effective siRNA sequences for mammalian and chick RNA interference. Nucleic Acids Res 2004;32(3):936-48.
181. Reynolds A, Leake D, Boese Q, Scaringe S, Marshall WS, Khvorova A. Rational siRNA design for RNA interference. Nat Biotechnol 2004;22(3):326-30.
182. Morita S, Kojima T, Kitamura T. Plat-E: an efficient and stable system for transient packaging of retroviruses. Gene Ther 2000;7(12):1063-6.
183. Kyba M, Perlingeiro RC, Daley GQ. HoxB4 confers definitive lymphoid-myeloid engraftment potential on embryonic stem cell and yolk sac hematopoietic progenitors. Cell 2002;109(1):29-37.
184. Ying QL, Stavridis M, Griffiths D, Li M, Smith A. Conversion of embryonic stem cells into neuroectodermal precursors in adherent monoculture. Nat Biotechnol 2003;21(2):183-6.
185. Ririe KM, Rasmussen RP, Wittwer CT. Product differentiation by analysis of DNA melting curves during the polymerase chain reaction. Anal Biochem 1997;245(2):154-60.
186. Herman GE, El-Hodiri HM. The role of ZIC3 in vertebrate development. Cytogenet Genome Res 2002;99(1-4):229-35.
187. Grinberg I, Millen KJ. The ZIC gene family in development and disease. Clin Genet 2005;67(4):290-6.
188. Chambers I, Smith A. Self-renewal of teratocarcinoma and embryonic stem cells. Oncogene 2004;23(43):7150-60.

189. Pease S, Braghetta P, Gearing D, Grail D, Williams RL. Isolation of embryonic stem (ES) cells in media supplemented with recombinant leukemia inhibitory factor (LIF). Dev Biol 1990;141(2):344-52.
190. Kunath T, Arnaud D, Uy GD, Okamoto I, Chureau C, Yamanaka Y, Heard E, Gardner RL, Avner P, Rossant J. Imprinted X-inactivation in extra-embryonic endoderm cell lines from mouse blastocysts. Development 2005;132(7):1649-61.
191. Mesnard D, Guzman-Ayala M, Constam DB. Nodal specifies embryonic visceral endoderm and sustains pluripotent cells in the epiblast before overt axial patterning. Development 2006;133(13):2497-505.
192. Hyslop L, Stojkovic M, Armstrong L, Walter T, Stojkovic P, Przyborski S, Herbert M, Murdoch A, Strachan T, Lako M. Downregulation of NANOG induces differentiation of human embryonic stem cells to extraembryonic lineages. Stem Cells 2005;23(8):1035-43.
193. Hough SR, Clements I, Welch PJ, Wiederholt KA. Differentiation of mouse embryonic stem cells after RNA interference-mediated silencing of OCT4 and Nanog. Stem Cells 2006;24(6):1467-75.
194. Mikkelsen TS, Hanna J, Zhang X, Ku M, Wernig M, Schorderet P, Bernstein BE, Jaenisch R, Lander ES, Meissner A. Dissecting direct reprogramming through integrative genomic analysis. Nature 2008.
195. Thomas PD, Kejariwal A, Guo N, Mi H, Campbell MJ, Muruganujan A, Lazareva-Ulitsky B. Applications for protein sequence-function evolution data: mRNA/protein expression analysis and coding SNP scoring tools. Nucleic Acids Res 2006;34(Web Server issue):W645-50.
196. Pavesi G, Mereghetti P, Zambelli F, Stefani M, Mauri G, Pesole G. MoD Tools: regulatory motif discovery in nucleotide sequences from co-regulated or homologous genes. Nucleic Acids Res 2006;34(Web Server issue):W566-70.
197. Ji H, Vokes SA, Wong WH. A comparative analysis of genome-wide chromatin immunoprecipitation data for mammalian transcription factors. Nucleic Acids Res 2006;34(21):e146.
198. Graham V, Khudyakov J, Ellis P, Pevny L. SOX2 functions to maintain neural progenitor identity. Neuron 2003;39(5):749-65.
199. Uwanogho D, Rex M, Cartwright EJ, Pearl G, Healy C, Scotting PJ, Sharpe PT. Embryonic expression of the chicken Sox2, Sox3 and Sox11 genes suggests an interactive role in neuronal development. Mech Dev 1995;49(1-2):23-36.
200. Klootwijk R, Franke B, van der Zee CE, de Boer RT, Wilms W, Hol FA, Mariman EC. A deletion encompassing Zic3 in bent tail, a mouse model for X-linked neural tube defects. Hum Mol Genet 2000;9(11):1615-22.
201. Inoue T, Ota M, Ogawa M, Mikoshiba K, Aruga J. Zic1 and Zic3 regulate medial forebrain development through expansion of neuronal progenitors. J Neurosci 2007;27(20):5461-73.
202. Al-Shahrour F, Minguez P, Tarraga J, Medina I, Alloza E, Montaner D, Dopazo J. FatiGO +: a functional profiling tool for genomic data. Integration of functional annotation, regulatory motifs and interaction data with microarray experiments. Nucleic Acids Res 2007;35(Web Server issue):W91-6.
203. Kim J, Chu J, Shen X, Wang J, Orkin SH. An extended transcriptional network for pluripotency of embryonic stem cells. Cell 2008;132(6):1049-61.
204. Haass C, Steiner H. Alzheimer disease gamma-secretase: a complex story of GxGD-type presenilin proteases. Trends Cell Biol 2002;12(12):556-62.
205. Hope RG, McLauchlan J. Sequence motifs required for lipid droplet association and protein stability are unique to the hepatitis C virus core protein. J Gen Virol 2000;81(Pt 8):1913-25.
206. Hua X, Nohturfft A, Goldstein JL, Brown MS. Sterol resistance in CHO cells traced to point mutation in SREBP cleavage-activating protein. Cell 1996;87(3):415-26.
207. Brown MS, Goldstein JL. A proteolytic pathway that controls the cholesterol content of membranes, cells, and blood. Proc Natl Acad Sci U S A 1999;96(20):11041-8.

208. Grinberg I, Northrup H, Ardinger H, Prasad C, Dobyns WB, Millen KJ. Heterozygous deletion of the linked genes ZIC1 and ZIC4 is involved in Dandy-Walker malformation. Nat Genet 2004;36(10):1053-5.
209. Haub O, Goldfarb M. Expression of the fibroblast growth factor-5 gene in the mouse embryo. Development 1991;112(2):397-406.
210. Lindholm D, Harikka J, da Penha Berzaghi M, Castren E, Tzimagiorgis G, Hughes RA, Thoenen H. Fibroblast growth factor-5 promotes differentiation of cultured rat septal cholinergic and raphe serotonergic neurons: comparison with the effects of neurotrophins. Eur J Neurosci 1994;6(2):244-52.
211. de Lecea L, Criado JR, Prospero-Garcia O, Gautvik KM, Schweitzer P, Danielson PE, Dunlop CL, Siggins GR, Henriksen SJ, Sutcliffe JG. A cortical neuropeptide with neuronal depressant and sleep-modulating properties. Nature 1996;381(6579):242-5.
212. de Lecea L, del Rio JA, Criado JR, Alcantara S, Morales M, Danielson PE, Henriksen SJ, Soriano E, Sutcliffe JG. Cortistatin is expressed in a distinct subset of cortical interneurons. J Neurosci 1997;17(15):5868-80.
213. Aoi T, Yae K, Nakagawa M, Ichisaka T, Okita K, Takahashi K, Chiba T, Yamanaka S. Generation of Pluripotent Stem Cells from Adult Mouse Liver and Stomach Cells. Science 2008.
214. Takahashi K, Okita K, Nakagawa M, Yamanaka S. Induction of pluripotent stem cells from fibroblast cultures. Nat Protoc 2007;2(12):3081-9.
215. Nakagawa M, Koyanagi M, Tanabe K, Takahashi K, Ichisaka T, Aoi T, Okita K, Mochiduki Y, Takizawa N, Yamanaka S. Generation of induced pluripotent stem cells without Myc from mouse and human fibroblasts. Nat Biotechnol 2008;26(1):101-6.
216. Adams IR, McLaren A. Identification and characterisation of mRif1: a mouse telomere-associated protein highly expressed in germ cells and embryo-derived pluripotent stem cells. Dev Dyn 2004;229(4):733-44.
217. Jung J, Mysliwiec MR, Lee Y. Roles of JUMONJI in mouse embryonic development. Dev Dyn 2005;232(1):21-32.
218. Jung J, Kim TG, Lyons GE, Kim HR, Lee Y. Jumonji regulates cardiomyocyte proliferation via interaction with retinoblastoma protein. J Biol Chem 2005;280(35):30916-23.
219. Schoor M, Schuster-Gossler K, Gossler A. The Etl-1 gene encodes a nuclear protein differentially expressed during early mouse development. Dev Dyn 1993;197(3):227-37.
220. Ueda J, Tachibana M, Ikura T, Shinkai Y. Zinc finger protein Wiz links G9a/GLP histone methyltransferases to the co-repressor molecule CtBP. J Biol Chem 2006;281(29):20120-8.
221. McGraw S, Vigneault C, Sirard MA. Temporal expression of factors involved in chromatin remodeling and in gene regulation during early bovine in vitro embryo development. Reproduction 2007;133(3):597-608.
222. De Robertis EM, Larrain J, Oelgeschlager M, Wessely O. The establishment of Spemann's organizer and patterning of the vertebrate embryo. Nat Rev Genet 2000;1(3):171-81.
223. Donner AL, Episkopou V, Maas RL. Sox2 and Pou2f1 interact to control lens and olfactory placode development. Dev Biol 2007;303(2):784-99.
224. Mansukhani A, Ambrosetti D, Holmes G, Cornivelli L, Basilico C. Sox2 induction by FGF and FGFR2 activating mutations inhibits Wnt signaling and osteoblast differentiation. J Cell Biol 2005;168(7):1065-76.
225. Solter D. From teratocarcinomas to embryonic stem cells and beyond: a history of embryonic stem cell research. Nat Rev Genet 2006;7(4):319-27.
226. Wernig M, Meissner A, Cassady JP, Jaenisch R. c-Myc is dispensable for direct reprogramming of mouse fibroblasts. Cell Stem Cell 2008;2(1):10-2.
227. Stadtfeld M, Maherali N, Breault DT, Hochedlinger K. Defining molecular cornerstones during fibroblast to iPS cell reprogramming in mouse. Cell Stem Cell 2008;2(3):230-40.
228. Brambrink T, Foreman R, Welstead GG, Lengner CJ, Wernig M, Suh H, Jaenisch R. Sequential expression of pluripotency markers during direct reprogramming of mouse somatic cells. Cell Stem Cell 2008;2(2):151-9.

229. Inoue T, Ota M, Mikoshiba K, Aruga J. Zic2 and Zic3 synergistically control neurulation and segmentation of paraxial mesoderm in mouse embryo. Dev Biol 2007;306(2):669-84.
230. Suh H, Consiglio A, Ray J, Sawai T, D'Amour KA, Gage FH. In Vivo Fate Analysis Reveals the Multipotent and Self-Renewal Capacities of Sox2(+) Neural Stem Cells in the Adult Hippocampus. Cell Stem Cell 2007;1(5):515-528.
231. Kishi M, Mizuseki K, Sasai N, Yamazaki H, Shiota K, Nakanishi S, Sasai Y. Requirement of Sox2-mediated signaling for differentiation of early Xenopus neuroectoderm. Development 2000;127(4):791-800.

APPENDICES

Appendix 1. Primers for ChIP-PCR assay

No.	Name	SEQUENCE (5' -> 3')	Grade	Quantity
1	60_Rik_375_F	TTCCGGGTCGCAAACGGAAGTG	PCRGrade	50nmole
2	60_Rik_375_R	AGTCCCAGGCTCGCCGCGTTAC	PCRGrade	50nmole
3	Agtrap_109F	AGAAGCCATATGGGAACCCATG	PCRGrade	50nmole
4	Agtrap_109R	ATTAAATTAGGTCTGCCCCGCC	PCRGrade	50nmole
5	Anxa11_432_F	GTCCTGGGGCGTCAGTTGAAAG	PCRGrade	50nmole
6	Anxa11_432_R	CCCCAGCTCACATTTAGGCACC	PCRGrade	50nmole
7	Btn2a2_399_F	GGCGGGCACCATAGGTCCTTTAAAG	PCRGrade	50nmole
8	Btn2a2_399_R	TAGTGCTGAGCCAGGAGACACGTGG	PCRGrade	50nmole
9	Cacna2d1_112F	TAAGTCGCTCTGGGGTGCCTTTG	PCRGrade	50nmole
10	Cacna2d1_112R	GGTTAGCTTTCCCGTCCCCCTT	PCRGrade	50nmole
11	Cd109_219_F	GCAGGAGGTGGCCAACCACACC	PCRGrade	50nmole
12	Cd109_219_R	CGCGCACAAGCAGAGAAGGTGG	PCRGrade	50nmole
13	Commd3_25_F	AGGTGTCAAGCTGCGGAGCTTTTC	PCRGrade	50nmole
14	Commd3_25_R	TATTCCACTTGCCCTTTGGCCC	PCRGrade	50nmole
15	D11Ertd636e_F	GCAGGCCAGAAGCATCGGAAAC	PCRGrade	50nmole
16	D11Ertd636e_R	CAGTGGATTCCTCGCTGGGAGG	PCRGrade	50nmole
17	Dido1_60_F	CAGAGCCACCTTTCAATTTTATG	PCRGrade	50nmole
18	Dido1_60_R	GGGCAATTAGGGTAGCTCTAGG	PCRGrade	50nmole
19	Dll1_523_F	CCCTCCCCCTATGCCTCTCCTTC	PCRGrade	50nmole
20	Dll1_523_R	CGGGCTGCAGCCGCAGGTAAAC	PCRGrade	50nmole
21	Emb_423_F	GTAGGGTCAGCTCATTTGCAGGAG	PCRGrade	50nmole
22	Emb_423_R	GCTTGCTAATTCACACCGGTGC	PCRGrade	50nmole
23	Fgf5_129_F	TCTTGTCTTCCTGGTGGCTCTCGG	PCRGrade	50nmole
24	Fgf5_129_R	TTTCCAAACCCTCCCCACAGGC	PCRGrade	50nmole
25	Fgfbp1_125_F	GCTGTGGAAGGAGGCAGACTGAG	PCRGrade	50nmole
26	Fgfbp1_125_R	TTCTTAGATTGATTCAGAATCG	PCRGrade	50nmole
27	Gja1_251_F	AGCTGTGCGCTTTGTCTTGGAG	PCRGrade	50nmole
28	Gja1_251_R	TGCCTAGGCAAAGGTAGCCAAG	PCRGrade	50nmole
29	Hesx1_434_F	TAACTCCTTAAGCCGCTGGCTG	PCRGrade	50nmole
30	Hesx1_434_R	TGGGATCTTCCAGCAGTTCACC	PCRGrade	50nmole
31	Hlf_333_F	TTCCTTCTAGCCCCACTGCATATCC	PCRGrade	50nmole
32	Hlf_333_R	TTAATTCCCTCGGACAGCGTGG	PCRGrade	50nmole
33	Hoxb13_339_F	CTGTGAAGCTGGAGAAAGGACTGGG	PCRGrade	50nmole
34	Hoxb13_339_R	CGGGGGTCCCACACAGAAACTG	PCRGrade	50nmole
35	Hs6st2_642_F	GGTTGACACAGTAGGTAGCTATCC	PCRGrade	50nmole
36	Hs6st2_642_R	TGTGGGCTTGAATGTGTGAACC	PCRGrade	50nmole
37	Hs6st2_644_F	AGGGTCCTTCAGTCACTTGACTGC	PCRGrade	50nmole
38	Hs6st2_644_R	AGCAAGGAAGTGGTTTCCCTGG	PCRGrade	50nmole
39	Itga1_421_F	AAGGCTGTGAGCTTAGCTACTG	PCRGrade	50nmole
40	Itga1_421_R	ACCCAAATGTCGCAGTGCTGTC	PCRGrade	50nmole
41	Jarid2_405_F	AACCACAAAGGACAATCCATTTTCC	PCRGrade	50nmole
42	Jarid2_405_R	CTCCAAGTCCCAGGCAAGTGTG	PCRGrade	50nmole
43	Klf2_202_F	ACACACACACACACACACACAC	PCRGrade	50nmole
44	Klf2_202_R	TTTTTTCCTGGTAGGTGGCCGG	PCRGrade	50nmole
45	Klf6_394_F	ACAGGGAAACCTGCGGGCACGTTTG	PCRGrade	50nmole
46	Klf6_394_R	TGTTCCCGGATCCTTCCCTGAC	PCRGrade	50nmole
47	Klf9_617_F	TCCCAATGTGAGGTCTGACACGTG	PCRGrade	50nmole
48	Klf9_617_R	CTGCCGATTCTGGCTTTTCTCG	PCRGrade	50nmole
49	Lbxcor1_211_F	GTGCGAGGGGGTTACTTGGCAG	PCRGrade	50nmole
50	Lbxcor1_211_R	CCTTTTCCTCCCTTAGCCCCCC	PCRGrade	50nmole
51	Liph_507_F	TAATGAACCTGCCCTGGAATGTGC	PCRGrade	50nmole
52	Liph_507_R	TGAGGATCGGATAGTTTCGCCC	PCRGrade	50nmole
53	Lmx1b_29_F	TGTCTTGATAACCACTACTCCGCCC	PCRGrade	50nmole
54	Lmx1b_29_R	AAAGGACCCCGGCTTTATCCTC	PCRGrade	50nmole
55	Map4k4_6_F	TGAAAGGGAGCCCTGTTAACAGC	PCRGrade	50nmole
56	Map4k4_6_R	CCGTGCTTAAACAAACTCTGGAGC	PCRGrade	50nmole

No.	Name	SEQUENCE (5' -> 3')	Grade	Quantity
57	Mllt6-342_F	ATCTCCTCTCCGAGCCCTCTGC	PCRGrade	50nmole
58	Mllt6-342_R	AATACCCCCTCAGCGGGAGGTT	PCRGrade	50nmole
59	Mycn_371_F	AGCAGGGGCTGTATGGTAAGTGTTC	PCRGrade	50nmole
60	Mycn_371_R	AAAAGGTTCTGGGAGCCACACC	PCRGrade	50nmole
61	Nid2_430_F	ACATTTCAGAGGGTGGCAGTGTCC	PCRGrade	50nmole
62	Nid2_430_R	GGCCCTCGGATAAAGAATCAAAGG	PCRGrade	50nmole
63	Nodal_255_F	GGCAGCTGCTAATGTGCTAGTTGG	PCRGrade	50nmole
64	Nodal_255_R	TTCAAAAGGGAAGGCGGGATAG	PCRGrade	50nmole
65	Pax6_40_F	GAGTGAGGAGGACAGAGGTCCAATG	PCRGrade	50nmole
66	Pax6_40_R	TCAGCCCAAACCCCTAGCCTAG	PCRGrade	50nmole
67	Pax9_376_F	GCGCTGCCCTACAACCACATTTAC	PCRGrade	50nmole
68	Pax9_376_R	GAGTGAGAGGAGGGCCAGGTGC	PCRGrade	50nmole
69	Pdpn_106_F	AACAGCGGGGGACCCTTTGTTC	PCRGrade	50nmole
70	Pdpn_106_R	AGAAGTGCAGCCCACCGCTCTC	PCRGrade	50nmole
71	Phc1_150_F	CCTTTGGGAAGGCTGAGCATATG	PCRGrade	50nmole
72	Phc1_150_R	GCTGTCTTTGCTAACAATGCTCTGG	PCRGrade	50nmole
73	Porcn_639_F	TGTGAACGGAGAAACACACCCAG	PCRGrade	50nmole
74	Porcn_639_R	TTAACAGAAAGGGACACCGCCC	PCRGrade	50nmole
75	Pou5f1_552_F	GGTTGGGGAGCAGGAAGTTGTCC	PCRGrade	50nmole
76	Pou5f1_552_R	AGGACAATGGCCTTGGCTGGAC	PCRGrade	50nmole
77	Pou5f1_550_F	CTGGGTGTGGGGAGGTTGTAGC	PCRGrade	50nmole
78	Pou5f1_550_R	AACCATCTTCTCTGCCCCCAGG	PCRGrade	50nmole
79	Pou5f1_549_F	GCTAACACGAGTGATTTCCCTGCTC	PCRGrade	50nmole
80	Pou5f1_549_R	AACAATAGGCGTTGACCCCCAC	PCRGrade	50nmole
81	Ppp2r5b_612F	AGCTCAGAACTGGACTCCCGAATTC	PCRGrade	50nmole
82	Ppp2r5b_612R	CAAATTGTGGGCCTGGCACATC	PCRGrade	50nmole
83	Rif1_30_F	CTCTACACCTGGGGTCCAATGGAAG	PCRGrade	50nmole
84	Rif1_30_R	TGGCGTGCATAACAAAGGCCTG	PCRGrade	50nmole
85	Ror1_92_F	CTGAGCCTGCACACAATGAGAGG	PCRGrade	50nmole
86	Ror1_92_R	AGAGTTCAGGGGCTCCAACACC	PCRGrade	50nmole
87	Sall4_57_F	AACCTGCATTCTCCTACAGACCGAC	PCRGrade	50nmole
88	Sall4_57_R	GGACCTCGATTGTGGTTTTGGG	PCRGrade	50nmole
89	Smarcd1_495F	ACTGCAGTTCACCACTCCTGCTGG	PCRGrade	50nmole
90	Smarcd1_495R	TCAACAGCAACCCAGACCCCAG	PCRGrade	50nmole
91	Snapc5_213_F	ACCACCACAGCTATGGCCACTG	PCRGrade	50nmole
92	Snapc5_213_R	AGGAACTGCCTTGTCTCAGGGAGT	PCRGrade	50nmole
93	Sox2_65_F	AACCCACTCAAATGCAGATGCAGG	PCRGrade	50nmole
94	Sox2_65_R	TGACAATGTTGTGGAGGTGCGG	PCRGrade	50nmole
95	Tcea1_2_F	CACCTTAACTTTGCCTTAGGCAGC	PCRGrade	50nmole
96	Tcea1_2_R	TTTCCTGCCTCCACCCAAGTAC	PCRGrade	50nmole
97	Tdgf1_223_F	TGAGACTGGAGGAGTGGAGAAGGG	PCRGrade	50nmole
98	Tdgf1_223_R	CCCCAAGTGATCATGGAAAGGC	PCRGrade	50nmole
99	Thbs2_518_F	GGTTCTCCCCGCCCTGTACATT	PCRGrade	50nmole
100	Thbs2_518_R	AGGAATGTCAAGAGATCTCTTG	PCRGrade	50nmole
101	Trp53_305_F	CTCCCTGCTCTTGCAATCTCTTTG	PCRGrade	50nmole
102	Trp53_305_R	TAAACAAGATGGGGCCTAGG	PCRGrade	50nmole
103	Twsg1_581_F	TAAAGGTAGAGGACCAAGTCACGG	PCRGrade	50nmole
104	Twsg1_581_R	TGTGTTCTGCCCCCCTCTATGTAG	PCRGrade	50nmole
105	Upp1_282_F	GAAAGGGCCAGTCTTTTCCGGG	PCRGrade	50nmole
106	Upp1_282_R	TCAGAGGTCACACCTGCCCCCT	PCRGrade	50nmole
107	Vegfc_198_F	GCAGAGTTCCTAGGTGCTTTTC	PCRGrade	50nmole
108	Vegfc_198_R	GACACACCCAAACTGTATCTGC	PCRGrade	50nmole
109	Vim_20_F	GCAGCATTCCCAGAACTGACTGAG	PCRGrade	50nmole
110	Vim_20_R	TGGAGCACAGAGTGTTCCCAGC	PCRGrade	50nmole
111	Vmp_403_F	AGGATTTTGCCTGGGGCTTACC	PCRGrade	50nmole
112	Vmp_403_R	TCCATCTGGCTGTCAAACCCAG	PCRGrade	50nmole
113	Zcrb1_492_F	ACAATGGACCCGGCACCCCGGAG	PCRGrade	50nmole
114	Zcrb1_492_R	TCCGGCCCCAGGAACGTCCAGC	PCRGrade	50nmole

No.	Name	SEQUENCE (5' -> 3')	Grade	Quantity
115	Zfp206_527_F	GGGGTGTAGGCTTACAGCACTGTG	PCRGrade	50nmole
116	Zfp206_527_R	TGCTGTGTGGCCTTGGAGTCTC	PCRGrade	50nmole
117	Zfp36l1_383F	GGGAATCGGTAACCCTGTAACCG	PCRGrade	50nmole
118	Zfp36l1_383R	GCTGCCCCGCTCTTTGATCTAT	PCRGrade	50nmole
119	Zfp36l1_385F	CACTGCACGGCCTTCGACTTTTC	PCRGrade	50nmole
120	Zfp36l1_385R	TTGGGGCAGCGACTTCAGACAG	PCRGrade	50nmole
121	Zfp499_171_F	GACCTTACCCCCTGCTGTTTAAACC	PCRGrade	50nmole
122	Zfp499_171_R	CAAGGGAAGGTGACAGGGACTAAGA	PCRGrade	50nmole
123	Zic5_471_F	TGGTCATCAGGAAGGCTCACTGTG	PCRGrade	50nmole
124	Zic5_471_R	TTAAGTGCGTTTCGGCTGGCTC	PCRGrade	50nmole

Appendix 2. FDR Analysis: ChIP-PCR results for Zic3/Sox2 common targets

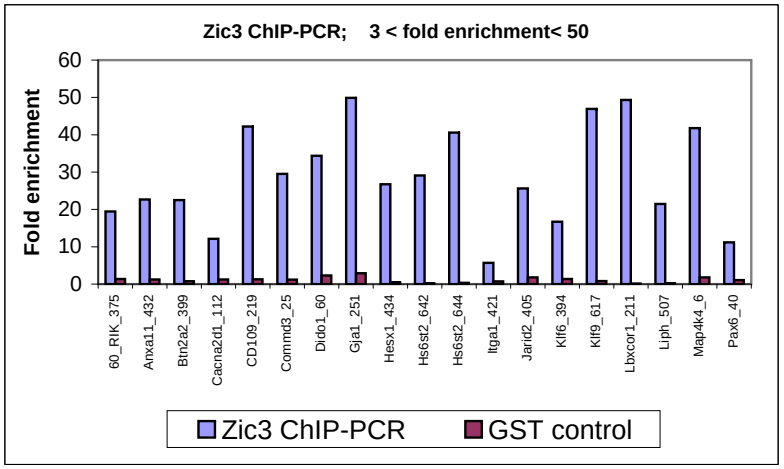

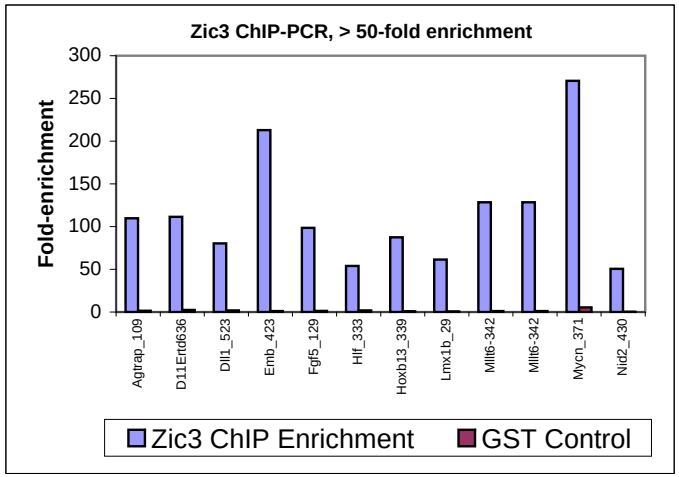

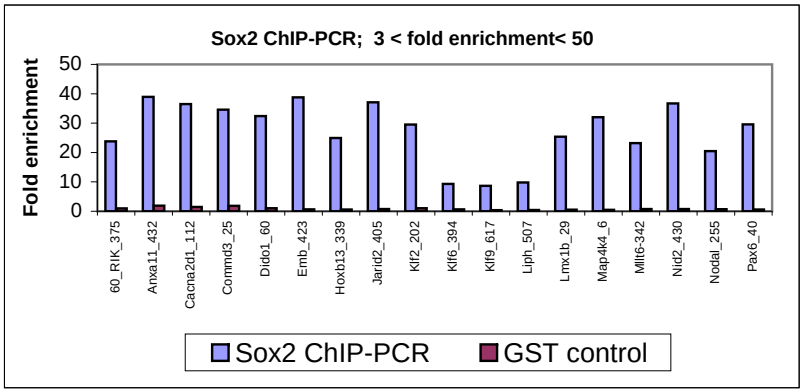

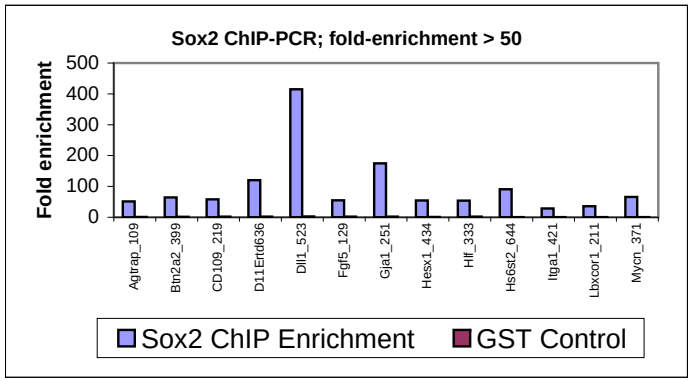

Appendix 3. Luciferase cloning primers for Zic3 chip-chip validation

No.	Name	SEQUENCE (5' -> 3')	Grade	Quantity
1	Mbtps2Luc-F	GCG-CGC-TAG-CACT-TTA-TTT-TTT-GAT-TTG-ACC-TTT-G	PCRGrade	50nmole
2	Mbtps2Luc-R	GCG-CAG-ATC-TCAA-AAT-GTT-TTG-CCA-ATT-AAG-C	PCRGrade	50nmole
3	Cort-Luc-F	GTC-AGC-TAG-CAC-TTG-CAC-GAG-GAG-AAG-GTT-TTC-C	PCRGrade	50nmole
4	Cort-Luc-R	GCT-AAG-ATC-TTGA-GCA-GTT-TCT-CTA-GAG-TCC-G	PCRGrade	50nmole
5	Zic5-2-Luc-F	GTC-AGC-TAG-CTT-CGT-TTC-CTT-GAA-GGA-CAT-TTC	PCRGrade	50nmole
6	Zic5-2-Luc-R	GCT-AAG-ATC-TTT-CAA-CGC-TCT-GGA-AAT-TGT-TG	PCRGrade	50nmole
7	NanogLuc-F	GTC-AGC-TAG-CAA-ATG-AGG-TAA-AGC-CTC-TTT-TT	PCRGrade	50nmole
8	NanogLuc-R	GCT-AAG-ATC-TGA-AGA-GTT-AAA-TGT-CTA-ATG-CA	PCRGrade	50nmole
9	Fgf5-Luc-F	GTC-AGC-TAG-CCT-GTG-TGC-ATG-CAT-GGG-ACT	PCRGrade	50nmole
10	Fgf5-Luc-R	GCT-AAG-ATC-TCG-AAC-GTC-AAG-AGA-AGG-GGT	PCRGrade	50nmole

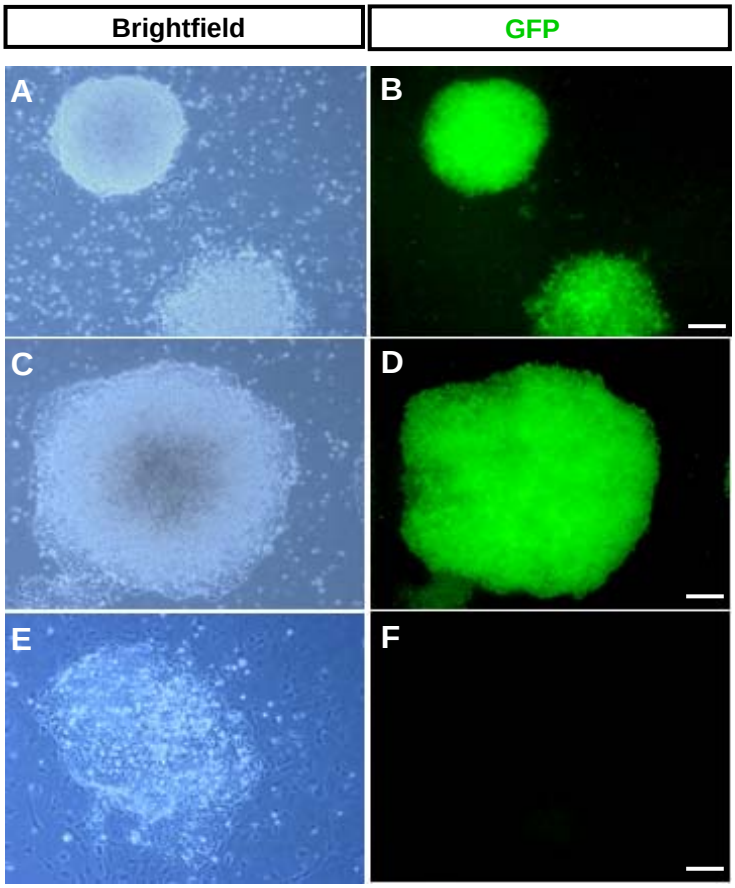

Appendix 4. GFP fluorescence in mES cells transfected with the pSUPER-GFP shRNA vector. (A – B) Three weeks post-transfection, non-targetting shRNA cells demonstrated robust GFP expression (C – D) mES cells were transfected with a pSUPER.GFP shRNA vector targetting the CoupTFII gene. As observed with the non-targetting cells, the CoupTFII knockdown cells expressed high levels of GFP protein. (E - F) In contrast to the non-targetting and CoupTFII RNAi cells, Zic3 shRNA transfected cells did not express GFP after 3 weeks in culture. This suggests that the lack of GFP expression is unique to the Zic3 knockdown cells, and could be an indicator that the colonies emerging from long-term selection were a result of low levels of expression from the shRNA construct, which conferred antibiotic resistance and reduced knockdown efficiency on the cells.

Appendix 5. Zic3 ChIP target gene and their associated promoter regions in mouse ES cells

"Bound Region" (column E) - the annotation assigned to each unique region
Genomic co-ordinates are with reference to UCSC build mm7 (August 2005)

Chr	Start	End	Length	Bound Region	First Gene	Accession #	Second gene	Accession #	Primary Annotation
chr1	4850110	4850610	500	Zic3_extended:1	Tcea1	NM_011541	NA	NA	PROMOTER
chr1	4850939	4851565	626	Zic3_extended:2	Tcea1	NM_011541	NA	NA	PROMOTER
chr1	36925610	36926110	500	Zic3_extended:3	BC050210	NM_201365	Cox5b	NM_009942	DIVERGENT
chr1	40141150	40141878	728	Zic3_extended:4	Map4k4	NM_008696	NA	NA	INSIDE
chr1	65548530	65549030	500	Zic3_extended:5	Pthr2	NM_139270	NA	NA	PROMOTER
chr1	96722860	96723535	675	Zic3_extended:6	Slco4c1	NM_172658	NA	NA	INSIDE
chr1	1.32E+08	1.32E+08	500	Zic3_extended:7	Slc26a9	NM_177243	NA	NA	INSIDE
chr1	1.33E+08	1.33E+08	649	Zic3_extended:8	Lrrn2	NM_010732	NA	NA	PROMOTER
chr1	1.34E+08	1.34E+08	500	Zic3_extended:9	Chi3l1	NM_007695	NA	NA	INSIDE
chr1	1.57E+08	1.57E+08	652	Zic3_extended:10	Ralgps2	NM_023884	NA	NA	INSIDE
chr1	1.66E+08	1.66E+08	500	Zic3_extended:11	Dusp27	NM_001033344	NA	NA	INSIDE
chr1	1.89E+08	1.89E+08	500	Zic3_extended:12	Kctd3	NM_172650	NA	NA	INSIDE
chr2	13511256	13512164	908	Zic3_extended:13	Vim	NM_011701	NA	NA	PROMOTER
chr2	18738918	18739815	897	Zic3_extended:14	Commd3	NM_147778	NA	NA	INSIDE
chr2	22604814	22605497	683	Zic3_extended:15	Gad2	NM_008078	NA	NA	PROMOTER
chr2	26306168	26306668	500	Zic3_extended:16	4932418E24Rik	NM_177841	NA	NA	PROMOTER
chr2	33644475	33644975	500	Zic3_extended:17	Lmx1b	NM_010725	NA	NA	INSIDE
chr2	52079235	52079735	500	Zic3_extended:18	Rif1	NM_175238	NA	NA	PROMOTER
chr2	69062444	69063255	811	Zic3_extended:19	Nostrin	NM_181547	NA	NA	PROMOTER
chr2	69152456	69153109	653	Zic3_extended:20	G6pc2	NM_021331	NA	NA	INSIDE
chr2	80291887	80292541	654	Zic3_extended:21	Frzb	NM_011356	NA	NA	PROMOTER
chr2	1.02E+08	1.02E+08	500	Zic3_extended:22	E430002G05Rik	NM_173749	NA	NA	PROMOTER
chr2	1.06E+08	1.06E+08	948	Zic3_extended:23	Pax6	NM_013627	NA	NA	INSIDE
chr2	1.17E+08	1.17E+08	718	Zic3_extended:24	Spred1	NM_033524	NA	NA	PROMOTER
chr2	1.21E+08	1.21E+08	796	Zic3_extended:25	Trp53bp1	NM_013735	NA	NA	PROMOTER
chr2	1.26E+08	1.26E+08	626	Zic3_extended:26	Slc27a2	NM_011978	NA	NA	PROMOTER
chr2	1.3E+08	1.3E+08	500	Zic3_extended:27	Stk35	NM_001038635	NA	NA	PROMOTER
chr2	1.47E+08	1.47E+08	500	Zic3_extended:28	Xrn2	NM_011917	NA	NA	PROMOTER
chr2	1.47E+08	1.47E+08	500	Zic3_extended:29	Nkx2-2	NM_010919	NA	NA	PROMOTER
chr2	1.48E+08	1.48E+08	500	Zic3_extended:30	Zfp336	NM_028986	NA	NA	PROMOTER
chr2	1.49E+08	1.49E+08	694	Zic3_extended:31	Cst3	NM_009976	NA	NA	INSIDE
chr2	1.53E+08	1.53E+08	500	Zic3_extended:32	Asxl1	NM_001039939	NA	NA	INSIDE
chr2	1.69E+08	1.69E+08	500	Zic3_extended:33	Sall4	NM_201396	NA	NA	INSIDE
chr2	1.72E+08	1.72E+08	614	Zic3_extended:34	Tcfap2c	NM_009335	NA	NA	PROMOTER
chr2	1.81E+08	1.81E+08	500	Zic3_extended:35	Dido1	NM_177852	2310003C23Rik	NM_029607	DIVERGENT
chr3	9009634	9010406	772	Zic3_extended:36	Tpd52	NM_001025263	NA	NA	INSIDE
chr3	34453440	34454092	652	Zic3_extended:37	Sox2	NM_011443	NA	NA	PROMOTER
chr3	51347657	51348396	739	Zic3_extended:38	Ccrn4l	NM_009834	NA	NA	PROMOTER
chr3	81139550	81140250	700	Zic3_extended:39	Pdgfc	NM_019971	NA	NA	PROMOTER
chr3	95534005	95534505	500	Zic3_extended:40	Mcl1	NM_008562	NA	NA	INSIDE
chr3	96432490	96433120	630	Zic3_extended:41	Txnip	NM_023719	NA	NA	INSIDE
chr3	97031441	97032125	684	Zic3_extended:42	Acp6	NM_019800	NA	NA	INSIDE
chr3	1.02E+08	1.02E+08	662	Zic3_extended:43	Casq2	NM_009814	NA	NA	PROMOTER
chr3	1.03E+08	1.03E+08	786	Zic3_extended:44	Dennd2c	NM_177857	NA	NA	INSIDE
chr3	1.05E+08	1.05E+08	680	Zic3_extended:45	Mov10	NM_008619	NA	NA	PROMOTER
chr3	1.21E+08	1.21E+08	644	Zic3_extended:46	Alg14	NM_024178	NA	NA	INSIDE
chr3	1.27E+08	1.27E+08	689	Zic3_extended:47	D3Wsu161e	NM_138593	mmu-mir-302	NA	DIVERGENT
chr4	35027618	35028342	724	Zic3_extended:48	Cga	NM_009889	NA	NA	PROMOTER
chr4	47107367	47107867	500	Zic3_extended:49	Galnt12	NM_172693	NA	NA	INSIDE
chr4	57961424	57962248	824	Zic3_extended:50	D630039A03Rik	NM_178727	NA	NA	PROMOTER
chr4	99473183	99474693	1510	Zic3_extended:51	Ror1	NM_013845	NA	NA	INSIDE
chr4	1.17E+08	1.17E+08	615	Zic3_extended:52	Plk3	NM_013807	NA	NA	INSIDE
chr4	1.23E+08	1.23E+08	745	Zic3_extended:53	Rragc	NM_017475	NA	NA	INSIDE
chr4	1.3E+08	1.3E+08	500	Zic3_extended:54	Pef1	NM_026441	NA	NA	PROMOTER
chr4	1.34E+08	1.34E+08	500	Zic3_extended:55	Stmn1	NM_019641	NA	NA	INSIDE
chr4	1.43E+08	1.43E+08	895	Zic3_extended:56	Pdpn	NM_010329	NA	NA	PROMOTER
chr4	1.47E+08	1.47E+08	794	Zic3_extended:57	Agtrap	NM_009642	NA	NA	PROMOTER
chr4	1.48E+08	1.48E+08	500	Zic3_extended:58	Cort	NM_007745	NA	NA	INSIDE
chr5	14920688	14921188	500	Zic3_extended:59	Cacna2d1	NM_009784	NA	NA	PROMOTER
chr5	28770547	28771193	646	Zic3_extended:60	Dnajb6	NM_001037941	NA	NA	INSIDE
chr5	32165192	32165692	500	Zic3_extended:61	Slc5a1	NM_019810	NA	NA	PROMOTER
chr5	37356800	37357725	925	Zic3_extended:62	Otop1	NM_178139	NA	NA	PROMOTER
chr5	43189306	43190241	935	Zic3_extended:63	Cd38	NM_007646	NA	NA	INSIDE
chr5	43303018	43304226	1208	Zic3_extended:64	Fgfbp1	NM_008009	NA	NA	PROMOTER

Chr	Start	End	Length	Bound Region	First Gene	Accession #	Second gene	Accession #	Primary Annotation
chr5	88619489	88620142	653	Zic3_extended:65	Grsf1	NM_178700	NA	NA	PROMOTER
chr5	97470559	97471301	742	Zic3_extended:66	Fgf5	NM_010203	NA	NA	INSIDE
chr5	99258407	99259361	954	Zic3_extended:67	2310057D15Rik	NM_026421	NA	NA	INSIDE
chr5	1.06E+08	1.06E+08	500	Zic3_extended:68	Tgfbr3	NM_011578	NA	NA	INSIDE
chr5	1.09E+08	1.09E+08	651	Zic3_extended:69	D5Ertd585e	NM_027922	NA	NA	PROMOTER
chr5	1.17E+08	1.17E+08	729	Zic3_extended:70	Wsb2	NM_021539	NA	NA	PROMOTER
chr5	1.47E+08	1.47E+08	895	Zic3_extended:71	Ubl3	NM_011908	NA	NA	INSIDE
chr6	28058167	28058667	500	Zic3_extended:72	Grm8	NM_008174	NA	NA	PROMOTER
chr6	92329962	92330617	655	Zic3_extended:73	Trh	NM_009426	NA	NA	PROMOTER
chr6	92899650	92900333	683	Zic3_extended:74	8430417A20Rik	NM_175209	NA	NA	PROMOTER
chr6	97296454	97297220	766	Zic3_extended:75	Ube1c	NM_011666	Arl6ip5	NM_022992	DIVERGENT
chr6	1.15E+08	1.15E+08	500	Zic3_extended:76	Timp4	NM_080639	NA	NA	PROMOTER
chr6	1.22E+08	1.22E+08	1212	Zic3_extended:77	Phc1	NM_007905	NA	NA	PROMOTER
chr6	1.22E+08	1.22E+08	804	Zic3_extended:78	Phc1	NM_007905	NA	NA	PROMOTER
chr6	1.27E+08	1.27E+08	653	Zic3_extended:79	Fgf23	NM_022657	NA	NA	INSIDE
chr6	1.37E+08	1.37E+08	717	Zic3_extended:80	Rerg	NM_181988	NA	NA	PROMOTER
chr6	1.41E+08	1.41E+08	500	Zic3_extended:81	Aebp2	NM_178803	NA	NA	PROMOTER
chr6	1.43E+08	1.43E+08	500	Zic3_extended:82	Ldhb	NM_008492	NA	NA	PROMOTER
chr7	6290797	6291881	1084	Zic3_extended:83	Usp29	NM_021323	NA	NA	INSIDE
chr7	11600570	11601510	940	Zic3_extended:84	Zfp499	NM_001024699	Trim28	NM_011588	DIVERGENT
chr7	24792012	24792512	500	Zic3_extended:85	4732475C15Rik	NM_001024726	NA	NA	PROMOTER
chr7	25367850	25368350	500	Zic3_extended:86	Samd4b	NM_175021	NA	NA	INSIDE
chr7	32228061	32228724	663	Zic3_extended:87	Rhpn2	NM_027897	NA	NA	INSIDE
chr7	41416413	41416913	500	Zic3_extended:88	Cd37	NM_007645	NA	NA	PROMOTER
chr7	55753819	55754609	790	Zic3_extended:89	Snurf	NM_033174	NA	NA	PROMOTER
chr7	93773043	93773543	500	Zic3_extended:90	Aqp11	NM_175105	NA	NA	PROMOTER
chr7	1.06E+08	1.06E+08	500	Zic3_extended:91	D930014E17Rik	NM_020616	NA	NA	PROMOTER
chr7	1.14E+08	1.14E+08	743	Zic3_extended:92	Arl6ip1	NM_019419	NA	NA	INSIDE
chr7	1.37E+08	1.37E+08	863	Zic3_extended:93	Ifitm2	NM_030694	Ifitm1	NM_026820	DIVERGENT
chr8	11608449	11609055	606	Zic3_extended:94	Ankrd10	NM_133971	NA	NA	PROMOTER
chr8	18819898	18820661	763	Zic3_extended:95	Agpat5	NM_026792	NA	NA	PROMOTER
chr8	23223678	23224286	608	Zic3_extended:96	1810011O10Rik	NM_026931	NA	NA	INSIDE
chr8	25840152	25840981	829	Zic3_extended:97	Gpr124	NM_054044	NA	NA	PROMOTER
chr8	52844954	52845644	690	Zic3_extended:98	Vegfc	NM_009506	NA	NA	PROMOTER
chr8	68450734	68451563	829	Zic3_extended:99	Gatad2a	NM_145596	NA	NA	PROMOTER
chr8	70838696	70839196	500	Zic3_extended:100	Klf2	NM_008452	NA	NA	PROMOTER
chr9	35452948	35453448	500	Zic3_extended:101	Ddx25	NM_013932	NA	NA	INSIDE
chr9	44239945	44240445	500	Zic3_extended:102	Mizf	NM_172162	NA	NA	PROMOTER
chr9	50637857	50638357	500	Zic3_extended:103	Dlat	NM_145614	NA	NA	INSIDE
chr9	52025216	52025716	500	Zic3_extended:104	Rdx	NM_009041	NA	NA	PROMOTER
chr9	59683361	59683861	500	Zic3_extended:105	Pkm2	NM_011099	NA	NA	INSIDE
chr9	61971493	61972167	674	Zic3_extended:106	Kif23	NM_024245	NA	NA	INSIDE
chr9	63174592	63175307	715	Zic3_extended:107	Lbxcor1	NM_172446	NA	NA	INSIDE
chr9	64051160	64051660	500	Zic3_extended:108	Smad6	NM_008542	NA	NA	PROMOTER
chr9	64206873	64207485	612	Zic3_extended:109	Snapc5	NM_183316	NA	NA	PROMOTER
chr9	70173572	70174072	500	Zic3_extended:110	6430514L14Rik	NM_029784	NA	NA	PROMOTER
chr9	73017831	73018331	500	Zic3_extended:111	Ccpg1	NM_028181	NA	NA	INSIDE
chr9	77583464	77583964	500	Zic3_extended:112	Lrrc1	NM_172528	NA	NA	PROMOTER
chr9	78663384	78663884	500	Zic3_extended:113	Slc17a5	NM_172773	NA	NA	INSIDE
chr9	78691267	78691767	500	Zic3_extended:114	Cd109	NM_153098	NA	NA	INSIDE
chr9	95051189	95051807	618	Zic3_extended:115	Chst2	NM_018763	NA	NA	INSIDE
chr9	98627445	98628296	851	Zic3_extended:116	Faim	NM_011810	NA	NA	PROMOTER
chr9	98884980	98885480	500	Zic3_extended:117	Cep70	NM_023873	NA	NA	INSIDE
chr9	1.06E+08	1.06E+08	500	Zic3_extended:118	Pcbp4	NM_021567	NA	NA	PROMOTER
chr9	1.08E+08	1.08E+08	500	Zic3_extended:119	Dag1	NM_010017	NA	NA	PROMOTER
chr9	1.08E+08	1.08E+08	500	Zic3_extended:120	Usp19	NM_027804	NA	NA	INSIDE
chr9	1.1E+08	1.1E+08	609	Zic3_extended:121	Mtap4	NM_008633	NA	NA	INSIDE
chr9	1.11E+08	1.11E+08	1085	Zic3_extended:122	Tdgf1	NM_011562	Lrrc2	NM_028838	DIVERGENT
chr9	1.12E+08	1.12E+08	626	Zic3_extended:123	Arpp21	NM_033264	NA	NA	INSIDE
chr9	1.18E+08	1.18E+08	636	Zic3_extended:124	Itga9	NM_133721	NA	NA	INSIDE
chr10	4540427	4540927	500	Zic3_extended:125	Fbxo5	NM_025995	NA	NA	PROMOTER
chr10	4795929	4796429	500	Zic3_extended:126	Syne1	NM_153399	NA	NA	INSIDE
chr10	13667365	13668247	882	Zic3_extended:127	Hivep2	NM_010437	NA	NA	PROMOTER
chr10	24587560	24588060	500	Zic3_extended:128	Enpp3	NM_134005	NA	NA	INSIDE
chr10	40087864	40088364	500	Zic3_extended:129	Amd2	NM_007444	NA	NA	INSIDE
chr10	43287733	43288387	654	Zic3_extended:130	AK122525	NM_199028	NA	NA	PROMOTER
chr10	56191057	56192221	1164	Zic3_extended:131	Gja1	NM_010288	NA	NA	PROMOTER
chr10	59469793	59470293	500	Zic3_extended:132	Ddit4	NM_029083	NA	NA	PROMOTER
chr10	60934099	60934599	500	Zic3_extended:133	Nodal	NM_013611	NA	NA	PROMOTER

Chr	Start	End	Length	Bound Region	First Gene	Accession #	Second gene	Accession #	Primary Annotation
chr10	61300254	61300930	676	Zic3_extended:134	H2afy2	NM_207000	NA	NA	INSIDE
chr10	61651300	61651917	617	Zic3_extended:135	Neurog3	NM_009719	NA	NA	PROMOTER
chr10	63609168	63609826	658	Zic3_extended:136	Lrrtm3	NM_178678	NA	NA	PROMOTER
chr10	66687292	66687909	617	Zic3_extended:137	D10Ucla1	NM_178606	NA	NA	PROMOTER
chr10	69847135	69847635	500	Zic3_extended:138	Slc16a9	NM_025807	NA	NA	PROMOTER
chr10	70886885	70887385	500	Zic3_extended:139	Ube2d1	NM_145420	NA	NA	INSIDE
chr10	75593367	75593995	628	Zic3_extended:140	Gm867	NM_001037714	NA	NA	INSIDE
chr10	79546773	79547388	615	Zic3_extended:141	Rnf126	NM_144528	NA	NA	PROMOTER
chr10	80131024	80131524	500	Zic3_extended:142	Adamtsl5	NM_025629	6330514A18Rik	NM_183152	DIVERGENT
chr10	85475173	85475673	500	Zic3_extended:143	Prdm4	NM_181650	NA	NA	PROMOTER
chr10	93101056	93101556	500	Zic3_extended:144	Ccdc38	NM_175488	NA	NA	INSIDE
chr10	94976124	94976827	703	Zic3_extended:145	Socs2	NM_007706	NA	NA	INSIDE
chr10	99577178	99577678	500	Zic3_extended:146	Kitl	NM_013598	NA	NA	INSIDE
chr10	1.17E+08	1.17E+08	500	Zic3_extended:147	Frs2	NM_177798	NA	NA	PROMOTER
chr10	1.2E+08	1.2E+08	500	Zic3_extended:148	Wif1	NM_011915	NA	NA	PROMOTER
chr10	1.27E+08	1.27E+08	500	Zic3_extended:149	Nab2	NM_008668	BC030440	NM_173732	DIVERGENT
chr10	1.28E+08	1.28E+08	500	Zic3_extended:150	Dgka	NM_016811	NA	NA	INSIDE
chr11	4112303	4112803	500	Zic3_extended:151	Sf3a1	NM_026175	NA	NA	INSIDE
chr11	6369586	6370086	500	Zic3_extended:152	Ppia	NM_008907	NA	NA	INSIDE
chr11	9067943	9068443	500	Zic3_extended:153	Upp1	NM_009477	NA	NA	PROMOTER
chr11	9069187	9069687	500	Zic3_extended:154	Upp1	NM_009477	NA	NA	PROMOTER
chr11	29644701	29645201	500	Zic3_extended:155	Rtn4	NM_194052	NA	NA	PROMOTER
chr11	31323146	31323646	500	Zic3_extended:156	Stc2	NM_011491	NA	NA	PROMOTER
chr11	34267223	34267723	500	Zic3_extended:157	MGC99845	NM_001025382	NA	NA	INSIDE
chr11	48827727	48828670	943	Zic3_extended:158	Irgm	NM_008326	NA	NA	PROMOTER
chr11	50167019	50167755	736	Zic3_extended:159	Sqstm1	NM_011018	NA	NA	INSIDE
chr11	50333864	50334576	712	Zic3_extended:160	Hnrph1	NM_021510	NA	NA	PROMOTER
chr11	51594711	51595211	500	Zic3_extended:161	Rmnd5b	NM_025346	NA	NA	PROMOTER
chr11	51607066	51607566	500	Zic3_extended:162	D930048N14Rik	NM_175289	NA	NA	PROMOTER
chr11	53721599	53722099	500	Zic3_extended:163	Irf1	NM_008390	NA	NA	PROMOTER
chr11	59531447	59531947	500	Zic3_extended:164	Jmjd4	NM_178659	NA	NA	INSIDE
chr11	64516893	64517393	500	Zic3_extended:165	F930015N05Rik	NM_001039541	NA	NA	INSIDE
chr11	68934435	68934935	500	Zic3_extended:166	Ndel1	NM_023668	NA	NA	PROMOTER
chr11	69199253	69199753	500	Zic3_extended:167	Hes7	NM_033041	NA	NA	PROMOTER
chr11	69662788	69664152	1364	Zic3_extended:168	Trp53	NM_011640	NA	NA	INSIDE
chr11	69686816	69687316	500	Zic3_extended:169	Atp1b2	NM_013415	NA	NA	INSIDE
chr11	72123511	72124346	835	Zic3_extended:170	Aipl1	NM_053245	6720460F02Rik	NM_144526	DIVERGENT
chr11	72491980	72492480	500	Zic3_extended:171	D130058I21Rik	NM_177776	NA	NA	INSIDE
chr11	73241691	73242191	500	Zic3_extended:172	P2rx5	NM_033321	NA	NA	PROMOTER
chr11	74126654	74127154	500	Zic3_extended:173	Olfr139	NM_147003	NA	NA	PROMOTER
chr11	74730687	74731419	732	Zic3_extended:174	E130309D14Rik	NM_001013784	NA	NA	DOWNSTREAM
chr11	74911605	74912105	500	Zic3_extended:175	Mnt	NM_010813	NA	NA	PROMOTER
chr11	75254608	75255258	650	Zic3_extended:176	Hic1	NM_010430	mmu-mir-212	NA	DIVERGENT
chr11	75276497	75277201	704	Zic3_extended:177	Rtn4rl1	NM_177708	NA	NA	INSIDE
chr11	75612874	75613724	850	Zic3_extended:178	Slc43a2	NM_173388	NA	NA	PROMOTER
chr11	82469836	82470475	639	Zic3_extended:179	Tmem132e	NM_023438	NA	NA	PROMOTER
chr11	84595929	84596429	500	Zic3_extended:180	Lhx1	NM_008498	NA	NA	PROMOTER
chr11	84939558	84940274	716	Zic3_extended:181	Ggnbp2	NM_153144	NA	NA	INSIDE
chr11	88169680	88170287	607	Zic3_extended:182	Cuedc1	NM_198013	NA	NA	INSIDE
chr11	89108200	89108822	622	Zic3_extended:183	Trim25	NM_009546	NA	NA	PROMOTER
chr11	90500291	90500791	500	Zic3_extended:184	Hlf	NM_172563	NA	NA	PROMOTER
chr11	95420611	95421258	647	Zic3_extended:185	Myst2	NM_177619	NA	NA	PROMOTER
chr11	95951212	95951712	500	Zic3_extended:186	Abi3	NM_025659	Gngt2	NM_023121	DIVERGENT
chr11	96116149	96116649	500	Zic3_extended:187	Igf2bp1	NM_009951	NA	NA	PROMOTER
chr11	96299162	96300038	876	Zic3_extended:188	Hoxb13	NM_008267	NA	NA	PROMOTER
chr11	97229180	97229680	500	Zic3_extended:189	Tbx21	NM_019507	NA	NA	PROMOTER
chr11	97770838	97771831	993	Zic3_extended:190	Mllt6	NM_139311	NA	NA	PROMOTER
chr11	99339714	99340338	624	Zic3_extended:191	Smarce1	NM_020618	NA	NA	PROMOTER
chr11	1.01E+08	1.01E+08	500	Zic3_extended:192	Jup	NM_010593	NA	NA	INSIDE
chr11	1.03E+08	1.03E+08	500	Zic3_extended:193	BC050840	BC050840	NA	NA	Unknown
chr11	1.1E+08	1.1E+08	833	Zic3_extended:194	Abca8b	NM_013851	NA	NA	PROMOTER
chr11	1.14E+08	1.14E+08	927	Zic3_extended:195	D11Ertd636e	NM_029794	NA	NA	PROMOTER
chr11	1.15E+08	1.15E+08	899	Zic3_extended:196	Slc9a3r1	NM_012030	NA	NA	PROMOTER
chr11	1.16E+08	1.16E+08	500	Zic3_extended:197	Grb2	NM_008163	NA	NA	INSIDE
chr11	1.16E+08	1.16E+08	500	Zic3_extended:198	Grb2	NM_008163	NA	NA	PROMOTER
chr11	1.16E+08	1.16E+08	500	Zic3_extended:199	H3f3b	NM_008211	NA	NA	INSIDE
chr11	1.17E+08	1.17E+08	500	Zic3_extended:200	St6galnac2	NM_009180	NA	NA	INSIDE
chr11	1.21E+08	1.21E+08	500	Zic3_extended:201	Pycr1	NM_144795	NA	NA	PROMOTER
chr12	8798692	8799433	741	Zic3_extended:202	Sdc1	NM_011519	NA	NA	INSIDE

Chr	Start	End	Length	Bound Region	First Gene	Accession #	Second gene	Accession #	Primary Annotation
chr12	11329562	11330209	647	Zic3_extended:203	Smc6l1	NM_025695	NA	NA	INSIDE
chr12	13005608	13006590	982	Zic3_extended:204	Mycn	NM_008709	NA	NA	PROMOTER
chr12	49359490	49360307	817	Zic3_extended:205	6030408C04Rik	NM_001015099	NA	NA	PROMOTER
chr12	49361345	49362049	704	Zic3_extended:206	6030408C04Rik	NM_001015099	NA	NA	PROMOTER
chr12	54627184	54627684	500	Zic3_extended:207	Pax9	NM_011041	NA	NA	INSIDE
chr12	68767854	68768354	500	Zic3_extended:208	Frmd6	NM_028127	NA	NA	PROMOTER
chr12	74328029	74328828	799	Zic3_extended:209	Zbtb25	NM_028356	Zbtb1	NM_178744	DIVERGENT
chr12	74920901	74921401	500	Zic3_extended:210	Max	NM_008558	NA	NA	PROMOTER
chr12	74923581	74924081	500	Zic3_extended:211	Max	NM_008558	NA	NA	PROMOTER
chr12	78074365	78074865	500	Zic3_extended:212	Zfp36l1	NM_007564	NA	NA	INSIDE
chr12	78079547	78080223	676	Zic3_extended:213	Zfp36l1	NM_007564	NA	NA	PROMOTER
chr12	78223037	78223537	500	Zic3_extended:214	Actn1	NM_134156	NA	NA	PROMOTER
chr12	81483154	81483654	500	Zic3_extended:215	Dpf3	NM_058212	NA	NA	INSIDE
chr12	82640889	82641389	500	Zic3_extended:216	7420416P09Rik	NM_001033776	NA	NA	PROMOTER
chr12	99453434	99454042	608	Zic3_extended:217	Mjd	NM_029705	NA	NA	PROMOTER
chr12	1.03E+08	1.03E+08	500	Zic3_extended:218	C630028L02Rik	NM_176899	NA	NA	INSIDE
chr12	1.04E+08	1.04E+08	500	Zic3_extended:219	Vrk1	NM_001029843	NA	NA	PROMOTER
chr12	1.08E+08	1.08E+08	500	Zic3_extended:220	2310040A13Rik	NM_027149	NA	NA	PROMOTER
chr13	5745679	5746179	500	Zic3_extended:221	Klf6	NM_011803	NA	NA	PROMOTER
chr13	21148419	21148919	500	Zic3_extended:222	Hist1h1b	NM_020034	NA	NA	PROMOTER
chr13	21155988	21156488	500	Zic3_extended:223	Hist1h2bp	NM_178202	NA	NA	DOWNSTREAM
chr13	21156519	21157406	887	Zic3_extended:224	Hist1h2bp	NM_178202	NA	NA	DOWNSTREAM
chr13	22858042	22858542	500	Zic3_extended:225	Btn2a2	NM_175938	NA	NA	PROMOTER
chr13	23105115	23105615	500	Zic3_extended:226	Hist1h1c	NM_015786	NA	NA	INSIDE
chr13	23110286	23110786	500	Zic3_extended:227	Hist1h3h	NM_178206	NA	NA	INSIDE
chr13	24197468	24197968	500	Zic3_extended:228	Ttrap	NM_019551	NA	NA	INSIDE
chr13	24640675	24641175	500	Zic3_extended:229	Vmp	NM_009513	NA	NA	PROMOTER
chr13	43054988	43055488	500	Zic3_extended:230	Rnf182	NM_183204	NA	NA	PROMOTER
chr13	44178546	44179261	715	Zic3_extended:231	Jarid2	NM_021878	NA	NA	PROMOTER
chr13	48671827	48672327	500	Zic3_extended:232	Ninj1	NM_013610	NA	NA	INSIDE
chr13	53693147	53693647	500	Zic3_extended:233	Cltb	NM_028870	NA	NA	INSIDE
chr13	54918449	54918949	500	Zic3_extended:234	Pitx1	NM_011097	NA	NA	INSIDE
chr13	61391226	61391915	689	Zic3_extended:235	Ptch1	NM_008957	NA	NA	PROMOTER
chr13	64425224	64425724	500	Zic3_extended:236	Mterfd1	NM_025547	NA	NA	PROMOTER
chr13	80810937	80811548	611	Zic3_extended:237	C130071C03Rik	NM_177100	NA	NA	INSIDE
chr13	94266754	94267254	500	Zic3_extended:238	Hexb	NM_010422	NA	NA	INSIDE
chr13	95885463	95885963	500	Zic3_extended:239	Fcho2	NM_172591	NA	NA	PROMOTER
chr13	1.1E+08	1.1E+08	693	Zic3_extended:240	Il6st	NM_010560	NA	NA	PROMOTER
chr13	1.12E+08	1.12E+08	500	Zic3_extended:241	Pelo	NM_134058	NA	NA	PROMOTER
chr13	1.12E+08	1.12E+08	627	Zic3_extended:242	Itga1	NM_001033228	Pelo	NM_134058	PROMOTER
chr13	1.14E+08	1.14E+08	500	Zic3_extended:243	Isl1	NM_021459	NA	NA	PROMOTER
chr13	1.14E+08	1.14E+08	947	Zic3_extended:244	Emb	NM_010330	NA	NA	PROMOTER
chr13	1.15E+08	1.15E+08	678	Zic3_extended:245	Hcn1	NM_010408	NA	NA	INSIDE
chr14	17407826	17408326	500	Zic3_extended:246	Nid2	NM_008695	NA	NA	PROMOTER
chr14	17408365	17409155	790	Zic3_extended:247	Nid2	NM_008695	NA	NA	PROMOTER
chr14	23512539	23513039	500	Zic3_extended:248	Anxa11	NM_013469	NA	NA	PROMOTER
chr14	24432904	24433818	914	Zic3_extended:249	Hesx1	NM_010420	NA	NA	INSIDE
chr14	24471440	24472072	632	Zic3_extended:250	Il17rd	NM_134437	NA	NA	PROMOTER
chr14	32320601	32321422	821	Zic3_extended:251	mmu-mir-346	mmu-mir-346	NA	NA	PROMOTER
chr14	40705759	40706259	500	Zic3_extended:252	Gnpnat1	NM_019425	NA	NA	INSIDE
chr14	47659796	47660296	500	Zic3_extended:253	Sall2	NM_015772	NA	NA	INSIDE
chr14	47665712	47666212	500	Zic3_extended:254	Sall2	NM_015772	NA	NA	PROMOTER
chr14	49278127	49278836	709	Zic3_extended:255	Slc7a7	NM_011405	NA	NA	INSIDE
chr14	50427122	50427881	759	Zic3_extended:256	Wdr23	NM_133734	NA	NA	INSIDE
chr14	51535675	51536380	705	Zic3_extended:257	4930548G07Rik	NM_023773	NA	NA	PROMOTER
chr14	52389235	52389735	500	Zic3_extended:258	Il17d	NM_145837	NA	NA	PROMOTER
chr14	58372276	58373106	830	Zic3_extended:259	Tdh	NM_021480	NA	NA	INSIDE
chr14	60983009	60983509	500	Zic3_extended:260	Ephx2	NM_007940	NA	NA	INSIDE
chr14	64996184	64997102	918	Zic3_extended:261	Slc39a14	NM_144808	NA	NA	PROMOTER
chr14	65279249	65279890	641	Zic3_extended:262	Epb4.9	NM_013514	NA	NA	PROMOTER
chr14	82130067	82130834	767	Zic3_extended:263	Tdrd3	NM_172605	NA	NA	INSIDE
chr14	97412017	97412632	615	Zic3_extended:264	Kctd12	NM_177715	NA	NA	INSIDE
chr14	1E+08	1E+08	697	Zic3_extended:265	Spry2	NM_011897	NA	NA	INSIDE
chr14	1.15E+08	1.15E+08	500	Zic3_extended:266	Rap2a	NM_029519	NA	NA	PROMOTER
chr14	1.17E+08	1.17E+08	500	Zic3_extended:267	Clybl	NM_029556	NA	NA	INSIDE
chr14	1.17E+08	1.17E+08	674	Zic3_extended:268	Zic5	NM_022987	Zic2	NM_009574	DIVERGENT
chr15	25468138	25468798	660	Zic3_extended:269	Basp1	NM_027395	NA	NA	PROMOTER
chr15	55172354	55172854	500	Zic3_extended:270	Depdc6	NM_145470	NA	NA	INSIDE
chr15	58278092	58278836	744	Zic3_extended:271	Fbxo32	NM_026346	NA	NA	INSIDE

Chr	Start	End	Length	Bound Region	First Gene	Accession #	Second gene	Accession #	Primary Annotation
chr15	79066470	79066970	500	Zic3_extended:272	Triobp	NM_001024716	NA	NA	INSIDE
chr15	79689154	79689973	819	Zic3_extended:273	Dmc1h	NM_010059	NA	NA	PROMOTER
chr15	82359817	82360317	500	Zic3_extended:274	Sep-03	NM_011889	NA	NA	INSIDE
chr15	84747325	84748166	841	Zic3_extended:275	BC024991	BC024991	NA	NA	Unknown
chr15	89157846	89158507	661	Zic3_extended:276	5730502D15Rik	NM_026485	NA	NA	PROMOTER
chr15	89278423	89278923	500	Zic3_extended:277	1700027J05Rik	NM_027081	NA	NA	INSIDE
chr15	93477634	93478595	961	Zic3_extended:278	Zcrb1	NM_026025	NA	NA	INSIDE
chr15	95791823	95792323	500	Zic3_extended:279	Tmem16f	NM_175344	NA	NA	INSIDE
chr15	99689343	99690118	775	Zic3_extended:280	Smarcd1	NM_031842	NA	NA	INSIDE
chr15	1.02E+08	1.02E+08	500	Zic3_extended:281	AI507495	NM_213728	NA	NA	PROMOTER
chr15	1.02E+08	1.02E+08	500	Zic3_extended:282	Eif4b	NM_145625	NA	NA	PROMOTER
chr15	1.04E+08	1.04E+08	500	Zic3_extended:283	Ppp1r1a	NM_021391	NA	NA	PROMOTER
chr16	10461960	10462763	803	Zic3_extended:284	Socs1	NM_009896	NA	NA	INSIDE
chr16	16695536	16696036	500	Zic3_extended:285	1810015A11Rik	NM_026940	NA	NA	PROMOTER
chr16	16759773	16760273	500	Zic3_extended:286	Gm603	NM_001033338	NA	NA	INSIDE
chr16	20282287	20282787	500	Zic3_extended:287	Thpo	NM_009379	NA	NA	INSIDE
chr16	21647513	21648253	740	Zic3_extended:288	Liph	NM_153404	NA	NA	PROMOTER
chr16	22092011	22092673	662	Zic3_extended:289	Etv5	NM_023794	NA	NA	PROMOTER
chr16	24055235	24055735	500	Zic3_extended:290	Lpp	NM_178665	NA	NA	INSIDE
chr16	32283306	32283806	500	Zic3_extended:291	Tfrc	NM_011638	NA	NA	INSIDE
chr16	32551851	32552351	500	Zic3_extended:292	1700021K19Rik	NM_172615	Fyttd1	NM_027226	DIVERGENT
chr16	45502007	45502716	709	Zic3_extended:293	Tagln3	NM_019754	NA	NA	PROMOTER
chr16	49616441	49617086	645	Zic3_extended:294	Cd47	NM_010581	NA	NA	INSIDE
chr17	12975566	12976632	1066	Zic3_extended:295	Thbs2	NM_011581	NA	NA	INSIDE
chr17	13241510	13242010	500	Zic3_extended:296	Phf10	NM_024250	NA	NA	INSIDE
chr17	13242296	13242904	608	Zic3_extended:297	Phf10	NM_024250	NA	NA	PROMOTER
chr17	13617464	13617964	500	Zic3_extended:298	Dll1	NM_007865	NA	NA	PROMOTER
chr17	13763847	13764347	500	Zic3_extended:299	Pdcd2	NM_008799	NA	NA	INSIDE
chr17	13940963	13941633	670	Zic3_extended:300	Chd1	NM_007690	NA	NA	PROMOTER
chr17	21780670	21781286	616	Zic3_extended:301	Zfp206	NM_001033425	NA	NA	INSIDE
chr17	21824850	21825510	660	Zic3_extended:302	Mmp25	NM_001033339	NA	NA	PROMOTER
chr17	24293450	24294656	1206	Zic3_extended:303	Tmem8	NM_021793	NA	NA	PROMOTER
chr17	25824460	25824960	500	Zic3_extended:304	Rps10	NM_025963	NA	NA	PROMOTER
chr17	26875656	26876156	500	Zic3_extended:305	Slc26a8	NM_146076	NA	NA	INSIDE
chr17	29577155	29577655	500	Zic3_extended:306	Pde9a	NM_008804	NA	NA	INSIDE
chr17	30584537	30585037	500	Zic3_extended:307	Wiz	NM_212438	NA	NA	PROMOTER
chr17	31758569	31759069	500	Zic3_extended:308	Hnrpm	NM_029804	NA	NA	INSIDE
chr17	31987259	31987907	648	Zic3_extended:309	Daxx	NM_007829	NA	NA	PROMOTER
chr17	31998414	31998914	500	Zic3_extended:310	Tapbp	NM_001025313	NA	NA	INSIDE
chr17	32008137	32008637	500	Zic3_extended:311	Rgl2	NM_009059	NA	NA	INSIDE
chr17	33008002	33008615	613	Zic3_extended:312	Ehmt2	NM_145830	NA	NA	INSIDE
chr17	33078929	33079429	500	Zic3_extended:313	Lsm2	NM_030597	NA	NA	PROMOTER
chr17	33156548	33157048	500	Zic3_extended:314	Ddah2	NM_016765	NA	NA	INSIDE
chr17	33300611	33301111	500	Zic3_extended:315	Lta	NM_010735	NA	NA	INSIDE
chr17	33603233	33603848	615	Zic3_extended:316	Pou5f1	NM_013633	NA	NA	PROMOTER
chr17	33605076	33605576	500	Zic3_extended:317	Pou5f1	NM_013633	NA	NA	PROMOTER
chr17	33605923	33606959	1036	Zic3_extended:318	Pou5f1	NM_013633	NA	NA	PROMOTER
chr17	34022197	34022837	640	Zic3_extended:319	Ppp1r10	NM_175934	NA	NA	INSIDE
chr17	34023624	34024124	500	Zic3_extended:320	Ppp1r10	NM_175934	NA	NA	INSIDE
chr17	35133524	35134024	500	Zic3_extended:321	2410137M14Rik	NM_029747	NA	NA	PROMOTER
chr17	35148896	35149508	612	Zic3_extended:322	Zfp57	NM_001013745	NA	NA	PROMOTER
chr17	38062191	38064808	2617	Zic3_extended:323	Pigt	NM_133779	NA	NA	PROMOTER
chr17	38066618	38067280	662	Zic3_extended:324	Pigt	NM_133779	NA	NA	DOWNSTREAM
chr17	45576769	45577374	605	Zic3_extended:325	1700001C19Rik	NM_029296	NA	NA	PROMOTER
chr17	54447794	54448610	816	Zic3_extended:326	M6prbp1	NM_025836	NA	NA	INSIDE
chr17	64173647	64174147	500	Zic3_extended:327	Twsg1	NM_023053	NA	NA	PROMOTER
chr17	65968212	65968712	500	Zic3_extended:328	Lama1	NM_008480	NA	NA	PROMOTER
chr17	77352355	77352855	500	Zic3_extended:329	BC020023	BC020023	NA	NA	Unknown
chr17	78357716	78358216	500	Zic3_extended:330	Hnrpll	NM_144802	NA	NA	PROMOTER
chr18	3551386	3551886	500	Zic3_extended:331	Cul2	NM_029402	NA	NA	INSIDE
chr18	3673646	3674259	613	Zic3_extended:332	Bambi	NM_026505	NA	NA	INSIDE
chr18	9414755	9415255	500	Zic3_extended:333	Fzd8	NM_008058	NA	NA	PROMOTER
chr18	9417236	9417873	637	Zic3_extended:334	Fzd8	NM_008058	NA	NA	INSIDE
chr18	9914004	9914504	500	Zic3_extended:335	Colec12	NM_130449	NA	NA	INSIDE
chr18	24587517	24588381	864	Zic3_extended:336	Galnt1	NM_013814	NA	NA	PROMOTER
chr18	34382606	34383106	500	Zic3_extended:337	Epb4.1l4a	NM_013512	NA	NA	PROMOTER
chr18	34749125	34749625	500	Zic3_extended:338	Reep5	NM_007874	NA	NA	PROMOTER
chr18	36037883	36038494	611	Zic3_extended:339	5133400G04Rik	NM_029485	NA	NA	PROMOTER
chr18	38977778	38978475	697	Zic3_extended:340	9630014M24Rik	NM_001033771	NA	NA	INSIDE

Chr	Start	End	Length	Bound Region	First Gene	Accession #	Second gene	Accession #	Primary Annotation
chr18	47746645	47747145	500	Zic3_extended:341	Sema6a	NM_018744	NA	NA	PROMOTER
chr18	61403019	61403684	665	Zic3_extended:342	Slc6a7	NM_201353	NA	NA	INSIDE
chr18	62115508	62116008	500	Zic3_extended:343	Grpel2	NM_021296	NA	NA	INSIDE
chr18	66335073	66335744	671	Zic3_extended:344	Rax	NM_013833	NA	NA	PROMOTER
chr18	67733626	67734310	684	Zic3_extended:345	Cidea	NM_007702	NA	NA	PROMOTER
chr19	4292818	4293318	500	Zic3_extended:346	9430078G10Rik	NM_001033811	NA	NA	INSIDE
chr19	4706247	4706747	500	Zic3_extended:347	Rbm14	NM_019869	NA	NA	PROMOTER
chr19	4962093	4962593	500	Zic3_extended:348	Cd248	NM_054042	NA	NA	PROMOTER
chr19	6130680	6131456	776	Zic3_extended:349	Ppp2r5b	NM_198168	1810013C15Rik	NM_194348	DIVERGENT
chr19	12474829	12475329	500	Zic3_extended:350	Zfp91	NM_053009	NA	NA	INSIDE
chr19	14298746	14299246	500	Zic3_extended:351	Tle4	NM_011600	NA	NA	PROMOTER
chr19	22834538	22835038	500	Zic3_extended:352	Klf9	NM_010638	NA	NA	PROMOTER
chr19	24600029	24600529	500	Zic3_extended:353	Foxd4	NM_008022	NA	NA	INSIDE
chr19	24602138	24602638	500	Zic3_extended:354	Foxd4	NM_008022	NA	NA	PROMOTER
chr19	29728705	29729393	688	Zic3_extended:355	Uhrf2	NM_144873	NA	NA	PROMOTER
chr19	30253011	30253511	500	Zic3_extended:356	Dkk1	NM_010051	NA	NA	PROMOTER
chr19	40164894	40165394	500	Zic3_extended:357	Pdlim1	NM_016861	NA	NA	INSIDE
chr19	41636979	41637479	500	Zic3_extended:358	Slit1	NM_015748	NA	NA	INSIDE
chr19	44187418	44187918	500	Zic3_extended:359	Scd2	NM_009128	NA	NA	PROMOTER
chr19	46044741	46045390	649	Zic3_extended:360	Pitx3	NM_008852	Gbf1	NM_178930	DIVERGENT
chr19	46225002	46225774	772	Zic3_extended:361	Fbxl15	NM_133694	NA	NA	INSIDE
chr19	46469726	46470226	500	Zic3_extended:362	Arl3	NM_019718	Sfxn2	NM_053196	DIVERGENT
chr19	53211495	53211995	500	Zic3_extended:363	Mxi1	NM_001008542	NA	NA	PROMOTER
chr19	55230271	55230968	697	Zic3_extended:364	Zdhhc6	NM_025883	Vti1a	NM_016862	DIVERGENT
chrX	6197914	6198414	500	Zic3_extended:365	Tcfe3	NM_172472	NA	NA	INSIDE
chrX	6639825	6640889	1064	Zic3_extended:366	Porcn	NM_145908	NA	NA	PROMOTER
chrX	46775012	46775824	812	Zic3_extended:367	Hs6st2	NM_015819	NA	NA	PROMOTER
chrX	46776734	46777586	852	Zic3_extended:368	Hs6st2	NM_015819	NA	NA	PROMOTER
chrX	47837278	47838363	1085	Zic3_extended:369	mmu-mir-106a	mmu-mir-106a	NA	NA	PROMOTER
chrX	48870422	48870922	500	Zic3_extended:370	Zfp36l3	NM_001009549	NA	NA	PROMOTER
chrX	96411551	96412051	500	Zic3_extended:371	Slc7a3	NM_007515	NA	NA	INSIDE
chrX	96964440	96964940	500	Zic3_extended:372	Ogt	NM_139144	NA	NA	PROMOTER
chrX	1.03E+08	1.03E+08	500	Zic3_extended:373	Itm2a	NM_008409	NA	NA	PROMOTER
chrX	1.39E+08	1.39E+08	1064	Zic3_extended:374	Glt28d1	NM_026247	NA	NA	INSIDE
chrX	1.46E+08	1.46E+08	754	Zic3_extended:375	ORF34	NM_198105	NA	NA	INSIDE
chrX	1.52E+08	1.52E+08	500	Zic3_extended:376	Sms	NM_009214	NA	NA	PROMOTER
chrX	1.52E+08	1.52E+08	686	Zic3_extended:377	Mbtps2	NM_178266	NA	NA	PROMOTER
chrX	1.55E+08	1.55E+08	500	Zic3_extended:378	Pdha1	NM_008810	NA	NA	PROMOTER
chrX	1.58E+08	1.58E+08	500	Zic3_extended:379	Rbbp7	NM_009031	NA	NA	PROMOTER

Appendix 6. Sox2 ChIP target gene and their associated promoter regions in mouse ES cells

"Bound Region" (column E) - the annotation assigned to each unique region
Genomic co-ordinates are with reference to UCSC build mm7 (August 2005)

Chr	Start	End	Bound Region	First Gene	Accession #	Second gene	Accession #	Primary Annotation
chr1	4850939	4851875	Sox2_bound:1	Tcea1	NM_011541	NA	NA	PROMOTER
chr1	5014069	5014840	Sox2_bound:2	Rgs20	NM_021374	NA	NA	INSIDE
chr1	7097722	7098222	Sox2_bound:3	BC110360	BC110360	NA	NA	Unknown
chr1	9844280	9845013	Sox2_bound:4	Mybl1	NM_008651	NA	NA	PROMOTER
chr1	9845140	9845834	Sox2_bound:5	Mybl1	NM_008651	NA	NA	PROMOTER
chr1	1.3E+07	1.3E+07	Sox2_bound:6	Sulf1	NM_172294	NA	NA	PROMOTER
chr1	1.3E+07	1.3E+07	Sox2_bound:7	Slco5a1	NM_172841	NA	NA	PROMOTER
chr1	1.4E+07	1.4E+07	Sox2_bound:8	Eya1	NM_010164	NA	NA	PROMOTER
chr1	1.7E+07	1.7E+07	Sox2_bound:9	Tceb1	NM_026456	Tmem70	NM_027415	DIVERGENT
chr1	1.9E+07	1.9E+07	Sox2_bound:10	Tcfap2b	NM_001025305	NA	NA	PROMOTER
chr1	3.5E+07	3.5E+07	Sox2_bound:11	C230030N03Rik	NM_172847	NA	NA	PROMOTER
chr1	3.6E+07	3.6E+07	Sox2_bound:12	Hs6st1	NM_015818	NA	NA	PROMOTER
chr1	4E+07	4E+07	Sox2_bound:13	Map4k4	NM_008696	NA	NA	INSIDE
chr1	4.1E+07	4.1E+07	Sox2_bound:14	Slc9a2	NM_001033289	NA	NA	PROMOTER
chr1	4.3E+07	4.3E+07	Sox2_bound:15	Tgfbrap1	NM_001013025	NA	NA	INSIDE
chr1	4.4E+07	4.4E+07	Sox2_bound:16	Nck2	NM_010879	NA	NA	INSIDE
chr1	5.2E+07	5.2E+07	Sox2_bound:17	5830411E10Rik	NM_028696	NA	NA	PROMOTER
chr1	5.2E+07	5.2E+07	Sox2_bound:18	Stat4	NM_011487	NA	NA	INSIDE
chr1	5.2E+07	5.2E+07	Sox2_bound:19	Stat4	NM_011487	NA	NA	INSIDE
chr1	5.5E+07	5.5E+07	Sox2_bound:20	Gtf3c3	NM_001033194	NA	NA	PROMOTER
chr1	5.5E+07	5.5E+07	Sox2_bound:21	Prei3	NM_025283	NA	NA	INSIDE
chr1	5.5E+07	5.5E+07	Sox2_bound:22	BC026871	BC026871	NA	NA	Unknown
chr1	5.7E+07	5.7E+07	Sox2_bound:23	Satb2	NM_139146	NA	NA	PROMOTER
chr1	5.9E+07	5.9E+07	Sox2_bound:24	Ppil3	NM_027351	Nif3l1	NM_022988	DIVERGENT
chr1	5.9E+07	5.9E+07	Sox2_bound:25	BC049806	NM_172513	Ndufb3	NM_025597	DIVERGENT
chr1	6E+07	6E+07	Sox2_bound:26	Fzd7	NM_008057	NA	NA	PROMOTER
chr1	6E+07	6E+07	Sox2_bound:27	Nol5	NM_018868	NA	NA	INSIDE
chr1	6.3E+07	6.3E+07	Sox2_bound:28	Nrp2	NM_010939	NA	NA	INSIDE
chr1	6.4E+07	6.4E+07	Sox2_bound:29	Klf7	NM_033563	NA	NA	PROMOTER
chr1	6.5E+07	6.5E+07	Sox2_bound:30	Crygd	NM_007776	NA	NA	INSIDE
chr1	6.7E+07	6.7E+07	Sox2_bound:31	Rpe	NM_025683	NA	NA	PROMOTER
chr1	7.2E+07	7.2E+07	Sox2_bound:32	Fn1	NM_010233	NA	NA	INSIDE
chr1	7.2E+07	7.2E+07	Sox2_bound:33	Fn1	NM_010233	NA	NA	PROMOTER
chr1	7.2E+07	7.2E+07	Sox2_bound:34	Wdt2	NM_001005423	NA	NA	PROMOTER
chr1	7.3E+07	7.3E+07	Sox2_bound:35	Smarcal1	NM_018817	NA	NA	PROMOTER
chr1	7.3E+07	7.3E+07	Sox2_bound:36	Igfbp2	NM_008342	NA	NA	PROMOTER
chr1	7.3E+07	7.3E+07	Sox2_bound:37	Igfbp2	NM_008342	NA	NA	INSIDE
chr1	7.3E+07	7.3E+07	Sox2_bound:38	Igfbp5	NM_010518	NA	NA	INSIDE
chr1	7.3E+07	7.3E+07	Sox2_bound:39	Igfbp5	NM_010518	NA	NA	INSIDE
chr1	7.5E+07	7.5E+07	Sox2_bound:40	Wnt6	NM_009526	NA	NA	INSIDE
chr1	7.6E+07	7.6E+07	Sox2_bound:41	Inha	NM_010564	NA	NA	INSIDE
chr1	7.6E+07	7.6E+07	Sox2_bound:42	Stk11ip	NM_027886	NA	NA	INSIDE
chr1	7.8E+07	7.8E+07	Sox2_bound:43	Epha4	NM_007936	NA	NA	INSIDE
chr1	8.6E+07	8.6E+07	Sox2_bound:44	Itm2c	NM_022417	NA	NA	INSIDE
chr1	8.6E+07	8.6E+07	Sox2_bound:45	Ptma	NM_008972	NA	NA	PROMOTER
chr1	8.6E+07	8.6E+07	Sox2_bound:46	Ptma	NM_008972	NA	NA	PROMOTER
chr1	8.8E+07	8.8E+07	Sox2_bound:47	6430706D22Rik	NM_198652	NA	NA	PROMOTER
chr1	8.9E+07	8.9E+07	Sox2_bound:48	Sh3bp4	NM_133816	NA	NA	INSIDE
chr1	9E+07	9E+07	Sox2_bound:49	Gbx2	NM_010262	NA	NA	PROMOTER
chr1	9E+07	9E+07	Sox2_bound:50	Gbx2	NM_010262	NA	NA	PROMOTER
chr1	9E+07	9E+07	Sox2_bound:51	Cmkor1	NM_007722	NA	NA	PROMOTER
chr1	9.1E+07	9.1E+07	Sox2_bound:52	Hes6	NM_019479	NA	NA	PROMOTER
chr1	9.7E+07	9.7E+07	Sox2_bound:53	Slco4c1	NM_172658	NA	NA	PROMOTER
chr1	1.2E+08	1.2E+08	Sox2_bound:54	Tcfcp2l1	NM_023755	NA	NA	PROMOTER
chr1	1.2E+08	1.2E+08	Sox2_bound:55	Tcfcp2l1	NM_023755	NA	NA	PROMOTER
chr1	1.2E+08	1.2E+08	Sox2_bound:56	Tmem37	NM_019432	NA	NA	PROMOTER
chr1	1.3E+08	1.3E+08	Sox2_bound:57	Cxcr4	NM_009911	NA	NA	PROMOTER
chr1	1.3E+08	1.3E+08	Sox2_bound:58	Dyrk3	NM_145508	NA	NA	PROMOTER
chr1	1.3E+08	1.3E+08	Sox2_bound:59	Lgtn	NM_010709	NA	NA	PROMOTER

chr1	1.3E+08	1.3E+08	Sox2_bound:60	Slc26a9	NM_177243	NA	NA	INSIDE
chr1	1.3E+08	1.3E+08	Sox2_bound:61	Rab7l1	NM_144875	NA	NA	PROMOTER
chr1	1.3E+08	1.3E+08	Sox2_bound:62	Nucks1	NM_175294	NA	NA	PROMOTER
chr1	1.3E+08	1.3E+08	Sox2_bound:63	mmu-mir-135b	mmu-mir-135b	NA	NA	PROMOTER
chr1	1.3E+08	1.3E+08	Sox2_bound:64	mmu-mir-135b	mmu-mir-135b	NA	NA	PROMOTER
chr1	1.3E+08	1.3E+08	Sox2_bound:65	Tmcc2	NM_178874	NA	NA	INSIDE
chr1	1.3E+08	1.3E+08	Sox2_bound:66	Rbbp5	NM_172517	NA	NA	PROMOTER
chr1	1.3E+08	1.3E+08	Sox2_bound:67	Lrrn2	NM_010732	NA	NA	PROMOTER
chr1	1.3E+08	1.3E+08	Sox2_bound:68	Ppp1r15b	NM_133819	NA	NA	PROMOTER
chr1	1.3E+08	1.3E+08	Sox2_bound:69	Ppp1r15b	NM_133819	NA	NA	PROMOTER
chr1	1.3E+08	1.3E+08	Sox2_bound:70	Ppp1r15b	NM_133819	NA	NA	PROMOTER
chr1	1.3E+08	1.3E+08	Sox2_bound:71	Chi3l1	NM_007695	NA	NA	INSIDE
chr1	1.3E+08	1.3E+08	Sox2_bound:72	4931440L10Rik	NM_183292	Jarid1b	NM_152895	DIVERGENT
chr1	1.4E+08	1.4E+08	Sox2_bound:73	5730559C18Rik	NM_028872	NA	NA	INSIDE
chr1	1.4E+08	1.4E+08	Sox2_bound:74	5730559C18Rik	NM_028872	NA	NA	PROMOTER
chr1	1.4E+08	1.4E+08	Sox2_bound:75	Lhx9	NM_010714	NA	NA	PROMOTER
chr1	1.4E+08	1.4E+08	Sox2_bound:76	Rgs2	NM_009061	NA	NA	PROMOTER
chr1	1.5E+08	1.5E+08	Sox2_bound:77	B830045N13Rik	NM_153539	NA	NA	INSIDE
chr1	1.5E+08	1.5E+08	Sox2_bound:78	1200016B10Rik	NM_025819	NA	NA	INSIDE
chr1	1.5E+08	1.5E+08	Sox2_bound:79	Rgs16	NM_011267	NA	NA	INSIDE
chr1	1.6E+08	1.6E+08	Sox2_bound:80	Mr1	NM_008209	Stx6	NM_021433	DIVERGENT
chr1	1.6E+08	1.6E+08	Sox2_bound:81	Ralgps2	NM_023884	NA	NA	INSIDE
chr1	1.6E+08	1.6E+08	Sox2_bound:82	BC026585	NM_001033284	NA	NA	INSIDE
chr1	1.6E+08	1.6E+08	Sox2_bound:83	6430517E21Rik	NM_207583	Astn1	NA	INSIDE
chr1	1.6E+08	1.6E+08	Sox2_bound:84	4930523C07Rik	NM_001024470	NA	NA	PROMOTER
chr1	1.6E+08	1.6E+08	Sox2_bound:85	Zbtb37	NM_173424	NA	NA	PROMOTER
chr1	1.6E+08	1.6E+08	Sox2_bound:86	Zbtb37	NM_173424	NA	NA	PROMOTER
chr1	1.6E+08	1.6E+08	Sox2_bound:87	Dars2	NM_172644	NA	NM_027429	DIVERGENT
chr1	1.7E+08	1.7E+08	Sox2_bound:88	Mpzl1	NM_001001880	NA	NA	PROMOTER
chr1	1.7E+08	1.7E+08	Sox2_bound:89	Pou2f1	NM_198932	NA	NA	PROMOTER
chr1	1.7E+08	1.7E+08	Sox2_bound:90	Dusp27	NM_001033344	NA	NA	INSIDE
chr1	1.7E+08	1.7E+08	Sox2_bound:91	Uck2	NM_030724	NA	NA	PROMOTER
chr1	1.7E+08	1.7E+08	Sox2_bound:92	Uck2	NM_030724	NA	NA	PROMOTER
chr1	1.7E+08	1.7E+08	Sox2_bound:93	Rxrg	NM_009107	NA	NA	INSIDE
chr1	1.7E+08	1.7E+08	Sox2_bound:94	Hsd17b7	NM_010476	NA	NA	PROMOTER
chr1	1.7E+08	1.7E+08	Sox2_bound:95	Ndufs2	NM_153064	Adamts4	NM_172845	DIVERGENT
chr1	1.7E+08	1.7E+08	Sox2_bound:96	Usf1	NM_009480	NA	NA	INSIDE
chr1	1.7E+08	1.7E+08	Sox2_bound:97	Refbp2	NM_019484	NA	NA	PROMOTER
chr1	1.7E+08	1.7E+08	Sox2_bound:98	Refbp2	NM_019484	NA	NA	PROMOTER
chr1	1.7E+08	1.7E+08	Sox2_bound:99	Tagln2	NM_178598	NA	NA	INSIDE
chr1	1.8E+08	1.8E+08	Sox2_bound:10	Hnrpu	NM_016805	NA	NA	PROMOTER
chr1	1.8E+08	1.8E+08	Sox2_bound:10	Efcab2	NM_026626	NA	NA	INSIDE
chr1	1.8E+08	1.8E+08	Sox2_bound:10	Parp1	NM_007415	NA	NA	INSIDE
chr1	1.8E+08	1.8E+08	Sox2_bound:10	BC031781	NM_145943	NA	NA	PROMOTER
chr1	1.8E+08	1.8E+08	Sox2_bound:10	Lefty2	NM_177099	NA	NA	PROMOTER
chr1	1.8E+08	1.8E+08	Sox2_bound:10	Lefty1	NM_010094	NA	NA	PROMOTER
chr1	1.8E+08	1.8E+08	Sox2_bound:10	LOC433384	NM_001007587	NA	NA	PROMOTER
chr1	1.8E+08	1.8E+08	Sox2_bound:10	Enah	NM_010135	NA	NA	INSIDE
chr1	1.8E+08	1.8E+08	Sox2_bound:10	Enah	NM_010135	NA	NA	PROMOTER
chr1	1.9E+08	1.9E+08	Sox2_bound:10	Kctd3	NM_172650	NA	NA	INSIDE
chr1	1.9E+08	1.9E+08	Sox2_bound:11	Prox1	NM_008937	NA	NA	INSIDE
chr1	1.9E+08	1.9E+08	Sox2_bound:11	mmu-mir-205	mmu-mir-205	NA	NA	PROMOTER
chr2	3337229	3338193	Sox2_bound:11	Meig1	NM_008579	NA	NA	INSIDE
chr2	9821702	9822582	Sox2_bound:11	Gata3	NM_008091	NA	NA	PROMOTER
chr2	1.1E+07	1.1E+07	Sox2_bound:11	Prkcq	NM_008859	NA	NA	PROMOTER
chr2	1.4E+07	1.4E+07	Sox2_bound:11	Vim	NM_011701	NA	NA	PROMOTER
chr2	1.8E+07	1.8E+07	Sox2_bound:11	2810030E01Rik	NM_028317	Mllt10	NM_010804	DIVERGENT
chr2	1.8E+07	1.8E+07	Sox2_bound:11	Mllt10	NM_010804	NA	NA	INSIDE
chr2	1.9E+07	1.9E+07	Sox2_bound:11	Commd3	NM_147778	NA	NA	INSIDE
chr2	2.3E+07	2.3E+07	Sox2_bound:11	Gad2	NM_008078	NA	NA	PROMOTER
chr2	2.5E+07	2.5E+07	Sox2_bound:12	Nrarp	NM_025980	NA	NA	PROMOTER
chr2	2.6E+07	2.6E+07	Sox2_bound:12	Btbd14a	NM_001037098	NA	NA	INSIDE
chr2	2.6E+07	2.6E+07	Sox2_bound:12	4932418E24Rik	NM_177841	NA	NA	PROMOTER
chr2	2.7E+07	2.7E+07	Sox2_bound:12	Notch1	NM_008714	NA	NA	INSIDE
chr2	2.7E+07	2.7E+07	Sox2_bound:12	Notch1	NM_008714	NA	NA	PROMOTER

chr2	2.9E+07	2.9E+07	ox2_bound:12	Ralgds	NM_009058	NA	NA	INSIDE
chr2	2.9E+07	2.9E+07	ox2_bound:12	Als4	NM_198033	NA	NA	PROMOTER
chr2	3E+07	3E+07	ox2_bound:12	Coq4	NM_178693	NA	NA	PROMOTER
chr2	3E+07	3E+07	ox2_bound:12	Set	NM_023871	NA	NA	PROMOTER
chr2	3E+07	3E+07	ox2_bound:12	Set	NM_023871	NA	NA	INSIDE
chr2	3E+07	3E+07	ox2_bound:13	Tbc1d13	NM_146252	NA	NA	INSIDE
chr2	3E+07	3E+07	ox2_bound:13	Ier5l	NM_030244	NA	NA	PROMOTER
chr2	3.1E+07	3.1E+07	ox2_bound:13	1700001O22Rik	NM_198000	2610205E22Ril	NM_170592	DIVERGENT
chr2	3.2E+07	3.2E+07	ox2_bound:13	Fubp3	NM_001033389	NA	NA	PROMOTER
chr2	3.2E+07	3.2E+07	ox2_bound:13	Lcn2	NM_008491	Ptges2	NM_133783	DIVERGENT
chr2	3.3E+07	3.3E+07	ox2_bound:13	C230093N12Rik	NM_153560	NA	NA	INSIDE
chr2	3.4E+07	3.4E+07	ox2_bound:13	Lmx1b	NM_010725	NA	NA	INSIDE
chr2	3.7E+07	3.7E+07	ox2_bound:13	Zbtb6	NM_146253	NA	NA	PROMOTER
chr2	3.9E+07	3.9E+07	ox2_bound:13	Nr6a1	NM_010264	NA	NA	INSIDE
chr2	4.5E+07	4.5E+07	ox2_bound:13	Zfhx1b	NM_015753	NA	NA	INSIDE
chr2	4.5E+07	4.5E+07	ox2_bound:14	Zfhx1b	NM_015753	NA	NA	PROMOTER
chr2	5.2E+07	5.2E+07	ox2_bound:14	Rif1	NM_175238	NA	NA	PROMOTER
chr2	5.2E+07	5.2E+07	ox2_bound:14	Rif1	NM_175238	NA	NA	PROMOTER
chr2	5.3E+07	5.3E+07	ox2_bound:14	Cacnb4	NM_146123	NA	NA	INSIDE
chr2	5.4E+07	5.4E+07	ox2_bound:14	Rprm	NM_023396	NA	NA	INSIDE
chr2	6E+07	6E+07	ox2_bound:14	Ly75	NM_013825	NA	NA	PROMOTER
chr2	6.2E+07	6.2E+07	ox2_bound:14	Dpp4	NM_010074	NA	NA	PROMOTER
chr2	6.3E+07	6.3E+07	ox2_bound:14	Kcnh7	NM_133207	NA	NA	PROMOTER
chr2	6.4E+07	6.4E+07	ox2_bound:14	Fign	NM_021716	NA	NA	PROMOTER
chr2	6.6E+07	6.6E+07	ox2_bound:14	A330102K23Rik	NM_153409	NA	NA	PROMOTER
chr2	6.6E+07	6.6E+07	ox2_bound:15	A330102K23Rik	NM_153409	NA	NA	INSIDE
chr2	6.9E+07	6.9E+07	ox2_bound:15	G6pc2	NM_021331	NA	NA	INSIDE
chr2	7.1E+07	7.1E+07	ox2_bound:15	4833418A01Rik	NM_198005	NA	NA	INSIDE
chr2	7.1E+07	7.1E+07	ox2_bound:15	Dlx1	NM_010053	NA	NA	INSIDE
chr2	7.2E+07	7.2E+07	ox2_bound:15	Pdk1	NM_172665	NA	NA	PROMOTER
chr2	7.3E+07	7.3E+07	ox2_bound:15	Sp3	NM_001018042	NA	NA	PROMOTER
chr2	7.5E+07	7.5E+07	ox2_bound:15	Evx2	NM_007967	NA	NA	INSIDE
chr2	7.5E+07	7.5E+07	ox2_bound:15	Hoxd13	NM_008275	NA	NA	INSIDE
chr2	7.5E+07	7.5E+07	ox2_bound:15	Hoxd12	NM_008274	NA	NA	PROMOTER
chr2	7.5E+07	7.5E+07	ox2_bound:15	Hoxd11	NM_008273	NA	NA	PROMOTER
chr2	7.5E+07	7.5E+07	ox2_bound:16	Hoxd10	NM_013554	NA	NA	PROMOTER
chr2	7.5E+07	7.5E+07	ox2_bound:16	Hoxd10	NM_013554	NA	NA	PROMOTER
chr2	7.5E+07	7.5E+07	ox2_bound:16	Hoxd10	NM_013554	NA	NA	PROMOTER
chr2	7.5E+07	7.5E+07	ox2_bound:16	Hoxd10	NM_013554	NA	NA	INSIDE
chr2	7.5E+07	7.5E+07	ox2_bound:16	Hoxd4	NM_010469	NA	NA	PROMOTER
chr2	7.6E+07	7.6E+07	ox2_bound:16	Hnrpa3	NM_198090	NA	NA	PROMOTER
chr2	7.6E+07	7.6E+07	ox2_bound:16	Nfe2l2	NM_010902	NA	NA	PROMOTER
chr2	7.7E+07	7.7E+07	ox2_bound:16	Fkbp7	NM_010222	NA	NA	INSIDE
chr2	7.9E+07	7.9E+07	ox2_bound:16	Neurod1	NM_010894	NA	NA	PROMOTER
chr2	8E+07	8E+07	ox2_bound:16	Pde1a	NM_016744	NA	NA	INSIDE
chr2	8E+07	8E+07	ox2_bound:17	Nup35	NM_027091	NA	NA	INSIDE
chr2	8.5E+07	8.5E+07	ox2_bound:17	2700094K13Rik	NM_001033166	NA	NA	INSIDE
chr2	8.5E+07	8.5E+07	ox2_bound:17	Zdhhc5	NM_144887	NA	NA	PROMOTER
chr2	8.5E+07	8.5E+07	ox2_bound:17	P2rx3	NM_145526	Ssrp1	NM_182990	DIVERGENT
chr2	9.2E+07	9.2E+07	ox2_bound:17	Chrm4	NM_007699	NA	NA	PROMOTER
chr2	9.2E+07	9.2E+07	ox2_bound:17	Mdk	NM_010784	NA	NA	PROMOTER
chr2	9.4E+07	9.4E+07	ox2_bound:17	2610203E10Rik	NM_183220	NA	NA	INSIDE
chr2	1E+08	1E+08	ox2_bound:17	B230118H07Rik	NM_026592	NA	NA	PROMOTER
chr2	1E+08	1E+08	ox2_bound:17	Nat10	NM_153126	NA	NA	PROMOTER
chr2	1E+08	1E+08	ox2_bound:17	Gpiap1	NM_016739	NA	NA	PROMOTER
chr2	1.1E+08	1.1E+08	ox2_bound:18	Rcn1	NM_009037	NA	NA	INSIDE
chr2	1.1E+08	1.1E+08	ox2_bound:18	Pax6	NM_013627	NA	NA	PROMOTER
chr2	1.1E+08	1.1E+08	ox2_bound:18	Pax6	NM_013627	NA	NA	INSIDE
chr2	1.1E+08	1.1E+08	ox2_bound:18	Kif18a	NM_139303	NA	NA	INSIDE
chr2	1.1E+08	1.1E+08	ox2_bound:18	Bdnf	NM_007540	NA	NA	PROMOTER
chr2	1.1E+08	1.1E+08	ox2_bound:18	Slc12a6	NM_133648	NA	NA	PROMOTER
chr2	1.1E+08	1.1E+08	ox2_bound:18	Arhgap11a	NM_181416	NA	NA	PROMOTER
chr2	1.2E+08	1.2E+08	ox2_bound:18	BC052040	NM_207264	NA	NA	PROMOTER
chr2	1.2E+08	1.2E+08	ox2_bound:18	Mrg1	NM_010825	NA	NA	INSIDE
chr2	1.2E+08	1.2E+08	ox2_bound:18	Spred1	NM_033524	NA	NA	PROMOTER

chr2	1.2E+08	1.2E+08	ox2_bound:19	Spred1	NM_033524	NA	NA	INSIDE
chr2	1.2E+08	1.2E+08	ox2_bound:19	2610510H03Rik	NM_026620	NA	NA	PROMOTER
chr2	1.2E+08	1.2E+08	ox2_bound:19	Bmf	NM_138313	NA	NA	PROMOTER
chr2	1.2E+08	1.2E+08	ox2_bound:19	Bub1b	NM_009773	NA	NA	PROMOTER
chr2	1.2E+08	1.2E+08	ox2_bound:19	Ivd	NM_019826	NA	NA	PROMOTER
chr2	1.2E+08	1.2E+08	ox2_bound:19	BC100358	BC100358	NA	NA	Unknown
chr2	1.2E+08	1.2E+08	ox2_bound:19	Rpusd2	NM_173450	NA	NA	DOWNSTREAM
chr2	1.2E+08	1.2E+08	ox2_bound:19	Dll4	NM_019454	NA	NA	PROMOTER
chr2	1.2E+08	1.2E+08	ox2_bound:19	Itpka	NM_146125	NA	NA	PROMOTER
chr2	1.2E+08	1.2E+08	ox2_bound:19	Pla2g4e	NM_177845	NA	NA	INSIDE
chr2	1.2E+08	1.2E+08	ox2_bound:20	Pla2g4e	NM_177845	NA	NA	INSIDE
chr2	1.2E+08	1.2E+08	ox2_bound:20	Trp53bp1	NM_013735	NA	NA	PROMOTER
chr2	1.2E+08	1.2E+08	ox2_bound:20	BC019755	NM_145395	NA	NA	INSIDE
chr2	1.2E+08	1.2E+08	ox2_bound:20	Shf	NM_001013829	NA	NA	PROMOTER
chr2	1.2E+08	1.2E+08	ox2_bound:20	Shf	NM_001013829	NA	NA	PROMOTER
chr2	1.3E+08	1.3E+08	ox2_bound:20	Shc4	NM_199022	NA	NA	PROMOTER
chr2	1.3E+08	1.3E+08	ox2_bound:20	Slc27a2	NM_011978	NA	NA	PROMOTER
chr2	1.3E+08	1.3E+08	ox2_bound:20	1810024B03Rik	NM_198630	Ascc3l1	NM_177214	DIVERGENT
chr2	1.3E+08	1.3E+08	ox2_bound:20	Zc3h8	NM_020594	NA	NA	PROMOTER
chr2	1.3E+08	1.3E+08	ox2_bound:20	BC058173	BC058173	NA	NA	Unknown
chr2	1.3E+08	1.3E+08	ox2_bound:21	Sirpa	NM_007547	NA	NA	PROMOTER
chr2	1.3E+08	1.3E+08	ox2_bound:21	Stk35	NM_001038635	NA	NA	PROMOTER
chr2	1.3E+08	1.3E+08	ox2_bound:21	Tgm3	NM_009374	NA	NA	PROMOTER
chr2	1.3E+08	1.3E+08	ox2_bound:21	4930402H24Rik	NM_029432	NA	NA	INSIDE
chr2	1.3E+08	1.3E+08	ox2_bound:21	D430028G21Rik	NM_144888	NA	NA	PROMOTER
chr2	1.3E+08	1.3E+08	ox2_bound:21	Pcna	NM_011045	Cds2	NM_138651	DIVERGENT
chr2	1.3E+08	1.3E+08	ox2_bound:21	B430119L13Rik	NM_177303	NA	NA	PROMOTER
chr2	1.4E+08	1.4E+08	ox2_bound:21	Jag1	NM_013822	NA	NA	PROMOTER
chr2	1.4E+08	1.4E+08	ox2_bound:21	2900006F19Rik	NM_028387	NA	NA	INSIDE
chr2	1.4E+08	1.4E+08	ox2_bound:21	Flrt3	NM_178382	NA	NA	PROMOTER
chr2	1.4E+08	1.4E+08	ox2_bound:22	LOC433479	NM_001013802	NA	NA	PROMOTER
chr2	1.4E+08	1.4E+08	ox2_bound:22	Dstn	NM_019771	NA	NA	INSIDE
chr2	1.5E+08	1.5E+08	ox2_bound:22	Insm1	NM_016889	NA	NA	PROMOTER
chr2	1.5E+08	1.5E+08	ox2_bound:22	Insm1	NM_016889	NA	NA	PROMOTER
chr2	1.5E+08	1.5E+08	ox2_bound:22	Xrn2	NM_011917	NA	NA	PROMOTER
chr2	1.5E+08	1.5E+08	ox2_bound:22	Nkx2-2	NM_010919	NA	NA	PROMOTER
chr2	1.5E+08	1.5E+08	ox2_bound:22	Nkx2-2	NM_010919	NA	NA	PROMOTER
chr2	1.5E+08	1.5E+08	ox2_bound:22	Pax1	NM_008780	NA	NA	PROMOTER
chr2	1.5E+08	1.5E+08	ox2_bound:22	Cst3	NM_009976	NA	NA	INSIDE
chr2	1.5E+08	1.5E+08	ox2_bound:22	2310001A20Rik	NM_027977	NA	NA	PROMOTER
chr2	1.5E+08	1.5E+08	ox2_bound:23	Nanp	NM_026086	NA	NA	INSIDE
chr2	1.5E+08	1.5E+08	ox2_bound:23	Gm123	NM_001009948	NA	NA	PROMOTER
chr2	1.5E+08	1.5E+08	ox2_bound:23	Id1	NM_010495	NA	NA	DOWNSTREAM
chr2	1.5E+08	1.5E+08	ox2_bound:23	Hck	NM_010407	NA	NA	PROMOTER
chr2	1.5E+08	1.5E+08	ox2_bound:23	Asxl1	NM_001039939	NA	NA	INSIDE
chr2	1.6E+08	1.6E+08	ox2_bound:23	Gdf5	NM_008109	NA	NA	PROMOTER
chr2	1.6E+08	1.6E+08	ox2_bound:23	Tgif2	NM_173396	NA	NA	INSIDE
chr2	1.6E+08	1.6E+08	ox2_bound:23	Src	NM_001025395	NA	NA	PROMOTER
chr2	1.6E+08	1.6E+08	ox2_bound:23	Gm691	NM_198627	NA	NA	PROMOTER
chr2	1.6E+08	1.6E+08	ox2_bound:23	Ppp1r16b	NM_153089	NA	NA	INSIDE
chr2	1.6E+08	1.6E+08	ox2_bound:24	Mafb	NM_010658	NA	NA	PROMOTER
chr2	1.6E+08	1.6E+08	ox2_bound:24	Mybl2	NM_008652	NA	NA	PROMOTER
chr2	1.6E+08	1.6E+08	ox2_bound:24	Sdc4	NM_011521	NA	NA	PROMOTER
chr2	1.6E+08	1.6E+08	ox2_bound:24	Spint4	NM_030058	NA	NA	INSIDE
chr2	1.6E+08	1.6E+08	ox2_bound:24	Zswim3	NM_178375	NA	NA	INSIDE
chr2	1.6E+08	1.6E+08	ox2_bound:24	Ppgb	NM_001038492	NA	NA	INSIDE
chr2	1.6E+08	1.6E+08	ox2_bound:24	Ncoa5	NM_144892	NA	NA	PROMOTER
chr2	1.7E+08	1.7E+08	ox2_bound:24	Prkcbp1	NM_027230	NA	NA	INSIDE
chr2	1.7E+08	1.7E+08	ox2_bound:24	Sulf2	NM_028072	NA	NA	PROMOTER
chr2	1.7E+08	1.7E+08	ox2_bound:24	Sulf2	NM_028072	NA	NA	PROMOTER
chr2	1.7E+08	1.7E+08	ox2_bound:25	Snai1	NM_011427	NA	NA	INSIDE
chr2	1.7E+08	1.7E+08	ox2_bound:25	Sall4	NM_201396	NA	NA	INSIDE
chr2	1.7E+08	1.7E+08	ox2_bound:25	Sall4	NM_175303	NA	NA	PROMOTER
chr2	1.7E+08	1.7E+08	ox2_bound:25	Sall4	NM_175303	NA	NA	PROMOTER
chr2	1.7E+08	1.7E+08	ox2_bound:25	Zfp64	NM_009564	NA	NA	PROMOTER

chr2	1.7E+08	1.7E+08	ox2_bound:25	Cbln4	NM_175631	NA	NA	INSIDE
chr2	1.7E+08	1.7E+08	ox2_bound:25	F730031O20Rik	NM_001033538	NA	NA	PROMOTER
chr2	1.7E+08	1.7E+08	ox2_bound:25	Tcfap2c	NM_009335	NA	NA	PROMOTER
chr2	1.7E+08	1.7E+08	ox2_bound:25	Gnas	NM_010309	NA	NA	PROMOTER
chr2	1.8E+08	1.8E+08	ox2_bound:25	Dido1	NM_011805	2310003C23Ri	NA	PROMOTER
chr2	1.8E+08	1.8E+08	ox2_bound:26	Dido1	NM_177852	NA	NM_029607	DIVERGENT
chr2	1.8E+08	1.8E+08	ox2_bound:26	BC019537	NM_183161	NA	NA	PROMOTER
chr2	1.8E+08	1.8E+08	ox2_bound:26	BC019537	NM_183161	NA	NA	INSIDE
chr2	1.8E+08	1.8E+08	ox2_bound:26	C030019F02Rik	NM_021426	NA	NA	INSIDE
chr2	1.8E+08	1.8E+08	ox2_bound:26	C030019F02Rik	NM_021426	NA	NA	INSIDE
chr2	1.8E+08	1.8E+08	ox2_bound:26	Chrna4	NM_015730	NA	NA	PROMOTER
chr2	1.8E+08	1.8E+08	ox2_bound:26	Kcnq2	NM_001006678	NA	NA	INSIDE
chr2	1.8E+08	1.8E+08	ox2_bound:26	2700038C09Rik	NM_025598	NA	NA	PROMOTER
chr2	1.8E+08	1.8E+08	ox2_bound:26	Myt1	NM_008665	NA	NA	PROMOTER
chr3	7374346	7375296	ox2_bound:26	Pkia	NM_008862	NA	NA	INSIDE
chr3	8515904	8517611	ox2_bound:27	Stmn2	NM_025285	NA	NA	INSIDE
chr3	8970645	8971423	ox2_bound:27	Tpd52	NM_001025262	NA	NA	PROMOTER
chr3	9009906	9010406	ox2_bound:27	Tpd52	NM_001025263	NA	NA	INSIDE
chr3	9014630	9015320	ox2_bound:27	Tpd52	NM_009412	NA	NA	PROMOTER
chr3	9616498	9617838	ox2_bound:27	Gig1	NM_133218	NA	NA	PROMOTER
chr3	1E+07	1E+07	ox2_bound:27	Fabp5	NM_010634	NA	NA	INSIDE
chr3	1E+07	1E+07	ox2_bound:27	Zfand1	NM_025512	NA	NA	PROMOTER
chr3	1.4E+07	1.4E+07	ox2_bound:27	Slc7a12	NM_080852	NA	NA	PROMOTER
chr3	1.5E+07	1.5E+07	ox2_bound:27	Car3	NM_007606	NA	NA	PROMOTER
chr3	1.8E+07	1.8E+07	ox2_bound:27	Bhlhb5	NM_021560	NA	NA	INSIDE
chr3	2E+07	2E+07	ox2_bound:28	Smarca3	NM_144959	NA	NA	INSIDE
chr3	2.2E+07	2.2E+07	ox2_bound:28	Tbl1xr1	NM_030732	NA	NA	PROMOTER
chr3	2.7E+07	2.7E+07	ox2_bound:28	Ect2	NM_007900	NA	NA	PROMOTER
chr3	3E+07	3E+07	ox2_bound:28	Arpm1	NM_029690	Mynn	NM_030557	DIVERGENT
chr3	3E+07	3E+07	ox2_bound:28	4930558O21Rik	NM_026668	NA	NA	INSIDE
chr3	3.1E+07	3.1E+07	ox2_bound:28	Prkci	NM_008857	NA	NA	PROMOTER
chr3	3.1E+07	3.1E+07	ox2_bound:28	Skil	NM_001039090	NA	NA	PROMOTER
chr3	3.2E+07	3.2E+07	ox2_bound:28	Kcnmb2	NM_028231	NA	NA	INSIDE
chr3	3.3E+07	3.3E+07	ox2_bound:28	Actl6a	NM_019673	NA	NA	INSIDE
chr3	3.3E+07	3.3E+07	ox2_bound:28	Mrpl47	NM_029017	Ndufb5	NM_025316	DIVERGENT
chr3	3.4E+07	3.4E+07	ox2_bound:29	Sox2	NM_011443	NA	NA	PROMOTER
chr3	3.4E+07	3.4E+07	ox2_bound:29	Sox2	NM_011443	NA	NA	PROMOTER
chr3	3.4E+07	3.4E+07	ox2_bound:29	Sox2	NM_011443	NA	NA	PROMOTER
chr3	3.4E+07	3.4E+07	ox2_bound:29	Sox2	NM_011443	NA	NA	INSIDE
chr3	4.5E+07	4.5E+07	ox2_bound:29	Pcdh10	NM_011043	NA	NA	PROMOTER
chr3	5.1E+07	5.1E+07	ox2_bound:29	Ccrn4l	NM_009834	NA	NA	PROMOTER
chr3	5.2E+07	5.2E+07	ox2_bound:29	Setd7	NM_080793	NA	NA	PROMOTER
chr3	7E+07	7E+07	ox2_bound:29	B3galt3	NM_020026	NA	NA	INSIDE
chr3	7E+07	7E+07	ox2_bound:29	1110032A04Rik	NM_133675	NA	NA	PROMOTER
chr3	8.1E+07	8.1E+07	ox2_bound:29	Pdgfc	NM_019971	NA	NA	PROMOTER
chr3	8.2E+07	8.2E+07	ox2_bound:30	Accn5	NM_021370	NA	NA	PROMOTER
chr3	8.5E+07	8.5E+07	ox2_bound:30	9930117H01Rik	NM_177260	NA	NA	PROMOTER
chr3	8.6E+07	8.6E+07	ox2_bound:30	Pet112l	NM_144896	NA	NA	INSIDE
chr3	8.6E+07	8.6E+07	ox2_bound:30	Gm1019	NM_001001650	NA	NA	PROMOTER
chr3	8.8E+07	8.8E+07	ox2_bound:30	Prcc	NM_033573	NA	NA	PROMOTER
chr3	8.8E+07	8.8E+07	ox2_bound:30	Cct3	NM_009836	NA	NA	PROMOTER
chr3	8.9E+07	8.9E+07	ox2_bound:30	Thbs3	NM_013691	NA	NA	INSIDE
chr3	8.9E+07	8.9E+07	ox2_bound:30	Muc1	NM_013605	NA	NA	PROMOTER
chr3	9E+07	9E+07	ox2_bound:30	Creb3l4	NM_030080	Slc39a1	NM_013901	DIVERGENT
chr3	9.1E+07	9.1E+07	ox2_bound:30	Ints3	NM_178876	NA	NA	PROMOTER
chr3	9.3E+07	9.3E+07	ox2_bound:31	2300002G24Rik	NM_028798	NA	NA	INSIDE
chr3	9.4E+07	9.4E+07	ox2_bound:31	2310007A19Rik	NM_025506	Tnrc4	NM_172434	DIVERGENT
chr3	9.5E+07	9.5E+07	ox2_bound:31	Scnm1	NM_027013	NA	NA	INSIDE
chr3	9.5E+07	9.5E+07	ox2_bound:31	Gabpb2	NM_172512	NA	NA	PROMOTER
chr3	9.5E+07	9.5E+07	ox2_bound:31	Cdc42se1	NM_001038708	NA	NA	INSIDE
chr3	9.5E+07	9.5E+07	ox2_bound:31	Arnt	NM_001037737	NA	NA	PROMOTER
chr3	9.6E+07	9.6E+07	ox2_bound:31	Za20d1	NM_001025613	NA	NA	PROMOTER
chr3	9.6E+07	9.6E+07	ox2_bound:31	Hist2h3c1	NM_178216	NA	NA	DOWNSTREAM
chr3	9.6E+07	9.6E+07	ox2_bound:31	Hist2h4	NM_033596	Hist2h3c1	NA	DOWNSTREAM
chr3	9.6E+07	9.6E+07	ox2_bound:31	Hist2h4	NM_033596	NA	NM_019469	DIVERGENT

chr3	9.6E+07	9.6E+07	ox2_bound:32	Polr3gl	NM_027241	NA	NA	INSIDE
chr3	9.7E+07	9.7E+07	ox2_bound:32	Acp6	NM_019800	NA	NA	INSIDE
chr3	1E+08	1E+08	ox2_bound:32	Ptgfrn	NM_011197	NA	NA	PROMOTER
chr3	1E+08	1E+08	ox2_bound:32	Casq2	NM_009814	NA	NA	PROMOTER
chr3	1E+08	1E+08	ox2_bound:32	Csde1	NM_144901	NA	NA	INSIDE
chr3	1E+08	1E+08	ox2_bound:32	Dennd2c	NM_177857	NA	NA	PROMOTER
chr3	1E+08	1E+08	ox2_bound:32	Dennd2c	NM_177857	NA	NA	INSIDE
chr3	1E+08	1E+08	ox2_bound:32	Trim33	NM_053170	NA	NA	PROMOTER
chr3	1E+08	1E+08	ox2_bound:32	Syt6	NM_018800	NA	NA	PROMOTER
chr3	1E+08	1E+08	ox2_bound:32	Ppm1j	NM_027982	NA	NA	INSIDE
chr3	1E+08	1E+08	ox2_bound:33	Cttnbp2nl	NM_030249	NA	NA	INSIDE
chr3	1.1E+08	1.1E+08	ox2_bound:33	Wdr77	NM_027432	NA	NA	PROMOTER
chr3	1.1E+08	1.1E+08	ox2_bound:33	Tmem77	NM_001025582	NA	NA	INSIDE
chr3	1.1E+08	1.1E+08	ox2_bound:33	Sypl2	NM_008596	NA	NA	PROMOTER
chr3	1.1E+08	1.1E+08	ox2_bound:33	Sars	NM_011319	NA	NA	PROMOTER
chr3	1.1E+08	1.1E+08	ox2_bound:33	Wdr47	NM_181400	NA	NA	PROMOTER
chr3	1.2E+08	1.2E+08	ox2_bound:33	BC072644	BC072644	NA	NA	Unknown
chr3	1.2E+08	1.2E+08	ox2_bound:33	Cnn3	NM_028044	NA	NA	INSIDE
chr3	1.2E+08	1.2E+08	ox2_bound:33	Gclm	NM_008129	NA	NA	PROMOTER
chr3	1.3E+08	1.3E+08	ox2_bound:33	Ank2	NM_178655	NA	NA	PROMOTER
chr3	1.3E+08	1.3E+08	ox2_bound:34	D3Wsu161e	NM_138593	mmu-mir-302	mmu-mir-302	DIVERGENT
chr3	1.3E+08	1.3E+08	ox2_bound:34	Neurog2	NM_009718	NA	NA	PROMOTER
chr3	1.3E+08	1.3E+08	ox2_bound:34	Pitx2	NM_011098	NA	NA	INSIDE
chr3	1.3E+08	1.3E+08	ox2_bound:34	Pitx2	NM_011098	NA	NA	INSIDE
chr3	1.3E+08	1.3E+08	ox2_bound:34	Lef1	NM_010703	NA	NA	PROMOTER
chr3	1.3E+08	1.3E+08	ox2_bound:34	Lef1	NM_010703	NA	NA	INSIDE
chr3	1.3E+08	1.3E+08	ox2_bound:34	Hadhsc	NM_008212	NA	NA	INSIDE
chr3	1.3E+08	1.3E+08	ox2_bound:34	Scye1	NM_007926	A630047E20Ri	NM_173032	DIVERGENT
chr3	1.3E+08	1.3E+08	ox2_bound:34	Cxxc4	NM_001004367	NA	NA	PROMOTER
chr3	1.4E+08	1.4E+08	ox2_bound:34	Ddit4l	NM_030143	NA	NA	PROMOTER
chr3	1.4E+08	1.4E+08	ox2_bound:35	Adh7	NM_009626	NA	NA	PROMOTER
chr3	1.4E+08	1.4E+08	ox2_bound:35	Tspan5	NM_019571	NA	NA	INSIDE
chr3	1.4E+08	1.4E+08	ox2_bound:35	Pdlim5	NM_019809	NA	NA	PROMOTER
chr3	1.4E+08	1.4E+08	ox2_bound:35	Ccbl2	NM_173763	NA	NA	PROMOTER
chr3	1.4E+08	1.4E+08	ox2_bound:35	Pkn2	NM_178654	NA	NA	PROMOTER
chr3	1.4E+08	1.4E+08	ox2_bound:35	Lmo4	NM_010723	NA	NA	INSIDE
chr3	1.4E+08	1.4E+08	ox2_bound:35	Lmo4	NM_010723	NA	NA	INSIDE
chr3	1.5E+08	1.5E+08	ox2_bound:35	Cyr61	NM_010516	NA	NA	PROMOTER
chr3	1.5E+08	1.5E+08	ox2_bound:35	Ddah1	NM_026993	NA	NA	PROMOTER
chr3	1.5E+08	1.5E+08	ox2_bound:35	Ddah1	NM_026993	NA	NA	INSIDE
chr3	1.5E+08	1.5E+08	ox2_bound:36	Gipc2	NM_016867	NA	NA	INSIDE
chr3	1.5E+08	1.5E+08	ox2_bound:36	Lhx8	NM_010713	NA	NA	INSIDE
chr3	1.6E+08	1.6E+08	ox2_bound:36	Sfrs11	NM_026989	Lrrc40	NM_024194	DIVERGENT
chr4	1.1E+07	1.1E+07	ox2_bound:36	Trp53inp1	NM_021897	NA	NA	PROMOTER
chr4	1.6E+07	1.6E+07	ox2_bound:36	Decr1	NM_026172	NA	NA	PROMOTER
chr4	1.6E+07	1.6E+07	ox2_bound:36	Nbn	NM_013752	NA	NA	INSIDE
chr4	2.1E+07	2.1E+07	ox2_bound:36	E130310K16Rik	NM_172987	NA	NA	INSIDE
chr4	2.2E+07	2.2E+07	ox2_bound:36	Coq3	NM_172687	NA	NA	INSIDE
chr4	2.2E+07	2.2E+07	ox2_bound:36	Pou3f2	NM_008899	NA	NA	PROMOTER
chr4	2.2E+07	2.2E+07	ox2_bound:36	Pou3f2	NM_008899	NA	NA	PROMOTER
chr4	2.6E+07	2.6E+07	ox2_bound:37	Fut9	NM_010243	NA	NA	INSIDE
chr4	3.3E+07	3.3E+07	ox2_bound:37	Ankrd6	NM_080471	NA	NA	PROMOTER
chr4	3.3E+07	3.3E+07	ox2_bound:37	Ankrd6	NM_001012451	NA	NA	INSIDE
chr4	4E+07	4E+07	ox2_bound:37	Ddx58	NM_172689	NA	NA	INSIDE
chr4	4.1E+07	4.1E+07	ox2_bound:37	B4galt1	NM_022305	NA	NA	PROMOTER
chr4	4.1E+07	4.1E+07	ox2_bound:37	Aqp3	NM_016689	NA	NA	PROMOTER
chr4	4.1E+07	4.1E+07	ox2_bound:37	Aqp3	NM_016689	NA	NA	PROMOTER
chr4	4.1E+07	4.1E+07	ox2_bound:37	Nol6	NM_139236	Ube2r2	NM_026275	DIVERGENT
chr4	4.3E+07	4.3E+07	ox2_bound:37	Dnajb5	NM_019874	NA	NA	PROMOTER
chr4	4.3E+07	4.3E+07	ox2_bound:37	Fancg	NM_053081	NA	NA	PROMOTER
chr4	4.4E+07	4.4E+07	ox2_bound:38	Gba2	NM_172692	NA	NA	INSIDE
chr4	4.5E+07	4.5E+07	ox2_bound:38	Pax5	NM_008782	NA	NA	PROMOTER
chr4	4.5E+07	4.5E+07	ox2_bound:38	D4Wsu132e	NM_138590	NA	NA	PROMOTER
chr4	4.6E+07	4.6E+07	ox2_bound:38	Hemgn	NM_053149	NA	NA	DOWNSTREAM
chr4	4.9E+07	4.9E+07	ox2_bound:38	Tmeff1	NM_021436	NA	NA	INSIDE

chr4	5.8E+07	5.8E+07	ox2_bound:38	D630039A03Rik	NM_178727	NA	NA	PROMOTER
chr4	5.8E+07	5.8E+07	ox2_bound:38	Musk	NM_001037127	NA	NA	INSIDE
chr4	8E+07	8E+07	ox2_bound:38	D4Bwg0951e	NM_026821	NA	NA	INSIDE
chr4	8.2E+07	8.2E+07	ox2_bound:38	Nfib	NM_008687	NA	NA	PROMOTER
chr4	8.3E+07	8.3E+07	ox2_bound:38	1810054D07Rik	NM_027238	NA	NA	PROMOTER
chr4	8.3E+07	8.3E+07	ox2_bound:39	Snapc3	NM_029949	NA	NA	PROMOTER
chr4	8.3E+07	8.3E+07	ox2_bound:39	Snapc3	NM_029949	NA	NA	PROMOTER
chr4	8.5E+07	8.5E+07	ox2_bound:39	BC062814	BC062814	NA	NA	Unknown
chr4	8.6E+07	8.6E+07	ox2_bound:39	Rraga	NM_178376	NA	NA	PROMOTER
chr4	8.6E+07	8.6E+07	ox2_bound:39	6230416J20Rik	NM_173400	NA	NA	PROMOTER
chr4	9.1E+07	9.1E+07	ox2_bound:39	Elavl2	NM_207685	NA	NA	INSIDE
chr4	9.7E+07	9.7E+07	ox2_bound:39	Nfia	NM_010905	NA	NA	PROMOTER
chr4	9.8E+07	9.8E+07	ox2_bound:39	Usp1	NM_146144	NA	NA	PROMOTER
chr4	9.9E+07	9.9E+07	ox2_bound:39	Itgb3bp	NM_026348	BC020077	NM_145549	DIVERGENT
chr4	9.9E+07	9.9E+07	ox2_bound:39	Ror1	NM_013845	NA	NA	INSIDE
chr4	1E+08	1E+08	ox2_bound:40	Cachd1	NM_198037	NA	NA	INSIDE
chr4	1E+08	1E+08	ox2_bound:40	Dab1	NM_010014	NA	NA	INSIDE
chr4	1E+08	1E+08	ox2_bound:40	Ppap2b	NM_080555	NA	NA	INSIDE
chr4	1.1E+08	1.1E+08	ox2_bound:40	Ssbp3	NM_023672	NA	NA	PROMOTER
chr4	1.1E+08	1.1E+08	ox2_bound:40	Tmem48	NM_028355	NA	NA	PROMOTER
chr4	1.1E+08	1.1E+08	ox2_bound:40	Btf3l4	NM_027453	Txndc12	NM_025334	DIVERGENT
chr4	1.1E+08	1.1E+08	ox2_bound:40	Tal1	NM_011527	NA	NA	PROMOTER
chr4	1.2E+08	1.2E+08	ox2_bound:40	Rad54l	NM_009015	NA	NA	PROMOTER
chr4	1.2E+08	1.2E+08	ox2_bound:40	Gpbp1l1	NM_029868	NA	NA	INSIDE
chr4	1.2E+08	1.2E+08	ox2_bound:40	Nasp	NM_016777	NA	NA	INSIDE
chr4	1.2E+08	1.2E+08	ox2_bound:41	Mmachc	NM_025962	6610037D15Ri	NM_026714	DIVERGENT
chr4	1.2E+08	1.2E+08	ox2_bound:41	Tesk2	NM_146151	NA	NA	PROMOTER
chr4	1.2E+08	1.2E+08	ox2_bound:41	Tesk2	NM_146151	NA	NA	INSIDE
chr4	1.2E+08	1.2E+08	ox2_bound:41	Zswim5	NM_001029912	NA	NA	PROMOTER
chr4	1.2E+08	1.2E+08	ox2_bound:41	Plk3	NM_013807	NA	NA	INSIDE
chr4	1.2E+08	1.2E+08	ox2_bound:41	Rps8	NM_009098	NA	NA	DOWNSTREAM
chr4	1.2E+08	1.2E+08	ox2_bound:41	Cdc20	NM_023223	NA	NA	PROMOTER
chr4	1.2E+08	1.2E+08	ox2_bound:41	Ybx1	NM_011732	NA	NA	INSIDE
chr4	1.2E+08	1.2E+08	ox2_bound:41	Hivep3	NM_010657	NA	NA	INSIDE
chr4	1.2E+08	1.2E+08	ox2_bound:41	Edn2	NM_007902	NA	NA	PROMOTER
chr4	1.2E+08	1.2E+08	ox2_bound:42	Smap1l	NM_133716	NA	NA	PROMOTER
chr4	1.2E+08	1.2E+08	ox2_bound:42	Zmpste24	NM_172700	NA	NA	INSIDE
chr4	1.2E+08	1.2E+08	ox2_bound:42	Mycl1	NM_008506	NA	NA	INSIDE
chr4	1.2E+08	1.2E+08	ox2_bound:42	Bmp8a	NM_007558	NA	NA	PROMOTER
chr4	1.3E+08	1.3E+08	ox2_bound:42	Eif2c1	NM_153403	NA	NA	INSIDE
chr4	1.3E+08	1.3E+08	ox2_bound:42	Gjb3	NM_008126	NA	NA	PROMOTER
chr4	1.3E+08	1.3E+08	ox2_bound:42	Trim62	NM_178110	NA	NA	PROMOTER
chr4	1.3E+08	1.3E+08	ox2_bound:42	Bsdc1	NM_133889	NA	NA	PROMOTER
chr4	1.3E+08	1.3E+08	ox2_bound:42	Tssk3	NM_080442	NA	NA	PROMOTER
chr4	1.3E+08	1.3E+08	ox2_bound:42	Pef1	NM_026441	NA	NA	PROMOTER
chr4	1.3E+08	1.3E+08	ox2_bound:43	Fabp3	NM_010174	NA	NA	PROMOTER
chr4	1.3E+08	1.3E+08	ox2_bound:43	Med18	NM_026039	NA	NA	INSIDE
chr4	1.3E+08	1.3E+08	ox2_bound:43	Sesn2	NM_144907	NA	NA	PROMOTER
chr4	1.3E+08	1.3E+08	ox2_bound:43	Rpa2	NM_011284	NA	NA	PROMOTER
chr4	1.3E+08	1.3E+08	ox2_bound:43	BC082554	BC082554	NA	NA	Unknown
chr4	1.3E+08	1.3E+08	ox2_bound:43	Lin28	NM_145833	NA	NA	INSIDE
chr4	1.3E+08	1.3E+08	ox2_bound:43	Slc30a2	NM_001039677	NA	NA	INSIDE
chr4	1.3E+08	1.3E+08	ox2_bound:43	Pafah2	NM_133880	NA	NA	PROMOTER
chr4	1.3E+08	1.3E+08	ox2_bound:43	Stmn1	NM_019641	NA	NA	INSIDE
chr4	1.3E+08	1.3E+08	ox2_bound:43	Stmn1	NM_019641	NA	NA	INSIDE
chr4	1.3E+08	1.3E+08	ox2_bound:44	Tmem57	NM_025382	NA	NA	INSIDE
chr4	1.3E+08	1.3E+08	ox2_bound:44	Grhl3	NM_001013756	NA	NA	PROMOTER
chr4	1.4E+08	1.4E+08	ox2_bound:44	Pnrc2	NM_026383	NA	NA	PROMOTER
chr4	1.4E+08	1.4E+08	ox2_bound:44	Id3	NM_008321	NA	NA	INSIDE
chr4	1.4E+08	1.4E+08	ox2_bound:44	Tcea3	NM_011542	NA	NA	PROMOTER
chr4	1.4E+08	1.4E+08	ox2_bound:44	Tcea3	NM_011542	NA	NA	PROMOTER
chr4	1.4E+08	1.4E+08	ox2_bound:44	6030445D17Rik	NM_177079	NA	NA	INSIDE
chr4	1.4E+08	1.4E+08	ox2_bound:44	4930549C01Rik	NM_026300	NA	NA	INSIDE
chr4	1.4E+08	1.4E+08	ox2_bound:44	Zbtb40	NM_198248	NA	NA	PROMOTER
chr4	1.4E+08	1.4E+08	ox2_bound:44	Akp2	NM_007431	NA	NA	PROMOTER

chr4	1.4E+08	1.4E+08	ox2_bound:45	Eif4g3	NM_172703	NA	NA	PROMOTER
chr4	1.4E+08	1.4E+08	ox2_bound:45	C79267	NM_183148	NA	NA	PROMOTER
chr4	1.4E+08	1.4E+08	ox2_bound:45	Pax7	NM_011039	NA	NA	PROMOTER
chr4	1.4E+08	1.4E+08	ox2_bound:45	Rcc2	NM_173867	NA	NA	PROMOTER
chr4	1.4E+08	1.4E+08	ox2_bound:45	Rcc2	NM_173867	NA	NA	INSIDE
chr4	1.4E+08	1.4E+08	ox2_bound:45	Arhgef19	NM_172520	NA	NA	PROMOTER
chr4	1.4E+08	1.4E+08	ox2_bound:45	Fblim1	NM_133754	NA	NA	PROMOTER
chr4	1.4E+08	1.4E+08	ox2_bound:45	Pdpn	NM_010329	NA	NA	PROMOTER
chr4	1.4E+08	1.4E+08	ox2_bound:45	Pdpn	NM_010329	NA	NA	PROMOTER
chr4	1.4E+08	1.4E+08	ox2_bound:45	Pdpn	NM_010329	NA	NA	PROMOTER
chr4	1.5E+08	1.5E+08	ox2_bound:46	Agtrap	NM_009642	NA	NA	INSIDE
chr4	1.5E+08	1.5E+08	ox2_bound:46	Agtrap	NM_009642	NA	NA	PROMOTER
chr4	1.5E+08	1.5E+08	ox2_bound:46	Cort	NM_007745	NA	NA	INSIDE
chr4	1.5E+08	1.5E+08	ox2_bound:46	Hes3	NM_008237	NA	NA	INSIDE
chr4	1.5E+08	1.5E+08	ox2_bound:46	D330010C22Rik	NM_001033489	Rpl22	NM_009079	DIVERGENT
chr5	5564922	5565540	ox2_bound:46	BC034507	NM_153116	NA	NA	INSIDE
chr5	8092083	8092583	ox2_bound:46	Sri	NM_025618	NA	NA	INSIDE
chr5	8461281	8462640	ox2_bound:46	B230315F11Rik	NM_178766	NA	NA	INSIDE
chr5	1.5E+07	1.5E+07	ox2_bound:46	Cacna2d1	NM_009784	NA	NA	PROMOTER
chr5	1.5E+07	1.5E+07	ox2_bound:46	Cacna2d1	NM_009784	NA	NA	INSIDE
chr5	2E+07	2E+07	ox2_bound:47	Phtf2	NM_172992	Tmem60	NM_177601	DIVERGENT
chr5	2E+07	2E+07	ox2_bound:47	Ptpn12	NM_011203	NA	NA	INSIDE
chr5	2.1E+07	2.1E+07	ox2_bound:47	Pmpcb	NM_028431	NA	NA	PROMOTER
chr5	2.7E+07	2.7E+07	ox2_bound:47	En2	NM_010134	NA	NA	INSIDE
chr5	2.9E+07	2.9E+07	ox2_bound:47	Dnajb6	NM_001037941	NA	NA	INSIDE
chr5	3E+07	3E+07	ox2_bound:47	9430057O19Rik	NM_174849	NA	NA	PROMOTER
chr5	3.1E+07	3.1E+07	ox2_bound:47	Fosl2	NM_008037	NA	NA	PROMOTER
chr5	3.2E+07	3.2E+07	ox2_bound:47	Slc5a1	NM_019810	NA	NA	PROMOTER
chr5	3.3E+07	3.3E+07	ox2_bound:47	Rnf4	NM_011278	NA	NA	INSIDE
chr5	3.4E+07	3.4E+07	ox2_bound:47	Lrpap1	NM_013587	NA	NA	INSIDE
chr5	3.6E+07	3.6E+07	ox2_bound:48	Crmp1	NM_007765	NA	NA	INSIDE
chr5	3.7E+07	3.7E+07	ox2_bound:48	Msx1	NM_010835	NA	NA	PROMOTER
chr5	3.7E+07	3.7E+07	ox2_bound:48	Otop1	NM_172709	NA	NA	PROMOTER
chr5	4.1E+07	4.1E+07	ox2_bound:48	Bapx1	NM_007524	NA	NA	PROMOTER
chr5	4.3E+07	4.3E+07	ox2_bound:48	Cd38	NM_007646	NA	NA	INSIDE
chr5	4.3E+07	4.3E+07	ox2_bound:48	Fgfbp1	NM_008009	NA	NA	PROMOTER
chr5	4.5E+07	4.5E+07	ox2_bound:48	Lap3	NM_024434	NA	NA	INSIDE
chr5	4.7E+07	4.7E+07	ox2_bound:48	Slit2	NM_178804	NA	NA	INSIDE
chr5	5.2E+07	5.2E+07	ox2_bound:48	Lgi2	NM_144945	NA	NA	PROMOTER
chr5	5.3E+07	5.3E+07	ox2_bound:48	Rbpsuh	NM_009035	NA	NA	INSIDE
chr5	5.3E+07	5.3E+07	ox2_bound:49	Cckar	NM_009827	NA	NA	PROMOTER
chr5	5.7E+07	5.7E+07	ox2_bound:49	Pcdh7	NM_018764	NA	NA	PROMOTER
chr5	6.3E+07	6.3E+07	ox2_bound:49	AA536743	NM_145923	NA	NA	PROMOTER
chr5	6.3E+07	6.3E+07	ox2_bound:49	AA536743	NM_145923	NA	NA	PROMOTER
chr5	6.4E+07	6.4E+07	ox2_bound:49	Tlr6	NM_011604	1130005N14Rik	NM_026667	DIVERGENT
chr5	6.4E+07	6.4E+07	ox2_bound:49	Klhl5	NM_175174	NA	NA	PROMOTER
chr5	6.5E+07	6.5E+07	ox2_bound:49	B3bp	NM_001024917	NA	NA	PROMOTER
chr5	6.6E+07	6.6E+07	ox2_bound:49	BC013481	NM_178446	NA	NA	PROMOTER
chr5	6.6E+07	6.6E+07	ox2_bound:49	Uchl1	NM_011670	NA	NA	INSIDE
chr5	6.6E+07	6.6E+07	ox2_bound:49	Uchl1	NM_011670	NA	NA	INSIDE
chr5	6.6E+07	6.6E+07	ox2_bound:50	Phox2b	NM_008888	NA	NA	PROMOTER
chr5	7.1E+07	7.1E+07	ox2_bound:50	Gabrb1	NM_008069	NA	NA	INSIDE
chr5	7.3E+07	7.3E+07	ox2_bound:50	9030227G01Rik	NM_177136	NA	NA	PROMOTER
chr5	7.4E+07	7.4E+07	ox2_bound:50	Gsh2	NM_133256	NA	NA	PROMOTER
chr5	7.5E+07	7.5E+07	ox2_bound:50	Kit	NM_021099	NA	NA	INSIDE
chr5	7.7E+07	7.7E+07	ox2_bound:50	Rest	NM_011263	NA	NA	PROMOTER
chr5	8.9E+07	8.9E+07	ox2_bound:50	Rufy3	NM_027530	NA	NA	INSIDE
chr5	8.9E+07	8.9E+07	ox2_bound:50	Grsf1	NM_178700	NA	NA	PROMOTER
chr5	9.2E+07	9.2E+07	ox2_bound:50	E430034L04Rik	NM_011816	NA	NA	PROMOTER
chr5	9.2E+07	9.2E+07	ox2_bound:50	Nup54	NM_183392	NA	NA	PROMOTER
chr5	9.2E+07	9.2E+07	ox2_bound:51	Scarb2	NM_007644	NA	NA	INSIDE
chr5	9.3E+07	9.3E+07	ox2_bound:51	4932413O14Rik	NM_177230	Shrm	NM_015756	DIVERGENT
chr5	9.3E+07	9.3E+07	ox2_bound:51	4932413O14Rik	NM_177230	Shrm	NM_015756	DIVERGENT
chr5	9.3E+07	9.3E+07	ox2_bound:51	Sept11	NM_001009818	NA	NA	INSIDE
chr5	9.3E+07	9.3E+07	ox2_bound:51	Ccni	NM_017367	NA	NA	PROMOTER

chr5	9.3E+07	9.3E+07	ox2_bound:51	Ccng2	NM_007635	NA	NA	INSIDE
chr5	9.7E+07	9.7E+07	ox2_bound:51	Fgf5	NM_010203	NA	NA	INSIDE
chr5	9.9E+07	9.9E+07	ox2_bound:51	2310057D15Rik	NM_026421	NA	NA	INSIDE
chr5	1E+08	1E+08	ox2_bound:51	Mrps18c	NM_026826	NA	NA	PROMOTER
chr5	1E+08	1E+08	ox2_bound:51	Arhgap24	NM_029270	NA	NA	PROMOTER
chr5	1E+08	1E+08	ox2_bound:52	Dhrs8	NM_053262	NA	NA	PROMOTER
chr5	1E+08	1E+08	ox2_bound:52	Spp1	NM_009263	NA	NA	PROMOTER
chr5	1E+08	1E+08	ox2_bound:52	Lrrc8c	NM_133897	NA	NA	PROMOTER
chr5	1.1E+08	1.1E+08	ox2_bound:52	Tgfbr3	NM_011578	NA	NA	INSIDE
chr5	1.1E+08	1.1E+08	ox2_bound:52	Mtf2	NM_013827	NA	NA	PROMOTER
chr5	1.1E+08	1.1E+08	ox2_bound:52	Dgkq	NM_199011	Idua	NM_008325	DIVERGENT
chr5	1.1E+08	1.1E+08	ox2_bound:52	D5Ertd585e	NM_027922	NA	NA	PROMOTER
chr5	1.1E+08	1.1E+08	ox2_bound:52	D5Ertd585e	NM_027922	NA	NA	PROMOTER
chr5	1.1E+08	1.1E+08	ox2_bound:52	Ulk1	NM_009469	NA	NA	INSIDE
chr5	1.1E+08	1.1E+08	ox2_bound:52	E130006D01Rik	NM_207252	NA	NA	INSIDE
chr5	1.2E+08	1.2E+08	ox2_bound:53	Ccdc60	NM_177759	NA	NA	PROMOTER
chr5	1.2E+08	1.2E+08	ox2_bound:53	1500001A10Rik	NM_026886	NA	NA	PROMOTER
chr5	1.2E+08	1.2E+08	ox2_bound:53	BC023744	NM_001033311	NA	NA	PROMOTER
chr5	1.2E+08	1.2E+08	ox2_bound:53	Wsb2	NM_021539	NA	NA	PROMOTER
chr5	1.2E+08	1.2E+08	ox2_bound:53	Tbx3	NM_011535	NA	NA	INSIDE
chr5	1.2E+08	1.2E+08	ox2_bound:53	Anapc7	NM_019805	NA	NA	PROMOTER
chr5	1.2E+08	1.2E+08	ox2_bound:53	Anapc5	NM_021505	NA	NA	PROMOTER
chr5	1.2E+08	1.2E+08	ox2_bound:53	Fbxl10	NM_001003953	NA	NA	PROMOTER
chr5	1.2E+08	1.2E+08	ox2_bound:53	Rhof	NM_175092	NA	NA	PROMOTER
chr5	1.2E+08	1.2E+08	ox2_bound:53	Mlxip	NM_177582	NA	NA	PROMOTER
chr5	1.2E+08	1.2E+08	ox2_bound:54	Zcchc8	NM_027494	NA	NA	PROMOTER
chr5	1.2E+08	1.2E+08	ox2_bound:54	1500011J06Rik	NM_001005523	NA	NA	PROMOTER
chr5	1.2E+08	1.2E+08	ox2_bound:54	6330548G22Rik	NM_029532	NA	NA	INSIDE
chr5	1.2E+08	1.2E+08	ox2_bound:54	Ncor2	NM_011424	NA	NA	INSIDE
chr5	1.3E+08	1.3E+08	ox2_bound:54	Fzd10	NM_175284	NA	NA	PROMOTER
chr5	1.3E+08	1.3E+08	ox2_bound:54	Gtf2i	NM_010365	NA	NA	INSIDE
chr5	1.3E+08	1.3E+08	ox2_bound:54	Cldn4	NM_009903	NA	NA	INSIDE
chr5	1.3E+08	1.3E+08	ox2_bound:54	Baz1b	NM_011714	NA	NA	PROMOTER
chr5	1.3E+08	1.3E+08	ox2_bound:54	Rhbdd2	NM_146002	NA	NA	PROMOTER
chr5	1.3E+08	1.3E+08	ox2_bound:54	Rhbdd2	NM_146002	NA	NA	PROMOTER
chr5	1.3E+08	1.3E+08	ox2_bound:55	Usmg1	NM_031398	NA	NA	INSIDE
chr5	1.3E+08	1.3E+08	ox2_bound:55	Ywhag	NM_018871	NA	NA	PROMOTER
chr5	1.4E+08	1.4E+08	ox2_bound:55	Ars2	NM_031405	NA	NA	INSIDE
chr5	1.4E+08	1.4E+08	ox2_bound:55	Ephb4	NM_010144	NA	NA	INSIDE
chr5	1.4E+08	1.4E+08	ox2_bound:55	Actl6b	NM_031404	NA	NA	PROMOTER
chr5	1.4E+08	1.4E+08	ox2_bound:55	Bcdin3	NM_144913	Zcwpw1	NM_001005420	DIVERGENT
chr5	1.4E+08	1.4E+08	ox2_bound:55	Zipro1	NM_011757	NA	NA	INSIDE
chr5	1.4E+08	1.4E+08	ox2_bound:55	Zfp113	NM_019747	Cops6	NM_012002	DIVERGENT
chr5	1.4E+08	1.4E+08	ox2_bound:55	Ap4m1	NM_021392	NA	NA	INSIDE
chr5	1.4E+08	1.4E+08	ox2_bound:55	Pdgfa	NM_008808	NA	NA	PROMOTER
chr5	1.4E+08	1.4E+08	ox2_bound:56	Uncx4.1	NM_013702	NA	NA	PROMOTER
chr5	1.4E+08	1.4E+08	ox2_bound:56	Zfp469	NM_178242	NA	NA	PROMOTER
chr5	1.4E+08	1.4E+08	ox2_bound:56	Nptx2	NM_016789	NA	NA	PROMOTER
chr5	1.4E+08	1.4E+08	ox2_bound:56	Atp5j2	NM_020582	NA	NA	PROMOTER
chr5	1.5E+08	1.5E+08	ox2_bound:56	Wasf3	NM_145155	NA	NA	INSIDE
chr5	1.5E+08	1.5E+08	ox2_bound:56	Gsh1	NM_008178	NA	NA	PROMOTER
chr5	1.5E+08	1.5E+08	ox2_bound:56	Cdx2	NM_007673	NA	NA	INSIDE
chr5	1.5E+08	1.5E+08	ox2_bound:56	Cdx2	NM_007673	NA	NA	INSIDE
chr5	1.5E+08	1.5E+08	ox2_bound:56	1200006F02Rik	NM_027872	NA	NA	INSIDE
chr5	1.5E+08	1.5E+08	ox2_bound:56	Ubl3	NM_011908	NA	NA	INSIDE
chr6	3450583	3451240	ox2_bound:57	1700034M03Rik	NM_024260	NA	NA	INSIDE
chr6	4039057	4040037	ox2_bound:57	Bet1	NM_009748	NA	NA	PROMOTER
chr6	5333718	5334218	ox2_bound:57	Asb4	NM_023048	NA	NA	PROMOTER
chr6	6833226	6834122	ox2_bound:57	Dlx5	NM_010056	NA	NA	INSIDE
chr6	7646962	7647708	ox2_bound:57	Asns	NM_012055	NA	NA	PROMOTER
chr6	1.4E+07	1.4E+07	ox2_bound:57	B630005N14Rik	NM_175312	NA	NA	PROMOTER
chr6	1.4E+07	1.4E+07	ox2_bound:57	2610001J05Rik	NM_183258	NA	NA	INSIDE
chr6	2.6E+07	2.6E+07	ox2_bound:57	Gpr37	NM_010338	NA	NA	INSIDE
chr6	2.9E+07	2.9E+07	ox2_bound:57	mmu-mir-129-1	mmu-mir-129-1	NA	NA	PROMOTER
chr6	2.9E+07	2.9E+07	ox2_bound:57	mmu-mir-129-1	mmu-mir-129-1	NA	NA	PROMOTER

chr6	2.9E+07	2.9E+07	ox2_bound:58	mmu-mir-129-1	mmu-mir-129-1	NA	NA	PROMOTER
chr6	3E+07	3E+07	ox2_bound:58	2700094F01Rik	NM_178625	700025E21Ri	NM_029373	DIVERGENT
chr6	3.8E+07	3.8E+07	ox2_bound:58	Trim24	NM_145076	NA	NA	INSIDE
chr6	3.8E+07	3.8E+07	ox2_bound:58	Zc3hav1	NM_028864	NA	NA	PROMOTER
chr6	3.8E+07	3.8E+07	ox2_bound:58	Zc3hav1	NM_028864	NA	NA	PROMOTER
chr6	3.8E+07	3.8E+07	ox2_bound:58	Ttc26	NM_153600	NA	NA	PROMOTER
chr6	3.8E+07	3.8E+07	ox2_bound:58	1110001J03Rik	NM_025363	NA	NA	PROMOTER
chr6	3.9E+07	3.9E+07	ox2_bound:58	Mkrn1	NM_018810	NA	NA	PROMOTER
chr6	4.7E+07	4.7E+07	ox2_bound:58	Cntnap2	NM_025771	NA	NA	PROMOTER
chr6	4.9E+07	4.9E+07	ox2_bound:58	Gimap9	NM_174960	NA	NA	INSIDE
chr6	4.9E+07	4.9E+07	ox2_bound:59	Igf2bp3	NM_023670	NA	NA	PROMOTER
chr6	4.9E+07	4.9E+07	ox2_bound:59	Igf2bp3	NM_023670	NA	NA	PROMOTER
chr6	5E+07	5E+07	ox2_bound:59	Npy	NM_023456	NA	NA	PROMOTER
chr6	5.1E+07	5.1E+07	ox2_bound:59	Hnrpa2b1	NM_016806	NA	NA	INSIDE
chr6	5.2E+07	5.2E+07	ox2_bound:59	Scap2	NM_018773	NA	NA	PROMOTER
chr6	5.2E+07	5.2E+07	ox2_bound:59	Hoxa2	NM_010451	730596B20Ri	NA	INSIDE
chr6	5.2E+07	5.2E+07	ox2_bound:59	Hoxa2	NM_010451	NA	NM_175261	DIVERGENT
chr6	5.2E+07	5.2E+07	ox2_bound:59	5730596B20Rik	NM_175261	NA	NA	PROMOTER
chr6	5.2E+07	5.2E+07	ox2_bound:59	Hoxa9	NM_010456	NA	NA	PROMOTER
chr6	5.2E+07	5.2E+07	ox2_bound:59	Hoxa10	NM_008263	NA	NA	INSIDE
chr6	5.2E+07	5.2E+07	ox2_bound:60	Hoxa10	NM_008263	NA	NA	PROMOTER
chr6	5.2E+07	5.2E+07	ox2_bound:60	Hoxa11	NM_010450	NA	NA	PROMOTER
chr6	5.2E+07	5.2E+07	ox2_bound:60	Hoxa11	NM_010450	NA	NA	PROMOTER
chr6	5.2E+07	5.2E+07	ox2_bound:60	Hoxa11	NM_010450	NA	NA	PROMOTER
chr6	5.2E+07	5.2E+07	ox2_bound:60	Hoxa11	NM_010450	NA	NA	PROMOTER
chr6	5.2E+07	5.2E+07	ox2_bound:60	Evx1	NM_007966	NA	NA	PROMOTER
chr6	5.2E+07	5.2E+07	ox2_bound:60	Evx1	NM_007966	NA	NA	INSIDE
chr6	7.1E+07	7.1E+07	ox2_bound:60	Fabp1	NM_017399	NA	NA	PROMOTER
chr6	7.1E+07	7.1E+07	ox2_bound:60	Smyd1	NM_009762	AA792894	NM_145568	DIVERGENT
chr6	7.2E+07	7.2E+07	ox2_bound:60	Jmjd1a	NM_173001	NA	NA	PROMOTER
chr6	7.3E+07	7.3E+07	ox2_bound:61	Tcf3	NM_009332	NA	NA	INSIDE
chr6	7.3E+07	7.3E+07	ox2_bound:61	BC043330	BC043330	NA	NA	Unknown
chr6	7.3E+07	7.3E+07	ox2_bound:61	BC043330	BC043330	NA	NA	Unknown
chr6	7.8E+07	7.8E+07	ox2_bound:61	Reg3g	NM_011260	NA	NA	INSIDE
chr6	8.3E+07	8.3E+07	ox2_bound:61	Hk2	NM_013820	NA	NA	INSIDE
chr6	8.6E+07	8.6E+07	ox2_bound:61	Figla	NM_012013	NA	NA	DOWNSTREAM
chr6	8.8E+07	8.8E+07	ox2_bound:61	8430410A17Rik	NM_173737	NA	NA	PROMOTER
chr6	9.2E+07	9.2E+07	ox2_bound:61	C130022K22Rik	NM_172730	NA	NA	PROMOTER
chr6	9.2E+07	9.2E+07	ox2_bound:61	Trh	NM_009426	NA	NA	PROMOTER
chr6	9.2E+07	9.2E+07	ox2_bound:61	Trh	NM_009426	NA	NA	PROMOTER
chr6	9.3E+07	9.3E+07	ox2_bound:62	8430417A20Rik	NM_175209	NA	NA	PROMOTER
chr6	9.7E+07	9.7E+07	ox2_bound:62	Ube1c	NM_011666	Arl6ip5	NM_022992	DIVERGENT
chr6	9.7E+07	9.7E+07	ox2_bound:62	Ube1c	NM_011666	Arl6ip5	NM_022992	DIVERGENT
chr6	9.9E+07	9.9E+07	ox2_bound:62	NSMUST000000892	MUST0000008	NA	NA	Unknown
chr6	1E+08	1E+08	ox2_bound:62	Rybp	NM_019743	NA	NA	INSIDE
chr6	1.1E+08	1.1E+08	ox2_bound:62	Setd5	NM_028385	NA	NA	PROMOTER
chr6	1.1E+08	1.1E+08	ox2_bound:62	Slc6a1	NM_178703	NA	NA	INSIDE
chr6	1.2E+08	1.2E+08	ox2_bound:62	Timp4	NM_080639	NA	NA	PROMOTER
chr6	1.2E+08	1.2E+08	ox2_bound:62	Rpl3	NM_172086	Syngr1	NA	PROMOTER
chr6	1.2E+08	1.2E+08	ox2_bound:62	BC060267	NM_198603	NA	NA	INSIDE
chr6	1.2E+08	1.2E+08	ox2_bound:63	Adipor2	NM_197985	NA	NA	PROMOTER
chr6	1.2E+08	1.2E+08	ox2_bound:63	Adipor2	NM_197985	NA	NA	PROMOTER
chr6	1.2E+08	1.2E+08	ox2_bound:63	Wnk1	NM_198703	NA	NA	PROMOTER
chr6	1.2E+08	1.2E+08	ox2_bound:63	M6pr	NM_010749	NA	NA	PROMOTER
chr6	1.2E+08	1.2E+08	ox2_bound:63	Phc1	NM_007905	NA	NA	PROMOTER
chr6	1.2E+08	1.2E+08	ox2_bound:63	Gdf3	NM_008108	NA	NA	INSIDE
chr6	1.2E+08	1.2E+08	ox2_bound:63	Gdf3	NM_008108	NA	NA	INSIDE
chr6	1.2E+08	1.2E+08	ox2_bound:63	Dppa3	NM_139218	NA	NA	PROMOTER
chr6	1.2E+08	1.2E+08	ox2_bound:63	Slc2a3	NM_011401	NA	NA	PROMOTER
chr6	1.2E+08	1.2E+08	ox2_bound:63	mmu-mir-141	mmu-mir-141	NA	NA	INSIDE
chr6	1.2E+08	1.2E+08	ox2_bound:64	Grcc10	NM_013535	NA	NA	INSIDE
chr6	1.2E+08	1.2E+08	ox2_bound:64	Usp5	NM_013700	NA	NA	INSIDE
chr6	1.3E+08	1.3E+08	ox2_bound:64	Ing4	NM_133345	NA	NA	INSIDE
chr6	1.3E+08	1.3E+08	ox2_bound:64	LOC14433	NM_008084	NA	NA	INSIDE
chr6	1.3E+08	1.3E+08	ox2_bound:64	Ntf3	NM_008742	NA	NA	INSIDE

chr6	1.3E+08	1.3E+08	ox2_bound:64	Ndufa9	NM_025358	Akap3	NM_009650	DIVERGENT
chr6	1.3E+08	1.3E+08	ox2_bound:64	Rad51ap1	NM_009013	D6Wsu163e	NM_138594	DIVERGENT
chr6	1.3E+08	1.3E+08	ox2_bound:64	Prmt8	NM_201371	NA	NA	PROMOTER
chr6	1.3E+08	1.3E+08	ox2_bound:64	Tspan9	NM_175414	NA	NA	INSIDE
chr6	1.3E+08	1.3E+08	ox2_bound:64	Etv6	NM_007961	NA	NA	PROMOTER
chr6	1.3E+08	1.3E+08	ox2_bound:65	Gpr19	NM_008157	NA	NA	PROMOTER
chr6	1.3E+08	1.3E+08	ox2_bound:65	Gpr19	NM_008157	NA	NA	PROMOTER
chr6	1.3E+08	1.3E+08	ox2_bound:65	Cdkn1b	NM_009875	NA	NA	PROMOTER
chr6	1.4E+08	1.4E+08	ox2_bound:65	Gprc5a	NM_181444	NA	NA	PROMOTER
chr6	1.4E+08	1.4E+08	ox2_bound:65	8430419L09Rik	NM_028982	NA	NA	PROMOTER
chr6	1.4E+08	1.4E+08	ox2_bound:65	Atf7ip	NM_019426	NA	NA	PROMOTER
chr6	1.4E+08	1.4E+08	ox2_bound:65	Pde6h	NM_023898	NA	NA	INSIDE
chr6	1.4E+08	1.4E+08	ox2_bound:65	Rerg	NM_181988	NA	NA	INSIDE
chr6	1.4E+08	1.4E+08	ox2_bound:65	BC027061	NM_183165	NA	NA	INSIDE
chr6	1.4E+08	1.4E+08	ox2_bound:65	Ldhb	NM_008492	NA	NA	INSIDE
chr6	1.4E+08	1.4E+08	ox2_bound:66	Ldhb	NM_008492	NA	NA	PROMOTER
chr6	1.4E+08	1.4E+08	ox2_bound:66	Ldhb	NM_008492	NA	NA	PROMOTER
chr6	1.4E+08	1.4E+08	ox2_bound:66	Kcnj8	NM_008428	NA	NA	PROMOTER
chr6	1.4E+08	1.4E+08	ox2_bound:66	Cmas	NM_009908	NA	NA	PROMOTER
chr6	1.4E+08	1.4E+08	ox2_bound:66	St8sia1	NM_011374	NA	NA	INSIDE
chr6	1.4E+08	1.4E+08	ox2_bound:66	St8sia1	NM_011374	NA	NA	PROMOTER
chr6	1.5E+08	1.5E+08	ox2_bound:66	Bcat1	NM_00102446	NA	NA	PROMOTER
chr6	1.5E+08	1.5E+08	ox2_bound:66	Lrmp	NM_008511	NA	NA	PROMOTER
chr6	1.5E+08	1.5E+08	ox2_bound:66	4930469P12Rik	NM_133688	NA	NA	INSIDE
chr6	1.5E+08	1.5E+08	ox2_bound:66	Tera	NM_019643	NA	NA	PROMOTER
chr6	1.5E+08	1.5E+08	ox2_bound:67	2810474O19Rik	NM_026054	NA	NA	INSIDE
chr7	3290067	3290567	ox2_bound:67	Leng1	NM_027203	NA	NA	PROMOTER
chr7	3326734	3327792	ox2_bound:67	Rps9	NM_029767	NA	NA	INSIDE
chr7	3712277	3712921	ox2_bound:67	Cdc42ep5	NM_021454	NA	NA	INSIDE
chr7	4108696	4110108	ox2_bound:67	6030429G01Rik	NM_00103354	NA	NA	PROMOTER
chr7	4326084	4326774	ox2_bound:67	Cox6b2	NM_183406	NA	NA	INSIDE
chr7	4590686	4591186	ox2_bound:67	Fiz1	NM_011813	Zfp524	NM_025324	DIVERGENT
chr7	6287731	6288231	ox2_bound:67	Peg3	NM_00101098	NA	NA	INSIDE
chr7	6290903	6291681	ox2_bound:67	Usp29	NM_021323	NA	NA	INSIDE
chr7	9149609	9150109	ox2_bound:67	Zik1	NM_009577	NA	NA	PROMOTER
chr7	1.2E+07	1.2E+07	ox2_bound:68	Zfp499	NM_00102469	Trim28	NA	INSIDE
chr7	1.2E+07	1.2E+07	ox2_bound:68	Zfp499	NM_00102469	Trim28	NM_011588	DIVERGENT
chr7	1.2E+07	1.2E+07	ox2_bound:68	Trim28	NM_011588	NA	NA	PROMOTER
chr7	1.2E+07	1.2E+07	ox2_bound:68	Zfp98	NM_145819	NA	NA	PROMOTER
chr7	1.5E+07	1.5E+07	ox2_bound:68	Slc1a5	NM_009201	NA	NA	PROMOTER
chr7	1.7E+07	1.7E+07	ox2_bound:68	Bloc1s3	NM_177692	Trappc6a	NM_025960	DIVERGENT
chr7	1.7E+07	1.7E+07	ox2_bound:68	Gemin7	NM_027189	Zfp296	NM_022409	DIVERGENT
chr7	1.7E+07	1.7E+07	ox2_bound:68	Clptm1	NM_019649	NA	NA	PROMOTER
chr7	1.7E+07	1.7E+07	ox2_bound:68	Apoe	NM_009696	NA	NA	PROMOTER
chr7	2.1E+07	2.1E+07	ox2_bound:68	Zfp93	NM_009567	NA	NA	PROMOTER
chr7	2.1E+07	2.1E+07	ox2_bound:69	2410005H09Rik	NM_146183	NA	NA	PROMOTER
chr7	2.1E+07	2.1E+07	ox2_bound:69	2410005H09Rik	NM_146183	NA	NA	PROMOTER
chr7	2.2E+07	2.2E+07	ox2_bound:69	Rps19	NM_023133	NA	NA	PROMOTER
chr7	2.2E+07	2.2E+07	ox2_bound:69	Rps19	NM_023133	NA	NA	PROMOTER
chr7	2.2E+07	2.2E+07	ox2_bound:69	Gsk3a	NM_00103166	NA	NA	PROMOTER
chr7	2.3E+07	2.3E+07	ox2_bound:69	Hnrpul1	NM_144922	NA	NA	PROMOTER
chr7	2.4E+07	2.4E+07	ox2_bound:69	Mia1	NM_019394	NA	NA	INSIDE
chr7	2.5E+07	2.5E+07	ox2_bound:69	BC089491	NM_175033	NA	NA	INSIDE
chr7	2.5E+07	2.5E+07	ox2_bound:69	Samd4b	NM_175021	Gmfg	NM_022024	DIVERGENT
chr7	2.6E+07	2.6E+07	ox2_bound:69	Fbxo27	NM_207238	NA	NA	PROMOTER
chr7	2.6E+07	2.6E+07	ox2_bound:70	Hnrpl	NM_177301	NA	NA	PROMOTER
chr7	2.6E+07	2.6E+07	ox2_bound:70	Neud4	NM_013874	NA	NA	INSIDE
chr7	2.7E+07	2.7E+07	ox2_bound:70	Zfp27	NM_00103770	NA	NA	INSIDE
chr7	2.7E+07	2.7E+07	ox2_bound:70	Zfp27	NM_011754	NA	NA	PROMOTER
chr7	2.7E+07	2.7E+07	ox2_bound:70	Zfp27	NM_011754	NA	NA	PROMOTER
chr7	2.7E+07	2.7E+07	ox2_bound:70	Zfp146	NM_011980	NA	NM_00103354	DIVERGENT
chr7	2.7E+07	2.7E+07	ox2_bound:70	Capns1	NM_009795	NA	NA	PROMOTER
chr7	2.7E+07	2.7E+07	ox2_bound:70	Prodh2	NM_019546	NA	NA	PROMOTER
chr7	2.7E+07	2.7E+07	ox2_bound:70	Prodh2	NM_019546	NA	NA	PROMOTER
chr7	2.8E+07	2.8E+07	ox2_bound:70	Lsr	NM_017405	NA	NA	INSIDE

chr7	3.2E+07	3.2E+07	ox2_bound:71	Rhpn2	NM_027897	NA	NA	PROMOTER
chr7	3.2E+07	3.2E+07	ox2_bound:71	Rhpn2	NM_027897	NA	NA	INSIDE
chr7	3.5E+07	3.5E+07	ox2_bound:71	C80913	NM_011274	NA	NA	PROMOTER
chr7	4E+07	4E+07	ox2_bound:71	BC043301	NM_00100854	NA	NA	PROMOTER
chr7	4E+07	4E+07	ox2_bound:71	4933405K07Rik	NM_028913	NA	NA	PROMOTER
chr7	4E+07	4E+07	ox2_bound:71	4933405K07Rik	NM_028913	NA	NA	INSIDE
chr7	4.1E+07	4.1E+07	ox2_bound:71	Napsa	NM_008437	NA	NA	PROMOTER
chr7	4.1E+07	4.1E+07	ox2_bound:71	Med25	NM_029365	NA	NA	PROMOTER
chr7	4.1E+07	4.1E+07	ox2_bound:71	Prrg2	NM_022999	Nosip	NM_025533	DIVERGENT
chr7	4.1E+07	4.1E+07	ox2_bound:71	Rps11	NM_013725	NA	NA	PROMOTER
chr7	4.1E+07	4.1E+07	ox2_bound:72	Nop17	NM_029406	NA	NA	PROMOTER
chr7	4.1E+07	4.1E+07	ox2_bound:72	Cd37	NM_007645	NA	NA	PROMOTER
chr7	4.2E+07	4.2E+07	ox2_bound:72	Snrp70	NM_009224	NA	NA	PROMOTER
chr7	4.2E+07	4.2E+07	ox2_bound:72	Ftl1	NM_010240	NA	NA	PROMOTER
chr7	4.2E+07	4.2E+07	ox2_bound:72	Dhrs10	NM_025330	NA	NA	PROMOTER
chr7	4.2E+07	4.2E+07	ox2_bound:72	Bcat2	NM_009737	NA	NA	PROMOTER
chr7	4.2E+07	4.2E+07	ox2_bound:72	Car11	NM_009800	NA	NA	INSIDE
chr7	4.2E+07	4.2E+07	ox2_bound:72	Pscd2	NM_011181	NA	NA	PROMOTER
chr7	4.2E+07	4.2E+07	ox2_bound:72	Tmem143	NM_144801	NA	NA	INSIDE
chr7	4.2E+07	4.2E+07	ox2_bound:72	Emp3	NM_010129	BC013491	NM_00103324	DIVERGENT
chr7	4.6E+07	4.6E+07	ox2_bound:73	Dbx1	NM_00100523	NA	NA	INSIDE
chr7	5.6E+07	5.6E+07	ox2_bound:73	Snurf	NM_033174	NA	NA	INSIDE
chr7	5.6E+07	5.6E+07	ox2_bound:73	Snurf	NM_033174	NA	NA	PROMOTER
chr7	5.6E+07	5.6E+07	ox2_bound:73	Snurf	NM_033174	NA	NA	PROMOTER
chr7	6.9E+07	6.9E+07	ox2_bound:73	Rgma	NM_177740	NA	NA	INSIDE
chr7	7.5E+07	7.5E+07	ox2_bound:73	Rlbp1	NM_020599	BC025462	NM_145946	DIVERGENT
chr7	7.6E+07	7.6E+07	ox2_bound:73	5730590G19Rik	NM_029835	NA	NA	INSIDE
chr7	7.7E+07	7.7E+07	ox2_bound:73	Zscan2	NM_009553	NA	NA	PROMOTER
chr7	7.7E+07	7.7E+07	ox2_bound:73	Pde8a	NM_008803	NA	NA	PROMOTER
chr7	7.7E+07	7.7E+07	ox2_bound:73	Pde8a	NM_008803	NA	NA	PROMOTER
chr7	7.7E+07	7.7E+07	ox2_bound:74	Rps17	NM_009092	NA	NA	DOWNSTREAM
chr7	8E+07	8E+07	ox2_bound:74	Mesdc1	NM_030705	Mesdc2	NM_023403	DIVERGENT
chr7	8E+07	8E+07	ox2_bound:74	Mesdc2	NM_023403	NA	NA	INSIDE
chr7	8.3E+07	8.3E+07	ox2_bound:74	Tyr	NM_011661	NA	NA	PROMOTER
chr7	8.4E+07	8.4E+07	ox2_bound:74	Rab38	NM_028238	NA	NA	PROMOTER
chr7	8.5E+07	8.5E+07	ox2_bound:74	Tmem135	NM_028343	NA	NA	PROMOTER
chr7	8.5E+07	8.5E+07	ox2_bound:74	Fzd4	NM_008055	NA	NA	INSIDE
chr7	8.9E+07	8.9E+07	ox2_bound:74	2310015N07Rik	NM_025515	NA	NA	PROMOTER
chr7	8.9E+07	8.9E+07	ox2_bound:74	Rab30	NM_029494	NA	NA	PROMOTER
chr7	8.9E+07	8.9E+07	ox2_bound:74	Rab30	NM_029494	NA	NA	INSIDE
chr7	8.9E+07	8.9E+07	ox2_bound:75	Prcp	NM_028243	NA	NA	PROMOTER
chr7	8.9E+07	8.9E+07	ox2_bound:75	Prcp	NM_028243	NA	NA	INSIDE
chr7	9.2E+07	9.2E+07	ox2_bound:75	Timd4	NM_178759	NA	NA	PROMOTER
chr7	9.3E+07	9.3E+07	ox2_bound:75	Alg8	NM_199035	NA	NA	INSIDE
chr7	9.4E+07	9.4E+07	ox2_bound:75	1810020D17Rik	NM_183251	NA	NA	PROMOTER
chr7	9.4E+07	9.4E+07	ox2_bound:75	Aqp11	NM_175105	NA	NA	PROMOTER
chr7	9.5E+07	9.5E+07	ox2_bound:75	NSMUST000000868	MUST0000008	NA	NA	Unknown
chr7	9.5E+07	9.5E+07	ox2_bound:75	Wnt11	NM_009519	NA	NA	PROMOTER
chr7	9.5E+07	9.5E+07	ox2_bound:75	Serpinh1	NM_009825	NA	NA	INSIDE
chr7	9.6E+07	9.6E+07	ox2_bound:75	Pgm2l1	NM_027629	NA	NA	INSIDE
chr7	9.6E+07	9.6E+07	ox2_bound:76	Ppme1	NM_028292	NA	NA	INSIDE
chr7	1E+08	1E+08	ox2_bound:76	Prkcdbp	NM_028444	NA	NA	INSIDE
chr7	1E+08	1E+08	ox2_bound:76	Prkcdbp	NM_028444	NA	NA	INSIDE
chr7	1.1E+08	1.1E+08	ox2_bound:76	Zfp143	NM_009281	NA	NA	PROMOTER
chr7	1.1E+08	1.1E+08	ox2_bound:76	Calca	NM_00103395	NA	NA	PROMOTER
chr7	1.1E+08	1.1E+08	ox2_bound:76	Plekha7	NM_172743	NA	NA	INSIDE
chr7	1.1E+08	1.1E+08	ox2_bound:76	Rps15a	NM_170669	NA	NA	PROMOTER
chr7	1.1E+08	1.1E+08	ox2_bound:76	Coq7	NM_009940	NA	NA	INSIDE
chr7	1.1E+08	1.1E+08	ox2_bound:76	9030624J02Rik	NM_027815	NA	NA	PROMOTER
chr7	1.1E+08	1.1E+08	ox2_bound:76	Gprc5b	NM_022420	NA	NA	INSIDE
chr7	1.2E+08	1.2E+08	ox2_bound:77	4930404J24Rik	NM_029610	NA	NA	INSIDE
chr7	1.2E+08	1.2E+08	ox2_bound:77	4930404J24Rik	NM_029610	NA	NA	INSIDE
chr7	1.2E+08	1.2E+08	ox2_bound:77	Eef2k	NM_007908	NA	NA	INSIDE
chr7	1.2E+08	1.2E+08	ox2_bound:77	Polr3e	NM_025298	NA	NA	PROMOTER
chr7	1.2E+08	1.2E+08	ox2_bound:77	Polr3e	NM_025298	NA	NA	PROMOTER

chr7	1.2E+08	1.2E+08	ox2_bound:77	Cdr2	NM_007672	NA	NA	PROMOTER
chr7	1.2E+08	1.2E+08	ox2_bound:77	Prkcb1	NM_008855	NA	NA	DOWNSTREAM
chr7	1.2E+08	1.2E+08	ox2_bound:77	Slc5a11	NM_146198	NA	NA	PROMOTER
chr7	1.2E+08	1.2E+08	ox2_bound:77	Slc5a11	NM_146198	NA	NA	INSIDE
chr7	1.2E+08	1.2E+08	ox2_bound:77	2210013K02Rik	NM_023712	NA	NA	PROMOTER
chr7	1.2E+08	1.2E+08	ox2_bound:78	Sh2bpsm1	NM_011363	NA	NA	PROMOTER
chr7	1.2E+08	1.2E+08	ox2_bound:78	Ppp4c	NM_019674	NA	NA	PROMOTER
chr7	1.2E+08	1.2E+08	ox2_bound:78	Qprt	NM_133686	NA	NA	INSIDE
chr7	1.2E+08	1.2E+08	ox2_bound:78	Cd2bp2	NM_027353	NA	NA	PROMOTER
chr7	1.2E+08	1.2E+08	ox2_bound:78	Sept1	NM_017461	NA	NA	INSIDE
chr7	1.2E+08	1.2E+08	ox2_bound:78	Zfp553	NM_146201	NA	NA	PROMOTER
chr7	1.2E+08	1.2E+08	ox2_bound:78	Zfp689	NM_175163	NA	NA	PROMOTER
chr7	1.2E+08	1.2E+08	ox2_bound:78	Fbxl19	NM_172748	NA	NA	PROMOTER
chr7	1.2E+08	1.2E+08	ox2_bound:78	Zfp668	NM_146259	6820429M01	NM_172749	DIVERGENT
chr7	1.2E+08	1.2E+08	ox2_bound:78	Prss8	NM_133351	NA	NA	PROMOTER
chr7	1.3E+08	1.3E+08	ox2_bound:79	Brwd2	NM_172255	NA	NA	PROMOTER
chr7	1.3E+08	1.3E+08	ox2_bound:79	Fgfr2	NM_010207	NA	NA	INSIDE
chr7	1.3E+08	1.3E+08	ox2_bound:79	Plekha1	NM_133942	NA	NA	PROMOTER
chr7	1.3E+08	1.3E+08	ox2_bound:79	Ebf3	NM_010096	NA	NA	PROMOTER
chr7	1.4E+08	1.4E+08	ox2_bound:79	Ppp2r2d	NM_026391	NA	NA	INSIDE
chr7	1.4E+08	1.4E+08	ox2_bound:79	Dpysl4	NM_011993	NA	NA	PROMOTER
chr7	1.4E+08	1.4E+08	ox2_bound:79	Utf1	NM_009482	NA	NA	DOWNSTREAM
chr7	1.4E+08	1.4E+08	ox2_bound:79	Msx3	NM_010836	NA	NA	INSIDE
chr7	1.4E+08	1.4E+08	ox2_bound:79	Drd1ip	NM_026769	Prap1	NM_009475	DIVERGENT
chr7	1.4E+08	1.4E+08	ox2_bound:79	Ifitm2	NM_030694	Ifitm1	NM_026820	DIVERGENT
chr7	1.4E+08	1.4E+08	ox2_bound:80	Ifitm2	NM_030694	Ifitm1	NM_026820	DIVERGENT
chr7	1.4E+08	1.4E+08	ox2_bound:80	Ifitm2	NM_030694	Ifitm1	NM_026820	DIVERGENT
chr7	1.4E+08	1.4E+08	ox2_bound:80	Ifitm1	NM_026820	NA	NA	DOWNSTREAM
chr7	1.4E+08	1.4E+08	ox2_bound:80	Ifitm3	NM_025378	NA	NA	DOWNSTREAM
chr7	1.4E+08	1.4E+08	ox2_bound:80	Drd4	NM_007878	NA	NA	INSIDE
chr7	1.4E+08	1.4E+08	ox2_bound:80	Igf2	NM_010514	NA	NA	PROMOTER
chr7	1.4E+08	1.4E+08	ox2_bound:80	Mrgprg	NM_203492	NA	NA	PROMOTER
chr7	1.4E+08	1.4E+08	ox2_bound:80	Fgf4	NM_010202	NA	NA	PROMOTER
chr8	3308637	3309559	ox2_bound:80	Arhgef18	NM_133962	NA	NA	INSIDE
chr8	1.1E+07	1.1E+07	ox2_bound:80	Col4a1	NM_009931	NA	NA	INSIDE
chr8	1.2E+07	1.2E+07	ox2_bound:81	Ankrd10	NM_133971	NA	NA	PROMOTER
chr8	1.3E+07	1.3E+07	ox2_bound:81	Tmco3	NM_172282	NA	NA	INSIDE
chr8	2.1E+07	2.1E+07	ox2_bound:81	Defb1	NM_007843	NA	NA	PROMOTER
chr8	2.6E+07	2.6E+07	ox2_bound:81	Gpr124	NM_054044	NA	NA	PROMOTER
chr8	2.6E+07	2.6E+07	ox2_bound:81	Got1l1	NM_029674	NA	NA	PROMOTER
chr8	2.6E+07	2.6E+07	ox2_bound:81	Adrb3	NM_013462	NA	NA	PROMOTER
chr8	3E+07	3E+07	ox2_bound:81	Rnf122	NM_175136	NA	NA	PROMOTER
chr8	3E+07	3E+07	ox2_bound:81	BC019943	NM_144927	NA	NA	PROMOTER
chr8	3E+07	3E+07	ox2_bound:81	BC019943	NM_144927	NA	NA	PROMOTER
chr8	3.4E+07	3.4E+07	ox2_bound:81	Dusp4	NM_176933	NA	NA	PROMOTER
chr8	3.4E+07	3.4E+07	ox2_bound:82	Dusp4	NM_176933	NA	NA	INSIDE
chr8	4.2E+07	4.2E+07	ox2_bound:82	Zfp42	NM_009556	NA	NA	INSIDE
chr8	4.2E+07	4.2E+07	ox2_bound:82	Zfp42	NM_009556	NA	NA	PROMOTER
chr8	4.4E+07	4.4E+07	ox2_bound:82	F11	NM_028066	NA	NA	PROMOTER
chr8	4.5E+07	4.5E+07	ox2_bound:82	Helt	NM_173789	NA	NA	PROMOTER
chr8	4.5E+07	4.5E+07	ox2_bound:82	Casp3	NM_009810	NA	NA	INSIDE
chr8	5.3E+07	5.3E+07	ox2_bound:82	Vegfc	NM_009506	NA	NA	PROMOTER
chr8	5.6E+07	5.6E+07	ox2_bound:82	Hand2	NM_010402	NA	NA	INSIDE
chr8	5.9E+07	5.9E+07	ox2_bound:82	BC042740	BC042740	NA	NA	Unknown
chr8	6.3E+07	6.3E+07	ox2_bound:82	BC031142	BC031142	NA	NA	Unknown
chr8	6.7E+07	6.7E+07	ox2_bound:83	Ints10	NM_027590	NA	NA	PROMOTER
chr8	6.9E+07	6.9E+07	ox2_bound:83	Cspg3	NM_007789	NA	NA	PROMOTER
chr8	6.9E+07	6.9E+07	ox2_bound:83	Ddx49	NM_001024922	Cope	NM_021538	DIVERGENT
chr8	6.9E+07	6.9E+07	ox2_bound:83	Fkbp8	NM_010223	NA	NA	PROMOTER
chr8	6.9E+07	6.9E+07	ox2_bound:83	Lsm4	NM_015816	NA	NA	INSIDE
chr8	7E+07	7E+07	ox2_bound:83	2010315L10Rik	NM_025917	NA	NA	PROMOTER
chr8	7E+07	7E+07	ox2_bound:83	Insl3	NM_013564	NA	NA	PROMOTER
chr8	7.1E+07	7.1E+07	ox2_bound:83	Tpm4	NM_001001491	NA	NA	INSIDE
chr8	7.1E+07	7.1E+07	ox2_bound:83	Klf2	NM_008452	NA	NA	PROMOTER
chr8	7.1E+07	7.1E+07	ox2_bound:83	Calr3	NM_028500	700030K09Ri	NM_028170	DIVERGENT

chr8	7.2E+07	7.2E+07	ox2_bound:84	Large	NM_010687	NA	NA	PROMOTER
chr8	7.4E+07	7.4E+07	ox2_bound:84	Hmox1	NM_010442	NA	NA	PROMOTER
chr8	7.7E+07	7.7E+07	ox2_bound:84	Pou4f2	NM_138944	NA	NA	INSIDE
chr8	7.7E+07	7.7E+07	ox2_bound:84	Pou4f2	NM_138944	NA	NA	PROMOTER
chr8	7.7E+07	7.7E+07	ox2_bound:84	2410193C02Rik	NM_001009980	NA	NA	INSIDE
chr8	7.7E+07	7.7E+07	ox2_bound:84	2410193C02Rik	NM_001009980	NA	NA	INSIDE
chr8	7.9E+07	7.9E+07	ox2_bound:84	Hhip	NM_020259	NA	NA	INSIDE
chr8	8.2E+07	8.2E+07	ox2_bound:84	Tbc1d9	NM_027758	NA	NA	PROMOTER
chr8	8.2E+07	8.2E+07	ox2_bound:84	Tbc1d9	NM_027758	NA	NA	PROMOTER
chr8	8.2E+07	8.2E+07	ox2_bound:84	Tbc1d9	NM_027758	NA	NA	PROMOTER
chr8	8.2E+07	8.2E+07	ox2_bound:85	Gipc1	NM_018771	NA	NA	PROMOTER
chr8	8.2E+07	8.2E+07	ox2_bound:85	Gipc1	NM_018771	NA	NA	INSIDE
chr8	8.3E+07	8.3E+07	ox2_bound:85	Ier2	NM_010499	NA	NA	INSIDE
chr8	8.4E+07	8.4E+07	ox2_bound:85	Prdx2	NM_011563	NA	NA	INSIDE
chr8	8.4E+07	8.4E+07	ox2_bound:85	Junb	NM_008416	NA	NA	PROMOTER
chr8	8.4E+07	8.4E+07	ox2_bound:85	Tnpo2	NM_145390	NA	NA	PROMOTER
chr8	8.4E+07	8.4E+07	ox2_bound:85	BC056474	NM_001001493	NA	NA	INSIDE
chr8	8.6E+07	8.6E+07	ox2_bound:85	Cbln1	NM_019626	NA	NA	PROMOTER
chr8	8.8E+07	8.8E+07	ox2_bound:85	Sall1	NM_021390	NA	NA	PROMOTER
chr8	8.9E+07	8.9E+07	ox2_bound:85	Chd9	NM_177224	NA	NA	PROMOTER
chr8	9E+07	9E+07	ox2_bound:86	Irx3	NM_008393	NA	NA	PROMOTER
chr8	9.3E+07	9.3E+07	ox2_bound:86	Amfr	NM_011787	NA	NA	INSIDE
chr8	9.3E+07	9.3E+07	ox2_bound:86	Mt1	NM_013602	NA	NA	PROMOTER
chr8	9.3E+07	9.3E+07	ox2_bound:86	Cpne2	NM_153507	NA	NA	INSIDE
chr8	9.3E+07	9.3E+07	ox2_bound:86	Pllp	NM_026385	NA	NA	PROMOTER
chr8	9.4E+07	9.4E+07	ox2_bound:86	Ccdc102a	NM_001033533	Gpr114	NM_001033468	DIVERGENT
chr8	9.4E+07	9.4E+07	ox2_bound:86	Kifc3	NM_010631	NA	NA	PROMOTER
chr8	9.4E+07	9.4E+07	ox2_bound:86	Kifc3	NM_010631	NA	NA	PROMOTER
chr8	9.4E+07	9.4E+07	ox2_bound:86	BC031853	NM_172758	NA	NA	PROMOTER
chr8	9.8E+07	9.8E+07	ox2_bound:86	Cdh8	NM_007667	NA	NA	INSIDE
chr8	1E+08	1E+08	ox2_bound:87	4931428F04Rik	NM_028888	NA	NA	PROMOTER
chr8	1E+08	1E+08	ox2_bound:87	Slc12a4	NM_009195	NA	NA	PROMOTER
chr8	1E+08	1E+08	ox2_bound:87	Smpd3	NM_021491	NA	NA	PROMOTER
chr8	1E+08	1E+08	ox2_bound:87	Smpd3	NM_021491	NA	NA	PROMOTER
chr8	1.1E+08	1.1E+08	ox2_bound:87	Zfp90	NM_011764	NA	NA	INSIDE
chr8	1.1E+08	1.1E+08	ox2_bound:87	6030452D12Rik	NM_177904	NA	NA	INSIDE
chr8	1.1E+08	1.1E+08	ox2_bound:87	Cdh3	NM_007665	NA	NA	PROMOTER
chr8	1.1E+08	1.1E+08	ox2_bound:87	Cdh1	NM_009864	NA	NA	PROMOTER
chr8	1.1E+08	1.1E+08	ox2_bound:87	Cdh1	NM_009864	NA	NA	INSIDE
chr8	1.1E+08	1.1E+08	ox2_bound:87	Has3	NM_008217	NA	NA	INSIDE
chr8	1.1E+08	1.1E+08	ox2_bound:88	Has3	NM_008217	NA	NA	INSIDE
chr8	1.1E+08	1.1E+08	ox2_bound:88	Has3	NM_008217	NA	NA	INSIDE
chr8	1.1E+08	1.1E+08	ox2_bound:88	Sntb2	NM_009229	NA	NA	PROMOTER
chr8	1.1E+08	1.1E+08	ox2_bound:88	Nqo1	NM_008706	NA	NA	PROMOTER
chr8	1.1E+08	1.1E+08	ox2_bound:88	Dhx38	NM_178380	Txnl4b	NM_175646	DIVERGENT
chr8	1.1E+08	1.1E+08	ox2_bound:88	2400003C14Rik	NM_028018	NA	NA	INSIDE
chr8	1.1E+08	1.1E+08	ox2_bound:88	Zfp1	NM_001037665	NA	NA	INSIDE
chr8	1.1E+08	1.1E+08	ox2_bound:88	Wwox	NM_019573	NA	NA	PROMOTER
chr8	1.1E+08	1.1E+08	ox2_bound:88	Maf	NM_001025577	NA	NA	INSIDE
chr8	1.2E+08	1.2E+08	ox2_bound:88	Plcg2	NM_172285	NA	NA	PROMOTER
chr8	1.2E+08	1.2E+08	ox2_bound:89	Cdh13	NM_019707	NA	NA	INSIDE
chr8	1.2E+08	1.2E+08	ox2_bound:89	Gse1	NM_198671	NA	NA	PROMOTER
chr8	1.2E+08	1.2E+08	ox2_bound:89	Cox4i1	NM_009941	NA	NA	INSIDE
chr8	1.2E+08	1.2E+08	ox2_bound:89	Cox4i1	NM_009941	NA	NA	INSIDE
chr8	1.2E+08	1.2E+08	ox2_bound:89	Car5a	NM_007608	Banp	NM_016812	DIVERGENT
chr8	1.2E+08	1.2E+08	ox2_bound:89	Spire2	NM_172287	NA	NA	INSIDE
chr8	1.2E+08	1.2E+08	ox2_bound:89	Tubb3	NM_023279	NA	NA	PROMOTER
chr8	1.2E+08	1.2E+08	ox2_bound:89	Tubb3	NM_023279	NA	NA	INSIDE
chr8	1.2E+08	1.2E+08	ox2_bound:89	Rab4a	NM_009003	NA	NA	INSIDE
chr8	1.2E+08	1.2E+08	ox2_bound:89	4933403G14Rik	NM_028908	NA	NA	PROMOTER
chr8	1.3E+08	1.3E+08	ox2_bound:90	2610044O15Rik	NM_153780	NA	NA	PROMOTER
chr9	4711313	4712169	ox2_bound:90	Gria4	NM_019691	NA	NA	INSIDE
chr9	1.4E+07	1.4E+07	ox2_bound:90	Sesn3	NM_030261	NA	NA	PROMOTER
chr9	1.9E+07	1.9E+07	ox2_bound:90	Zfp75	NM_172918	NA	NA	INSIDE
chr9	2.1E+07	2.1E+07	ox2_bound:90	Edg5	NM_010333	NA	NA	PROMOTER

chr9	2.1E+07	2.1E+07	ox2_bound:90	Tmed1	NM_010744	NA	NA	PROMOTER
chr9	2.5E+07	2.5E+07	ox2_bound:90	Tbx20	NM_020496	NA	NA	PROMOTER
chr9	2.5E+07	2.5E+07	ox2_bound:90	Tbx20	NM_020496	NA	NA	PROMOTER
chr9	2.7E+07	2.7E+07	ox2_bound:90	Acad8	NM_025862	Thyn1	NM_144543	DIVERGENT
chr9	3.2E+07	3.2E+07	ox2_bound:90	Fli1	NM_008026	NA	NA	PROMOTER
chr9	3.7E+07	3.7E+07	ox2_bound:91	BC024479	NM_146222	NA	NA	PROMOTER
chr9	4.3E+07	4.3E+07	ox2_bound:91	Tmem136	NM_001034863	NA	NA	INSIDE
chr9	4.3E+07	4.3E+07	ox2_bound:91	Pou2f3	NM_011139	NA	NA	PROMOTER
chr9	4.3E+07	4.3E+07	ox2_bound:91	D9Ucla1	NM_178644	NA	NA	PROMOTER
chr9	4.4E+07	4.4E+07	ox2_bound:91	Pvrl1	NM_021424	NA	NA	PROMOTER
chr9	4.4E+07	4.4E+07	ox2_bound:91	Tmem24	NM_027909	Dpagt1	NM_007875	DIVERGENT
chr9	4.4E+07	4.4E+07	ox2_bound:91	Dpagt1	NM_007875	NA	NA	INSIDE
chr9	4.5E+07	4.5E+07	ox2_bound:91	Atp5l	NM_013795	NA	NA	PROMOTER
chr9	4.5E+07	4.5E+07	ox2_bound:91	Amica1	NM_001005421	NA	NA	PROMOTER
chr9	4.9E+07	4.9E+07	ox2_bound:91	Zw10	NM_012039	NA	NA	PROMOTER
chr9	4.9E+07	4.9E+07	ox2_bound:92	Zw10	NM_012039	NA	NA	PROMOTER
chr9	5E+07	5E+07	ox2_bound:92	Ncam1	NM_010875	NA	NA	INSIDE
chr9	5E+07	5E+07	ox2_bound:92	1600029D21Rik	NM_029639	NA	NA	INSIDE
chr9	5.1E+07	5.1E+07	ox2_bound:92	Dixdc1	NM_178118	NA	NA	INSIDE
chr9	5.1E+07	5.1E+07	ox2_bound:92	Dixdc1	NM_178118	NA	NA	PROMOTER
chr9	5.5E+07	5.5E+07	ox2_bound:92	Acsbg1	NM_053178	NA	NA	PROMOTER
chr9	5.6E+07	5.6E+07	ox2_bound:92	C230081A13Rik	NM_172924	Hmg20a	NM_025812	DIVERGENT
chr9	6E+07	6E+07	ox2_bound:92	Pkm2	NM_011099	NA	NA	INSIDE
chr9	6E+07	6E+07	ox2_bound:92	Pkm2	NM_011099	NA	NA	INSIDE
chr9	6.1E+07	6.1E+07	ox2_bound:92	Tle3	NM_009389	NA	NA	PROMOTER
chr9	6.1E+07	6.1E+07	ox2_bound:93	Tle3	NM_009389	NA	NA	PROMOTER
chr9	6.2E+07	6.2E+07	ox2_bound:93	Anp32a	NM_009672	NA	NA	PROMOTER
chr9	6.3E+07	6.3E+07	ox2_bound:93	Fem1b	NM_010193	NA	NA	PROMOTER
chr9	6.3E+07	6.3E+07	ox2_bound:93	Lbxcor1	NM_172446	NA	NA	INSIDE
chr9	6.4E+07	6.4E+07	ox2_bound:93	Snapc5	NM_183316	NA	NA	PROMOTER
chr9	6.4E+07	6.4E+07	ox2_bound:93	AV340375	NM_172519	NA	NA	INSIDE
chr9	6.6E+07	6.6E+07	ox2_bound:93	Plekhq1	NM_153119	AI449441	NM_172453	DIVERGENT
chr9	7E+07	7E+07	ox2_bound:93	Foxb1	NM_022378	NA	NA	INSIDE
chr9	7E+07	7E+07	ox2_bound:93	Foxb1	NM_022378	NA	NA	PROMOTER
chr9	7.3E+07	7.3E+07	ox2_bound:93	Nedd4	NM_010890	NA	NA	INSIDE
chr9	7.3E+07	7.3E+07	ox2_bound:94	BC003885	NM_198609	NA	NA	PROMOTER
chr9	7.5E+07	7.5E+07	ox2_bound:94	BC023444	BC023444	NA	NA	Unknown
chr9	7.5E+07	7.5E+07	ox2_bound:94	Gnb5	NM_010313	NA	NA	PROMOTER
chr9	7.8E+07	7.8E+07	ox2_bound:94	Gsta4	NM_010357	NA	NA	PROMOTER
chr9	7.8E+07	7.8E+07	ox2_bound:94	Gsta4	NM_010357	NA	NA	PROMOTER
chr9	7.8E+07	7.8E+07	ox2_bound:94	Dppa5	NM_025274	NA	NA	PROMOTER
chr9	7.9E+07	7.9E+07	ox2_bound:94	Cd109	NM_153098	NA	NA	PROMOTER
chr9	8E+07	8E+07	ox2_bound:94	Col12a1	NM_007730	NA	NA	INSIDE
chr9	8.9E+07	8.9E+07	ox2_bound:94	NSMUST000000937	MUST0000009	NA	NA	Unknown
chr9	8.9E+07	8.9E+07	ox2_bound:94	NSMUST000000937	MUST0000009	NA	NA	Unknown
chr9	9E+07	9E+07	ox2_bound:95	Rasgrf1	NM_001039655	NA	NA	PROMOTER
chr9	9E+07	9E+07	ox2_bound:95	Tbc1d2b	NM_194334	NA	NA	PROMOTER
chr9	9.2E+07	9.2E+07	ox2_bound:95	BC002017	BC002017	NA	NA	Unknown
chr9	9.4E+07	9.4E+07	ox2_bound:95	1190002N15Rik	NM_001033145	NA	NA	INSIDE
chr9	9.4E+07	9.4E+07	ox2_bound:95	Slc9a9	NM_177909	NA	NA	PROMOTER
chr9	9.4E+07	9.4E+07	ox2_bound:95	Slc9a9	NM_177909	NA	NA	INSIDE
chr9	9.6E+07	9.6E+07	ox2_bound:95	BC043934	NM_177770	NA	NA	INSIDE
chr9	9.6E+07	9.6E+07	ox2_bound:95	Zbtb38	NM_175537	NA	NA	INSIDE
chr9	9.7E+07	9.7E+07	ox2_bound:95	Slc25a36	NM_138756	NA	NA	PROMOTER
chr9	1E+08	1E+08	ox2_bound:95	Stag1	NM_009282	NA	NA	PROMOTER
chr9	1E+08	1E+08	ox2_bound:96	Stag1	NM_009282	NA	NA	PROMOTER
chr9	1.1E+08	1.1E+08	ox2_bound:96	Rpl29	NM_009082	NA	NA	INSIDE
chr9	1.1E+08	1.1E+08	ox2_bound:96	Tex264	NM_011573	NA	NA	PROMOTER
chr9	1.1E+08	1.1E+08	ox2_bound:96	Zmynd10	NM_053253	NA	NA	INSIDE
chr9	1.1E+08	1.1E+08	ox2_bound:96	Gnat1	NM_008140	NA	NA	INSIDE
chr9	1.1E+08	1.1E+08	ox2_bound:96	Gnat1	NM_008140	NA	NA	INSIDE
chr9	1.1E+08	1.1E+08	ox2_bound:96	Camkv	NM_145621	NA	NA	INSIDE
chr9	1.1E+08	1.1E+08	ox2_bound:96	Ihpk1	NM_013785	NA	NA	PROMOTER
chr9	1.1E+08	1.1E+08	ox2_bound:96	Amt	NM_001013814	NA	NA	PROMOTER
chr9	1.1E+08	1.1E+08	ox2_bound:96	1700102P08Rik	NM_053216	NA	NA	PROMOTER

chr9	1.1E+08	1.1E+08	ox2_bound:97	Celsr3	NM_080437	NA	NA	PROMOTER
chr9	1.1E+08	1.1E+08	ox2_bound:97	Tdgf1	NM_011562	Lrrc2	NM_028838	DIVERGENT
chr9	1.1E+08	1.1E+08	ox2_bound:97	Lrrc2	NM_028838	NA	NA	INSIDE
chr9	1.1E+08	1.1E+08	ox2_bound:97	Arpp21	NM_033264	NA	NA	INSIDE
chr9	1.1E+08	1.1E+08	ox2_bound:97	Cnot10	NM_153585	NA	NA	PROMOTER
chr9	1.2E+08	1.2E+08	ox2_bound:97	Eomes	NM_010136	NA	NA	PROMOTER
chr9	1.2E+08	1.2E+08	ox2_bound:97	Itga9	NM_133721	NA	NA	INSIDE
chr9	1.2E+08	1.2E+08	ox2_bound:97	BC060645	BC060645	NA	NA	Unknown
chr9	1.2E+08	1.2E+08	ox2_bound:97	Mobp	NM_001039365	NA	NA	INSIDE
chr9	1.2E+08	1.2E+08	ox2_bound:97	Zfp105	NM_009544	NA	NA	INSIDE
chr9	1.2E+08	1.2E+08	ox2_bound:98	Tmem42	NM_025339	NA	NA	PROMOTER
chr1	4521461	4522150	ox2_bound:98	Mtrf1l	NM_175374	NA	NA	PROMOTER
chr1	6078900	6079534	ox2_bound:98	Akap12	NM_031185	NA	NA	INSIDE
chr1	8585796	8586731	ox2_bound:98	Sash1	NM_175155	NA	NA	PROMOTER
chr1	8588747	8589372	ox2_bound:98	Sash1	NM_175155	NA	NA	PROMOTER
chr1	8589806	8590306	ox2_bound:98	Sash1	NM_175155	NA	NA	PROMOTER
chr1	1.4E+07	1.4E+07	ox2_bound:98	1110059P08Rik	NM_025418	NA	NA	INSIDE
chr1	1.7E+07	1.7E+07	ox2_bound:98	Cited2	NM_010828	NA	NA	PROMOTER
chr1	1.8E+07	1.8E+07	ox2_bound:98	BC030842	BC030842	NA	NA	Unknown
chr1	1.9E+07	1.9E+07	ox2_bound:98	Olig3	NM_053008	NA	NA	PROMOTER
chr1	2.1E+07	2.1E+07	ox2_bound:99	Ahi1	NM_026203	NA	NA	PROMOTER
chr1	2.4E+07	2.4E+07	ox2_bound:99	Rps12	NM_011295	NA	NA	PROMOTER
chr1	2.4E+07	2.4E+07	ox2_bound:99	Ctgf	NM_010217	NA	NA	PROMOTER
chr1	2.5E+07	2.5E+07	ox2_bound:99	Enpp3	NM_134005	NA	NA	INSIDE
chr1	2.9E+07	2.9E+07	ox2_bound:99	6330407J23Rik	NM_026138	NA	NA	PROMOTER
chr1	3.7E+07	3.7E+07	ox2_bound:99	Marcks	NM_008538	6930403N24Ri	NM_177177	DIVERGENT
chr1	4E+07	4E+07	ox2_bound:99	Bxdc1	NM_023323	NA	NA	INSIDE
chr1	4E+07	4E+07	ox2_bound:99	2410016F19Rik	NM_026113	NA	NA	PROMOTER
chr1	4E+07	4E+07	ox2_bound:99	Cdc2l6	NM_198164	NA	NA	PROMOTER
chr1	4.1E+07	4.1E+07	ox2_bound:99	Wasf1	NM_031877	NA	NA	PROMOTER
chr1	4.1E+07	4.1E+07	ox2_bound:10(	Mical1	NM_138315	NA	NA	INSIDE
chr1	4.3E+07	4.3E+07	ox2_bound:10(	AK122525	NM_199028	NA	NA	PROMOTER
chr1	4.3E+07	4.3E+07	ox2_bound:10(	Cd24a	NM_009846	NA	NA	INSIDE
chr1	4.3E+07	4.3E+07	ox2_bound:10(	Cd24a	NM_009846	NA	NA	INSIDE
chr1	4.4E+07	4.4E+07	ox2_bound:10(	Prdm1	NM_007548	NA	NA	PROMOTER
chr1	4.5E+07	4.5E+07	ox2_bound:10(	Lin28b	NM_001031772	NA	NA	INSIDE
chr1	5.1E+07	5.1E+07	ox2_bound:10(	Sim1	NM_011376	NA	NA	PROMOTER
chr1	5.6E+07	5.6E+07	ox2_bound:10(	Gja1	NM_010288	NA	NA	PROMOTER
chr1	5.6E+07	5.6E+07	ox2_bound:10(	Gja1	NM_010288	NA	NA	PROMOTER
chr1	5.6E+07	5.6E+07	ox2_bound:10(	Gja1	NM_010288	NA	NA	PROMOTER
chr1	6E+07	6E+07	ox2_bound:101	Unc5b	NM_029770	NA	NA	INSIDE
chr1	6.1E+07	6.1E+07	ox2_bound:101	Nodal	NM_013611	NA	NA	PROMOTER
chr1	6.1E+07	6.1E+07	ox2_bound:101	Nodal	NM_013611	NA	NA	PROMOTER
chr1	6.1E+07	6.1E+07	ox2_bound:101	Nodal	NM_013611	NA	NA	PROMOTER
chr1	6.1E+07	6.1E+07	ox2_bound:101	H2afy2	NM_207000	NA	NA	INSIDE
chr1	6.2E+07	6.2E+07	ox2_bound:101	Tspan15	NM_197996	NA	NA	PROMOTER
chr1	6.4E+07	6.4E+07	ox2_bound:101	Lrrtm3	NM_178678	NA	NA	PROMOTER
chr1	6.7E+07	6.7E+07	ox2_bound:101	D10Ucla1	NM_178606	NA	NA	INSIDE
chr1	6.7E+07	6.7E+07	ox2_bound:101	D10Ucla1	NM_178606	NA	NA	PROMOTER
chr1	6.7E+07	6.7E+07	ox2_bound:101	D10Ucla1	NM_178606	NA	NA	PROMOTER
chr1	6.7E+07	6.7E+07	ox2_bound:102	D10Ucla1	NM_178606	NA	NA	PROMOTER
chr1	6.8E+07	6.8E+07	ox2_bound:102	Arid5b	NM_023598	NA	NA	PROMOTER
chr1	7E+07	7E+07	ox2_bound:102	Ank3	NM_009670	NA	NA	INSIDE
chr1	7E+07	7E+07	ox2_bound:102	Phyhipl	NM_178621	NA	NA	INSIDE
chr1	7.2E+07	7.2E+07	ox2_bound:102	Zwint	NM_025635	NA	NA	PROMOTER
chr1	7.2E+07	7.2E+07	ox2_bound:102	Zwint	NM_025635	NA	NA	INSIDE
chr1	7.5E+07	7.5E+07	ox2_bound:102	Ggtla1	NM_011820	NA	NA	PROMOTER
chr1	7.6E+07	7.6E+07	ox2_bound:102	Gm867	NM_001037714	NA	NA	INSIDE
chr1	7.6E+07	7.6E+07	ox2_bound:102	Gm867	NM_001037714	NA	NM_009514	DIVERGENT
chr1	7.6E+07	7.6E+07	ox2_bound:102	Ftcd	NM_080845	NA	NA	PROMOTER
chr1	7.8E+07	7.8E+07	ox2_bound:103	Aire	NM_009646	Dnmt3l	NM_019448	DIVERGENT
chr1	8E+07	8E+07	ox2_bound:103	Thrap5	NM_198107	NA	NA	PROMOTER
chr1	8E+07	8E+07	ox2_bound:103	Midn	NM_021565	NA	NA	INSIDE
chr1	8E+07	8E+07	ox2_bound:103	Ndufs7	NM_029272	NA	NA	PROMOTER
chr1	8E+07	8E+07	ox2_bound:103	Tcfe2a	NM_011548	NA	NA	PROMOTER

chr1	8.1E+07	8.1E+07	ox2_bound:103	Atcay	NM_178662	NA	NA	INSIDE
chr1	8.1E+07	8.1E+07	ox2_bound:103	Tle2	NM_019725	NA	NA	PROMOTER
chr1	8.1E+07	8.1E+07	ox2_bound:103	Sirt6	NM_181586	Ankrd24	NA	INSIDE
chr1	8.4E+07	8.4E+07	ox2_bound:103	Rfx4	NM_001024918	NA	NA	PROMOTER
chr1	8.4E+07	8.4E+07	ox2_bound:103	Rfx4	NM_001024918	NA	NA	INSIDE
chr1	8.4E+07	8.4E+07	ox2_bound:104	Rfx4	NM_001024918	NA	NA	INSIDE
chr1	8.4E+07	8.4E+07	ox2_bound:104	Rfx4	NM_001024918	NA	NA	INSIDE
chr1	8.4E+07	8.4E+07	ox2_bound:104	Rfx4	NM_027689	NA	NA	PROMOTER
chr1	8.4E+07	8.4E+07	ox2_bound:104	Rfx4	NM_027689	NA	NA	INSIDE
chr1	8.4E+07	8.4E+07	ox2_bound:104	Ric8b	NM_183172	NA	NA	PROMOTER
chr1	8.6E+07	8.6E+07	ox2_bound:104	Bpil2	NM_177772	Fbxo7	NM_153195	DIVERGENT
chr1	8.7E+07	8.7E+07	ox2_bound:104	Ascl1	NM_008553	NA	NA	PROMOTER
chr1	8.7E+07	8.7E+07	ox2_bound:104	Igf1	NM_010512	NA	NA	PROMOTER
chr1	8.8E+07	8.8E+07	ox2_bound:104	Spic	NM_011461	NA	NA	PROMOTER
chr1	8.9E+07	8.9E+07	ox2_bound:104	Tmem16d	NM_178773	NA	NA	INSIDE
chr1	9.3E+07	9.3E+07	ox2_bound:105	Ccdc38	NM_175488	NA	NA	INSIDE
chr1	9.3E+07	9.3E+07	ox2_bound:105	Usp44	NM_183199	NA	NA	PROMOTER
chr1	9.5E+07	9.5E+07	ox2_bound:105	Cradd	NM_009950	NA	NA	INSIDE
chr1	9.5E+07	9.5E+07	ox2_bound:105	Socs2	NM_007706	NA	NA	INSIDE
chr1	9.5E+07	9.5E+07	ox2_bound:105	Socs2	NM_007706	NA	NA	INSIDE
chr1	9.5E+07	9.5E+07	ox2_bound:105	Nudt4	NM_027722	NA	NA	PROMOTER
chr1	9.9E+07	9.9E+07	ox2_bound:105	Dusp6	NM_026268	NA	NA	PROMOTER
chr1	9.9E+07	9.9E+07	ox2_bound:105	Dusp6	NM_026268	NA	NA	INSIDE
chr1	9.9E+07	9.9E+07	ox2_bound:105	B530045E10Rik	NM_177302	NA	NA	INSIDE
chr1	1E+08	1E+08	ox2_bound:105	Mgat4c	NM_026243	NA	NA	PROMOTER
chr1	1E+08	1E+08	ox2_bound:106	Cart1	NM_172553	NA	NA	INSIDE
chr1	1E+08	1E+08	ox2_bound:106	Slc6a15	NM_175328	NA	NA	INSIDE
chr1	1.1E+08	1.1E+08	ox2_bound:106	Thap2	NM_025780	NA	NA	INSIDE
chr1	1.2E+08	1.2E+08	ox2_bound:106	Frs2	NM_177798	NA	NA	PROMOTER
chr1	1.2E+08	1.2E+08	ox2_bound:106	Irak3	NM_028679	Tmbim4	NM_026617	DIVERGENT
chr1	1.2E+08	1.2E+08	ox2_bound:106	Hmga2	NM_178057	NA	NA	INSIDE
chr1	1.3E+08	1.3E+08	ox2_bound:106	4632413K17Rik	NM_177614	NA	NA	PROMOTER
chr1	1.3E+08	1.3E+08	ox2_bound:106	Kif5a	NM_008447	Dctn2	NM_027151	DIVERGENT
chr1	1.3E+08	1.3E+08	ox2_bound:106	Nxph4	NM_183297	NA	NA	PROMOTER
chr1	1.3E+08	1.3E+08	ox2_bound:106	Il23a	NM_031252	Usp52	NM_133992	DIVERGENT
chr1	1.3E+08	1.3E+08	ox2_bound:107	Rpl41	NM_018860	NA	NA	INSIDE
chr1	1.3E+08	1.3E+08	ox2_bound:107	Rps26	NM_013765	NA	NA	PROMOTER
chr1	1.3E+08	1.3E+08	ox2_bound:107	Dgka	NM_016811	Wibg	NM_030100	DIVERGENT
chr1	3244576	3245076	ox2_bound:107	Zfp278	NM_019574	NA	NA	INSIDE
chr1	3915769	3916269	ox2_bound:107	Pes1	NM_022889	NA	NA	INSIDE
chr1	4656808	4657536	ox2_bound:107	Zmat5	NM_026015	NA	NA	INSIDE
chr1	7166409	7167017	ox2_bound:107	Igfbp3	NM_008343	NA	NA	PROMOTER
chr1	9067309	9067809	ox2_bound:107	Upp1	NM_009477	NA	NA	PROMOTER
chr1	9067943	9068443	ox2_bound:107	Upp1	NM_009477	NA	NA	PROMOTER
chr1	9069065	9069947	ox2_bound:107	Upp1	NM_009477	NA	NA	PROMOTER
chr1	9071367	9072240	ox2_bound:108	Upp1	NM_009477	NA	NA	INSIDE
chr1	1.2E+07	1.2E+07	ox2_bound:108	Cobl	NM_172496	NA	NA	PROMOTER
chr1	1.9E+07	1.9E+07	ox2_bound:108	Meis1	NM_010789	NA	NA	PROMOTER
chr1	2E+07	2E+07	ox2_bound:108	Spred2	NM_033523	NA	NA	INSIDE
chr1	2E+07	2E+07	ox2_bound:108	Slc1a4	NM_018861	NA	NA	PROMOTER
chr1	2E+07	2E+07	ox2_bound:108	Sertad2	NM_021372	NA	NA	PROMOTER
chr1	2E+07	2E+07	ox2_bound:108	Sertad2	NM_021372	NA	NA	PROMOTER
chr1	2.2E+07	2.2E+07	ox2_bound:108	Otx1	NM_011023	NA	NA	INSIDE
chr1	2.2E+07	2.2E+07	ox2_bound:108	Otx1	NM_011023	NA	NA	PROMOTER
chr1	2.3E+07	2.3E+07	ox2_bound:108	Xpo1	NM_001035226	NA	NA	INSIDE
chr1	2.4E+07	2.4E+07	ox2_bound:109	4933435A13Rik	NM_028304	NA	NA	INSIDE
chr1	2.4E+07	2.4E+07	ox2_bound:109	A830031A19Rik	NM_207251	Bcl11a	NM_016707	DIVERGENT
chr1	2.9E+07	2.9E+07	ox2_bound:109	Ccdc85a	NM_181577	NA	NA	INSIDE
chr1	3E+07	3E+07	ox2_bound:109	Rtn4	NM_024226	NA	NA	PROMOTER
chr1	3.1E+07	3.1E+07	ox2_bound:109	2510006C20Rik	NM_026527	NA	NA	PROMOTER
chr1	3.2E+07	3.2E+07	ox2_bound:109	Nsg2	NM_008741	NA	NA	INSIDE
chr1	3.3E+07	3.3E+07	ox2_bound:109	Fgf18	NM_008005	NA	NA	INSIDE
chr1	3.4E+07	3.4E+07	ox2_bound:109	MGC99845	NM_001025382	NA	NA	INSIDE
chr1	4.1E+07	4.1E+07	ox2_bound:109	Nudcd2	NM_026023	NA	NA	INSIDE
chr1	4.5E+07	4.5E+07	ox2_bound:109	Ebf1	NM_007897	NA	NA	PROMOTER

chr1	4.6E+07	4.6E+07	ox2_bound:110	Sox30	NM_173384	NA	NA	PROMOTER
chr1	4.9E+07	4.9E+07	ox2_bound:110	Irgm	NM_008326	NA	NA	INSIDE
chr1	4.9E+07	4.9E+07	ox2_bound:110	Zfp62	NM_001024846	NA	NA	INSIDE
chr1	5E+07	5E+07	ox2_bound:110	Scgb3a1	NM_054037	NA	NA	PROMOTER
chr1	5E+07	5E+07	ox2_bound:110	Canx	NM_007597	NA	NA	PROMOTER
chr1	5E+07	5E+07	ox2_bound:110	Hnrph1	NM_021510	NA	NA	PROMOTER
chr1	5.1E+07	5.1E+07	ox2_bound:110	Zfp2	NM_178447	NA	NA	INSIDE
chr1	5.2E+07	5.2E+07	ox2_bound:110	Rmnd5b	NM_025346	NA	NA	PROMOTER
chr1	5.2E+07	5.2E+07	ox2_bound:110	D930048N14Rik	NM_175289	NA	NA	PROMOTER
chr1	5.2E+07	5.2E+07	ox2_bound:110	Ube2b	NM_009458	Cdkl3	NM_153785	DIVERGENT
chr1	5.2E+07	5.2E+07	ox2_bound:111	Tcf7	NM_009331	NA	NA	PROMOTER
chr1	5.2E+07	5.2E+07	ox2_bound:111	Vdac1	NM_011694	NA	NA	PROMOTER
chr1	5.3E+07	5.3E+07	ox2_bound:111	Aff4	NM_033565	NA	NA	INSIDE
chr1	5.3E+07	5.3E+07	ox2_bound:111	Sept8	NM_033144	NA	NA	INSIDE
chr1	5.8E+07	5.8E+07	ox2_bound:111	Zfp692	NM_182996	NA	NA	PROMOTER
chr1	6E+07	6E+07	ox2_bound:111	Flcn	NM_146018	NA	NA	PROMOTER
chr1	6.1E+07	6.1E+07	ox2_bound:111	Llgl1	NM_008502	NA	NA	PROMOTER
chr1	6.1E+07	6.1E+07	ox2_bound:111	Top3a	NM_009410	Smcr8	NM_175491	DIVERGENT
chr1	6.1E+07	6.1E+07	ox2_bound:111	Aldh3a2	NM_007437	NA	NA	INSIDE
chr1	6.3E+07	6.3E+07	ox2_bound:111	Ubb	NM_011664	NA	NA	PROMOTER
chr1	6.3E+07	6.3E+07	ox2_bound:112	Fbxw10	NM_001033669	NA	NA	INSIDE
chr1	6.4E+07	6.4E+07	ox2_bound:112	Hs3st3b1	NM_018805	NA	NA	PROMOTER
chr1	6.7E+07	6.7E+07	ox2_bound:112	A730055C05Rik	NM_177392	NA	NA	PROMOTER
chr1	6.7E+07	6.7E+07	ox2_bound:112	A730055C05Rik	NM_177392	NA	NA	PROMOTER
chr1	6.8E+07	6.8E+07	ox2_bound:112	Usp43	NM_173754	NA	NA	PROMOTER
chr1	6.9E+07	6.9E+07	ox2_bound:112	Aurkb	NM_011496	NA	NA	PROMOTER
chr1	6.9E+07	6.9E+07	ox2_bound:112	Aloxe3	NM_011786	NA	NA	PROMOTER
chr1	6.9E+07	6.9E+07	ox2_bound:112	Trappc1	NM_001024206	NA	NA	INSIDE
chr1	6.9E+07	6.9E+07	ox2_bound:112	Jmjd3	NM_001017426	NA	NA	PROMOTER
chr1	7E+07	7E+07	ox2_bound:112	Trp53	NM_011640	NA	NA	INSIDE
chr1	7E+07	7E+07	ox2_bound:113	Cd68	NM_009853	NA	NA	PROMOTER
chr1	7E+07	7E+07	ox2_bound:113	Tnfsf13	NM_023517	NA	NA	INSIDE
chr1	7E+07	7E+07	ox2_bound:113	2810408A11Rik	NM_027419	NA	NA	INSIDE
chr1	7E+07	7E+07	ox2_bound:113	Gabarap	NM_019749	NA	NA	INSIDE
chr1	7E+07	7E+07	ox2_bound:113	Pelp1	NM_029231	NA	NA	PROMOTER
chr1	7.3E+07	7.3E+07	ox2_bound:113	Ube2g1	NM_025985	NA	NA	INSIDE
chr1	7.6E+07	7.6E+07	ox2_bound:113	Slc43a2	NM_173388	NA	NA	PROMOTER
chr1	7.8E+07	7.8E+07	ox2_bound:113	Nufip2	NM_001024205	NA	NA	PROMOTER
chr1	7.8E+07	7.8E+07	ox2_bound:113	Myo18a	NM_011586	NA	NA	PROMOTER
chr1	7.8E+07	7.8E+07	ox2_bound:113	Pipox	NM_008952	NA	NA	PROMOTER
chr1	7.8E+07	7.8E+07	ox2_bound:114	Sez6	NM_021286	NA	NA	PROMOTER
chr1	7.8E+07	7.8E+07	ox2_bound:114	Phf12	NM_174852	NA	NA	PROMOTER
chr1	7.9E+07	7.9E+07	ox2_bound:114	Wsb1	NM_019653	NA	NA	INSIDE
chr1	8.5E+07	8.5E+07	ox2_bound:114	Lhx1	NM_008498	NA	NA	INSIDE
chr1	8.7E+07	8.7E+07	ox2_bound:114	Cltc	NM_001003908	NA	NA	INSIDE
chr1	8.7E+07	8.7E+07	ox2_bound:114	Cltc	NM_001003908	NA	NA	PROMOTER
chr1	8.7E+07	8.7E+07	ox2_bound:114	Gdpd1	NM_025638	NA	NA	PROMOTER
chr1	8.7E+07	8.7E+07	ox2_bound:114	mmu-mir-301	mmu-mir-301	NA	NA	PROMOTER
chr1	8.8E+07	8.8E+07	ox2_bound:114	Mrps23	NM_024174	NA	NA	PROMOTER
chr1	8.9E+07	8.9E+07	ox2_bound:114	BC065135	BC065135	NA	NA	Unknown
chr1	8.9E+07	8.9E+07	ox2_bound:115	Trim25	NM_009546	NA	NA	PROMOTER
chr1	9E+07	9E+07	ox2_bound:115	Tmem100	NM_026433	NA	NA	INSIDE
chr1	9.1E+07	9.1E+07	ox2_bound:115	Hlf	NM_172563	NA	NA	PROMOTER
chr1	9.4E+07	9.4E+07	ox2_bound:115	Nme1	NM_008704	NA	NA	INSIDE
chr1	9.4E+07	9.4E+07	ox2_bound:115	Spag9	NM_001025428	NA	NA	INSIDE
chr1	9.5E+07	9.5E+07	ox2_bound:115	Myst2	NM_177619	NA	NA	PROMOTER
chr1	9.5E+07	9.5E+07	ox2_bound:115	Myst2	NM_177619	NA	NA	PROMOTER
chr1	9.6E+07	9.6E+07	ox2_bound:115	Nxph3	NM_130858	NA	NA	PROMOTER
chr1	9.6E+07	9.6E+07	ox2_bound:115	Ngfr	NM_033217	NA	NA	INSIDE
chr1	9.6E+07	9.6E+07	ox2_bound:115	Phb	NM_008831	NA	NA	PROMOTER
chr1	9.6E+07	9.6E+07	ox2_bound:116	LOC544809	NM_001024710	NA	NA	PROMOTER
chr1	9.6E+07	9.6E+07	ox2_bound:116	Hoxb13	NM_008267	NA	NA	PROMOTER
chr1	9.6E+07	9.6E+07	ox2_bound:116	Hoxb13	NM_008267	NA	NA	PROMOTER
chr1	9.6E+07	9.6E+07	ox2_bound:116	Hoxb5	NM_008268	NA	NA	PROMOTER
chr1	9.6E+07	9.6E+07	ox2_bound:116	mmu-mir-10a	mmu-mir-10a	NA	NA	PROMOTER

chr1	9.6E+07	9.6E+07	ox2_bound:116	Hoxb1	NM_008266	NA	NA	PROMOTER
chr1	9.7E+07	9.7E+07	ox2_bound:116	Snx11	NM_028965	Cbx1	NM_007622	DIVERGENT
chr1	9.7E+07	9.7E+07	ox2_bound:116	Npepps	NM_008942	NA	NA	PROMOTER
chr1	9.7E+07	9.7E+07	ox2_bound:116	Mrpl45	NM_025927	NA	NA	PROMOTER
chr1	9.8E+07	9.8E+07	ox2_bound:116	Mllt6	NM_139311	NA	NA	PROMOTER
chr1	9.8E+07	9.8E+07	ox2_bound:117	Lasp1	NM_010688	NA	NA	PROMOTER
chr1	9.8E+07	9.8E+07	ox2_bound:117	Lasp1	NM_010688	NA	NA	INSIDE
chr1	9.8E+07	9.8E+07	ox2_bound:117	Stac2	NM_146028	NA	NA	PROMOTER
chr1	9.8E+07	9.8E+07	ox2_bound:117	Pparbp	NM_134027	Crkrs	NM_026952	DIVERGENT
chr1	9.9E+07	9.9E+07	ox2_bound:117	6330509G02Rik	NM_172946	NA	NA	PROMOTER
chr1	1E+08	1E+08	ox2_bound:117	Krt1-17	NM_010663	NA	NA	PROMOTER
chr1	1E+08	1E+08	ox2_bound:117	Jup	NM_010593	NA	NA	INSIDE
chr1	1E+08	1E+08	ox2_bound:117	Cnp1	NM_009923	NA	NA	PROMOTER
chr1	1E+08	1E+08	ox2_bound:117	Gcn5l2	NM_020004	NA	NA	PROMOTER
chr1	1E+08	1E+08	ox2_bound:117	Stat5a	NM_011488	NA	NA	PROMOTER
chr1	1E+08	1E+08	ox2_bound:118	Stat3	NM_213660	NA	NA	PROMOTER
chr1	1E+08	1E+08	ox2_bound:118	Rnd2	NM_009708	NA	NA	INSIDE
chr1	1E+08	1E+08	ox2_bound:118	Brca1	NM_009764	Nbr1	NA	INSIDE
chr1	1E+08	1E+08	ox2_bound:118	Brca1	NM_009764	NA	NM_008676	DIVERGENT
chr1	1E+08	1E+08	ox2_bound:118	Nbr1	NM_008676	NA	NA	INSIDE
chr1	1E+08	1E+08	ox2_bound:118	Rdm1	NM_025654	NA	NA	PROMOTER
chr1	1E+08	1E+08	ox2_bound:118	Etv4	NM_008815	NA	NA	PROMOTER
chr1	1E+08	1E+08	ox2_bound:118	Etv4	NM_008815	NA	NA	PROMOTER
chr1	1E+08	1E+08	ox2_bound:118	BC030867	NM_153544	NA	NA	PROMOTER
chr1	1E+08	1E+08	ox2_bound:118	BC030867	NM_153544	NA	NA	INSIDE
chr1	1E+08	1E+08	ox2_bound:119	Rap2ip	NM_016759	NA	NA	PROMOTER
chr1	1E+08	1E+08	ox2_bound:119	Fzd2	NM_020510	NA	NA	PROMOTER
chr1	1E+08	1E+08	ox2_bound:119	BC050840	BC050840	NA	NA	Unknown
chr1	1E+08	1E+08	ox2_bound:119	Acbd4	NM_025988	NA	NA	INSIDE
chr1	1E+08	1E+08	ox2_bound:119	Hexim1	NM_138753	NA	NA	PROMOTER
chr1	1E+08	1E+08	ox2_bound:119	Nsf	NM_008740	Arf2	NM_007477	DIVERGENT
chr1	1.1E+08	1.1E+08	ox2_bound:119	2610204L23Rik	NM_026009	Ddx42	NM_028074	DIVERGENT
chr1	1.1E+08	1.1E+08	ox2_bound:119	Pitpnc1	NM_145823	NA	NA	INSIDE
chr1	1.1E+08	1.1E+08	ox2_bound:119	Pitpnc1	NM_145823	NA	NA	INSIDE
chr1	1.1E+08	1.1E+08	ox2_bound:119	Gna13	NM_010303	NA	NA	PROMOTER
chr1	1.1E+08	1.1E+08	ox2_bound:120	Slc16a6	NM_001029842	NA	NA	PROMOTER
chr1	1.1E+08	1.1E+08	ox2_bound:120	Slc39a11	NM_027216	NA	NA	PROMOTER
chr1	1.1E+08	1.1E+08	ox2_bound:120	D11Ertd636e	NM_029794	NA	NA	PROMOTER
chr1	1.2E+08	1.2E+08	ox2_bound:120	Galr2	NM_010254	NA	NA	INSIDE
chr1	1.2E+08	1.2E+08	ox2_bound:120	Sphk1	NM_025367	NA	NA	PROMOTER
chr1	1.2E+08	1.2E+08	ox2_bound:120	Tha1	NM_027919	NA	NA	PROMOTER
chr1	1.2E+08	1.2E+08	ox2_bound:120	Baiap2	NM_001037755	NA	NA	PROMOTER
chr1	1.2E+08	1.2E+08	ox2_bound:120	P4hb	NM_011032	NA	NA	PROMOTER
chr1	8523865	8524705	ox2_bound:120	Rhob	NM_007483	NA	NA	INSIDE
chr1	8947667	8948379	ox2_bound:120	Laptm4a	NM_008640	NA	NA	INSIDE
chr1	9602816	9603316	ox2_bound:121	Osr1	NM_011859	NA	NA	INSIDE
chr1	1.2E+07	1.2E+07	ox2_bound:121	D12Ertd553e	NM_029758	NA	NA	INSIDE
chr1	1.3E+07	1.3E+07	ox2_bound:121	Mycn	NM_008709	NA	NA	PROMOTER
chr1	1.3E+07	1.3E+07	ox2_bound:121	Mycn	NM_008709	NA	NA	PROMOTER
chr1	1.5E+07	1.5E+07	ox2_bound:121	BC058368	BC058368	NA	NA	Unknown
chr1	1.6E+07	1.6E+07	ox2_bound:121	Trib2	NM_144551	NA	NA	INSIDE
chr1	2E+07	2E+07	ox2_bound:121	Ywhaq	NM_011739	NA	NA	PROMOTER
chr1	2.3E+07	2.3E+07	ox2_bound:121	Id2	NM_010496	NA	NA	PROMOTER
chr1	2.6E+07	2.6E+07	ox2_bound:121	Rps7	NM_011300	NA	NA	PROMOTER
chr1	3.2E+07	3.2E+07	ox2_bound:121	Twist1	NM_011658	NA	NA	INSIDE
chr1	3.2E+07	3.2E+07	ox2_bound:122	Hdac9	NM_024124	NA	NA	PROMOTER
chr1	3.3E+07	3.3E+07	ox2_bound:122	Snx13	NM_001014973	NA	NA	PROMOTER
chr1	3.4E+07	3.4E+07	ox2_bound:122	Bzw2	NM_025840	NA	NA	INSIDE
chr1	3.7E+07	3.7E+07	ox2_bound:122	Etv1	NM_007960	NA	NA	PROMOTER
chr1	3.7E+07	3.7E+07	ox2_bound:122	Etv1	NM_007960	NA	NA	INSIDE
chr1	4.9E+07	4.9E+07	ox2_bound:122	6030408C04Rik	NM_001015099	NA	NA	PROMOTER
chr1	4.9E+07	4.9E+07	ox2_bound:122	6030408C04Rik	NM_001015099	NA	NA	INSIDE
chr1	5E+07	5E+07	ox2_bound:122	Coch	NM_007728	NA	NA	INSIDE
chr1	5.1E+07	5.1E+07	ox2_bound:122	Npas3	NM_013780	NA	NA	PROMOTER
chr1	5.1E+07	5.1E+07	ox2_bound:122	Npas3	NM_013780	NA	NA	INSIDE

chr1	5.3E+07	5.3E+07	ox2_bound:123	1810011O16Rik	NM_025456	NA	NA	PROMOTER
chr1	5.3E+07	5.3E+07	ox2_bound:123	Nfkbia	NM_010907	NA	NA	PROMOTER
chr1	5.4E+07	5.4E+07	ox2_bound:123	Titf1	NM_009385	NA	NA	INSIDE
chr1	5.4E+07	5.4E+07	ox2_bound:123	Titf1	NM_009385	NA	NA	INSIDE
chr1	5.5E+07	5.5E+07	ox2_bound:123	Nkx2-9	NM_008701	NA	NA	PROMOTER
chr1	5.5E+07	5.5E+07	ox2_bound:123	Pax9	NM_011041	NA	NA	INSIDE
chr1	6.7E+07	6.7E+07	ox2_bound:123	Klhdc2	NM_027117	NA	NA	INSIDE
chr1	6.9E+07	6.9E+07	ox2_bound:123	Psma3	NM_011184	NA	NA	PROMOTER
chr1	6.9E+07	6.9E+07	ox2_bound:123	Timm9	NM_013896	NA	NA	PROMOTER
chr1	7E+07	7E+07	ox2_bound:123	1200003C05Rik	NM_024205	NA	NA	INSIDE
chr1	7E+07	7E+07	ox2_bound:124	Rtn1	NM_001007596	NA	NA	INSIDE
chr1	7.1E+07	7.1E+07	ox2_bound:124	Mnat1	NM_008612	NA	NA	INSIDE
chr1	7.5E+07	7.5E+07	ox2_bound:124	Max	NM_008558	NA	NA	PROMOTER
chr1	7.8E+07	7.8E+07	ox2_bound:124	Zfp36l1	NM_007564	NA	NA	INSIDE
chr1	7.8E+07	7.8E+07	ox2_bound:124	Zfp36l1	NM_007564	NA	NA	PROMOTER
chr1	7.8E+07	7.8E+07	ox2_bound:124	Zfp36l1	NM_007564	NA	NA	PROMOTER
chr1	7.8E+07	7.8E+07	ox2_bound:124	Actn1	NM_134156	NA	NA	INSIDE
chr1	7.9E+07	7.9E+07	ox2_bound:124	Gm1568	NM_001008423	NA	NA	INSIDE
chr1	8.1E+07	8.1E+07	ox2_bound:124	Dpf3	NM_058212	NA	NA	PROMOTER
chr1	8.2E+07	8.2E+07	ox2_bound:124	Papln	NM_130887	NA	NA	PROMOTER
chr1	8.2E+07	8.2E+07	ox2_bound:125	Acot1	NM_012006	NA	NA	PROMOTER
chr1	8.3E+07	8.3E+07	ox2_bound:125	Abcd4	NM_008992	NA	NA	PROMOTER
chr1	8.3E+07	8.3E+07	ox2_bound:125	7420416P09Rik	NM_001033776	NA	NA	PROMOTER
chr1	8.3E+07	8.3E+07	ox2_bound:125	7420416P09Rik	NM_001033776	NA	NA	PROMOTER
chr1	8.3E+07	8.3E+07	ox2_bound:125	Acyp1	NM_025421	NA	NA	DOWNSTREAM
chr1	8.3E+07	8.3E+07	ox2_bound:125	Fos	NM_010234	NA	NA	PROMOTER
chr1	8.3E+07	8.3E+07	ox2_bound:125	Fos	NM_010234	NA	NA	INSIDE
chr1	8.5E+07	8.5E+07	ox2_bound:125	6430527G18Rik	NM_145836	NA	NA	PROMOTER
chr1	8.5E+07	8.5E+07	ox2_bound:125	2310044G17Rik	NM_173735	NA	NA	PROMOTER
chr1	9.3E+07	9.3E+07	ox2_bound:125	Flrt2	NM_201518	NA	NA	INSIDE
chr1	9.6E+07	9.6E+07	ox2_bound:126	Ptpn21	NM_011877	NA	NA	PROMOTER
chr1	9.8E+07	9.8E+07	ox2_bound:126	Rps6ka5	NM_153587	NA	NA	PROMOTER
chr1	1E+08	1E+08	ox2_bound:126	Itpk1	NM_172584	NA	NA	INSIDE
chr1	1E+08	1E+08	ox2_bound:126	Itpk1	NM_172584	NA	NA	PROMOTER
chr1	1E+08	1E+08	ox2_bound:126	Moap1	NM_022323	NA	NA	PROMOTER
chr1	1E+08	1E+08	ox2_bound:126	Gsc	NM_010351	NA	NA	PROMOTER
chr1	1E+08	1E+08	ox2_bound:126	Tcl1	NM_009337	NA	NA	PROMOTER
chr1	1E+08	1E+08	ox2_bound:126	Tcl1	NM_009337	NA	NA	PROMOTER
chr1	1.1E+08	1.1E+08	ox2_bound:126	Rcor1	NM_198023	NA	NA	PROMOTER
chr1	1.1E+08	1.1E+08	ox2_bound:126	Ckb	NM_021273	NA	NA	INSIDE
chr1	1.2E+08	1.2E+08	ox2_bound:127	Sp8	NM_177082	NA	NA	PROMOTER
chr1	1.2E+08	1.2E+08	ox2_bound:127	Sp8	NM_177082	NA	NA	PROMOTER
chr1	5745679	5746179	ox2_bound:127	Klf6	NM_011803	NA	NA	PROMOTER
chr1	1.3E+07	1.3E+07	ox2_bound:127	Tbce	NM_178337	NA	NA	PROMOTER
chr1	1.7E+07	1.7E+07	ox2_bound:127	2810021B07Rik	NM_025479	NA	NA	INSIDE
chr1	2.1E+07	2.1E+07	ox2_bound:127	Hist1h3h	NM_178206	NA	NA	PROMOTER
chr1	2.1E+07	2.1E+07	ox2_bound:127	Hist1h2bm	NM_178200	NA	NA	PROMOTER
chr1	2.1E+07	2.1E+07	ox2_bound:127	Hist1h4j	NM_178210	NA	NA	PROMOTER
chr1	2.1E+07	2.1E+07	ox2_bound:127	Hist1h4j	NM_178210	NA	NA	DOWNSTREAM
chr1	2.1E+07	2.1E+07	ox2_bound:127	Hist1h4k	NM_178211	NA	NA	DOWNSTREAM
chr1	2.1E+07	2.1E+07	ox2_bound:128	Hist1h1b	NM_020034	NA	NA	PROMOTER
chr1	2.1E+07	2.1E+07	ox2_bound:128	Hist1h3i	NM_178207	NA	NA	PROMOTER
chr1	2.1E+07	2.1E+07	ox2_bound:128	Hist1h3i	NM_178207	NA	NA	PROMOTER
chr1	2.1E+07	2.1E+07	ox2_bound:128	Hist1h2an	NM_178184	Hist1h2bp	NM_178202	DIVERGENT
chr1	2.1E+07	2.1E+07	ox2_bound:128	Hist1h2bp	NM_178202	NA	NA	DOWNSTREAM
chr1	2.1E+07	2.1E+07	ox2_bound:128	Hist1h2bp	NM_178202	NA	NA	DOWNSTREAM
chr1	2.1E+07	2.1E+07	ox2_bound:128	Zfp184	NM_183014	NA	NA	PROMOTER
chr1	2.1E+07	2.1E+07	ox2_bound:128	Hist1h2ah	NM_175659	Hist1h2bk	NA	DOWNSTREAM
chr1	2.1E+07	2.1E+07	ox2_bound:128	Hist1h2ah	NM_175659	NA	NM_175665	DIVERGENT
chr1	2.1E+07	2.1E+07	ox2_bound:128	Hist1h2bk	NM_175665	NA	NA	DOWNSTREAM
chr1	2.1E+07	2.1E+07	ox2_bound:129	Hist1h4i	NM_175656	NA	NA	DOWNSTREAM
chr1	2.1E+07	2.1E+07	ox2_bound:129	Hist1h4i	NM_175656	NA	NA	PROMOTER
chr1	2.1E+07	2.1E+07	ox2_bound:129	Hist1h2ag	NM_178186	Hist1h2bj	NM_178198	DIVERGENT
chr1	2.3E+07	2.3E+07	ox2_bound:129	Abt1	NM_013924	NA	NA	PROMOTER
chr1	2.3E+07	2.3E+07	ox2_bound:129	Btn2a2	NM_175938	NA	NA	PROMOTER

chr1	2.3E+07	2.3E+07	ox2_bound:12	Hist1h4h	NM_153173	NA	NA	PROMOTER
chr1	2.3E+07	2.3E+07	ox2_bound:12	Hist1h4h	NM_153173	NA	NA	PROMOTER
chr1	2.3E+07	2.3E+07	ox2_bound:12	Hist1h2af	NM_175661	NA	NA	PROMOTER
chr1	2.3E+07	2.3E+07	ox2_bound:12	Hist1h2af	NM_175661	NA	NA	PROMOTER
chr1	2.3E+07	2.3E+07	ox2_bound:12	Hist1h3f	NM_013548	NA	NA	INSIDE
chr1	2.3E+07	2.3E+07	ox2_bound:13	Hist1h3h	NM_178206	NA	NA	INSIDE
chr1	2.3E+07	2.3E+07	ox2_bound:13	Hist1h1d	NM_145713	NA	NA	INSIDE
chr1	2.3E+07	2.3E+07	ox2_bound:13	Hist1h3e	NM_178205	NA	NA	PROMOTER
chr1	2.3E+07	2.3E+07	ox2_bound:13	Hist1h3e	NM_178205	NA	NA	PROMOTER
chr1	2.3E+07	2.3E+07	ox2_bound:13	Hist1h2ae	NM_178187	NA	NM_178196	DIVERGENT
chr1	2.3E+07	2.3E+07	ox2_bound:13	Hist1h3h	NM_178206	NA	NA	INSIDE
chr1	2.3E+07	2.3E+07	ox2_bound:13	Hist1h3d	NM_178204	NA	NA	PROMOTER
chr1	2.3E+07	2.3E+07	ox2_bound:13	Hist1h4d	NM_175654	NA	NA	INSIDE
chr1	2.3E+07	2.3E+07	ox2_bound:13	Hist1h2bc	NM_023422	NA	NA	INSIDE
chr1	2.3E+07	2.3E+07	ox2_bound:13	Hist1h3h	NM_178206	NA	NA	INSIDE
chr1	2.3E+07	2.3E+07	ox2_bound:13	Hist1h1c	NM_015786	NA	NA	INSIDE
chr1	2.3E+07	2.3E+07	ox2_bound:13	Hist1h3h	NM_178206	NA	NA	INSIDE
chr1	2.3E+07	2.3E+07	ox2_bound:13	Hist1h2ab	NM_175660	NA	NA	PROMOTER
chr1	2.3E+07	2.3E+07	ox2_bound:13	Hist1h4a	NM_178192	NA	NA	PROMOTER
chr1	2.3E+07	2.3E+07	ox2_bound:13	Hist1h1a	NM_030609	NA	NA	DOWNSTREAM
chr1	2.3E+07	2.3E+07	ox2_bound:13	Scgn	NM_145399	NA	NA	PROMOTER
chr1	2.5E+07	2.5E+07	ox2_bound:13	Vmp	NM_009513	NA	NA	PROMOTER
chr1	3.4E+07	3.4E+07	ox2_bound:13	Tubb2b	NM_023716	NA	NA	PROMOTER
chr1	3.4E+07	3.4E+07	ox2_bound:13	Tubb2b	NM_023716	NA	NA	PROMOTER
chr1	3.4E+07	3.4E+07	ox2_bound:13	Tubb2b	NM_023716	NA	NA	PROMOTER
chr1	4E+07	4E+07	ox2_bound:13	Tcfap2a	NM_011547	NA	NA	INSIDE
chr1	4E+07	4E+07	ox2_bound:13	Gcnt2	NM_008105	NA	NA	PROMOTER
chr1	4E+07	4E+07	ox2_bound:13	Gcnt2	NM_133219	NA	NA	PROMOTER
chr1	4.2E+07	4.2E+07	ox2_bound:13	Edn1	NM_010104	NA	NA	PROMOTER
chr1	4.3E+07	4.3E+07	ox2_bound:13	Rnf182	NM_183204	NA	NA	PROMOTER
chr1	4.4E+07	4.4E+07	ox2_bound:13	Jarid2	NM_021878	NA	NA	PROMOTER
chr1	4.6E+07	4.6E+07	ox2_bound:13	Nup153	NM_175749	NA	NA	PROMOTER
chr1	4.6E+07	4.6E+07	ox2_bound:13	Kif13a	NM_010617	NA	NA	INSIDE
chr1	4.9E+07	4.9E+07	ox2_bound:13	1700022C02Rik	NM_025495	NA	NA	PROMOTER
chr1	5.1E+07	5.1E+07	ox2_bound:13	Shc3	NM_009167	NA	NA	PROMOTER
chr1	5.1E+07	5.1E+07	ox2_bound:13	Gadd45g	NM_011817	NA	NA	INSIDE
chr1	5.3E+07	5.3E+07	ox2_bound:13	Msx2	NM_013601	NA	NA	INSIDE
chr1	5.3E+07	5.3E+07	ox2_bound:13	Sfxn1	NM_027324	NA	NA	PROMOTER
chr1	5.4E+07	5.4E+07	ox2_bound:13	Higd2a	NM_025933	NA	NA	INSIDE
chr1	6E+07	6E+07	ox2_bound:13	Dapk1	NM_029653	NA	NA	INSIDE
chr1	6.1E+07	6.1E+07	ox2_bound:13	Ptch1	NM_008957	NA	NA	PROMOTER
chr1	6.1E+07	6.1E+07	ox2_bound:13	Ptch1	NM_008957	NA	NA	PROMOTER
chr1	6.5E+07	6.5E+07	ox2_bound:13	6820416H06Rik	NM_198322	NA	NA	INSIDE
chr1	6.5E+07	6.5E+07	ox2_bound:13	BC048507	BC048507	NA	NA	Unknown
chr1	7E+07	7E+07	ox2_bound:13	Irx2	NM_010574	NA	NA	INSIDE
chr1	7.2E+07	7.2E+07	ox2_bound:13	Pcsk1	NM_013628	NA	NA	INSIDE
chr1	7.9E+07	7.9E+07	ox2_bound:13	Lysmd3	NM_030257	NA	NA	PROMOTER
chr1	8.1E+07	8.1E+07	ox2_bound:13	mmu-mir-9-2	mmu-mir-9-2	NA	NA	PROMOTER
chr1	8.1E+07	8.1E+07	ox2_bound:13	C130071C03Rik	NM_177100	NA	NA	INSIDE
chr1	8.1E+07	8.1E+07	ox2_bound:13	C130071C03Rik	NM_177100	NA	NA	INSIDE
chr1	8.8E+07	8.8E+07	ox2_bound:13	Rps23	NM_024175	NA	NA	DOWNSTREAM
chr1	9.3E+07	9.3E+07	ox2_bound:13	F2rl1	NM_007974	NA	NA	PROMOTER
chr1	9.4E+07	9.4E+07	ox2_bound:13	Hmgcr	NM_008255	NA	NA	PROMOTER
chr1	9.4E+07	9.4E+07	ox2_bound:13	Hmgcr	NM_008255	NA	NA	PROMOTER
chr1	9.4E+07	9.4E+07	ox2_bound:13	Hexb	NM_010422	NA	NA	INSIDE
chr1	9.7E+07	9.7E+07	ox2_bound:13	Mtap1b	NM_008634	NA	NA	INSIDE
chr1	1E+08	1E+08	ox2_bound:13	2410002O22Rik	NM_025879	NA	NA	INSIDE
chr1	1.1E+08	1.1E+08	ox2_bound:13	Il6st	NM_010560	NA	NA	PROMOTER
chr1	1.1E+08	1.1E+08	ox2_bound:13	mmu-mir-449	mmu-mir-449	NA	NA	PROMOTER
chr1	1.1E+08	1.1E+08	ox2_bound:13	mmu-mir-449	mmu-mir-449	NA	NA	PROMOTER
chr1	1.1E+08	1.1E+08	ox2_bound:13	Ndufs4	NM_010887	NA	NA	PROMOTER
chr1	1.1E+08	1.1E+08	ox2_bound:13	Itga1	NM_001033228	NA	NA	INSIDE
chr1	1.1E+08	1.1E+08	ox2_bound:13	Emb	NM_010330	NA	NA	PROMOTER
chr1	1.1E+08	1.1E+08	ox2_bound:13	Emb	NM_010330	NA	NA	PROMOTER
chr1	5985472	5985972	ox2_bound:13	Pdhb	NM_024221	NA	NA	PROMOTER

chr1	9368570	9369324	ox2_bound:13(	Ptprg	NM_008981	NA	NA	PROMOTER
chr1	1E+07	1E+07	ox2_bound:13(	Zfp312	NM_080433	NA	NA	INSIDE
chr1	1E+07	1E+07	ox2_bound:13(	Zfp312	NM_080433	NA	NA	INSIDE
chr1	1.7E+07	1.7E+07	ox2_bound:13(	Nid2	NM_008695	NA	NA	PROMOTER
chr1	1.8E+07	1.8E+07	ox2_bound:13(	Nudt13	NM_026341	NA	NA	INSIDE
chr1	2E+07	2E+07	ox2_bound:13(	Zfp503	NM_145459	NA	NA	PROMOTER
chr1	2.3E+07	2.3E+07	ox2_bound:13(	Rai17	NM_183208	NA	NA	PROMOTER
chr1	2.4E+07	2.4E+07	ox2_bound:13(	Anxa11	NM_013469	NA	NA	PROMOTER
chr1	2.4E+07	2.4E+07	ox2_bound:13(	Slmap	NM_032008	NA	NA	PROMOTER
chr1	2.4E+07	2.4E+07	ox2_bound:13(	E430028B21Rik	NM_178668	NA	NA	INSIDE
chr1	2.4E+07	2.4E+07	ox2_bound:13'	Hesx1	NM_010420	NA	NA	INSIDE
chr1	2.7E+07	2.7E+07	ox2_bound:13'	Selk	NM_019979	NA	NA	PROMOTER
chr1	3.2E+07	3.2E+07	ox2_bound:13'	Glud1	NM_008133	NA	NA	INSIDE
chr1	3.2E+07	3.2E+07	ox2_bound:13'	Mmrn2	NM_153127	NA	NA	INSIDE
chr1	3.2E+07	3.2E+07	ox2_bound:13'	mmu-mir-346	mmu-mir-346	NA	NA	PROMOTER
chr1	3.8E+07	3.8E+07	ox2_bound:13'	Sh2d4b	NM_177816	NA	NA	INSIDE
chr1	3.8E+07	3.8E+07	ox2_bound:13'	Sh2d4b	NM_177816	NA	NA	INSIDE
chr1	4.1E+07	4.1E+07	ox2_bound:13'	Gnpnat1	NM_019425	NA	NA	INSIDE
chr1	4.2E+07	4.2E+07	ox2_bound:13'	Bmp4	NM_007554	NA	NA	PROMOTER
chr1	4.4E+07	4.4E+07	ox2_bound:13'	Otx2	NM_144841	NA	NA	PROMOTER
chr1	4.4E+07	4.4E+07	ox2_bound:13(	Otx2	NM_144841	NA	NA	PROMOTER
chr1	4.6E+07	4.6E+07	ox2_bound:13(	Rnase9	NM_183032	NA	NA	PROMOTER
chr1	4.6E+07	4.6E+07	ox2_bound:13(	Rnase4	NM_021472	NA	NA	PROMOTER
chr1	4.7E+07	4.7E+07	ox2_bound:13(	Zfp219	NM_027248	NA	NA	PROMOTER
chr1	4.7E+07	4.7E+07	ox2_bound:13(	Hnrpc	NM_016884	Rpgrip1	NM_023879	DIVERGENT
chr1	4.8E+07	4.8E+07	ox2_bound:13(	5730589K01Rik	NM_023434	NA	NA	INSIDE
chr1	4.8E+07	4.8E+07	ox2_bound:13(	Sall2	NM_015772	NA	NA	PROMOTER
chr1	4.9E+07	4.9E+07	ox2_bound:13(	Slc7a7	NM_011405	Mrpl52	NA	INSIDE
chr1	4.9E+07	4.9E+07	ox2_bound:13(	Slc7a7	NM_011405	NA	NA	INSIDE
chr1	4.9E+07	4.9E+07	ox2_bound:13(	Slc7a7	NM_011405	NA	NM_026851	DIVERGENT
chr1	4.9E+07	4.9E+07	ox2_bound:13'	Prmt5	NM_013768	NA	NA	PROMOTER
chr1	5E+07	5E+07	ox2_bound:13'	1500001L15Rik	NM_026890	NA	NA	PROMOTER
chr1	5E+07	5E+07	ox2_bound:13'	Wdr23	NM_133734	NA	NA	INSIDE
chr1	5.1E+07	5.1E+07	ox2_bound:13'	Nfatc4	NM_023699	NA	NA	PROMOTER
chr1	5.4E+07	5.4E+07	ox2_bound:13'	Tmem46	NM_145463	NA	NA	PROMOTER
chr1	5.6E+07	5.6E+07	ox2_bound:13'	Sacs	NM_172809	NA	NA	PROMOTER
chr1	5.6E+07	5.6E+07	ox2_bound:13'	Sacs	NM_172809	NA	NA	INSIDE
chr1	5.7E+07	5.7E+07	ox2_bound:13'	Dleu8	NM_026001	NA	NA	PROMOTER
chr1	5.8E+07	5.8E+07	ox2_bound:13'	Fdft1	NM_010191	NA	NA	PROMOTER
chr1	5.8E+07	5.8E+07	ox2_bound:13'	Tdh	NM_021480	NA	NA	INSIDE
chr1	5.9E+07	5.9E+07	ox2_bound:14(	mmu-mir-124a-1	nmu-mir-124a-	NA	NA	PROMOTER
chr1	5.9E+07	5.9E+07	ox2_bound:14(	mmu-mir-124a-1	nmu-mir-124a-	NA	NA	DOWNSTREAM
chr1	6E+07	6E+07	ox2_bound:14(	Hmbox1	NM_177338	D14Ertd231e	NM_153414	DIVERGENT
chr1	6E+07	6E+07	ox2_bound:14(	Fbxo16	NM_015795	NA	NA	PROMOTER
chr1	6.1E+07	6.1E+07	ox2_bound:14(	Pbk	NM_023209	NA	NA	INSIDE
chr1	6.1E+07	6.1E+07	ox2_bound:14(	Ephx2	NM_007940	NA	NA	INSIDE
chr1	6.2E+07	6.2E+07	ox2_bound:14(	Dpysl2	NM_009955	NA	NA	INSIDE
chr1	6.2E+07	6.2E+07	ox2_bound:14(	Ebf2	NM_010095	NA	NA	PROMOTER
chr1	6.2E+07	6.2E+07	ox2_bound:14(	Ebf2	NM_010095	NA	NA	PROMOTER
chr1	6.2E+07	6.2E+07	ox2_bound:14(	Ebf2	NM_010095	NA	NA	INSIDE
chr1	6.3E+07	6.3E+07	ox2_bound:141	Nefl	NM_010910	NA	NA	PROMOTER
chr1	6.4E+07	6.4E+07	ox2_bound:141	Chmp7	NM_134078	NA	NA	PROMOTER
chr1	6.4E+07	6.4E+07	ox2_bound:141	Chmp7	NM_134078	NA	NA	PROMOTER
chr1	6.5E+07	6.5E+07	ox2_bound:141	Slc39a14	NM_144808	NA	NA	PROMOTER
chr1	6.5E+07	6.5E+07	ox2_bound:141	Epb4.9	NM_013514	NA	NA	PROMOTER
chr1	6.8E+07	6.8E+07	ox2_bound:141	P2ry5	NM_175116	NA	NA	PROMOTER
chr1	6.8E+07	6.8E+07	ox2_bound:141	P2ry5	NM_175116	NA	NA	INSIDE
chr1	7.2E+07	7.2E+07	ox2_bound:141	LOC629678	NM_00103793[illegible]	NA	NA	PROMOTER
chr1	7.4E+07	7.4E+07	ox2_bound:141	Pcdh8	NM_021543	NA	NA	PROMOTER
chr1	7.4E+07	7.4E+07	ox2_bound:141	Pcdh8	NM_021543	NA	NA	PROMOTER
chr1	8.2E+07	8.2E+07	ox2_bound:142	Tdrd3	NM_172605	NA	NA	INSIDE
chr1	1E+08	1E+08	ox2_bound:142	Spry2	NM_011897	NA	NA	PROMOTER
chr1	1.1E+08	1.1E+08	ox2_bound:142	Gpc6	NM_011821	NA	NA	INSIDE
chr1	1.1E+08	1.1E+08	ox2_bound:142	Tgds	NM_029578	Gpr180	NM_021434	DIVERGENT
chr1	1.2E+08	1.2E+08	ox2_bound:142	Slc15a1	NM_053079	NA	NA	PROMOTER

chr1	1.2E+08	1.2E+08	ox2_bound:142	6530402A20	NM_177817	NA	NA	INSIDE
chr1	1.2E+08	1.2E+08	ox2_bound:142	Zic5	NM_022987	Zic2	NM_009574	DIVERGENT
chr1	1.2E+08	1.2E+08	ox2_bound:142	Zic2	NM_009574	NA	NA	INSIDE
chr1	3853269	3853769	ox2_bound:142	Oxct1	NM_024188	NA	NA	PROMOTER
chr1	7639552	7640218	ox2_bound:142	Gdnf	NM_010275	NA	NA	INSIDE
chr1	1.1E+07	1.1E+07	ox2_bound:143	Rai14	NM_030690	NA	NA	PROMOTER
chr1	1.1E+07	1.1E+07	ox2_bound:143	C1qtnf3	NM_030888	NA	NA	INSIDE
chr1	1.1E+07	1.1E+07	ox2_bound:143	C1qtnf3	NM_030888	NA	NA	INSIDE
chr1	1.1E+07	1.1E+07	ox2_bound:143	C1qtnf3	NM_030888	NA	NA	INSIDE
chr1	1.2E+07	1.2E+07	ox2_bound:143	Zfr	NM_011767	NA	NA	PROMOTER
chr1	1.2E+07	1.2E+07	ox2_bound:143	Mtmr12	NM_172958	NA	NA	PROMOTER
chr1	1.2E+07	1.2E+07	ox2_bound:143	Mtmr12	NM_172958	NA	NA	INSIDE
chr1	1.2E+07	1.2E+07	ox2_bound:143	Golph3	NM_025673	NA	NA	INSIDE
chr1	1.3E+07	1.3E+07	ox2_bound:143	Cdh6	NM_007666	NA	NA	PROMOTER
chr1	1.3E+07	1.3E+07	ox2_bound:143	Cdh6	NM_007666	NA	NA	PROMOTER
chr1	2.5E+07	2.5E+07	ox2_bound:144	Basp1	NM_027395	NA	NA	PROMOTER
chr1	2.6E+07	2.6E+07	ox2_bound:144	LOC432939	NM_001013791	NA	NA	PROMOTER
chr1	3.2E+07	3.2E+07	ox2_bound:144	Cct5	NM_007637	A930016P21Ri	NM_026546	DIVERGENT
chr1	3.5E+07	3.5E+07	ox2_bound:144	Osr2	NM_054049	NA	NA	PROMOTER
chr1	3.5E+07	3.5E+07	ox2_bound:144	Osr2	NM_054049	NA	NA	PROMOTER
chr1	3.7E+07	3.7E+07	ox2_bound:144	Zfp706	NM_026521	NA	NA	PROMOTER
chr1	3.7E+07	3.7E+07	ox2_bound:144	Grhl2	NM_026496	NA	NA	INSIDE
chr1	4E+07	4E+07	ox2_bound:144	Dpys	NM_022722	NA	NA	INSIDE
chr1	4.3E+07	4.3E+07	ox2_bound:144	Angpt1	NM_009640	NA	NA	INSIDE
chr1	5.3E+07	5.3E+07	ox2_bound:144	Ext1	NM_010162	NA	NA	INSIDE
chr1	5.5E+07	5.5E+07	ox2_bound:145	Depdc6	NM_145470	NA	NA	INSIDE
chr1	5.6E+07	5.6E+07	ox2_bound:145	Mtbp	NM_134092	NA	NA	INSIDE
chr1	5.7E+07	5.7E+07	ox2_bound:145	Has2	NM_008216	NA	NA	INSIDE
chr1	5.9E+07	5.9E+07	ox2_bound:145	Mtss1	NM_144800	NA	NA	INSIDE
chr1	5.9E+07	5.9E+07	ox2_bound:145	Mtss1	NM_144800	NA	NA	PROMOTER
chr1	6.7E+07	6.7E+07	ox2_bound:145	Wisp1	NM_018865	NA	NA	PROMOTER
chr1	7.5E+07	7.5E+07	ox2_bound:145	Ly6e	NM_008529	NA	NA	INSIDE
chr1	7.6E+07	7.6E+07	ox2_bound:145	Mafa	NM_194350	NA	NA	PROMOTER
chr1	7.7E+07	7.7E+07	ox2_bound:145	Foxh1	NM_007989	Ppp1r16a	NM_033371	DIVERGENT
chr1	7.8E+07	7.8E+07	ox2_bound:145	D15Bwg0759e	NM_001017983	NA	NA	INSIDE
chr1	7.9E+07	7.9E+07	ox2_bound:146	Cdc42ep1	NM_027219	NA	NA	INSIDE
chr1	8E+07	8E+07	ox2_bound:146	Dmc1h	NM_010059	NA	NA	PROMOTER
chr1	8E+07	8E+07	ox2_bound:146	Apobec3	NM_030255	NA	NA	PROMOTER
chr1	8E+07	8E+07	ox2_bound:146	Cbx7	NM_144811	NA	NA	PROMOTER
chr1	8E+07	8E+07	ox2_bound:146	Cbx7	NM_144811	NA	NA	PROMOTER
chr1	8E+07	8E+07	ox2_bound:146	Cbx7	NM_144811	NA	NA	PROMOTER
chr1	8E+07	8E+07	ox2_bound:146	Rpl3	NM_013762	Syngr1	NA	INSIDE
chr1	8E+07	8E+07	ox2_bound:146	Rpl32	NM_013762	NA	NM_009303	DIVERGENT
chr1	8E+07	8E+07	ox2_bound:146	Rpl36	NM_013762	NA	NM_009303	DIVERGENT
chr1	8.2E+07	8.2E+07	ox2_bound:146	L3mbtl2	NM_145993	NA	NA	PROMOTER
chr1	8.2E+07	8.2E+07	ox2_bound:147	Tob2	NM_020507	NA	NA	PROMOTER
chr1	8.2E+07	8.2E+07	ox2_bound:147	Phf5a	NM_026737	Aco2	NM_080633	DIVERGENT
chr1	8.3E+07	8.3E+07	ox2_bound:147	Poldip3	NM_178627	NA	NA	PROMOTER
chr1	8.4E+07	8.4E+07	ox2_bound:147	Samm50	NM_178614	NA	NA	PROMOTER
chr1	8.5E+07	8.5E+07	ox2_bound:147	BC024991	BC024991	NA	NA	Unknown
chr1	9E+07	9E+07	ox2_bound:147	Arsa	NM_009713	NA	NA	PROMOTER
chr1	9E+07	9E+07	ox2_bound:147	Shank3	NM_021423	NA	NA	PROMOTER
chr1	9.3E+07	9.3E+07	ox2_bound:147	Zcrb1	NM_026025	NA	NA	INSIDE
chr1	9.6E+07	9.6E+07	ox2_bound:147	Tmem16f	NM_175344	NA	NA	PROMOTER
chr1	9.7E+07	9.7E+07	ox2_bound:147	Slc38a2	NM_175121	NA	NA	PROMOTER
chr1	9.7E+07	9.7E+07	ox2_bound:148	Slc38a2	NM_175121	NA	NA	PROMOTER
chr1	9.8E+07	9.8E+07	ox2_bound:148	Col2a1	NM_031163	NA	NA	INSIDE
chr1	9.9E+07	9.9E+07	ox2_bound:148	Cacnb3	NM_007581	NA	NA	INSIDE
chr1	9.9E+07	9.9E+07	ox2_bound:148	Tuba1	NM_011653	NA	NA	INSIDE
chr1	1E+08	1E+08	ox2_bound:148	Smarcd1	NM_031842	NA	NA	INSIDE
chr1	1E+08	1E+08	ox2_bound:148	BC031490	BC031490	NA	NA	Unknown
chr1	1E+08	1E+08	ox2_bound:148	BC031490	BC031490	NA	NA	Unknown
chr1	1E+08	1E+08	ox2_bound:148	BC004728	NM_174992	NA	NA	INSIDE
chr1	1E+08	1E+08	ox2_bound:148	LOC432988	NM_001004171	NA	NA	INSIDE
chr1	1E+08	1E+08	ox2_bound:148	Aaas	NM_153416	NA	NA	PROMOTER

chr1	1E+08	1E+08	ox2_bound:14	Prr13	NM_025385	NA	NA	INSIDE
chr1	1E+08	1E+08	ox2_bound:14	Hoxc12	NM_010463	NA	NA	PROMOTER
chr1	1E+08	1E+08	ox2_bound:14	Hoxc5	NM_175730	NA	NA	INSIDE
chr1	1E+08	1E+08	ox2_bound:14	Smug1	NM_027885	NA	NA	PROMOTER
chr1	1E+08	1E+08	ox2_bound:14	Hnrpa1	NM_001039129	NA	NA	INSIDE
chr1	4558866	4559366	ox2_bound:14	Mgrn1	NM_029657	NA	NA	PROMOTER
chr1	1.3E+07	1.3E+07	ox2_bound:14	Parn	NM_028761	Bfar	NM_025976	DIVERGENT
chr1	1.3E+07	1.3E+07	ox2_bound:14	Pla2g10	NM_011987	NA	NA	PROMOTER
chr1	1.3E+07	1.3E+07	ox2_bound:14	Rrn3	NM_001039521	NA	NA	INSIDE
chr1	1.4E+07	1.4E+07	ox2_bound:14	2900011O08Rik	NM_144518	NA	NA	INSIDE
chr1	1.6E+07	1.6E+07	ox2_bound:15	Yars2	NM_198246	NA	NA	PROMOTER
chr1	1.6E+07	1.6E+07	ox2_bound:15	Fgd4	NM_139234	NA	NA	PROMOTER
chr1	1.7E+07	1.7E+07	ox2_bound:15	Thap7	NM_026909	NA	NA	PROMOTER
chr1	1.7E+07	1.7E+07	ox2_bound:15	Slc25a1	NM_153150	NA	NA	PROMOTER
chr1	2E+07	2E+07	ox2_bound:15	Ap2m1	NM_009679	NA	NA	PROMOTER
chr1	2.2E+07	2.2E+07	ox2_bound:15	Liph	NM_153404	NA	NA	PROMOTER
chr1	2.2E+07	2.2E+07	ox2_bound:15	Liph	NM_153404	NA	NA	PROMOTER
chr1	2.2E+07	2.2E+07	ox2_bound:15	C330012H03Rik	NM_183029	NA	NA	INSIDE
chr1	2.2E+07	2.2E+07	ox2_bound:15	Sfrs10	NM_009186	NA	NA	INSIDE
chr1	2.2E+07	2.2E+07	ox2_bound:15	Etv5	NM_023794	NA	NA	PROMOTER
chr1	2.2E+07	2.2E+07	ox2_bound:15	Etv5	NM_023794	NA	NA	PROMOTER
chr1	2.3E+07	2.3E+07	ox2_bound:15	Eif4a2	NM_013506	NA	NA	INSIDE
chr1	2.3E+07	2.3E+07	ox2_bound:15	B630019A10Rik	NM_177072	NA	NA	PROMOTER
chr1	2.4E+07	2.4E+07	ox2_bound:15	Lpp	NM_178665	NA	NA	PROMOTER
chr1	3.3E+07	3.3E+07	ox2_bound:15	Slc12a8	NM_134251	NA	NA	PROMOTER
chr1	3.6E+07	3.6E+07	ox2_bound:15	Parp14	NM_001039530	NA	NA	INSIDE
chr1	3.8E+07	3.8E+07	ox2_bound:15	Tmem39a	NM_026407	NA	NA	PROMOTER
chr1	4.5E+07	4.5E+07	ox2_bound:15	Cd200r1	NM_021325	NA	NA	PROMOTER
chr1	4.6E+07	4.6E+07	ox2_bound:15	Tagln3	NM_019754	NA	NA	PROMOTER
chr1	4.6E+07	4.6E+07	ox2_bound:15	Tagln3	NM_019754	NA	NA	PROMOTER
chr1	4.8E+07	4.8E+07	ox2_bound:15	Dppa4	NM_001018002	NA	NA	PROMOTER
chr1	5.6E+07	5.6E+07	ox2_bound:15	Nfkbiz	NM_030612	NA	NA	PROMOTER
chr1	8.5E+07	8.5E+07	ox2_bound:15	Jam2	NM_023844	NA	NA	PROMOTER
chr1	8.6E+07	8.6E+07	ox2_bound:15	Adamts1	NM_009621	NA	NA	PROMOTER
chr1	9E+07	9E+07	ox2_bound:15	BC065126	BC065126	NA	NA	Unknown
chr1	9.2E+07	9.2E+07	ox2_bound:15	Ifngr2	NM_008338	NA	NA	INSIDE
chr1	9.2E+07	9.2E+07	ox2_bound:15	Cryzl1	NM_133679	NA	NA	PROMOTER
chr1	9.2E+07	9.2E+07	ox2_bound:15	1190017O12Rik	NM_138743	NA	NA	INSIDE
chr1	9.6E+07	9.6E+07	ox2_bound:15	Brwd1	NM_145125	NA	NA	PROMOTER
chr1	5385118	5385765	ox2_bound:15	5730437N04Rik	NM_027457	NA	NA	INSIDE
chr1	5435942	5436570	ox2_bound:15	Zdhhc14	NM_146073	NA	NA	PROMOTER
chr1	1.3E+07	1.3E+07	ox2_bound:15	Thbs2	NM_011581	NA	NA	INSIDE
chr1	1.3E+07	1.3E+07	ox2_bound:15	Tcte3	NM_011560	NA	NA	INSIDE
chr1	1.4E+07	1.4E+07	ox2_bound:15	Dll1	NM_007865	NA	NA	PROMOTER
chr1	1.4E+07	1.4E+07	ox2_bound:15	Dll1	NM_007865	NA	NA	PROMOTER
chr1	1.4E+07	1.4E+07	ox2_bound:15	Dll1	NM_007865	NA	NA	PROMOTER
chr1	1.6E+07	1.6E+07	ox2_bound:15	Lnpep	NM_172827	NA	NA	PROMOTER
chr1	1.9E+07	1.9E+07	ox2_bound:15	Zfp160	NM_145483	NA	NA	PROMOTER
chr1	2.2E+07	2.2E+07	ox2_bound:15	Zfp206	NM_001033425	NA	NA	INSIDE
chr1	2.2E+07	2.2E+07	ox2_bound:15	Zfp206	NM_001033425	NA	NA	INSIDE
chr1	2.2E+07	2.2E+07	ox2_bound:15	2810417J12Rik	NM_029798	NA	NA	PROMOTER
chr1	2.2E+07	2.2E+07	ox2_bound:15	Tbc1d24	NM_173186	NA	NA	INSIDE
chr1	2.3E+07	2.3E+07	ox2_bound:15	Traf7	NM_153792	NA	NA	PROMOTER
chr1	2.3E+07	2.3E+07	ox2_bound:15	Fahd1	NM_023480	NA	NA	INSIDE
chr1	2.4E+07	2.4E+07	ox2_bound:15	Msln	NM_018857	NA	NA	PROMOTER
chr1	2.4E+07	2.4E+07	ox2_bound:15	Tmem8	NM_021793	NA	NA	PROMOTER
chr1	2.5E+07	2.5E+07	ox2_bound:15	Dusp1	NM_013642	NA	NA	PROMOTER
chr1	2.5E+07	2.5E+07	ox2_bound:15	Itpr3	NM_080553	NA	NA	PROMOTER
chr1	2.6E+07	2.6E+07	ox2_bound:15	Grm4	NM_001013385	NA	NA	INSIDE
chr1	2.7E+07	2.7E+07	ox2_bound:15	Gm749	NM_001034871	NA	NA	PROMOTER
chr1	2.7E+07	2.7E+07	ox2_bound:15	Gm749	NM_001034871	NA	NA	PROMOTER
chr1	2.7E+07	2.7E+07	ox2_bound:15	Stk38	NM_134115	NA	NA	PROMOTER
chr1	2.7E+07	2.7E+07	ox2_bound:15	Stk38	NM_134115	NA	NA	PROMOTER
chr1	2.9E+07	2.9E+07	ox2_bound:15	Slc37a1	NM_153062	NA	NA	INSIDE
chr1	3.1E+07	3.1E+07	ox2_bound:15	Morc2b	NM_177719	NA	NA	INSIDE

chr1	3.1E+07	3.1E+07	ox2_bound:15	Zfp422	NM_029952	rs1	NA	INSIDE
chr1	3.2E+07	3.2E+07	ox2_bound:15	Daxx	NM_007829	NA	NA	PROMOTER
chr1	3.2E+07	3.2E+07	ox2_bound:15	Rps18	NM_011296	Vps52	NM_172620	DIVERGENT
chr1	3.3E+07	3.3E+07	ox2_bound:15	Notch4	NM_010929	NA	NA	INSIDE
chr1	3.4E+07	3.4E+07	ox2_bound:15	Pou5f1	NM_013633	NA	NA	PROMOTER
chr1	3.4E+07	3.4E+07	ox2_bound:15	Pou5f1	NM_013633	NA	NA	PROMOTER
chr1	3.4E+07	3.4E+07	ox2_bound:15	Cdsn	NM_001008424	NA	NA	PROMOTER
chr1	3.4E+07	3.4E+07	ox2_bound:15	Tubb5	NM_011655	Myg1	NA	INSIDE
chr1	3.4E+07	3.4E+07	ox2_bound:15	Tubb5	NM_011655	NA	NM_021713	DIVERGENT
chr1	3.4E+07	3.4E+07	ox2_bound:15	Ppp1r10	NM_175934	NA	NA	INSIDE
chr1	3.5E+07	3.5E+07	ox2_bound:15	Ppp1r11	NM_029632	NA	NA	PROMOTER
chr1	3.5E+07	3.5E+07	ox2_bound:15	2410137M14Rik	NM_029747	NA	NA	PROMOTER
chr1	3.5E+07	3.5E+07	ox2_bound:15	Zfp57	NM_001013745	NA	NA	PROMOTER
chr1	3.5E+07	3.5E+07	ox2_bound:15	Zfp57	NM_009559	NA	NA	PROMOTER
chr1	3.5E+07	3.5E+07	ox2_bound:15	Mog	NM_010814	NA	NA	PROMOTER
chr1	4.4E+07	4.4E+07	ox2_bound:15	Hsp90ab1	NM_008302	NA	NA	PROMOTER
chr1	4.4E+07	4.4E+07	ox2_bound:15	Slc29a1	NM_022880	NA	NA	PROMOTER
chr1	4.5E+07	4.5E+07	ox2_bound:15	Slc22a7	NM_144856	NA	NA	PROMOTER
chr1	4.5E+07	4.5E+07	ox2_bound:15	Rpl7l1	NM_025433	NA	NA	PROMOTER
chr1	5E+07	5E+07	ox2_bound:15	Satb1	NM_009122	NA	NA	PROMOTER
chr1	5.1E+07	5.1E+07	ox2_bound:15	Kcnh8	NM_001031811	NA	NA	PROMOTER
chr1	5.2E+07	5.2E+07	ox2_bound:15	Pcaf	NM_020005	NA	NA	PROMOTER
chr1	5.2E+07	5.2E+07	ox2_bound:15	Pcaf	NM_020005	NA	NA	PROMOTER
chr1	5.2E+07	5.2E+07	ox2_bound:15	Pcaf	NM_020005	NA	NA	PROMOTER
chr1	5.4E+07	5.4E+07	ox2_bound:15	BC031441	NM_146249	Ebi3	NM_015766	DIVERGENT
chr1	5.4E+07	5.4E+07	ox2_bound:15	Ccdc94	NM_028381	NA	NA	INSIDE
chr1	5.4E+07	5.4E+07	ox2_bound:15	M6prbp1	NM_025836	NA	NA	INSIDE
chr1	5.4E+07	5.4E+07	ox2_bound:15	Jmjd2b	NM_172132	NA	NA	PROMOTER
chr1	5.5E+07	5.5E+07	ox2_bound:15	Rpl3	NM_018730	Syngr1	NA	INSIDE
chr1	5.5E+07	5.5E+07	ox2_bound:15	Ranbp3	NM_027933	NA	NA	PROMOTER
chr1	5.5E+07	5.5E+07	ox2_bound:15	Nrtn	NM_008738	Dus3l	NM_144858	DIVERGENT
chr1	6.4E+07	6.4E+07	ox2_bound:15	E130009J12Rik	NM_001008973	NA	NA	PROMOTER
chr1	6.4E+07	6.4E+07	ox2_bound:15	Twsg1	NM_023053	NA	NA	PROMOTER
chr1	6.6E+07	6.6E+07	ox2_bound:15	Lama1	NM_008480	NA	NA	PROMOTER
chr1	6.6E+07	6.6E+07	ox2_bound:15	Lama1	NM_008480	NA	NA	INSIDE
chr1	6.6E+07	6.6E+07	ox2_bound:15	Arhgap28	NM_172964	NA	NA	PROMOTER
chr1	6.9E+07	6.9E+07	ox2_bound:15	Tgif	NM_009372	NA	NA	INSIDE
chr1	6.9E+07	6.9E+07	ox2_bound:15	Mylc2b	NM_023402	NA	NA	PROMOTER
chr1	7.7E+07	7.7E+07	ox2_bound:15	Vit	NM_028813	NA	NA	INSIDE
chr1	7.9E+07	7.9E+07	ox2_bound:15	Sfrs7	NM_146083	NA	NA	PROMOTER
chr1	8.3E+07	8.3E+07	ox2_bound:15	Ppm1b	NM_011151	NA	NA	PROMOTER
chr1	8.4E+07	8.4E+07	ox2_bound:15	Six3os1	NM_175267	Six3	NA	INSIDE
chr1	8.4E+07	8.4E+07	ox2_bound:15	Six3os1	NM_175267	Six3	NA	INSIDE
chr1	8.4E+07	8.4E+07	ox2_bound:15	Six3os1	NM_175267	NA	NM_011381	DIVERGENT
chr1	8.6E+07	8.6E+07	ox2_bound:15	Msh6	NM_010830	NA	NA	PROMOTER
chr1	6720080	6721211	ox2_bound:16	Epc1	NM_007935	NA	NA	PROMOTER
chr1	9414640	9415405	ox2_bound:16	Fzd8	NM_008058	NA	NA	PROMOTER
chr1	9418194	9419299	ox2_bound:16	Fzd8	NM_008058	NA	NA	DOWNSTREAM
chr1	1.3E+07	1.3E+07	ox2_bound:16	Npc1	NM_008720	NA	NA	INSIDE
chr1	1.3E+07	1.3E+07	ox2_bound:16	Cabyr	NM_027687	NA	NA	PROMOTER
chr1	2.1E+07	2.1E+07	ox2_bound:16	Rnf125	NM_026301	NA	NA	PROMOTER
chr1	2.1E+07	2.1E+07	ox2_bound:16	Rnf125	NM_026301	NA	NA	PROMOTER
chr1	2.1E+07	2.1E+07	ox2_bound:16	Rnf125	NM_026301	NA	NA	PROMOTER
chr1	2.1E+07	2.1E+07	ox2_bound:16	Rnf125	NM_026301	NA	NA	INSIDE
chr1	3.4E+07	3.4E+07	ox2_bound:16	D0H4S114	NM_053078	NA	NA	INSIDE
chr1	3.5E+07	3.5E+07	ox2_bound:16	Wnt8a	NM_009290	NA	NA	PROMOTER
chr1	3.6E+07	3.6E+07	ox2_bound:16	Paip2	NM_026420	NA	NA	INSIDE
chr1	3.7E+07	3.7E+07	ox2_bound:16	Pura	NM_008989	NA	NA	PROMOTER
chr1	3.7E+07	3.7E+07	ox2_bound:16	Dnd1	NM_173383	NA	NA	INSIDE
chr1	3.7E+07	3.7E+07	ox2_bound:16	Pcdha12	NM_138663	NA	NA	PROMOTER
chr1	3.8E+07	3.8E+07	ox2_bound:16	Pcdhb1	NM_053126	NA	NA	INSIDE
chr1	3.8E+07	3.8E+07	ox2_bound:16	Pcdhb3	NM_053128	NA	NA	INSIDE
chr1	3.8E+07	3.8E+07	ox2_bound:16	Pcdhb11	NM_053136	NA	NA	INSIDE
chr1	3.8E+07	3.8E+07	ox2_bound:16	Pcdhb16	NM_053141	NA	NA	INSIDE
chr1	3.8E+07	3.8E+07	ox2_bound:16	Pcdhgb2	NM_033575	NA	NA	PROMOTER

chr1	3.8E+07	3.8E+07	ox2_bound:162	Pcdhgb6	NM_033578	NA	NA	PROMOTER
chr1	3.8E+07	3.8E+07	ox2_bound:162	Diap1	NM_007858	NA	NA	INSIDE
chr1	3.9E+07	3.9E+07	ox2_bound:162	9630014M24Rik	NM_001033771	NA	NA	INSIDE
chr1	4.3E+07	4.3E+07	ox2_bound:162	BC052715	BC052715	NA	NA	Unknown
chr1	4.4E+07	4.4E+07	ox2_bound:162	Stk32a	NM_178749	NA	NA	INSIDE
chr1	4.4E+07	4.4E+07	ox2_bound:162	Spink3	NM_009258	NA	NA	PROMOTER
chr1	4.6E+07	4.6E+07	ox2_bound:162	Kcnn2	NM_080465	NA	NA	PROMOTER
chr1	4.7E+07	4.7E+07	ox2_bound:162	Trim36	NM_178872	NA	NA	PROMOTER
chr1	4.8E+07	4.8E+07	ox2_bound:162	Sema6a	NM_018744	NA	NA	INSIDE
chr1	5.5E+07	5.5E+07	ox2_bound:162	BC092219	BC092219	NA	NA	Unknown
chr1	5.8E+07	5.8E+07	ox2_bound:163	Slc12a2	NM_009194	NA	NA	PROMOTER
chr1	6.1E+07	6.1E+07	ox2_bound:163	Slc6a7	NM_201353	NA	NA	INSIDE
chr1	6.1E+07	6.1E+07	ox2_bound:163	Cdx1	NM_009880	NA	NA	INSIDE
chr1	6.2E+07	6.2E+07	ox2_bound:163	BC060677	NM_172832	NA	NA	INSIDE
chr1	6.6E+07	6.6E+07	ox2_bound:163	Zfp532	NM_207255	NA	NA	PROMOTER
chr1	6.6E+07	6.6E+07	ox2_bound:163	Zfp532	NM_207255	NA	NA	INSIDE
chr1	6.6E+07	6.6E+07	ox2_bound:163	5330437I02Rik	NM_177028	NA	NA	PROMOTER
chr1	6.6E+07	6.6E+07	ox2_bound:163	Rax	NM_013833	NA	NA	PROMOTER
chr1	6.8E+07	6.8E+07	ox2_bound:163	Impa2	NM_053261	NA	NA	PROMOTER
chr1	6.8E+07	6.8E+07	ox2_bound:163	Cidea	NM_007702	NA	NA	PROMOTER
chr1	6.8E+07	6.8E+07	ox2_bound:164	D18Ertd653e	NM_172631	NA	NA	PROMOTER
chr1	6.9E+07	6.9E+07	ox2_bound:164	Mc5r	NM_013596	NA	NA	PROMOTER
chr1	7.4E+07	7.4E+07	ox2_bound:164	Mapk4	NM_172632	NA	NA	INSIDE
chr1	7.5E+07	7.5E+07	ox2_bound:164	Lipg	NM_010720	NA	NA	PROMOTER
chr1	7.5E+07	7.5E+07	ox2_bound:164	Rpl17	NM_001002239	NA	NA	INSIDE
chr1	8.1E+07	8.1E+07	ox2_bound:164	Sall3	NM_178280	NA	NA	INSIDE
chr1	8.5E+07	8.5E+07	ox2_bound:164	Fbxo15	NM_015798	NA	NA	PROMOTER
chr1	8.5E+07	8.5E+07	ox2_bound:164	Fbxo15	NM_015798	NA	NA	PROMOTER
chr1	8.9E+07	8.9E+07	ox2_bound:164	Rttn	NM_175542	NA	NA	INSIDE
chr1	3470790	3471290	ox2_bound:164	Saps3	NM_029456	NA	NA	PROMOTER
chr1	3473388	3473888	ox2_bound:165	Saps3	NM_029456	NA	NA	PROMOTER
chr1	3953852	3954352	ox2_bound:165	BC021614	NM_144869	NA	NA	PROMOTER
chr1	4693633	4694133	ox2_bound:165	Rbm4	NM_009032	NA	NA	PROMOTER
chr1	4704473	4706060	ox2_bound:165	Rbm14	NM_019869	NA	NA	INSIDE
chr1	4822741	4823417	ox2_bound:165	Dpp3	NM_133803	NA	NA	PROMOTER
chr1	5261359	5261966	ox2_bound:165	Banf1	NM_011793	2010003J03Rik	NM_027236	DIVERGENT
chr1	5382746	5383827	ox2_bound:165	Mus81	NM_027877	Cfl1	NA	INSIDE
chr1	5979720	5980913	ox2_bound:165	Cdca5	NM_026410	NA	NA	INSIDE
chr1	6130680	6131180	ox2_bound:165	Ppp2r5b	NM_198168	810013C15Rik	NM_194348	DIVERGENT
chr1	6166232	6166896	ox2_bound:165	Ehd1	NM_010119	NA	NA	PROMOTER
chr1	7301904	7302404	ox2_bound:166	Rtn3	NM_001003930	NA	NA	INSIDE
chr1	8392938	8393984	ox2_bound:166	Slc3a2	NM_008577	NA	NA	INSIDE
chr1	9658526	9659531	ox2_bound:166	Fth1	NM_010239	NA	NA	PROMOTER
chr1	9693228	9693728	ox2_bound:166	Rab3il1	NM_144538	NA	NA	PROMOTER
chr1	1.1E+07	1.1E+07	ox2_bound:166	Tmem109	NM_134142	NA	NA	PROMOTER
chr1	1.1E+07	1.1E+07	ox2_bound:166	Ms4a10	NM_023529	NA	NA	INSIDE
chr1	1.6E+07	1.6E+07	ox2_bound:166	Cep78	NM_198019	NA	NA	INSIDE
chr1	1.6E+07	1.6E+07	ox2_bound:166	Gna14	NM_008137	NA	NA	INSIDE
chr1	1.7E+07	1.7E+07	ox2_bound:166	Foxb2	NM_008023	NA	NA	DOWNSTREAM
chr1	1.8E+07	1.8E+07	ox2_bound:166	2410127L17Rik	NM_026120	NA	NA	INSIDE
chr1	2.3E+07	2.3E+07	ox2_bound:167	Klf9	NM_010638	NA	NA	PROMOTER
chr1	2.3E+07	2.3E+07	ox2_bound:167	Mamdc2	NM_174857	NA	NA	INSIDE
chr1	2.3E+07	2.3E+07	ox2_bound:167	1700028P14Rik	NM_026188	NA	NA	PROMOTER
chr1	2.5E+07	2.5E+07	ox2_bound:167	Foxd4	NM_008022	NA	NA	INSIDE
chr1	2.5E+07	2.5E+07	ox2_bound:167	Foxd4	NM_008022	NA	NA	PROMOTER
chr1	3E+07	3E+07	ox2_bound:167	Uhrf2	NM_144873	NA	NA	PROMOTER
chr1	3E+07	3E+07	ox2_bound:167	Dkk1	NM_010051	NA	NA	PROMOTER
chr1	3E+07	3E+07	ox2_bound:167	Dkk1	NM_010051	NA	NA	PROMOTER
chr1	3.4E+07	3.4E+07	ox2_bound:167	Stambpl1	NM_029682	NA	NA	INSIDE
chr1	4E+07	4E+07	ox2_bound:167	Pdlim1	NM_016861	NA	NA	PROMOTER
chr1	4.1E+07	4.1E+07	ox2_bound:168	Tm9sf3	NM_133352	NA	NA	PROMOTER
chr1	4.1E+07	4.1E+07	ox2_bound:168	Morf4l1	NM_001039147	NA	NA	PROMOTER
chr1	4.2E+07	4.2E+07	ox2_bound:168	Frat2	NM_177603	NA	NA	PROMOTER
chr1	4.2E+07	4.2E+07	ox2_bound:168	Avpi1	NM_027106	NA	NA	PROMOTER
chr1	4.2E+07	4.2E+07	ox2_bound:168	D19Ertd386e	NM_177464	NA	NA	PROMOTER

chr1	4.4E+07	4.4E+07	ox2_bound:168	Scd2	NM_009128	NA	NA	PROMOTER
chr1	4.6E+07	4.6E+07	ox2_bound:168	Ldb1	NM_010697	NA	NA	INSIDE
chr1	4.6E+07	4.6E+07	ox2_bound:168	BC066048	BC066048	NA	NA	Unknown
chr1	4.6E+07	4.6E+07	ox2_bound:168	Nolc1	NM_001039351	NA	NA	PROMOTER
chr1	4.6E+07	4.6E+07	ox2_bound:168	Cuedc2	NM_024192	NA	NA	INSIDE
chr1	4.6E+07	4.6E+07	ox2_bound:169	4930538D17Rik	NM_029186	NA	NA	INSIDE
chr1	4.6E+07	4.6E+07	ox2_bound:169	Trim8	NM_053100	NA	NA	PROMOTER
chr1	4.6E+07	4.6E+07	ox2_bound:169	Trim8	NM_053100	NA	NA	INSIDE
chr1	4.7E+07	4.7E+07	ox2_bound:169	Nt5c2	NM_029810	NA	NA	INSIDE
chr1	4.8E+07	4.8E+07	ox2_bound:169	BC063749	NM_001001738	NA	NA	PROMOTER
chr1	5.5E+07	5.5E+07	ox2_bound:169	Acsl5	NM_027976	NA	NA	INSIDE
chr1	5.6E+07	5.6E+07	ox2_bound:169	Dclre1a	NM_018831	Nhlrc2	NM_025811	DIVERGENT
chr1	5.9E+07	5.9E+07	ox2_bound:169	Hspa12a	NM_175199	NA	NA	INSIDE
chrX	6197699	6198537	ox2_bound:169	Tcfe3	NM_172472	NA	NA	INSIDE
chrX	6359451	6360920	ox2_bound:169	Eras	NM_181548	NA	NA	INSIDE
chrX	6453322	6454137	ox2_bound:170	2010001H14Rik	NM_027227	NA	NA	PROMOTER
chrX	6639825	6641207	ox2_bound:170	Porcn	NM_145908	NA	NA	PROMOTER
chrX	1.2E+07	1.2E+07	ox2_bound:170	Usp9x	NM_009481	NA	NA	PROMOTER
chrX	1.6E+07	1.6E+07	ox2_bound:170	Fundc1	NM_028058	NA	NA	INSIDE
chrX	1.9E+07	1.9E+07	ox2_bound:170	Cfp	NM_008823	NA	NA	PROMOTER
chrX	1.9E+07	1.9E+07	ox2_bound:170	Zfp182	NM_001013387	NA	NA	PROMOTER
chrX	2E+07	2E+07	ox2_bound:170	D930016N04Rik	NM_183185	NA	NA	PROMOTER
chrX	2.2E+07	2.2E+07	ox2_bound:170	BC068151	BC068151	NA	NA	Unknown
chrX	3.3E+07	3.3E+07	ox2_bound:170	Zbtb33	NM_020256	NA	NA	PROMOTER
chrX	3.6E+07	3.6E+07	ox2_bound:170	Gria3	NM_016886	NA	NA	INSIDE
chrX	4.4E+07	4.4E+07	ox2_bound:171	Pdcd8	NM_012019	Rab33a	NM_011228	DIVERGENT
chrX	4.4E+07	4.4E+07	ox2_bound:171	Suhw3	NM_153532	NA	NA	PROMOTER
chrX	4.7E+07	4.7E+07	ox2_bound:171	Hs6st2	NM_015819	NA	NA	PROMOTER
chrX	4.7E+07	4.7E+07	ox2_bound:171	Hs6st2	NM_015819	NA	NA	PROMOTER
chrX	4.7E+07	4.7E+07	ox2_bound:171	Gpc4	NM_008150	NA	NA	INSIDE
chrX	4.7E+07	4.7E+07	ox2_bound:171	Gpc4	NM_008150	NA	NA	PROMOTER
chrX	4.8E+07	4.8E+07	ox2_bound:171	mmu-mir-106a	mmu-mir-106a	NA	NA	PROMOTER
chrX	5.3E+07	5.3E+07	ox2_bound:171	Rbmx	NM_011252	NA	NA	PROMOTER
chrX	5.4E+07	5.4E+07	ox2_bound:171	Zic3	NM_009575	NA	NA	INSIDE
chrX	5.4E+07	5.4E+07	ox2_bound:171	Zic3	NM_009575	NA	NA	INSIDE
chrX	5.6E+07	5.6E+07	ox2_bound:172	Mcf2	NM_133197	NA	NA	PROMOTER
chrX	6.9E+07	6.9E+07	ox2_bound:172	Mecp2	NM_010788	NA	NA	PROMOTER
chrX	7E+07	7E+07	ox2_bound:172	Rpl10	NM_052835	NA	NA	PROMOTER
chrX	7.3E+07	7.3E+07	ox2_bound:172	Tbl1x	NM_020601	NA	NA	PROMOTER
chrX	7.3E+07	7.3E+07	ox2_bound:172	Tbl1x	NM_020601	NA	NA	PROMOTER
chrX	8.2E+07	8.2E+07	ox2_bound:172	Nr0b1	NM_007430	NA	NA	PROMOTER
chrX	8.2E+07	8.2E+07	ox2_bound:172	Nr0b1	NM_007430	NA	NA	INSIDE
chrX	8.9E+07	8.9E+07	ox2_bound:172	Pcyt1b	NM_211138	NA	NA	PROMOTER
chrX	8.9E+07	8.9E+07	ox2_bound:172	Pcyt1b	NM_211138	NA	NA	INSIDE
chrX	9E+07	9E+07	ox2_bound:172	Klhl15	NM_001039059	NA	NA	PROMOTER
chrX	9.1E+07	9.1E+07	ox2_bound:173	Las1l	NM_152822	NA	NA	PROMOTER
chrX	9.6E+07	9.6E+07	ox2_bound:173	Slc7a3	NM_007515	NA	NA	INSIDE
chrX	9.7E+07	9.7E+07	ox2_bound:173	Snx12	NM_018875	NA	NA	PROMOTER
chrX	9.7E+07	9.7E+07	ox2_bound:173	Ogt	NM_139144	NA	NA	PROMOTER
chrX	9.7E+07	9.7E+07	ox2_bound:173	Ogt	NM_139144	NA	NA	PROMOTER
chrX	9.7E+07	9.7E+07	ox2_bound:173	Ogt	NM_139144	NA	NA	PROMOTER
chrX	9.9E+07	9.9E+07	ox2_bound:173	Cdx4	NM_007674	NA	NA	PROMOTER
chrX	9.9E+07	9.9E+07	ox2_bound:173	Rnf12	NM_011276	NA	NA	PROMOTER
chrX	9.9E+07	9.9E+07	ox2_bound:173	Rnf12	NM_011276	NA	NA	PROMOTER
chrX	1E+08	1E+08	ox2_bound:173	2610529C04Rik	NM_025952	Cox7b	NM_025379	DIVERGENT
chrX	1E+08	1E+08	ox2_bound:174	Pgk1	NM_008828	NA	NA	INSIDE
chrX	1E+08	1E+08	ox2_bound:174	Cysltr1	NM_021476	NA	NA	INSIDE
chrX	1E+08	1E+08	ox2_bound:174	Gpr23	NM_175271	NA	NA	PROMOTER
chrX	1E+08	1E+08	ox2_bound:174	Nsbp1	NM_016710	NA	NA	INSIDE
chrX	1E+08	1E+08	ox2_bound:174	Nsbp1	NM_016710	NA	NA	PROMOTER
chrX	1.3E+08	1.3E+08	ox2_bound:174	Armcx1	NM_030066	NA	NA	PROMOTER
chrX	1.3E+08	1.3E+08	ox2_bound:174	Gprasp1	NM_001004359	NA	NA	PROMOTER
chrX	1.3E+08	1.3E+08	ox2_bound:174	2900062L11Rik	NM_029823	NA	NA	PROMOTER
chrX	1.3E+08	1.3E+08	ox2_bound:174	Zcchc18	NM_001035509	NA	NA	PROMOTER
chrX	1.4E+08	1.4E+08	ox2_bound:174	Prps1	NM_021463	NA	NA	PROMOTER

chrX	1.4E+08	1.4E+08	ox2_bound:175	Prps1	NM_021463	NA	NA	INSIDE
chrX	1.4E+08	1.4E+08	ox2_bound:175	AW547186	NM_177592	NA	NA	PROMOTER
chrX	1.5E+08	1.5E+08	ox2_bound:175	Gnl3l	NM_198110	NA	NA	PROMOTER
chrX	1.5E+08	1.5E+08	ox2_bound:175	ORF34	NM_198105	NA	NA	INSIDE
chrX	1.5E+08	1.5E+08	ox2_bound:175	Huwe1	NM_021523	NA	NA	INSIDE
chrX	1.5E+08	1.5E+08	ox2_bound:175	Acot9	NM_019736	NA	NA	PROMOTER
chrX	1.5E+08	1.5E+08	ox2_bound:175	Sms	NM_009214	NA	NA	PROMOTER
chrX	1.5E+08	1.5E+08	ox2_bound:175	Mbtps2	NM_178266	NA	NA	PROMOTER
chrX	1.6E+08	1.6E+08	ox2_bound:175	Rbbp7	NM_009031	NA	NA	PROMOTER
chrX	1.6E+08	1.6E+08	ox2_bound:175	4932441K18Rik	NM_178935	NA	NA	PROMOTER
chrX	1.6E+08	1.6E+08	ox2_bound:176	4932441K18Rik	NM_178935	NA	NA	PROMOTER
chrX	1.6E+08	1.6E+08	ox2_bound:176	4932441K18Rik	NM_178935	NA	NA	PROMOTER
chrX	1.6E+08	1.6E+08	ox2_bound:176	Glra2	NM_183427	NA	NA	PROMOTER
chrX	1.6E+08	1.6E+08	ox2_bound:176	Tmsb4x	NM_021278	NA	NA	INSIDE
chrX	1.6E+08	1.6E+08	ox2_bound:176	Prps2	NM_026662	NA	NA	INSIDE

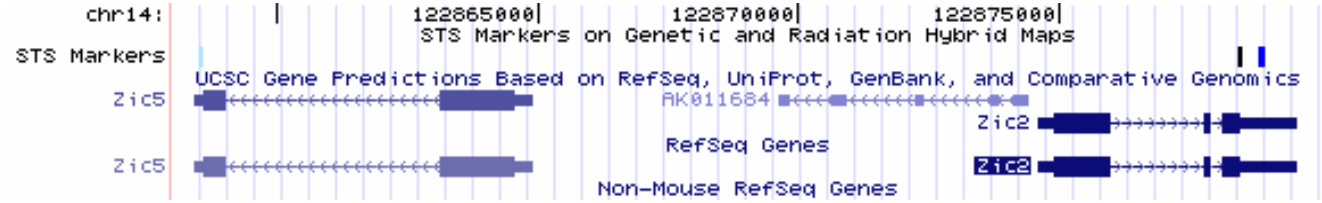

Appendix 7. Zic5 and Zic2 are transcribed by a divergent promoter. The divergent promoter regulates the expression of Zic5 and Zic2 by regulating the transcription of their genes in opposite directions (Zic2 forward and Zic5 reverse). This divergent promoter is approximately 9800 bp in length. *Source: UCSC genome browser Build mm7 (August 2005).*

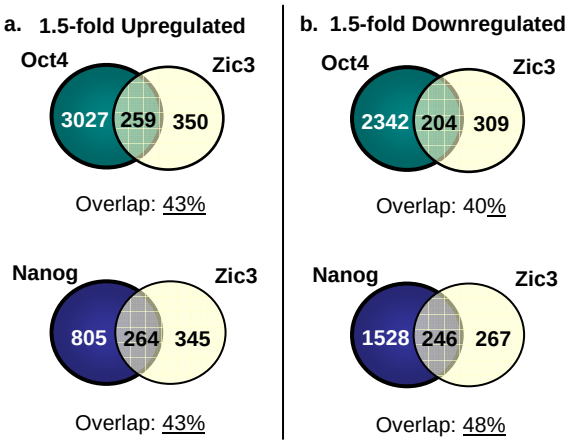

Appendix 8. Zic3 shares regulatory pathways with Oct4 and Nanog in ES cells. RNA was harvested from mouse ES cells treated with Oct4 and Nanog shRNA for 4 days with puromycin selection. The transfected cells that survived were assayed for their gene expression profiles on Illumina mouse Ref8 microarrays. The number of significantly-regulated genes following each RNAi experiment is presented here and compared with that of the Zic3 gene expression profile.

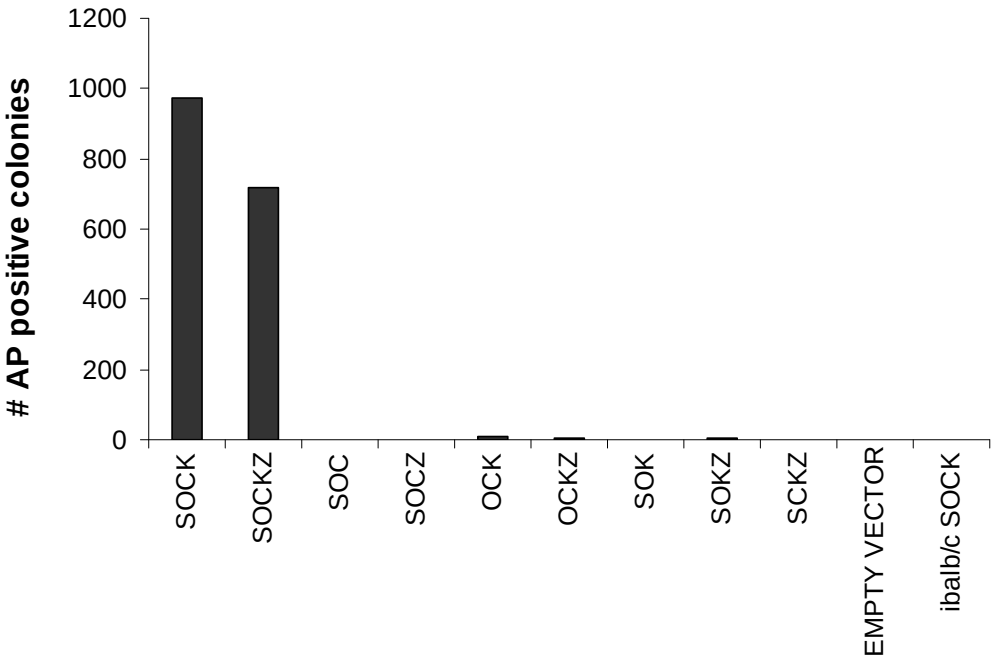

Appendix 9. Reprogramming assay with Oct4, Sox2, Klf4, C-Myc and Zic3. Oct4, Sox2, Klf4, C-Myc and Zic3 were ectopically expressed in mouse embryonic fibroblast cells (Balb/c; Passage 3), using combinations reflected in the graph above. Details of the reprogramming assay may be found in Section 2.3.5. Three weeks following infection of the reprogramming factors, pluripotent colonies were stained for alkaline phosphatase (AP) and quantified. Assays were performed in biological triplicate in 6 cm^2 tissue culture dishes. Overexpression of Zic3 in a variety of combinations of Oct4, Sox2, Klf4 and C-Myc did not result in a significant increase in pluripotent AP-positive colonies, relative to the positive control (SOCK). Legend – S: Sox2, O: Oct4, C: C-Myc, K: Klf4, Z- Zic3.

Credits: Zic3-pMXs vector created by Linda Lim; reprogramming assays optimized by Linda Lim & Tahira Allapitchay; Zic3 reprogramming experiment and quantification of colonies performed by Tahira Allapitchay.

APPENDIX 10

Zic3 is required for maintenance of pluripotency in embryonic stem cells

Mol Biol Cell. 2007 Apr;18(4):1348-58.

Molecular Biology of the Cell
Vol. 18, 1348–1358, April 2007

Zic3 Is Required for Maintenance of Pluripotency in Embryonic Stem Cells[D]

Linda Shushan Lim,*† Yuin-Han Loh,†‡ Weiwei Zhang,‡§ Yixun Li,‖ Xi Chen,‡§ Yinan Wang,‡§ Manjiri Bakre,* Huck-Hui Ng,‡§ and Lawrence W. Stanton*§

*Stem Cell and Developmental Biology Group, ‡Gene Regulation Laboratory, and ‖Information and Mathematical Sciences Group, Genome Institute of Singapore, Singapore 138672; and §Department of Biological Sciences, National University of Singapore, Singapore 117543

Submitted July 24, 2006; Revised November 9, 2006; Accepted January 22, 2007
Monitoring Editor: Marianne Bronner-Fraser

Embryonic stem (ES) cell pluripotency is dependent upon sustained expression of the key transcriptional regulators Oct4, Nanog, and Sox2. Dissection of the regulatory networks downstream of these transcription factors has provided critical insight into the molecular mechanisms that regulate ES cell pluripotency and early differentiation. Here we describe a role for Zic3, a member of the Gli family of zinc finger transcription factors, in the maintenance of pluripotency in ES cells. We show that Zic3 is expressed in ES cells and that this expression is repressed upon differentiation. The expression of Zic3 in pluripotent ES cells is also directly regulated by Oct4, Sox2, and Nanog. Targeted repression of Zic3 in human and mouse ES cells by RNA interference–induced expression of several markers of the endodermal lineage. Notably, the expression of Nanog, a key pluripotency regulator and repressor of extraembryonic endoderm specification in ES cells, was significantly reduced in Zic3 knockdown cells. This suggests that Zic3 may prevent endodermal marker expression through Nanog-regulated pathways. Thus our results extend the ES cell transcriptional network beyond Oct4, Nanog, and Sox2, and further establish that Zic3 plays an important role in the maintenance of pluripotency by preventing endodermal lineage specification in embryonic stem cells.

INTRODUCTION

The transcription factors Oct4, Nanog, and Sox2 are key regulatory players in embryonic stem (ES) cell biology. These core factors contribute to the hallmark characteristics of ES cells by 1) activation of target genes that encode pluripotency and self-renewal mechanisms and 2) repression of signaling pathways that promote differentiation (Orkin, 2005). In ES cells Oct4, Nanog, and Sox2 co-occupy promoters of hundreds of genes that are both expressed and repressed in the pluripotent state (Boyer *et al.*, 2005; Loh *et al.*, 2006). This suggests complex regulatory circuitry in which Oct4, Nanog, and Sox2 collectively and uniquely regulate downstream genes to control ES cell differentiation. However, it remains unclear what are the downstream effectors of these transcription factors that contribute to maintaining the pluripotent status of ES cells. It also not understood how these "master regulators" of pluripotency are involved in controlling lineage-specific differentiation of ES cells. It is therefore useful to elucidate the transcriptional networks surrounding Oct4, Nanog, and Sox2, where detailed knowledge of these pathways remain key to harnessing the potential to direct differentiation of ES cells into therapeutically useful cell types.

To expand our understanding of the transcriptional networks that control stem cell differentiation, we have looked at transcription factors whose expression is directly regulated by Oct4, Nanog, and Sox2. We have identified Zic3 (Zinc finger protein of the cerebellum 3) as a transcription factor of interest for two main reasons. First, Oct4, Nanog, and Sox2 binding have been mapped to the Zic3 promoter regions in ES cells (Boyer *et al.*, 2005; Loh *et al.*, 2006), implying that these key factors may regulate Zic3 expression. The overlap between mouse and human ES cells further highlights the significance of Zic3 and suggests possible conservation of the gene's pathways between the two species. Second, Zic3 demonstrates differential gene expression between the pluripotent and early differentiation phases, where its expression is higher in the pluripotent state (Brandenberger *et al.*, 2004; Wei *et al.*, 2005). The changes in gene expression between these states suggest a potential role for Zic3 in controlling differentiation of mouse and human ES cells.

Zic3 belongs to the GLI superfamily of transcription factors and is a vertebrate homologue of the *Drosophila* pair-rule gene odd-paired (*opa*; Aruga *et al.*, 1996a). The five known mammalian Zic genes (Zic1-5) encode five tandem C_2H_2 zinc finger domains that are highly conserved across species (Herman and El-Hodiri, 2002; Grinberg and Millen, 2005). Although the expression of Zic3 is restricted to the cerebellum of adult mammals, dynamic patterns of expression have been observed during embryonic development in mouse (Herman and El-Hodiri, 2002), *Xenopus* (Nakata *et al.*,

This article was published online ahead of print in *MBC in Press* (http://www.molbiolcell.org/cgi/doi/10.1091/mbc.E06–07–0624) on January 31, 2007.

[D] The online version of this article contains supplemental material at *MBC Online* (http://www.molbiolcell.org).

† These authors contributed equally to this work.

Address correspondence to: Lawrence W. Stanton (stantonl@gis.a-star.edu.sg).

Abbreviations used: ES, embryonic stem; RA, retinoic acid; RNAi, RNA interference; ChIP, chromatin immunoprecipitation; AVE, anterior visceral endoderm.

1997, 1998), chick (Warner *et al.*, 2003), and zebrafish (Grinblat and Sive, 2001). The expression of Zic3 in the embryonic ectoderm and mesoderm during gastrulation (Kitaguchi *et al.*, 2002; Elms *et al.*, 2004), and throughout the tailbud, retina and limb bud during neurulation and organogenesis (Herman and El-Hodiri, 2002; Orkin, 2005), suggests an important role for this transcription factor in embryonic ectoderm and mesoderm development. This is further supported by molecular pathways in which Zic3 has been implicated. For example the mesoderm-associated gene Brachyury induces Zic3 expression in *Xenopus* (Kitaguchi *et al.*, 2002), and the embryonic patterning gene Nodal is regulated by Zic3 during gastrulation through interaction with an upstream enhancer region in mouse and *Xenopus* embryos (Ware *et al.*, 2006a). In ectodermal development, Zic3 is a potent inducer of *Xenopus* proneural and neural crest genes (Nakata *et al.*, 1997) and is induced directly downstream of transcription factors Pbx1b and Meis1 in the *Xenopus* ectoderm (Maeda *et al.*, 2002; Kelly *et al.*, 2006).

Zic3 mutations are associated with X-linked heterotaxy, a disorder characterized by disruptions in embryonic laterality and midline developmental field defect (Gebbia *et al.*, 1997). In Zic3 mutant organisms s*itus ambiguus* is frequently observed, encompassing failure in lateralization of internal organs, mirror-image inversions, and left-right isomerism (Aylsworth, 2001). Several mutations have been identified in humans that render the Zic3 protein unstable and absent in cells or incapable of nuclear localization where its transcriptional effect is exerted (Gebbia *et al.*, 1997; Ware *et al.*, 2004).

Consistent with its expression in the involuting mesoderm and presumptive neural plate during gastrulation, Zic3 is involved in regulating left–right asymmetry and neural tube development. Zic3-null mice exhibit a wide spectrum of phenotypes. Fifty percent of null mice succumb to embryonic lethality over different gestational stages, and 30% to perinatal lethality as a result of congenital heart defects, pulmonary isomerism, and defects in the CNS (Purandare *et al.*, 2002). The earliest and most profound Zic3-null defects have been attributed to failure in establishment of the anterior-posterior axis by the anterior visceral endoderm (AVE) before gastrulation (Ware *et al.*, 2006b). In less severely affected embryos, abnormalities are observed at gastrulation in the distribution and accumulation of excess mesoderm tissue. Taken together, the defects in embryonic lethal mice demonstrate a key role for Zic3 in early embryonic patterning that encompasses anterior visceral endoderm formation, initiation of gastrulation, and primitive streak morphogenesis (Ware *et al.*, 2006b).

The varying degrees of severity in failure to complete gastrulation displayed by Zic3 null mice may perhaps be attributed to compensatory mechanisms in developing embryos, as indicated by the distinct and partially overlapping expression patterns exhibited by members of the Zic gene family (Nagai *et al.*, 1997; Elms *et al.*, 2004). It is important to note that Zic3 shares overall 64 and 59% homology with Zic1 and Zic2, respectively, and this homology increases to 91% within the zinc finger domain. Thus members of Zic family are strong candidates for redundancy in molecular signaling owing to the high degree of homology and overlapping expression observed among the members of this family.

Although Zic3 expression has been implicated in embryonic development, still lacking is a detailed understanding of what regulates Zic3 expression and what the downstream effectors of Zic3 are. The Zic3 gene has been identified as a target of Oct4, Nanog, and Sox2 in ES cells (Boyer *et al.*, 2005; Loh *et al.*, 2006), and Zic3 is preferentially expressed in pluripotent state (Brandenberger *et al.*, 2004; Wei *et al.*, 2005). Questions arising from these data are as follows: 1) How do Oct4, Nanog, and Sox2 interact with the Zic3 regulatory region, and what results from this interaction and, 2) what

Table 1. List of marker genes used to assess lineage development in ES cells

Gene symbol	Description	Lineage
Sox17	SRY-box containing gene 17	Endoderm
PDGFRA	Platelet-derived growth factor receptor, alpha	Endoderm
Gata4	GATA binding protein 4	Endoderm
Gata6	GATA binding protein 6	Endoderm
Foxa2	Forkhead box A2	Endoderm
GSC	Goosecoid	Mesendoderm
Nodal	Nodal	Mesendoderm
MixL1	Mix1 homeobox-like 1	Mesendoderm
Hand1	Heart and neural crest derivatives expressed 1	Mesoderm
Nkx2.5	NK2 transcription factor related, locus 5	Mesoderm
Gata2	GATA binding protein 2	Mesoderm
Nestin	Nestin	Ectoderm
GFAP	Glial fibrillary acidic protein	Ectoderm
Pax6	Paired box gene 6	Ectoderm
TDGF1	Teratocarcinoma-derived growth factor/Cripto	Ectoderm
Sox1	SRY-box containing gene 1	Ectoderm
REST	RE1-silencing transcription factor	Ectoderm
CoREST	REST Co-repressor 1	Ectoderm
FGF5	Fibroblast growth factor 5	Ectoderm
BMP4	Bone morphogenetic protein 4	Trophectoderm
CDX2	Caudal type homeobox 2	Trophectoderm
DKK3	Dickkopf homolog 3	Wnt pathway
Gsk3beta	Glycogen synthase kinase 3 beta	Wnt pathway

role does Zic3 play in the embryonic stem cell? We have addressed these questions using the loss-of-function approach for Zic3 and the key regulatory genes in ES cells. In this study, we examined the function of Zic3 as a regulatory target of Oct4, Nanog, and Sox2 in ES cells. We report that Zic3 shares significant overlap with the Oct4, Nanog, and Sox2 transcriptional networks and is important in maintaining ES cell pluripotency by preventing differentiation of cells into endodermal lineages. Thus our results extend the current knowledge of the ES cell transcriptional circuitry beyond Oct4, Nanog, and Sox2.

MATERIALS AND METHODS

ES Cell Maintenance

Feeder-free E14 Mouse ES cells were maintained on 0.1% gelatin-coated dishes in E14 proliferative medium containing DMEM/15% ES FBS (Invitrogen, Carlsbad, CA), 0.1 mM MEM nonessential amino acids (Invitrogen), 2 mM L-glutamine (Invitrogen), 0.1 mM β-mercaptoethanol (Invitrogen), and Chinese hamster ovary-Leukaemia Inhibitory Factor (CHO-LIF) (1000 U/ml). Feeder-free undifferentiated HuES9 human ES cells were maintained on matrigel-coated dishes in conditioned medium containing knockout DMEM/10% serum replacement (Invitrogen), 0.1 mM MEM nonessential amino acids (Invitrogen), 1 mM L-glutamine (Invitrogen), 0.1 mM β-mercaptoethanol (Invitrogen), 8% plasmanate (National University Hospital Pharmacy, Singapore), 12 ng/ml LIF, and 10 ng/ml human recombinant basic fibroblast growth factor (bFGF; Invitrogen). Conditioned medium was obtained by culturing mouse embryonic fibroblast (MEF) cells with HuES9 media. The medium was collected at 24 h intervals, filter sterilized, and further supplemented with 8 ng/ml bFGF for HuES9 cell culture.

RNA Interference and Establishment of Clonal Knockdown Lines

Small Interfering RNA (siRNA) Experiments. RNA interference (RNAi) experiments were performed with Dharmacon siGENOME SMARTpool reagents (Boulder, CO) against human or mouse Zic3. The Dharmacon si*CONTROL* nontargeting siRNA pool was used as a negative control. Mouse ES cells were transfected according to manufacturer's instructions in 12-well plates at a density of 2×10^5 cells per well. Retransfections were performed on preadherent cells at 48-h intervals, and RNA expression analysis was performed on samples from day 5. Human ES cells were transfected in 12-well plates with 2×10^5 cells, in suspension, per well. Subsequent retransfections were performed on adherent cells at 24-h intervals and RNA was harvested for analysis at day 5.

Short Hairpin RNA (shRNA) Experiments. The Oct4 and Nanog RNAi experiments were previously published (Loh *et al.*, 2006). The Zic3 shRNA construct was designed as described (Chew *et al.*, 2005) with a target sequence of 5′-GAATTCGAAGGCTGTGACA-3′. E14 cells in six-well plates were transfected with 2.0 μg pSUPERpuro vector or Zic3-pSUPER.puro (OligoEngine, Seattle, WA) at a density of 4×10^5 cells per well. Puromycin selection was introduced 1 d after transfection at 1.0 μg/ml and was maintained for 3 d before RNA isolation. ES cells were maintained in proliferative medium at all times.

Clonal Zic3 knockdown lines were established by transfection of shRNA constructs as described above. The Zic3 knockdown and vector control colonies were picked after 7 d of puromycin selection (1.0 μg/ml). Colonies were dissociated into single-cell suspensions by treatment with 0.05% Trypsin (Invitrogen) and plated on puromycin-resistant mitomycin-inactivated DR4 MEFs (ATCC, Manassas, VA). In total, 15 Zic3 clonal knockdown and 7 vector control lines were established and maintained under constant puromycin selection. The lines analyzed in this article were maintained feeder-free in ES cell proliferative media on 0.1% gelatin-coated dishes over a period of eight passages.

Secondary ES Colony-replating Assay

ES cells were transfected with Zic3- or empty pSUPER shRNA constructs and selected 24 h later with puromycin at 1.0 μg/ml over 4 d. At the end of 4 d few cells remained in the untransfected control wells indicating that selection was effective. The surviving cells were trypsinized and resuspended in E14 medium without LIF. Ten thousand or 20,000 cells were plated onto mouse feeder layers in six-well plates for secondary ES cell-colony formation. After 7 d, emerging colonies were stained with the Wright-Giemsa (Sigma, St. Louis, MO) stain. The extent of differentiated colonies was defined as the percentage of unstained colonies out of the total number of colonies in the well.

RNAi Rescue Experiments

The Zic3 open reading frame (ORF; NM_009575) was cloned from reverse-transcribed cDNA from mouse embryonic stem cells, using the primers indicated in Supplementary Table 1A. The PCR product was subsequently cloned into a vector driven by the CAG promoter. The RNAi-immune Zic3 ORF R3M (Supplementary Figure 1) was generated from this template using site-specific mutagenesis. To perform the rescue experiments, 4×10^5 mouse ES cells were seeded per well in six-well plates and transfected according to the scheme in Supplementary Table 1B. Hygromycin selection (1.0 μg/ml) was introduced 1 d after transfection.

RNA Extraction, cDNA Synthesis, and Quantitative Real-Time PCR

To minimize genomic DNA contamination, RNA was extracted with TriZol reagent (Invitrogen) and further purified with the RNeasy minikit (Qiagen, Chatsworth, CA). cDNA was synthesized with 1.0 μg total RNA using the High Capacity cDNA Archive kit (Applied Biosystems, Foster City, CA). For each qPCR reaction, cDNA samples diluted 10 times in water were mixed with 5.0 μl TaqMan Universal PCR Master Mix reagent (Applied Biosystems) and 0.5 μl of a single TaqMan probe from the following list: Zic3, Oct4, Nanog, Sox2, or the lineage markers in Table 1 (20× TaqMan Gene Expression

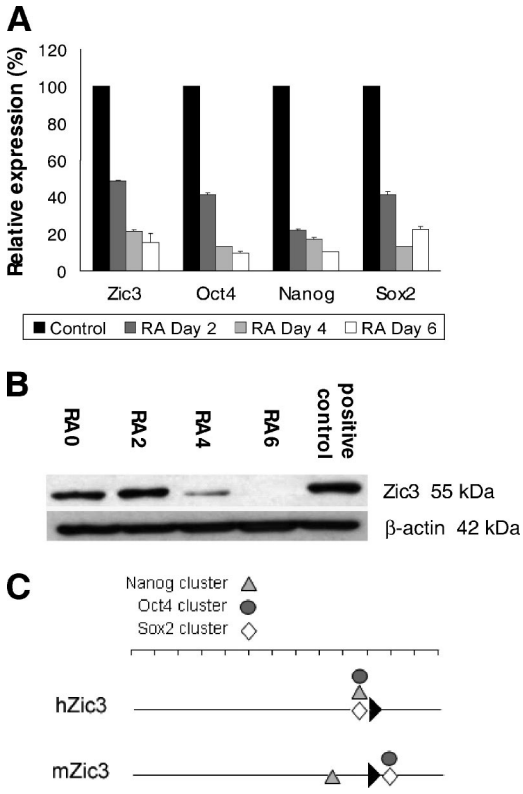

Figure 1. A profile of Zic3 expression in differentiating E14 cells. (A) Real-time PCR analysis of differentiation induced by retinoic acid. Samples were assayed at 2-d intervals (untreated control, and treated samples day 2, day 4, and day 6). Mean levels ± SE are expressed as percentages relative to undifferentiated E14 cells (100%). The assays were conducted in duplicate and normalized to β-actin control. (B) Verification of Zic3 protein expression during the process of RA differentiation. (C) A summary of ChIP mapping of Oct4, Nanog, and Sox2 binding sites on the Zic3 regulatory regions in mouse ES cells (Loh *et al.*, 2006; Sox2, Ng, unpublished data) and human ES cells (Boyer *et al.*, 2005). We examined transcription factor binding sites within 100 kb up- and downstream of the Zic3 coding region. In human ES cells, Oct4, Nanog, and Sox2 binding sites were located within 3.5 kb upstream of the Zic3 transcription start site, whereas in mouse ES cells, the Nanog binding site was found within 18.5 kb upstream, and the Oct4 and Sox2 binding sites were within 9.5 kb downstream of the gene, respectively (Loh *et al.*, 2006). Each unit on the scale represents 10 kb.

Assay reagents; Applied Biosystems) with a final volume of 10 μl. Quantitative real-time PCR analysis was conducted in 384-well clear optical reaction plate (Applied Biosystems) on the ABI Prism 7900 machine (Columbia, MD).

Western Blots and Immunocytochemistry

Zic3 protein detection was performed with goat-anti-Zic3 antibody (1:800 dilution; C-12, Santa Cruz Biotechnology, Santa Cruz, CA) and donkey anti-goat horseradish peroxidase (HRP; 1:5000; Santa Cruz Biotechnology). Loading consistency was determined with mouse anti-β-actin (1:3000; Invitrogen) and goat anti-mouse HRP (1:5000; Santa Cruz Biotechnology). For immunocytochemistry, cells were seeded at a density of 1.0×10^5 cells per well on fibronectin-coated chamber slides, fixed in 4% paraformaldehyde, and permeabilized with 0.3% Triton X-100. Blocking was performed with 5% fetal bovine serum and 1% bovine serum albumin in PBS solution for 30 min. Cells were stained with the following primary antibodies (1:100): goat or mouse anti-Oct4 (Santa Cruz Biotechnology, N-19 and C-10, respectively), rabbit-anti-Nanog (Chemicon, Temecula, CA; AB5731), goat anti-FoxA2 (M-20, Santa Cruz Biotechnology), goat-anti-Gata6 (C-20, Santa Cruz Biotechnology), or mouse anti-CD140a (PDGFRA; eBioscience, San Diego, CA; 16-1401). This was followed by the appropriate secondary antibodies detecting mouse or goat IgG Alexa Fluor 488 (Molecular Probes, Eugene, OR; 1:500) for Oct4 staining, rabbit IgG Alexa Fluor 594 (Molecular Probes; 1:500) for Nanog staining, or Qdot 655 anti-goat or anti-mouse antibodies (Molecular Probes) for FoxA2, Gata6, and PDGFRA staining (1:150) according to the manufacturer's protocol. Images were captured with the Zeiss LSM 5 Duo inverted confocal microscope (Zeiss, Thornwood, NY).

Luciferase Reporter Construct and Assays

The 300-base pair Zic3 enhancer region containing the Nanog-binding site was cloned from mouse genomic DNA. The primers used were as follows: forward, 5′ ATATAacgcgtTTAGAGGTCAAACCAT-3′ and reverse, 5′-TATATagatctTAGTAGTCAAACTGGATT-3′ with restriction sites indicated in lower case letters. The PCR fragment was digested with MluI and BglII and cloned into the pGL3-Basic vector (Promega, Madison, WI) containing a basal promoter comprising the 500-bp region immediately upstream of the mouse Oct4 gene. The following constructs were transfected into cells 2.5×10^4 cells in 96-well plates for the luciferase assay: 100 ng firefly luciferase reporter, 1.0 ng of the *Renilla* luciferase vector, pRL-SV40 plasmid normalization control, and 250 ng of the respective knock-down construct. Puromycin selection (1.0 μg/ml) was introduced 20 h after transfection and cultured for 2 d. Luciferase activity measured using the Dual Luciferase System (Promega) in a Centro LB960 96-well luminometer (Berthold Technologies, Natick, MA).

RESULTS

Zic3 Expression Is Associated with ES Cell Pluripotency

Comprehensive expression profiling of mouse and human ES cells has identified numerous genes that are expressed in undifferentiated cells and quickly repressed upon differentiation (Brandenberger *et al.*, 2004; Wei *et al.*, 2005). Among these genes are transcription factors Oct4, Nanog, and Sox2, which are required to maintain pluripotency of ES cells. Zic3, a zinc-finger transcription factor, was also found to be expressed in undifferentiated ES and suppressed in differentiated cells, and thus, may play a role in regulating ES cell differentiation. We assayed the expression of Zic3 in mouse ES cells induced to differentiate over 6 d by addition of retinoic acid (RA; Figure 1A). Similar to the trends observed for Oct4, Nanog, and Sox2 genes, Zic3 transcript levels decreased between 1.5- and 10-fold for each 2-d interval (D2, D4, and D6), relative to the undifferentiated control. Zic3

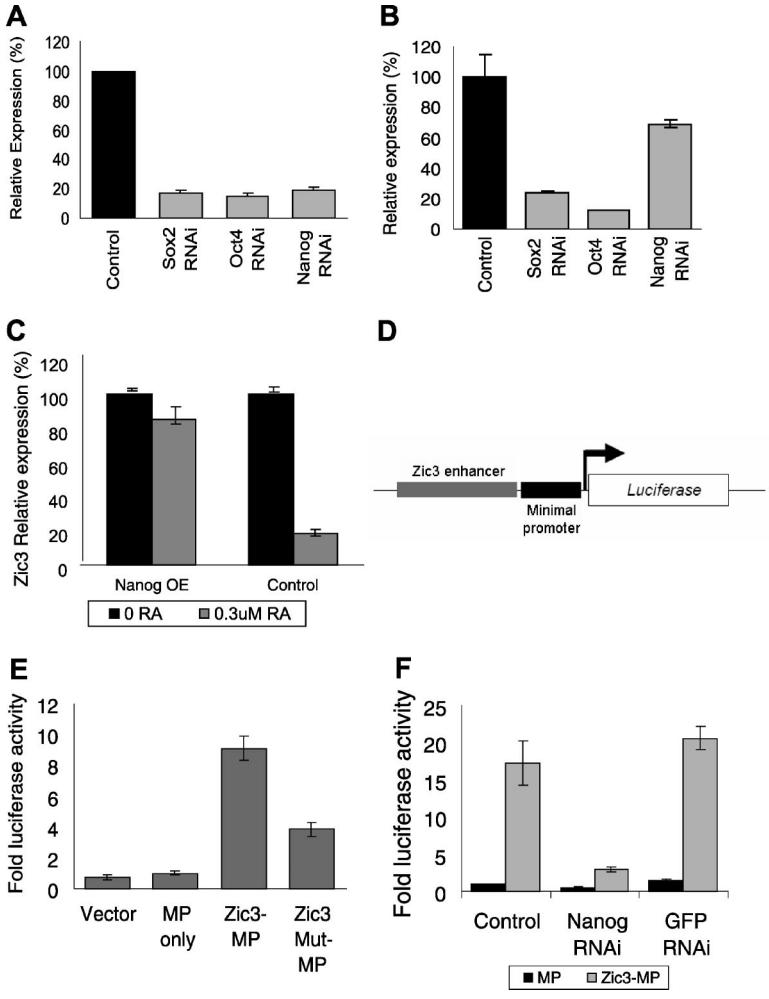

Figure 2. Oct4, Sox2, and Nanog regulate Zic3 expression. (A) Changes in endogenous gene expression levels of Oct4, Nanog, and Sox2 after gene-specific RNAi and (B) corresponding changes in endogenous *Zic3* gene levels. cDNAs were prepared from the RNAi knockdown ES cells and analyzed using real-time PCR. The levels of the transcripts were normalized against values derived from control RNAi-transfected ES cells (100%). (C) Changes in ES cell endogenous Zic3 gene level after Nanog overexpression with RA induced differentiation. Nanog overexpression cell line and control cell line were treated with no RA or 0.3 μM RA for 2 d. Transcript levels of 0.3 μM RA-treated sample were normalized against no RA treatment sample. (D) Diagram of the construct with putative Zic3 enhancer region fused upstream of a minimal Pou5f1 promoter and firefly luciferase gene. (E) The effects of luciferase activity in deletion of the putative Nanog binding site on Zic3 enhancer were tested by transfecting into ES cells. Activity were measured relative to the minimal promoter only (MP) construct without the Nanog enhancer. (F) Effects of Nanog RNAi on Zic3 enhancer activity were tested by cotransfecting the Nanog RNAi with the reporter construct into ES cells and luciferase activity measured. Activity were normalized against the Control RNAi with mOct4 promoter-only construct. An RNAi targeting the GFP sequence was used as a non-specific control.

RNA levels were also significantly decreased in mouse ES cells differentiated by treatment with HMBA (hexamethylene bisacetamide) or dimethyl sulfoxide, and also by aggregation into embryoid bodies (data not shown). The decrease in Zic3 mRNA correlated with a comparable decrease in protein expression (Figure 1B). Thus, Zic3 gene expression is associated with the mouse ES pluripotent state and its expression decreases as cells differentiate.

Chromatin immunoprecipitation experiments in both mouse and human ES cells have identified binding sites for the transcription factors Oct4, Nanog, and Sox2 at the Zic3 gene locus (Figure 1C; Boyer *et al.*, 2005; Loh *et al.*, 2006). The binding of these transcription factors, which are demonstrated regulators of pluripotency, suggests that Zic3 is a direct target for regulation by these TFs and may play a role in regulating ES cell differentiation.

Regulation of Zic3 by Oct4, Sox2, and Nanog

To further validate that Oct4, Sox2, and Nanog regulate Zic3 expression, we performed gene expression knockdown experiments in mouse ES cells using RNA interference. Mouse ES cells were thrice transfected with gene-specific siRNAs against Oct4, Sox2, and Nanog on alternate days to achieve 80–90% reduction in expression of the targeted gene (Figure 2A). Down-regulation of Oct4 and Sox2 reduced the level of endogenous Zic3 to <25%, whereas Nanog RNAi reduced the level of Zic3 to 70% (Figure 2B). These data indicate that Zic3 expression is regulated by Oct4, Sox2, and Nanog.

It has been shown that Nanog-overexpressing ES cells are resistant to differentiation induced by LIF withdrawal and RA addition (Chambers and Smith, 2004). As the endogenous levels of Zic3 decreased in the presence of RA-induced differentiation (Figure 1), we were interested in determining if Nanog overexpression would sustain Zic3 levels under RA treatment. ES cells were stably transfected with a construct that expresses Nanog from a constitutively active promoter. The Nanog-expressing cells and cells transfected with empty vector were treated for 2 d with 0.3 μM RA. Vector-only control cells showed a decrease in Zic3 RNA levels typical of RA-induced differentiation. In contrast, mouse ES cells overexpressing Nanog sustained the level of Zic3 at greater than 80%, relative to the control ES cell line (Figure 2C). Thus, overexpression and knockdown of Nanog in ES cells results in an increase and decrease, respectively, of Zic3, suggesting that Zic3 expression is regulated by Nanog, perhaps directly or indirectly.

Our previous study identified a Nanog binding site in the enhancer region, 16.4 kb upstream of the transcription start site, of the Zic3 gene (Loh *et al.*, 2006). As this DNA region was available for further study in our lab, we sought to determine if Zic3 expression was directly regulated by Nanog. We fused the 292-base pair portion of the Zic3 enhancer that contains the Nanog-binding site upstream of a minimal Pou5f1 promoter driving the firefly luciferase gene (Figure 2D). The minimal promoter was weakly active in ES cells, whereas activity of the Zic3 enhancer region linked to the minimal promoter was ninefold up-regulated as quantified by luciferase (Figure 2E). When the sequences of this putative Nanog binding site were deleted from the Zic3 enhancer the corresponding reporter activity decreased (Figure 2E). We then transfected Nanog RNAi together with the wild-type reporter construct and showed that the activity of the Zic3 enhancer decreased fourfold relative to the controls (Figure 2F). Collectively, our data show that Zic3 expression is directly regulated by Nanog and thus, may be a downstream effector in controlling ES cell differentiation.

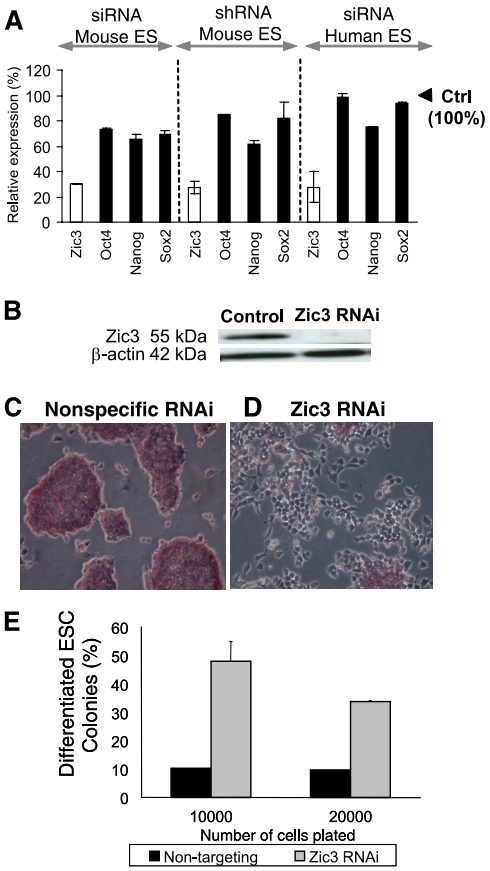

Figure 3. Effect of Zic3 RNAi on endogenous Oct4, Nanog, and Sox2 levels. (A) Zic3 levels were depleted by RNAi using siRNA and shRNA in mouse E14 cells and siRNA in human HuES9 cells. RNA was harvested between 4 and 5 d of transfection and transcript levels assayed by real-time PCR. Shown in this figure are the levels of Zic3 transcript and the corresponding changes in Oct4, Nanog, and Sox2 expression. Mean values ± SE are plotted as percentages relative to the nontargeting control (100%). The samples were assayed in duplicate and normalized to endogenous β-actin. (B) Corresponding decrease in protein levels after Zic3 RNAi treatment. The Zic3 protein species was depleted in the Zic3 RNAi sample, whereas β-actin protein levels remained high in the control. β-actin protein was used as a loading control. (C and D) Alkaline phosphatase staining revealed that the extent of differentiation in Zic3 RNAi-treated cells was greater than mock-transfected cells. (E) Secondary replating assays were used to quantitate the extent of differentiation in Zic3 RNAi cells. A 3- to 5-fold increase in differentiated colonies were observed with Zic3 RNAi relative to mock-transfected control.

Effect of Zic3 Depletion on ES Cell Differentiation

To investigate the role of Zic3 in ES cells, we used RNAi to achieve knockdown of gene expression. Both the siRNA and shRNA methods resulted in a 70% reduction of Zic3 transcript levels relative to the nontargeting controls (Figure 3A). Zic3 protein levels reflect this decrease in gene expression after Zic3 RNAi treatment, whereas protein expression remained high in vector-only–treated cells (Figure 3B).

Zic3 RNAi transfections resulted in a marked decrease in pluripotent colonies that stained for alkaline phosphatase (AP) relative to the mock RNAi control (Figures 3, C and D). The extent of differentiation was quantified with secondary replating assays that revealed a three- to fivefold increase in differentiated colonies in comparison with the nontargeting control (Figure 3E). To assess the differentiation state of Zic3

knockdown cells, we assayed for changes in expression of key pluripotency genes (Figure 3A). Though the mouse ES cells showed clear morphological changes (Figure 3, C and D), surprisingly, there were only modest decreases (15–25%) in the expression of the key pluripotency genes Oct4 and Sox2 (Figure 3A), whereas Nanog expression decreased 40% relative to the nontargeting control. We performed the same experiment with human ES cells (HuES9). Although there was 70% decrease in Zic3 transcript levels, Oct4 and Sox2 transcript levels remained unchanged and Nanog levels decreased by 25% (Figure 3A). These results indicate that Zic3 plays a role in maintaining ES cell pluripotency and its action is downstream of the dominant pluripotency factors Oct4, Sox2, and Nanog.

It is interesting that targeted repression of Zic3 induced morphological differentiation of ES cells while maintaining the expression of pluripotency marker genes in the transient knockdown experiments. We were interested in assessing the role of Zic3 in the maintenance of pluripotency. To determine the differentiation status of these cells we assayed by Q-RT-PCR for expression of markers that represent lineage-specific ES cell differentiation (Table 1). Zic3 knockdown in mouse and human ES cells resulted in an up-regulation of a panel of endodermal markers: Sox17 (3.5-fold), PDGFRA (3.2- to 5.5-fold in mouse ES cells; 2.7-fold in human ES cells), and Gata6 (2.5- to 3.5-fold; Figure 4). In addition, two more endodermal lineage genes Gata4 and Foxa2 were up-regulated in the E14 RNAi cells (2.5-fold). We also assayed the expression of mesendodermal, mesodermal, ectodermal, trophectodermal and Wnt-pathway markers in Zic3 RNAi cells. These markers remained unchanged relative to the nontargeting control in both mouse and human RNAi experiments (Figure 4). These results indicate that Zic3 could play a specific role in maintaining ES cell pluripotency by suppressing endodermal specification.

Rescue of RNAi-induced Zic3 Phenotype

Our RNAi experiments have established a link between the expression of Zic3 and suppression of endodermal lineage specification. We observed consistent results using multiple siRNAs and shRNAs in both mouse and human ES cells. However, there is still concern that ES cell differentiation and marker gene expression were due to off-target effects of the RNAi. To address this concern we designed a Zic3 expression construct that was immune to RNAi and tested whether this construct could rescue the knockdown phenotypes.

The Zic3 RNAi-immune expression construct was engineered with five silent mutations in protein coding domain sequence (Supplementary Figure 1). As such, this construct (mutZic3) produces functional Zic3 protein, but with the added feature that it is resistant to RNAi targeting and

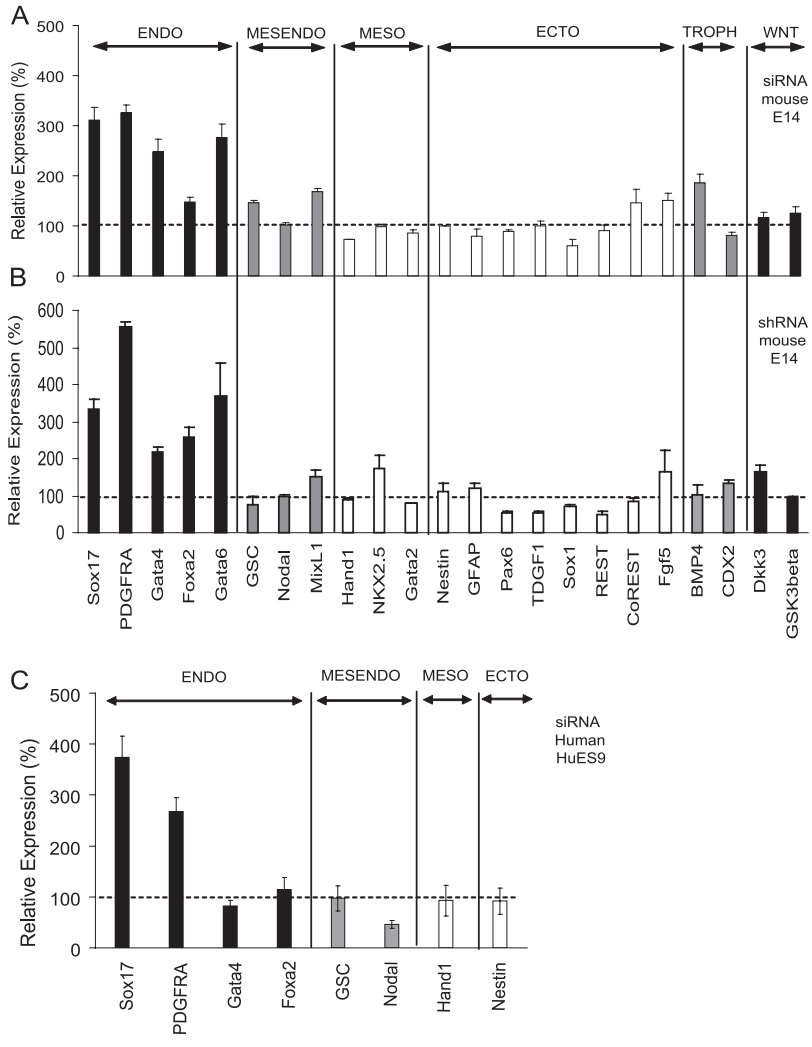

Figure 4. Effect of Zic3 RNAi on lineage marker gene expression. The panel of genes above was selected for their lineage specificity. Transcript levels of genes from the endodermal (ENDO), mesendodermal (MESENDO), mesdodermal (MESO), ectodermal (ECTO), trophectordermal (TROPH), and Wnt pathways in mouse and human ES cells were assayed by real-time PCR after Zic3 depletion by RNAi. (A) siRNA in mouse E14 cells. (B) shRNA in mouse E14 cells. (C) siRNA in human HuES9 cells. Mean levels ± SE are expressed as percentages relative to the nontargeting control (100%). The assays were read in duplicate and results were normalized to β-actin.

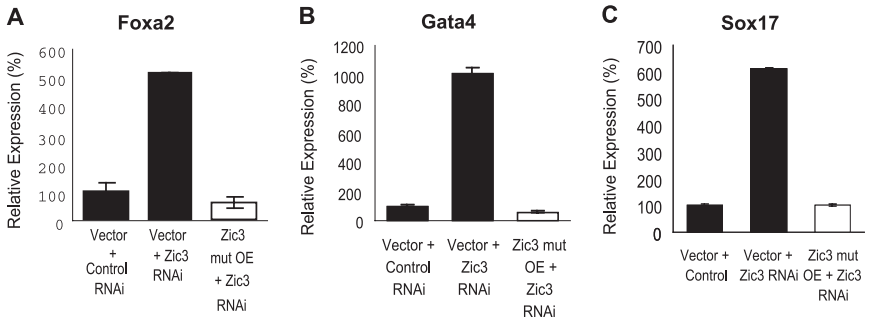

Figure 5. Zic3-immune construct specifically reverses changes in lineage marker expression levels caused by Zic3 RNAi. (A–C) Zic3 rescue experiments demonstrating the specificity of Zic3 RNAi and reversibility of lineage marker expression. E14 cells cotransfected with the Zic3 RNAi-immune overexpression construct and Zic3 RNAi vector demonstrated notable suppression of endodermal markers Foxa2, Gata4, and Sox17, relative to Zic3 RNAi cotransfected with the empty vector control. Zic3 immune real-time PCR analysis was conducted 3 d after transfection. β-Actin was used as an internal control for normalization. The measurements were done in duplicates and the average of the normalized ratio of target gene/β-actin was calculated and presented with SD. Relative expressions calculated with respect to the control experiment (Vector + control RNAi) at 100%. Transfection schemes are represented in Supplementary Table 1b.

degradation. Using this mutZic3 construct, we determined the specificity of the endodermal lineage specification produced by Zic3 knockdown. First, the expression levels of endodermal markers Foxa2, Gata4, and Sox17 were induced in ES cells cotransfected with empty vector and Zic3-RNAi, compared with cells cotransfeceted with empty vector and GFP-RNAi (6.5-, 10.1-, and 8.7-fold, for Foxa2, Gata4, and Sox17, respectively, Figure 5, A–C). However, ES cells that express the mutZic3 (RNAi immune construct) showed no induction of endodermal markers by Zic3-RNAi. (Figure 5, A–C). These experiments indicate that our RNAi results are not due to off-target effects and further support our conclusions that Zic3 plays a role in maintaining the pluripotency of ES cells.

Effects of Simultaneous Reduction of Zic2 and Zic3 Expression

Zic2 is another member of the Zic-family of transcription factors. Zic2 is expressed in ES cells and its expression is down-regulated upon differentiation (Brandenberger *et al.*, 2004; Wei *et al.*, 2005). Zic2 may also be regulated by Oct4, Sox2, and Nanog as binding sites for these TFs have been mapped to the Zic2 gene by chromatin immunoprecipitation (ChIP; Supplementary Figure 2). It was interesting that Zic3 RNAi resulted in a twofold increase in Zic2 (Figure 6A), and this raised the possibility that Zic2 may be compensating for the reduction in Zic3 levels. Knockdown of Zic2 expression by siRNA (75% reduction in RNA levels) did not produce any effect on lineage marker expression (Figure 6B). To determine if Zic2 compensated for the absence of Zic3, we performed a double RNAi experiment with Zic2 and Zic3 in ES cells. The double knockdown prevented Zic2 levels from increasing in a compensatory manner as observed in the Zic3 single knockdown (Figure 6C). Interestingly, endodermal specification was markedly enhanced after the Zic2 and Zic3 double knockdown as demonstrated by increased expression of Sox17 (4.7-fold), PDGFRA (8.7-fold), and Gata4 (3.1-fold), which is more robust than observed for all three markers (Sox17, 3.1-fold; PDGFRA, 3.3-fold; Gata4, 1.5-fold) when Zic3 alone was reduced (Figure 6D). Thus, we demonstrate that in the absence of Zic3, Zic2 is able to compensate at least partially to reduce the extent of endodermal specification in ES cells.

Zic3 Clonal Knockdown Lines Show Enhanced Endodermal Specification

To determine if endodermal markers were up-regulated in the same cells in which Zic3 was depleted, three clonal lines were generated that stably expressed Zic3 shRNA. As anticipated, Zic3 expression in the clonal lines was down-regulated 60% relative to vector-only control lines (Figure 7A). This knockdown is slightly less robust than in the transient Zic3 knockdowns where depletion of Zic3 expression by 70–80% was observed (Figure 3A). The pluripotency genes Oct4 and Sox2 were reduced between 20 and 30% relative to controls in all three clonal knockdown lines, whereas Nanog was reduced by 80% (Figure 7A). The endodermal genes PDGFRA, Gata4, Gata6, and Sox7 were 30-fold higher than in the controls, whereas Sox17 was up-regulated between 60- to 80-fold and FoxA2 was increased by 80- to 120-fold in all three Zic3 knockdown lines (Figure 7B). The induction of endodermal markers here was substantially greater than observed in the transient Zic3 knockdowns. Markers of the mesendoderm, mesoderm, ectoderm, trophectoderm, and Wnt pathways remained essentially unchanged (<2-fold) in the Zic3 knockdown lines (Figure 7C). Thus the specific up-regulation of endodermal gene expression in the clonal lines is consistent, in fact more pronounced, with our observations in the transient knockdowns (Figure 4).

To ascertain if there were corresponding increases in endodermal protein levels, immunocytochemistry was performed against FoxA2, Gata6, and PDGFRA in the clonal lines. The Zic3 knockdown lines consistently demonstrated robust endodermal marker staining (Figure 8A) that was absent in the vector control lines (Supplementary Figure 3). Oct4 staining was also observed in the cells that were positive for endodermal marker expression (Figure 8A). Interestingly, although the Zic3 clonal knockdown lines expressed Oct4 and SSEA-1 (Figure 8B), Nanog protein expression was significantly reduced relative to the vector control lines (Figure 8C). This agreed with the down-regulation observed in Nanog gene expression levels in the Zic3 knockdown lines (Figure 7A) and raises the possibility that Nanog gene expression is regulated by Zic3.

DISCUSSION

The work presented here demonstrates that Zic3 plays a key regulatory role in controlling ES cell differentiation. In this article, we have demonstrated that the expression pattern of Zic3 in ES cells corresponds closely with that of known regulators of pluripotency Oct4, Nanog, Sox2, which have high levels of expression in the undifferentiated state and decrease rapidly upon differentiation (Figure 1). Our findings in mouse ES cells are consistent with results from human ES cells (Brandenberger *et al.*, 2004). The differences we observed in Zic3 expression levels between pluripotent and early differentiation phases imply a potentially significant role for Zic3 in ES cell pluripotency. In addition, ChIP mapping by us and others has revealed Oct4, Nanog, and

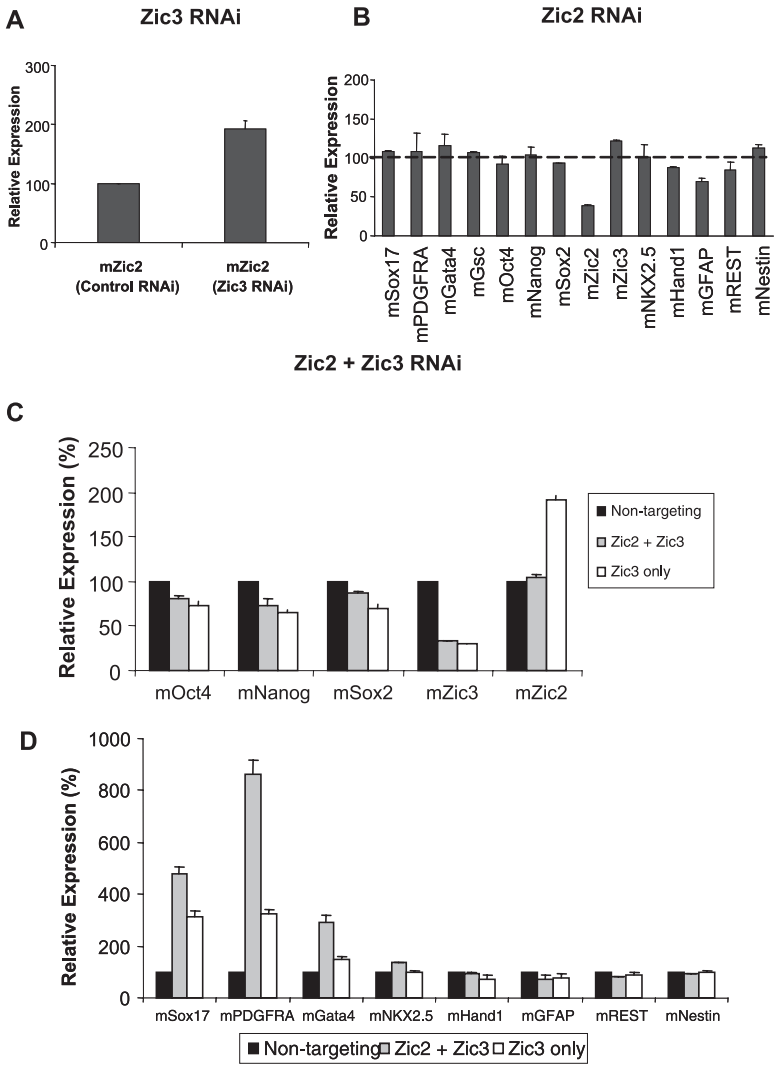

Figure 6. Effect of Zic2 and Zic3 double knockdown. The genes were assayed by real-time PCR in triplicate and normalized to a β-actin control. Mean levels $\pm$ SE are expressed as percentages relative to the nontargeting control. (A) Zic2 gene expression increased twofold with Zic3 transient knockdown 4 d after transfection. (B) Zic2 knockdown by siRNA was specific but did not produce changes in lineage markers assayed. (C) Zic2 and Zic3 coknockdown produced specific knockdown of Zic3 and at the same time prevented compensatory increase of Zic2 expression in ES cells. (D) The expression of endodermal lineage markers Sox17, PDGFRA, and Gata4 showed a similar pattern of up-regulation as in the Zic3 single knockdown, but was significantly enhanced in this Zic2/Zic3 coknockdown.

Sox2 co-occupancy on the Zic3 regulatory region, suggesting that Zic3 may be coordinately regulated by Oct4, Nanog, and Sox2 in mouse and human ES cells (Boyer *et al.,* 2005; Loh *et al.,* 2006; Figure 1C). These observations together led to our hypothesis that Zic3 functions to maintain the pluripotent state of ES cells. Here we characterized the relationship of Zic3 with that of the key stem cell regulatory factors and uncovered a role for Zic3 in the maintenance of ES cell pluripotency.

Our first objective was to assess the nature of interactions between Oct4, Nanog, and Sox2 with the Zic3 regulatory region. In constructing the transcriptional network around the key pluripotency genes, it is important to establish the outcome of transcription factor binding on downstream genes. We addressed this using a combinatorial approach encompassing the results of ChIP mapping and RNAi, demonstrating that ablation of Oct4, Nanog, and Sox2 in mouse ES cells resulted in a significant decrease in Zic3 expression (Figure 3A). Because Zic3 has already been implicated as a target of Oct4, Nanog, and Sox2 in ChIP experiments (Boyer *et al.,* 2005; Loh *et al.,* 2006), the concern of nondirect or secondary effects of RNAi was significantly reduced (Blais and Dynlacht, 2005). We thus concluded that the interaction of Oct4, Nanog, and Sox2 with the regulatory region of the Zic3 gene serves to enhance target gene expression. In other words, the key pluripotency regulators function as transcriptional activators of Zic3 in ES cells (Figure 9). This point is underscored by our results with Nanog overexpression and binding site mutagenesis assays, which demonstrate a positive association between Nanog binding and Zic3 expression. We thus demonstrate positive functional interactions between the key pluripotency regulators and the Zic3 gene regulatory region.

Because transcriptional networks are also known to feature autoregulatory loops (Lee *et al.,* 2002; Blais and Dynlacht, 2005), we also asked if the inverse relationship was true, that is, whether Zic3 regulates expression of the key regulatory genes. We observed that Oct4 and Sox2 levels remained largely unperturbed by the ablation of Zic3 expression (Figures 3A and 7A). In the absence of clear changes despite a robust Zic3 knockdown, our data places Zic3 downstream of Oct4 and Sox2 in the ES cell transcriptional networks as illustrated in Figure 9. In addition, we found that Nanog expression decreased significantly in the Zic3 clonal knockdown lines (Figures 7A and 8C). It remains to be determined whether Zic3 directly regulates the expression of Nanog in embryonic stem cells.

ES cells are derived from the inner cell mass of the blastocyst and, as such, are able to undergo unlimited self-renewal and differentiation into the three germ layers of the

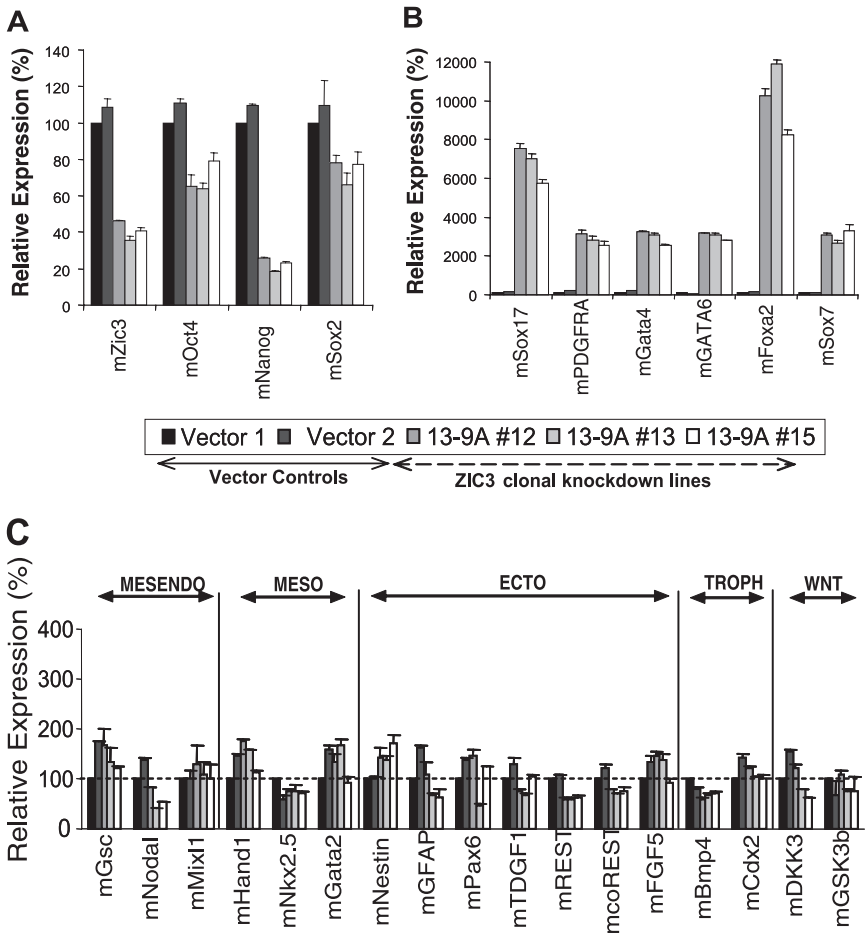

Figure 7. Zic3 knockdown clonal lines demonstrate endodermal gene marker specification. Three Zic3 knockdown clonal lines and two vector controls were assayed as indicated in the diagrams. (A) The pluripotency markers Oct4 and Sox2 were slightly down-regulated between 20 and 30%, whereas Zic3 and Nanog decreased significantly between 60 and 80% relative to the vector controls. (B) All endodermal markers assayed in the knockdown lines were significantly up-regulated between 20- and 120-fold relative to the control lines. (C) Mesendodermal, mesodermal, ectodermal, trophectodermal, and Wnt pathway genes did not change significantly in knockdown lines, demonstrating <2-fold changes relative to the vector controls. Gene expression levels were assayed by real-time PCR. The samples were assayed in triplicate and normalized to endogenous β-actin. Mean values $\pm$ SE are plotted as percentages relative to the vector control.

embryo: mesoderm, ectoderm, and endoderm (Evans and Kaufman, 1981; Martin, 1981). In the pluripotent state, ES cells remain undifferentiated and do not express specific lineage markers. We were interested in examining the effect of Zic3 knockdown on the maintenance of ES pluripotency using specific lineage markers as an assessment of differentiation after Zic3 knockdown (Table 1). Here we show that ablation of Zic3 expression in both mouse and human ES cells resulted in a significant increase in markers of endodermal lineage (Figures 4, 7, and 8). These results suggest that Zic3 may have an important role in preventing endodermal specification in ES cells.

Many reports support this observation: First, Zic3 knockdown in ES cells induced expression of Gata4 and Gata6, and forced expression of Gata4 and Gata 6 in ES cells result in differentiation toward extraembryonic endoderm (Fujikura *et al.*, 2002). Further strengthening this association is the fact that all other endodermal markers assayed (PDGFRA, Sox17, and FoxA2) are also expressed in extraembryonic endoderm derivatives (Kunath *et al.*, 2005). Second, Zic3 regulates Nodal expression through direct interaction with its promoter during gastrulation, and it has been shown that Nodal expression is essential in proper specification of the embryonic visceral endoderm (Mesnard *et al.*, 2006). This significance is underscored by studies reporting that the earliest abnormalities observed in Zic3 null mice are defects in proper patterning of the anterior visceral endoderm (Ware *et al.*, 2006b). Finally, Zic3 clonal knockdown lines exhibit a significant decrease in Nanog gene expression (Figures 7A and 8C), and several groups have reported that RNAi-mediated depletion of Nanog expression resulted in an induction of extraembryonic endoderm markers Gata4 and Gata6 (Mitsui *et al.*, 2003; Hyslop *et al.*, 2005; Hough *et al.*, 2006).

Here we have shown that Zic3 functions as a gatekeeper of pluripotency in ES cells by preventing their differentiation into cells that express endodermal markers. Corroborating this, we have found that Nanog expression is significantly reduced in the Zic3 clonal lines. This reduction is noteworthy as Nanog is a key regulator of pluripotency in ES cells (Chambers *et al.*, 2003), and it is well established that disruption of Nanog expression results in development of extraembryonic endoderm character in ES cells (Mitsui *et al.*, 2003; Hyslop *et al.*, 2005; Hough *et al.*, 2006). Thus, we demonstrate here an important role for Zic3 in the maintenance of pluripotency in ES cells through prevention of endodermal lineage specification, and we suggest that its action may in part be mediated through the key pluripotency regulator Nanog (Figure 9).

The role of Zic3 in preventing endodermal specification is further supported by evidence indicating its restricted expression within the mesoderm and ectoderm lineages during gastrulation (Herman and El-Hodiri, 2002). In addition, Zic3 activity has been specifically implicated in the mesodermal and ectodermal molecular pathways in the early developing embryo (Nakata *et al.*, 1997; Kitaguchi *et al.*, 2002; Maeda *et al.*, 2002; Kelly *et al.*, 2006). These data in combination with our results suggest that although Zic3 is instructive for mesodermal and ectodermal specification in embryonic development, it may simultaneously function as a repressor of ectopic endodermal induction in these tissues.

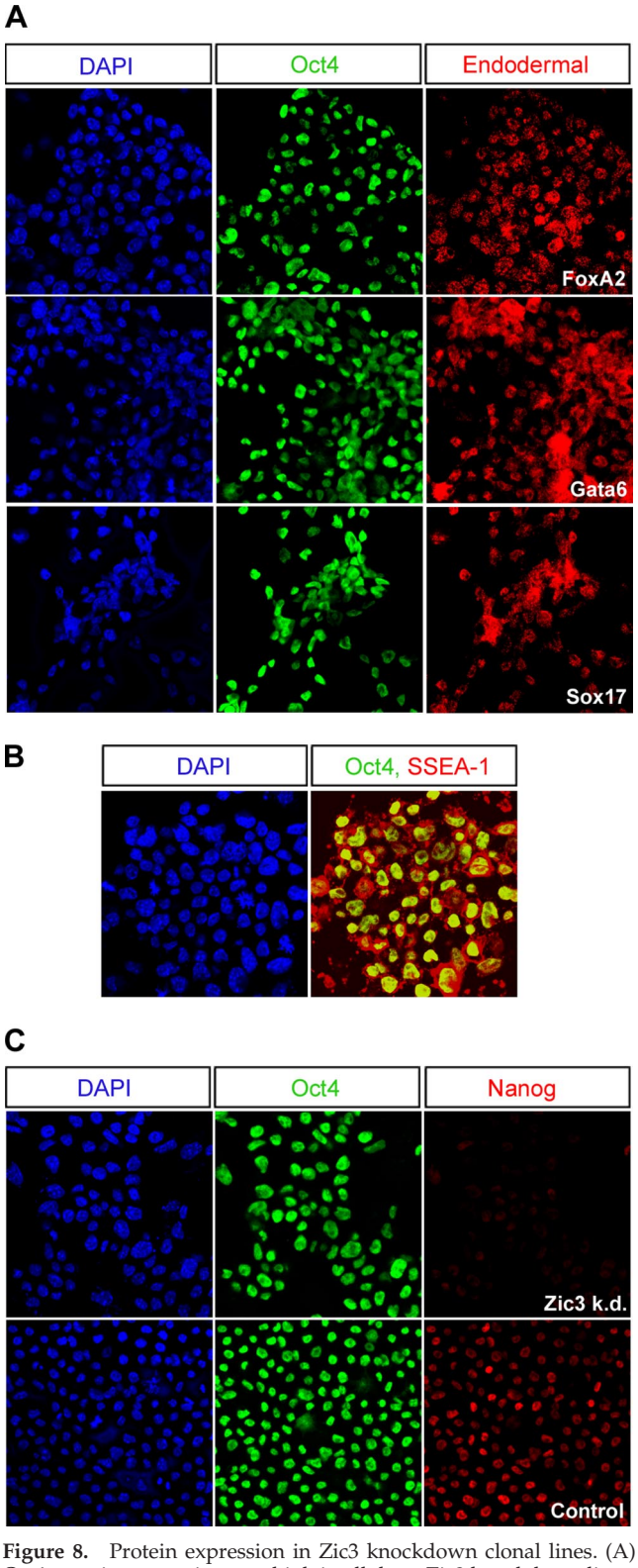

Figure 8. Protein expression in Zic3 knockdown clonal lines. (A) Oct4 protein expression was high in all three Zic3 knockdown lines, and the expression of specific endodermal marker proteins Foxa2, Gata6, and Sox17 was observed in the same cells. (B) The Zic3 knockdown lines expressed stem cell surface protein, SSEA-1, which is specific to murine ES cells. (C) The Zic3 clonal knockdown lines demonstrated a significant decrease in Nanog expression.

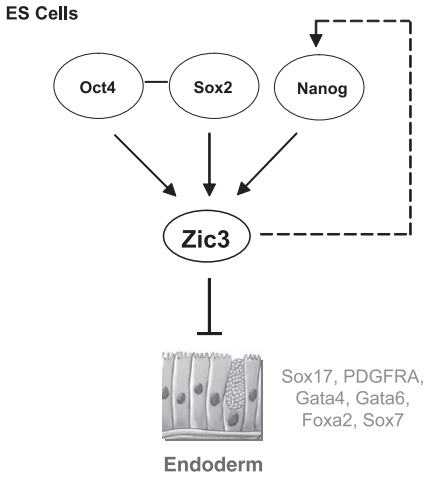

Figure 9. A model of Zic3 function in embryonic stem cells. Zic3 contributes to the maintenance of pluripotency by operating downstream of Oct4, Nanog, and Sox2 to inhibit endoderm lineage specification as characterized by endodermal markers Sox17, PDGFRA, Gata4, Gata6, Foxa2, and Sox7. The presence of Zic3 also maintains the expression of the homeodomain protein Nanog, a key regulator of pluripotency in embryonic stem cells.

The transcription factor Zic3 shares five highly conserved Zinc finger domains with family members Zic1, Zic2, Zic4, and Zic5 (Aruga *et al.*, 1994, 1996a,b, 2004). Their partially overlapping spatial and temporal patterns of expression during early development suggests potential functional redundancy between the Zic family members (Nagai *et al.*, 1997; Elms *et al.*, 2004). We observed that Zic2 gene levels were up-regulated when Zic3 expression was reduced (Figure 6A). Because Zic2 is also differentially expressed between pluripotent and differentiation states of ES cells (Brandenberger *et al.*, 2004; Wei *et al.*, 2005) and binding of the key pluripotency transcription factor Nanog has been mapped to the Zic2 regulatory region (Supplementary Figure 2), we reasoned that Zic2 may participate in the regulation of ES cell pluripotency along with Zic3. To unveil the possible effects of functional redundancy between Zic2 and Zic3, a double knockdown was performed in mouse ES cells. We report that repression of Zic2 and Zic3 expression significantly enhanced endoderm specification in ES cells (Figure 6C). The evidence that Nanog binds to the Zic2 regulatory region suggests that it may be involved in similar pathways as Zic3 in repressing endoderm expression. Thus, Zic2 and Zic3 may participate in redundant or partially overlapping networks to silence endoderm specifying gene expression and contribute to the maintenance of pluripotency in ES cells.

CONCLUSION

In this article, we expand on the significance of Zic3 as a target of the key stem cell regulatory factors in ES cells. Our results highlight a role for Zic3 in the maintenance of pluripotency downstream of Oct4 and Sox2, and uncovers its role as a gatekeeper controlling differentiation of ES cells into endoderm-specific lineages. In support of this, we present evidence that a key regulator of pluripotency, Nanog, which is shown to be important in repressing endodermal lineage specification, may directly or indirectly be regulated by Zic3 in ES cells. Having now established that Zic3 plays an important role in maintenance of pluripotency,

it will be valuable to search for Zic3-regulated target genes, which will extend our understanding of the transcriptional network that governs lineage specification. The elucidation of molecular signatures of early ES cells in this manner will contribute to validation and extension of the ES cell transcriptional network beyond Oct4, Nanog, and Sox2. The critical need to dissect their transcriptional networks is underscored by their potential to yield critical insights into genetic mechanisms at the earliest stages of embryo development and to provide significant inroads into the properties ES cell unlimited growth and differentiation potential that will render them therapeutically useful.

ACKNOWLEDGMENTS

We thank Drs. Noel Buckley, Paul Robson, Thomas Lufkin, and Bing Lim for helpful discussions. We also thank Li Pin, Aina Hoi, Joon-Lin Chew, and Boon Seng Soh for their invaluable assistance. We thank the Biomedical Research Council and Agency for Science, Technology and Research (A*STAR) for funding. L.S.L. and Y-H.L. are recipients of the A*STAR graduate scholarship. W.Z. and X.C. are supported by the National University of Singapore graduate scholarship.

REFERENCES

Aruga, J. (2004). The role of Zic genes in neural development. Mol. Cell Neurosci. *26*, 205–221.

Aruga, J., Nagai, T., Tokuyama, T., Hayashizaki, Y., Okazaki, Y., Chapman, V. M., and Mikoshiba, K. (1996a). The mouse zic gene family. Homologues of the *Drosophila* pair-rule gene odd-paired. J. Biol. Chem. *271*, 1043–1047.

Aruga, J., Yokota, N., Hashimoto, M., Furuichi, T., Fukuda, M., and Mikoshiba, K. (1994). A novel zinc finger protein, zic, is involved in neurogenesis, especially in the cell lineage of cerebellar granule cells. J. Neurochem. *63*, 1880–1890.

Aruga, J., Yozu, A., Hayashizaki, Y., Okazaki, Y., Chapman, V. M., and Mikoshiba, K. (1996b). Identification and characterization of Zic4, a new member of the mouse Zic gene family. Gene *172*, 291–294.

Aylsworth, A. S. (2001). Clinical aspects of defects in the determination of laterality. Am. J. Med. Genet. *101*, 345–355.

Blais, A., and Dynlacht, B. D. (2005). Constructing transcriptional regulatory networks. Genes Dev. *19*, 1499–1511.

Boyer, L. A. *et al.* (2005). Core transcriptional regulatory circuitry in human embryonic stem cells. Cell *122*, 947–956.

Brandenberger, R. *et al.* (2004). Transcriptome characterization elucidates signaling networks that control human ES cell growth and differentiation. Nat. Biotechnol. *22*, 707–716.

Chambers, I., Colby, D., Robertson, M., Nichols, J., Lee, S., Tweedie, S., and Smith, A. (2003). Functional expression cloning of Nanog, a pluripotency sustaining factor in embryonic stem cells. Cell *113*, 643–655.

Chambers, I., and Smith, A. (2004). Self-renewal of teratocarcinoma and embryonic stem cells. Oncogene *23*, 7150–7160.

Chew, J. L. *et al.* (2005). Reciprocal transcriptional regulation of Pou5f1 and Sox2 via the Oct4/Sox2 complex in embryonic stem cells. Mol. Cell Biol. *25*, 6031–6046.

Elms, P., Scurry, A., Davies, J., Willoughby, C., Hacker, T., Bogani, D., and Arkell, R. (2004). Overlapping and distinct expression domains of Zic2 and Zic3 during mouse gastrulation. Gene Expr. Patterns *4*, 505–511.

Evans, M. J., and Kaufman, M. H. (1981). Establishment in culture of pluripotential cells from mouse embryos. Nature *292*, 154–156.

Fujikura, J., Yamato, E., Yonemura, S., Hosoda, K., Masui, S., Nakao, K., Miyazaki Ji, J., and Niwa, H. (2002). Differentiation of embryonic stem cells is induced by GATA factors. Genes Dev. *16*, 784–789.

Gebbia, M. *et al.* (1997). X-linked situs abnormalities result from mutations in ZIC3. Nat. Genet. *17*, 305–308.

Grinberg, I., and Millen, K. J. (2005). The ZIC gene family in development and disease. Clin. Genet. *67*, 290–296.

Grinblat, Y., and Sive, H. (2001). zic Gene expression marks anteroposterior pattern in the presumptive neurectoderm of the zebrafish gastrula. Dev. Dyn. *222*, 688–693.

Herman, G. E., and El-Hodiri, H. M. (2002). The role of ZIC3 in vertebrate development. Cytogenet. Genome. Res. *99*, 229–235.

Hough, S. R., Clements, I., Welch, P. J., and Wiederholt, K. A. (2006). Differentiation of mouse embryonic stem cells after RNA interference-mediated silencing of OCT4 and Nanog. Stem. Cells *24*, 1467–1475.

Hyslop, L., Stojkovic, M., Armstrong, L., Walter, T., Stojkovic, P., Przyborski, S., Herbert, M., Murdoch, A., Strachan, T., and Lako, M. (2005). Downregulation of NANOG induces differentiation of human embryonic stem cells to extraembryonic lineages. Stem Cells *23*, 1035–1043.

Kelly, L. E., Carrel, T. L., Herman, G. E., and El-Hodiri, H. M. (2006). Pbx1 and Meis1 regulate activity of the *Xenopus laevis* Zic3 promoter through a highly conserved region. Biochem. Biophys. Res. Commun. *344*, 1031–1037.

Kitaguchi, T., Mizugishi, K., Hatayama, M., Aruga, J., and Mikoshiba, K. (2002). *Xenopus* Brachyury regulates mesodermal expression of Zic3, a gene controlling left-right asymmetry. Dev. Growth Differ. *44*, 55–61.

Kunath, T., Arnaud, D., Uy, G. D., Okamoto, I., Chureau, C., Yamanaka, Y., Heard, E., Gardner, R. L., Avner, P., and Rossant, J. (2005). Imprinted X-inactivation in extra-embryonic endoderm cell lines from mouse blastocysts. Development *132*, 1649–1661.

Lee, T. I. *et al.* (2002). Transcriptional regulatory networks in *Saccharomyces cerevisiae*. Science *298*, 799–804.

Loh, Y. H. *et al.* (2006). The Oct4 and Nanog transcription network regulates pluripotency in mouse embryonic stem cells. Nat. Genet. *38*, 431–440.

Maeda, R., Ishimura, A., Mood, K., Park, E. K., Buchberg, A. M., and Daar, I. O. (2002). Xpbx1b and Xmeis1b play a collaborative role in hindbrain and neural crest gene expression in *Xenopus* embryos. Proc. Natl. Acad. Sci. USA *99*, 5448–5453.

Martin, G. R. (1981). Isolation of a pluripotent cell line from early mouse embryos cultured in medium conditioned by teratocarcinoma stem cells. Proc. Natl. Acad. Sci. USA *78*, 7634–7638.

Mesnard, D., Guzman-Ayala, M., and Constam, D. B. (2006). Nodal specifies embryonic visceral endoderm and sustains pluripotent cells in the epiblast before overt axial patterning. Development *133*, 2497–2505.

Mitsui, K., Tokuzawa, Y., Itoh, H., Segawa, K., Murakami, M., Takahashi, K., Maruyama, M., Maeda, M., and Yamanaka, S. (2003). The homeoprotein Nanog is required for maintenance of pluripotency in mouse epiblast and ES cells. Cell *113*, 631–642.

Nagai, T., Aruga, J., Takada, S., Gunther, T., Sporle, R., Schughart, K., and Mikoshiba, K. (1997). The expression of the mouse Zic1, Zic2, and Zic3 gene suggests an essential role for Zic genes in body pattern formation. Dev. Biol. *182*, 299–313.

Nakata, K., Nagai, T., Aruga, J., and Mikoshiba, K. (1997). *Xenopus* Zic3, a primary regulator both in neural and neural crest development. Proc. Natl. Acad. Sci. USA *94*, 11980–11985.

Nakata, K., Nagai, T., Aruga, J., and Mikoshiba, K. (1998). *Xenopus* Zic family and its role in neural and neural crest development. Mech. Dev. *75*, 43–51.

Orkin, S. H. (2005). Chipping away at the embryonic stem cell network. Cell *122*, 828–830.

Purandare, S. M., Ware, S. M., Kwan, K. M., Gebbia, M., Bassi, M. T., Deng, J. M., Vogel, H., Behringer, R. R., Belmont, J. W., and Casey, B. (2002). A complex syndrome of left-right axis, central nervous system and axial skeleton defects in Zic3 mutant mice. Development *129*, 2293–2302.

Ware, S. M., Harutyunyan, K. G., and Belmont, J. W. (2006a). Heart defects in X-linked heterotaxy: evidence for a genetic interaction of Zic3 with the nodal signaling pathway. Dev. Dyn. *235*, 1631–1637.

Ware, S. M., Harutyunyan, K. G., and Belmont, J. W. (2006b). Zic3 is critical for early embryonic patterning during gastrulation. Dev. Dyn. *235*, 776–785.

Ware, S. M., Peng, J., Zhu, L., Fernbach, S., Colicos, S., Casey, B., Towbin, J., and Belmont, J. W. (2004). Identification and functional analysis of ZIC3 mutations in heterotaxy and related congenital heart defects. Am. J. Hum. Genet. *74*, 93–105.

Warner, S. J., Hutson, M. R., Oh, S. H., Gerlach-Bank, L. M., Lomax, M. I., and Barald, K. F. (2003). Expression of ZIC genes in the development of the chick inner ear and nervous system. Dev. Dyn. *226*, 702–712.

Wei, C. L. *et al.* (2005). Transcriptome profiling of human and murine ESCs identifies divergent paths required to maintain the stem cell state. Stem Cells *23*, 166–185.